[^{14}C] RADIOTRACER STUDIES OF THE HYDROGENATION REACTIONS OVER SUPPORTED PLATINUM CATALYSTS

THESIS

SUBMITTED FOR THE DEGREE OF

DOCTOR OF PHILOSOPHY

OF THE

UNIVERSITY OF GLASGOW

BY

© EZZIDDIN AHMED ARAFA, M.Sc.

NOVEMBER, 1988

Department of Chemistry

University of Glasgow

TO

ALAUDIN and IMADUDIN

Acknowledgements

I would like to record my sincere thanks to my supervisor, Professor G. Webb for suggesting the topic which is the subject of this thesis and for his advice throughout the course of this work.

Thanks are also due to Dr. G. McLellan for his assistance in the IR and TPR Measurements; Drs. A. El-Gadi and A. Legrouri for the electron micrographs; staff members, Dr. K.C. Campbell, Dr. J.M. Winfield and Professor S.J. Thomson, for their advice and encouragement.

I am indebted to Messrs. T. Boyle, K. Shepherd and R. Wilson for technical assistance; my colleagues in the Catalysis Research Laboratory and Fluorine Chemistry Group for encouragement and discussions, and to the staff of the Glassblowing workshop for the construction and maintenance of the vacuum apparatus.

I am grateful to Tajoura Research Centre and Al-Fateh University (Libya), for the award of a scholarship, and to my colleague, Dr. M.F. Ghorab for reading the manuscript and for his company during the past four years. Also thanks to Mrs. J. Anthony for her skilful preparation of the typescript.

Last, but not least, my special thanks go to my wife, and to the other members of the family for their patience and encouragement, and also my friends for their advice.

E.A. Arafa

November 1988

CONTENTS

Page No.

SUMMARY

The adsorption of acetylene, ethylene and carbon monoxide; the hydrogenation of acetylene and buta-1,3-diene; the effects of sulphur poisoning on the adsorption, and the hydrogenation reactions, have been studied at ambient temperature in a static system using a variety of supported platinum catalysts. The catalysts used were EUROPT-1 (6% Pt/SiO_2), EUROPT-3 (0.3% Pt/Al_2O_3), 0.5% Pt/MoO_3, 0.8% Pt/SiO_2 and 0.8% Pt/Al_2O_3.

Using the [14-C] radiotracer technique, the shape of acetylene adsorption isotherms over each catalyst showed two distinct adsorption regions, a steep primary region followed (except Pt/MoO_3) by a linear secondary region. The Pt/MoO_3 catalyst showed a non-linear secondary region. The adsorption of ethylene also occurred in two distinct stages, but the primary region was less steep than was found with acetylene. The adsorptive capacity of the catalysts for ethylene was approximately one quarter that for acetylene.

In contrast, the adsorption isotherms of carbon monoxide showed distinct dissimilarities between catalysts. On EUROPT-1, 0.8% Pt/SiO_2 and 0.8% Pt/Al_2O_3 catalysts, the isotherms displayed different behaviour from that observed with the hydrocarbons in that they showed a prolonged secondary region with a positive gradient. The adsorption isotherm of CO on EUROPT-3 was of a similar shape to the isotherms observed with the hydrocarbons. The Pt/MoO_3 catalyst exhibited the expected Langmuir-type CO adsorption isotherm.

On steady state catalysts the amount of each adsorbate that can be adsorbed was substantially less than that on freshly reduced catalysts. This has been suggested as being due to the permanently retained hydrocarbon species located at the primary adsorption region.

With each catalyst the experimental observations are consistent with the dissociative adsorption of the hydrocarbons on the primary region, whilst the species involved in the actual catalysis process are located on the secondary region and are associatively adsorbed.

From the H_2S poisoning experiments, evidence has been obtained to show that a surface reconstruction process accompanies the initial adsorption. The results are interpreted in terms of a model involving the migration of metal atoms into the adsorbate ad-layer.

The adsorption of acetylene in the presence of gas phase ethylene and vice versa indicates that the adsorption of the two hydrocarbons takes place on the same adsorption sites with acetylene being more strongly adsorbed than ethylene. However, during the hydrogenation of acetylene, hydrogen was found to create sites which were active for the non-competitive adsorption of ethylene.

IR evidence has been obtained for the formation of an ethylidyne ($\equiv C\text{-}CH_3$) species upon the exposure of a freshly reduced EUROPT-1 to C_2H_2 or C_2H_4, while bands characteristic of hydrocarbon polymeric species were detected with C_2H_2/H_2 deactivated catalysts. On each catalyst, the adsorbed carbon monoxide was found to exist in the linear form.

From the experimental observations regarding the hydrogenation of acetylene in the presence of various pressures of [14-C]-ethylene

and determination of the kinetics and product distribution, it has been established that the major route to ethane formation is *via* a route involving direct hydrogenation of acetylene, rather than *via* ethylene as an intermediate. The results have been interpreted in terms of the presence of separate surface sites for the hydrogenation of acetylene to ethylene, the hydrogenation of acetylene to ethane and for the hydrogenation of ethylene to ethane.

From the kinetics and variations of the product compositions with the experimental variables for buta-1,3-diene hydrogenation, it has been proposed that, whilst 1:2 addition of hydrogen to the buta-1,3-diene was responsible for but-1-ene formation, 1:4 addition of hydrogen to buta-1,3-diene, rather than the isomerisation of but-1-ene, was responsible for the production of *trans*-but-2-ene and *cis*-but-2-ene. The initial formation of n-butane was predominantly by a direct route from adsorbed buta-1,3-diene not involving the intermediate formation of butene.

The effect of sulphur poisoning on the selectivity of mono-olefin formation from acetylene and buta-1,3-diene hydrogenation was found to be beneficial using the alumina-supported catalysts, but detrimental when the silica-supported catalysts were used. These results are interpreted in terms of a site blocking mechanism.

The physical characterisation of EUROPT-1 and EUROPT-3 by TPR, TEM and SEM techniques has showed that, although the catalysts were resistant to sintering under H_2, C_2H_2/H_2 or heating at 250°C/H_2 for extended periods of time, deactivation by C_4H_6/H_2 induced changes to both the particle size and shape.

SECTION ONE

INTRODUCTORY

CHAPTER ONE

INTRODUCTION

1.1 Historical Background

The word "Catalysis" originally came from the two Greek words Cata and Lysin meaning to break-down. J.J. Berzelius (1) in 1836 first used the word catalysis to describe some observations of events which occurred on both homogeneous and heterogeneous catalytic actions. He concluded "It is then proved that several simple and compound bodies soluble and insoluble, have the property of exercising on other bodies an action very different from chemical affinity.....and I will therefore call this force the catalytic force and I will call catalysis the decomposition of bodies by this force".

Although the phenomena of catalytic activity was recognised by many workers at that time, H. Davy (2) in 1815 was the first to be particularly concerned with gas reactions on surfaces. He was asked to investigate the explosions in coal mines which were occurring too frequently at that time by the lights used in mines. He examined the combustion of a mixture of coal gas and air, using a safety-lamp in which a flame was surrounded by a cylinder of Pt gauze. When additional coal gas was introduced into the lamp, the flame went out but the platinum remained hot for many minutes. Davy wrote, "It was immediately obvious that oxygen and coal gas in contact with the hot wire combined without flame, and yet produced heat enough to preserve the wire ignited, and to keep up their own combustion". Davy was also

the first to recognise the phenomenon of catalyst poisoning when he noticed that coating the platinum wire with sulphur decreased its ability for ignition.

Since then, many studies have been made to try and understand the role behind the influence of solid substances on the rates of a chemical reaction and to develop catalytical processes of industrial importance.

The first heterogeneous catalytic process of industrial importance was introduced by P. Phillips in 1831, who used platinum to oxidize SO_2 to SO_3 in the production of H_2SO_4. In the following years other industrially important processes were developed, notably, the oxidation of ammonia on platinum gauze to form nitrogen oxide for the production of nitric acid, by W. Ostwald in 1901-1918; the synthesis of methanol from carbon monoxide and hydrogen in 1923; the synthesis of hydrocarbons from carbon monoxide and hydrogen using the Fischer-Tropsch Process in 1930 and the catalytic cracking of petroleum for fuels around 1937.

1.2 Adsorption of Molecules at Solid Surfaces

In heterogeneous catalysis the plane that separates two phases is known as a surface or an interface. When atoms or molecules come into contact with this interface the phenomenon is known as adsorption. This process mainly arises from the additional available valence bonds at the surface. For example, if we consider a crystal of a covalent solid (Figure 1a), each atom at the surface exists in an unusual situation with

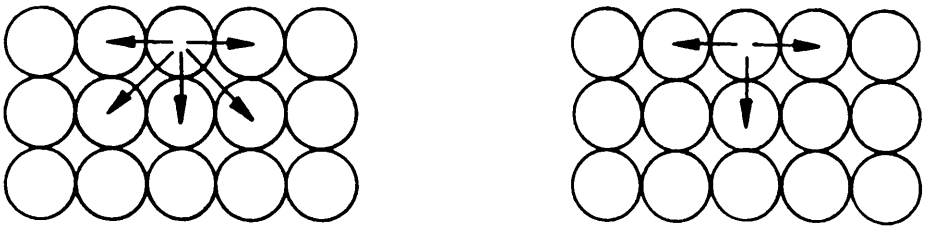

(a) (b)

Figure 1

respect to the bulk atoms in terms of its neighbouring atoms and its coordination number. Consequently, each surface atom possesses one or more free valencies which depends on the nature of the bonding between the atoms in the bulk solid. This in turn gives rise to an imbalance of forces at the surface with a net force acting inwards on the bulk atoms, which is identical to the phenomenon of surface tension in liquids. A similar situation occurs with ionic solids (Figure 1b).

Since the adsorption causes a reduction in the freedom of the molecules, the adsorption process is expected in most cases to be an exothermic process.

In heterogeneous catalysis, two types of adsorption phenomena have been recognised for many years - physical adsorption "physisorption", and chemical adsorption "chemisorption". The former involves van der Waals' attraction forces such as dipole-dipole and induced dipole interactions between an atom or a molecule and the surface, and is analogous in its character to a condensation of vapour molecules on to liquids, whereas the latter type of adsorption involves chemical bonding which is similar in its character to a chemical reaction and involves transfer of electrons between the adsorbent (solid) and the adsorbate (adsorbing species).

In terms of potential energy curves, the two adsorptions can be distinguished, as shown in Figure 2. At zero potential energy molecules are far from the surface. As the molecule reaches the surface, energy is liberated, accompanied with a fall in the potential energy. In the case of physical adsorption (curve A), the heat of adsorption (ΔH_a) is small, ~ 10 kJ mol^{-1}, at a distance of approximately 6Å from the surface, which corresponds to the adsorbate-adsorbent van der Waals' envelopes (Figure 3a).

The process of chemical adsorption is represented by curve B (Figure 2). At D_{XX} the adsorbate molecule is infinitely far from the surface with a potential energy corresponding to the X-X bond dissociation energy. As the molecule approaches the surface and dissociates, the pair of atoms undergo stabilization by the formation of chemisorption bonds and, as a result, the potential energy falls to a minimum at a distance of ca. 3Å from the surface, which is the sum of the covalent radii of the adsorbent and the adsorbate atoms (Figure 3c). The heat of chemisorption (ΔH_b) varies between 80 and 800 kJ mol^{-1}, depending on the surface coverage. However, it is important to note that the physically adsorbed molecule can undergo chemisorption if an energy of $E + (-\Delta H_b)$ is supplied to the system, as shown in Figure 2.

1.3 Adsorption Isotherms

The relationship between the quantity of gas adsorbed and the pressure with which it is in equilibrium at constant temperature is known as the adsorption isotherm. The first mathematical derivation which correlates the fractional surface coverage and pressure was

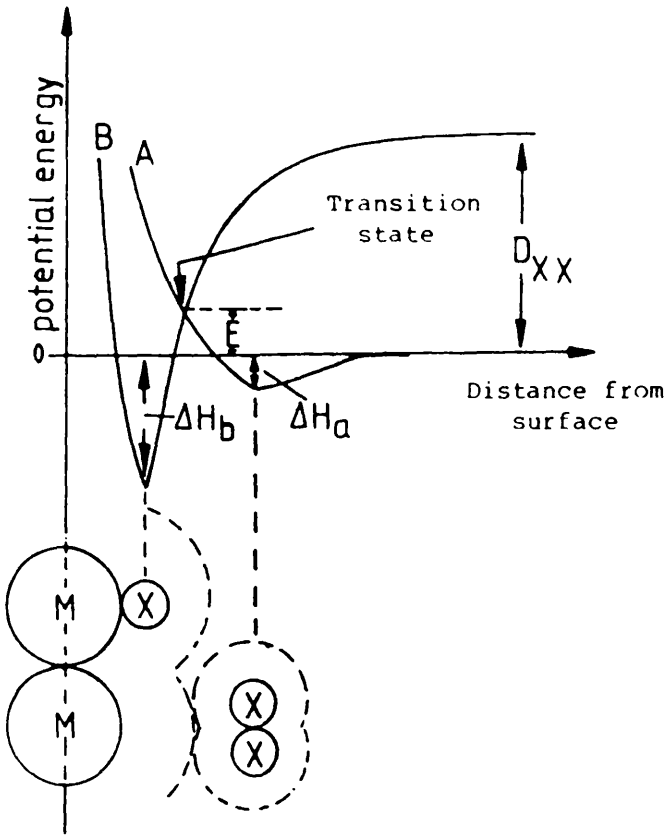

Figure 2. Potential energy curves for physical and chemical adsorptions.

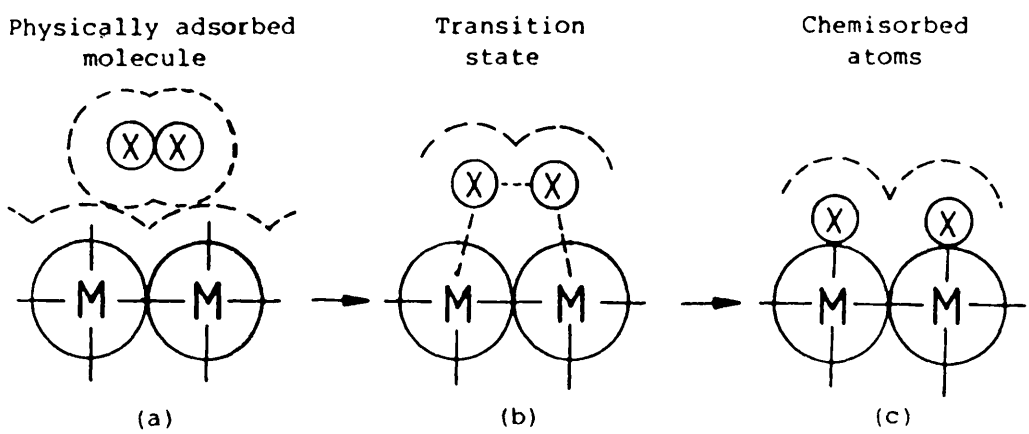

Figure 3. Physical and chemical adsorbed states.

developed by Irving Langmuir in 1916 (3) and has the form

$$\theta = \frac{bp}{1 + bp}$$

where θ = the fractional surface coverage with adsorbed atoms or molecules

p = the gas pressure

b = the adsorption coefficient of the adsorbate system which can be expressed in the form $b = A.e^{-\Delta H_a/RT}$ where $-\Delta H_a$ is the heat of adsorption, A is a constant, R is the standard gas constant and T is the temperature of the system.

The derivation of Langmuir is based on the following assumptions:

(i) the adsorbed species are held on to definite sites on the surface, i.e. the maximum adsorption corresponds to monolayer coverage,

(ii) the surface is energetically uniform, i.e. there is the same sticking probability of adsorption on all sites and the heat of adsorption is independent of surface coverage.

Although the Langmuir approach has been applied in heterogeneous surfaces, experimentally, few chemisorption isotherms correspond to the Langmuir equation and the major problem is that the heat of adsorption is found to decrease with surface coverage (4), which is

contrary to the second assumption. The phenomenon of decrease in heat of adsorption with surface coverage has been interpreted by De Boer (5) and Bond (6) and attributed to one or more of the following:

(i) the existence of repulsion forces between the adjacently adsorbed molecules

(ii) the heterogeneous character of the surface,

(iii) the existence of more than one type of bonding between the adsorbed molecules and surface,

Other isotherms have been devised by Freundlich (7) and Temkin (8) to eliminate the assumption of energetic equivalence of Langmuir. The Freundlich isotherm may be written in the form:

$$\Theta = k\, p^{1/n} \qquad k,n = \text{constants } (n > 1).$$

This isotherm, however, does not give any limit to the amount of adsorption Θ, as the gas pressure increases, and hence, considered by many scientists to be unrealistic. The Temkin isotherm is of the formula:

$$\Theta = \frac{RT}{\Delta H_o \alpha} \ln (b_o\, p)$$

where ΔH_o is the heat of adsorption at zero coverage and proportional to $e^{-\Delta H_o/RT}$ and α is a constant ranging between 0 and 1.

It is important to note that the Temkin isotherm is applicable if the drop in energy is caused by repulsive forces on heterogeneous surfaces.

Although the above derivations can be applied to chemisorption, Brunauer et al. (9) developed and specified five types of physical adsorption isotherms (Figure 4). Type I is known as the Langmuir isotherm and is commonly assigned for solids with very fine pores, such as silica gel and zeolites (10). The plateau region represents complete filling of the micro pores by the condensed gas. Type II isotherm is commonly encountered on non-porous solids, such as zinc oxide and titania and permits calculation of the monolayer capacity which in turn gives an estimate for the surface area of the solid by using the Brunauer, Emmet and Teller (BET) equation (9)

$$\frac{P}{V(P_o-P)} = \frac{1}{V_m c} + \frac{c-1}{Vm^c} \cdot \frac{P}{P_o}$$

where V is the volume of the gas adsorbed; V_m is the volume required to cover the adsorbent surface with a monolayer of adsorbate; P_o is the saturation vapour pressure of the adsorbate; c is a constant given by $c = e^{H_a - H_2/RT}$ where, H_a is the heat of adsorption in the first layer, and H_2 is the heat liberated on forming the subsequent layers. Point "B" corresponds to the stage at which monolayer coverage is completed. Type III and V isotherms show a complex behaviour over the entire pressure range and do not exhibit a point B. However, such isotherms are rare and their behaviour suggests that the adsorbent-adsorbate interactions are very weak and a multilayer build-up occurs, whereas the first layer is complete. Isotherms of type IV are of great interest and are mainly encountered with porous solids, such as glass and alumina (10). This isotherm shows similar behaviour to that of

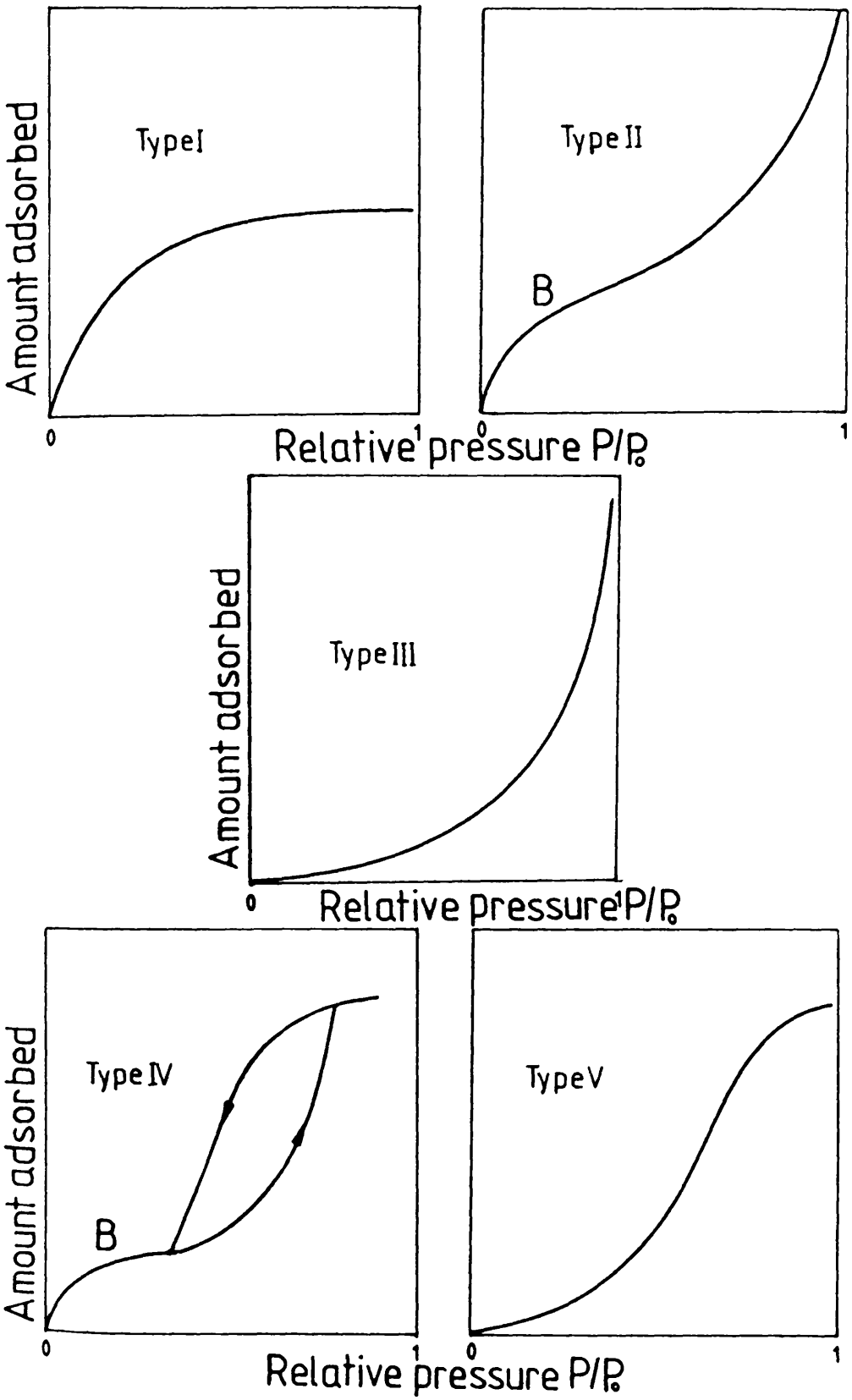

Figure 4. The five types of isotherms as classified by Brunauer et al. (9).

type II at low values of P/P_o. The adsorption increases markedly at higher P/P_o values where pore condensation takes place. The other feature from this isotherm is that, on desorption, the isotherm does not follow the same path of adsorption. This has been explained as being due to the existence of highly curved pores in which, on desorption, molecules undergo an evaporation-recondensation cycle.

1.4 Supported Metal Catalysts

Supported metal catalysts are of particular interest for reactions involving hydrogen, such as, hydrogenation, dehydrogenation and hydrogenolysis. The most commonly used and efficient catalysts for such reactions are the group VIII metals dispersed on a variety of support materials, such as, silica, alumina or titania, which have been considered as being catalytically inactive and not undergoing interactions with the metal. However, during the last two decades or so, there is a growing body of information in the catalytic literature (11) which stresses that this view is too simplistic and incorrect and carriers might indeed play a significant role in determining catalyst activities. Some of the publications dealing with what is referred to as Strong Metal Support Interactions (SMSI) will be reviewed later in this section.

The choice of the support is usually governed by the purpose for which the catalyst is to be used. For example, supports of low surface areas $< 1\ m^2\ g^{-1}$, such as, ground glass and silica, are commonly used when the metal is extremely active, whereas high surface area carriers $> 1\ m^2\ g^{-1}$, such as, alumina and asbestos, are usually

used when a higher selective activity and stability are required (12). This variation in surface area and also porosity of the support can play an important role in creating small metal particles, controlling their distribution and location within the support granules which, in turn, determine the catalyst's effectiveness. This shows the importance of the physical effects of the support.

Three types of process are generally used in making supported metal catalysts, namely, deposition, co-precipitation and impregnation. The latter method is the most commonly used and involves soaking the carrier material with an aqueous solution of the metal salt. The resultant slurry is evaporated in a steam-bath before finally being dried in a hot air oven. The catalyst material is then reduced in a flow of hydrogen at ~ 100°C. However, the recent advances made in the design and preparation of supported metal catalysts (12) showed that variations in the recipes of these preparation methods and pre-treatment conditions can also have a considerable impact on the catalyst activity and selectivity.

Despite the complexity involved in understanding the physics and chemistry of supported metal catalysts, they do have very attractive advantages, such as, high surface area per unit weight of the metal, greater stability to heat, poisoning and sintering, and can be easily regenerated after use. For these reasons, supported catalysts have found diverse applications in the chemical industry.

As stated above, the belief that the function of carrier materials in supported catalysts is purely physical, that is, to disperse and to retard its sintering, is under reconsideration, and is the subject of a fascinating dispute. Bond and Burch (11) have comprehensively

reviewed this subject and have considered the possible factors which could contribute to the existence of the so-called Strong Metal-Support Interaction (SMSI).

Historically, the phenomenon of SMSI was recognised in 1964 by Taylor and his colleagues (13) who observed an apparent variation in the catalytic activity as the support material was varied or changed. They suggested that the effect was electronic in its nature. Schwab (14), in 1966, produced the first convincing evidence for the transfer of electrons from the support to the metal. In the oxidation of CO and HCOOH decomposition over various catalysts, this effect altered significantly the activation energy of these reactions. Similar observations were also reported at that time by Solymosi and co-workers (15). Since then this idea was widely used as one form of explanation of the peculiar effects observed in the field of heterogeneous catalysis.

Tauster and co-workers (16,17), in 1978, reported what could be the basis of a real SMSI. Their results showed that, after reduction at elevated temperatures ~ 500°C, Group VIII metals supported on transition metal oxides, such as TiO_2, lost the ability to adsorb H_2 or CO. Though contamination by many means or as a result of some other factors, such as sintering, could suppress the extent of chemisorption of adsorbate molecules such as H_2 and CO, the results of Tauster et al. (16,17) are now generally accepted as conclusive evidence for the existence of SMSI.

Despite the vast number of investigators who have examined this phenomenon, the nature of the SMSI effect is not yet understood with any certainty. The information reported in the literature suggests

two approaches by which the support may affect the characteristics of the metal particles for chemisorption and catalysis and hence stimulate SMSI.

One of these approaches is based on the view that the metal and the support may interact together under the reduction conditions to form an intermetallic compound:

$$TO_2 + 2H_2 + 3M \longrightarrow M_3T + 2H_2O$$

TO_2 = Transition and non-transition metal oxides

M = Group VIII metals

Meschter and Worrell (18) have investigated the thermodyamics of the formation of such interactions using Pt/TiO_2. The standard free energy of formation, ΔH_f, of Pt_3Ti at 500°C was measured and found to be -75.5 k cal mol^{-1}. Denotter and Dautzenberg (19) reported the formation of $PtAl_3$ when Pt/Al_2O_3 was heated in H_2 above 497°C. Similarly, the alloy, $PtAl_3$ was suggested to form by Sprys and Mencik (20) in their TEM study of the interaction of Pt with γ-alumina. More recently, Martin et al. (21) have also demonstrated the formation of Ni-Si in Ni/SiO_2 and Pt-Si in Pt/SiO_2 catalyst systems, when these were reduced in H_2 at 500°C. Thus, interactions between the noble metals and the metals of Group 4B and 5B in this form are possible and even thermodynamically feasible under catalyst reduction conditions.

Another possible kind of interaction, this time involving the formation of metal-metal bonds between the cation of the support metal and the noble atoms (or cations), has been proposed. This possibility

came from the work of Dickinson et al. (22), who showed that in a class of oxides of the general formula

$$Ba\ M_{1/3}\ Ti_{2/3}\ O_3{}^{-x} \quad , \quad x \neq 0$$

where M = Group VIII metals

$Ti_{2/3}\ O_3{}^{-x}$ = Titania

the donor cations which stabilize this complex were those of Group VIII metals (Pt, Ir, Rh, Ru, Co, Fe). These authors suggested that one in every two metal oxide cations which acted as a host was metal-metal bonded to a donor ion. The state of the metal in the reduced supported catalysts is either a zero valent, slightly ionic atom or, more probably, aggregates of metal atoms. Therefore, the possibility of interaction between the d-electrons of these aggregates and the d-electrons of the metal oxide cations that lie at the surface should not be excluded as a dominant factor in SMSI. The formation of such complexes has been reported for Pt/Al_2O_3 ($Pt\text{-}Al_2O_x$) (23). However, as mentioned above, there is some contention in the literature that encapsulation or contamination of the metal particles by sub-oxide ions from the support formed during reduction at temperatures of ca. 500°C could be the cause of the inhibition of CO and H_2 chemisorption. For example, Huizinga and Prins (24), from their e.s.r. measurements on Pt/TiO_2, postulated that reduction of the catalyst in H_2 at 300°C and 500°C created O^{2-} vacancies with the formation of 0.3% Ti^{3+} ions. These species in the presence of H_2 are converted into OH^- ions:

$$Ti^{4+} + H + O^{2-} \rightleftharpoons Ti^{3+} + OH^{-} \quad \text{at } 300°C$$

$$2Ti^{4+} + 2H + 2O^{2-} \rightleftharpoons 2Ti^{3+} + 2OH^{-} \quad \text{at } 500°C$$

$$\rightleftharpoons 2Ti^{3+} + O^{2-} + H_2O$$

The OH^- ions have been suggested to migrate to the metal surface and consequently suppress the adsorption. Similar mechanisms have been suggested to account for Rh/TiO_2 (25), Ni/SiO_2 (26) and Pt supported on Al_2O_3, MgO and SiO_2 (27).

Another process which could account for SMSI is electronic in its nature. Katzer et al. (28) using EXAFS, observed an electron transfer to Rh from TiO_2 when a Rh/TiO_2 catalyst was reduced at 200°C. They also observed a large transfer of electrons to the support in Pt/Al_2O_3 compared to Pt/TiO_2. Similarly, Bouman and Biloen (29), from their XPS studies on calcined and reduced Pt/Al_2O_3, suggested that Pt was present in an electron deficient state, even after hydrogen treatment at 650°C, which was an indication of electron transfer towards the support. These results, however, place some doubt on the importance of electron transfer in the context of SMSI. An increase in the electron density on the transition metal atom should increase the strength of the M-CO bond with the result that adsorption should be enhanced, and not the reverse, as the study of Katzer et al. (28) showed.

1.5 The Adsorption of Unsaturated Hydrocarbons at Pt Surfaces

Although the chemical nature of the adsorbed species at metal surfaces has been the subject of debate for more than four decades, since the pioneering work of Horiuti and Polanyi (30), it can be said with confidence that, so far, these studies have not yet brought about a clear and unambiguous picture of the adsorbed states of even the most simple molecules, such as, acetylene and ethylene at these surfaces.

Knowledge concerning the adsorbed states of olefins and di-olefins has been obtained in part from the application of the recent direct instrumental methods developed by surface physicists, such as, AES, LEED, XPS, etc. (see section 1.10), which have been mainly concentrated on the adsorption of ethylene and acetylene on single crystals. However, the application of the results of these methods to interpret catalytic processes is not straightforward. This is due to the fact that most of these studies are carried out over clean surfaces (generally without hydrogen), under ultra-high vacuum conditions, and usually at low temperatures, whereas catalytic reactions take place on surfaces covered with adsorbed species and under several pressures of reactant gases at ambient or elevated temperatures. The other source of information regarding the adsorbed states of unsaturated hydrocarbons comes indirectly from the kinetics and product distributions of various processes such as hydrogenation, deuterium exchange and isomerisation of these compounds.

1.5.1 Adsorbed States of Ethylene

The adsorption of olefins on metal films and on supported metals was first reviewed by Bond in 1962 (6), Bond and Wells in 1964 (31) and, more recently, Webb (32) and Thomson (33). From these reviews, various states of ethylene adsorptions have been proposed and these are presented in the formulae a-j:

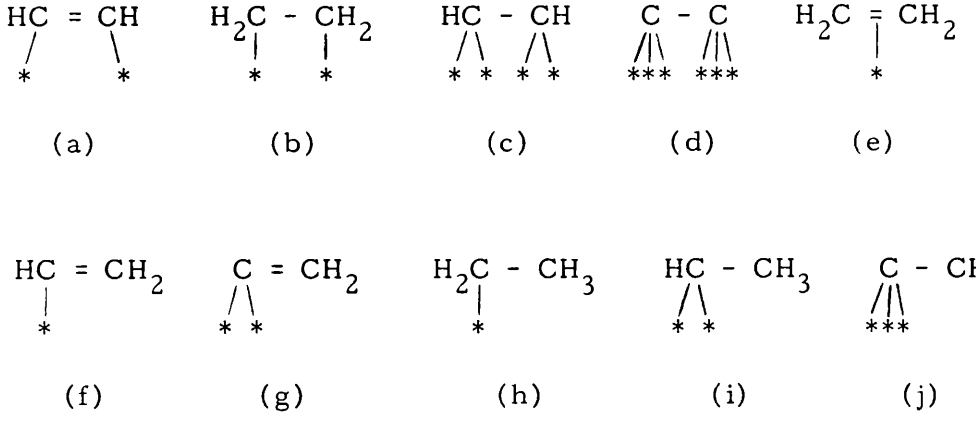

(a) (b) (c) (d) (e)

(f) (g) (h) (i) (j)

The presence of any of these adsorbed species on any particular metal surface is the subject of the literature data reported by many investigators. Following the early proposals of Horiuti and Polanyi (30) and Bond (6) that ethylene was adsorbed associatively as a di-σ-adsorbed species (structures a,b) by the rehybridization of its carbon atoms ($sp^2 \rightarrow sp^3$) followed by the formation of two σ-bonds between the carbons and two metal atoms at a suitable distance apart, or a π-adsorbed species (structure e) to one metal atom with the carbon atoms retaining their sp^2 hybridization, detailed studies (34-36) using LEED, ELS, UPS and TPD techniques have been reported regarding C_2H_4 adsorption on Pt(111) surface. The results of these studies can be summarized as

follows: below room temperature, the adsorption occurred reversibly in an associative form (structures a,b,c); this structure underwent irreversible dissociative adsorption (structures f-j) at room temperature and accompanied by self hydrogenation to ethane. Recent studies by Somorjai and co-workers (37-39) stressed the formation of a strongly adsorbed stable ethylidyne species (structure j) at room temperature, in which the C-C bond was perpendicular to the surface, with the species depicted in structures f, g, i acting as intermediates. They also suggested that ethylene hydrogenation took place on the top of these carbonaceous fragments, rather than on a clean metallic surface.

Infrared (IR) spectroscopy has been a widely used technique for investigating the adsorption of hydrocarbons on supported metal catalysts. In a recent study, Sheppard and co-workers (40), using an extremely sensitive infrared interferometry technique, have obtained evidence for the existence of both a di-σ-bonded (structure b) and a π-bonded (structure e) species when ethylene was chemisorbed on a hydrogen precovered silica-supported Pt catalysts. The former species gave bands at 2885 cm^{-1} and 2800 cm^{-1} while the latter produced bands at 3000 cm^{-1} and 1500 cm^{-1}. These workers claimed that, although both species were easily hydrogenated, the π-complex was the more reactive.

Thomson, Webb and their colleagues (41-44) using radiotracer techniques have made detailed studies of the adsorption of [14-C]-ethylene and its reaction with hydrogen on pure metals and supported catalysts. From these investigations it was observed that only a fraction of the initially adsorbed ethylene could be removed either by molecular exchange with non-radioactive ethylene, by evacuation, or

during the subsequent hydrogenation of ethylene-hydrogen mixtures. While the adsorptive capacity of the catalysts increased in the order Pd > Pt > Ir > Ru > Rh > Ni, the percentage of the initially adsorbed ethylene retained by the surface decreased in the order Pd > Ru > Ni > Rh > Ir > Pt. It was also demonstrated from these studies that as the temperature of the system was raised in presence of H_2, quantities of lower hydrocarbons (methane) were formed. These workers have suggested that the retained species in ethylene adsorption arises from the formation of multiply bonded hydrogen-deficient surface complexes (structures a,c,d,g) and one or more of the dissociative species (structures h,i, or j) may play a role as the hydrogen transfer media in hydrogenation reactions.

1.5.2 Adsorbed States of Acetylene

Acetylene is extremely important in preparative organic chemistry. Through the relatively simple alkylation of acetylene, it is possible to form new carbon-carbon bonds while the triple bond is retained. The resulting alkylacetylenes participate in numerous transformations involving addition reactions. One such reaction is the selective hydrogenation of the triple bond to yield cis-alkenes (6,45).

The early studies of acetylene adsorption on metal surfaces have been reviewed by Bond and Wells (31), and those studies published up to 1977 have been reviewed by Thomson (33) and Webb (32,45). The findings of these studies on adsorption and hydrogenation of acetylene on various metal surfaces including Pt, led to the postulation of the adsorbed species presented below.

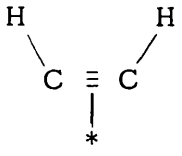

(k)

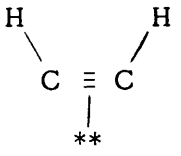

(l)

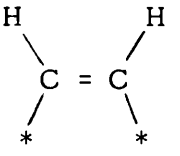

(m)

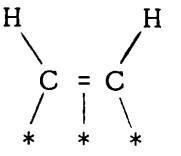

(n)

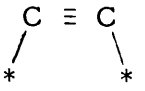

(o)

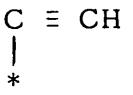

(p)

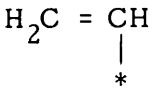

(q)

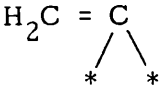

(r)

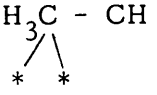

(s)

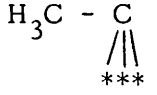

(t)

From the studies of the adsorption and hydrogenation of acetylene at various metal catalysts, it has been suggested (46) that the adsorbate forms two σ-bonds with two surface metal atoms to give a structure which is ethylene-like (structure m). However, as was the case for the adsorbed state of ethylene (section 1.5.1), an alternative structure has been proposed in which acetylene is π-bonded to the surface (structure l). This means that each π-electron system of the triple bond interacts with a metal atom, so that two atoms in the surface constitute a site for acetylene adsorption.

Although a reasonable agreement amongst the surface physicists exists regarding the adsorption of acetylene on a Pt(111) surface at low temperature (~-70°C), in which the π-bonded complex (structure k) has been postulated (47-49), several different species have been proposed at room and higher temperatures. For example, Fisher et al. (50), from their ESCA study and measurements of work function changes recorded during acetylene adsorption on Pt(111) at 55°C, pointed to the existence of adsorbed states similar to those of structures (k,m,o).

The authors attributed the decrease in the work function accompanying acetylene adsorption to the charge transfer from the adsorbed molecules the the metal atoms.

Studies using the UPS technique (34,35,48,49) have indicated that the simple π-complex (structure k) which was favoured at low temperature on a Pt(111) surface, transformed to the σ-complex (structure m) at room temperature. Although there was no dissociation of acetylene encountered on the Pt(111) surface at room temperature, fragmentation to CH and CH_2 species was reported to occur on Ni(111), Ni(110), Re(100) and W(111) (34,35).

LEED has also been used by Kesmodel et al. (51) to investigate the adsorption of acetylene on Pt(111) in the temperature range 27°-127°C. From the LEED profiles, these authors concluded that the adsorbed acetylene molecule was located at a site above the centre of a triangle of Pt atoms (structure t) at a vertical distance of 1.95Å from the top of the Pt layer. They also concluded that the structures r and s are most unlikely species and suggested that the hydrogenation of acetylene occurred over the primary adsorbed layer.

Sheppard and Ward (52) have obtained infrared spectra of acetylene adsorbed on silica-supported Pt catalysts. These spectra showed bands attributable to the olefinic species (structure m) and to surface alkyl groups. Addition of H_2 to the C_2H_2 precovered surface resulted in an intensification of the spectra and the appearance of new bands corresponding to surface alkyl groups of structure $CH_3(CH_2)_3$. These authors concluded that polymerisation occurred before hydrogenation via partially hydrogenated species (structures m,q). Addition of

a premixed sample of acetylene and hydrogen, in the ratio of 1:1, to a clean catalyst, resulted in no detectable formation of ethylene or ethane. Randhava and Rehmat (53) from their IR study of adsorbed acetylene on Pt/Al_2O_3 at room temperature have also proposed the adsorbed species shown (structures m and 4), which produced an intense band at 1690 cm^{-1}.

In a recent NMR study of C_2H_2 + Pt/alumina at ~ 25°C, Wang et al. (54) proposed a model involving a mixture of species which resemble those of structures (m) and (r).

The existence of several adsorbed states of acetylene on supported platinum group metals has been demonstrated in [14-C]radiotracer studies by Webb and co-workers (42,55-57). These studies showed the co-existence of at least two adsorbed states, one of which was retained on the surface, the other which was reactive and underwent molecular exchange and reaction with hydrogen. In comparison with their results of ethylene adsorption (41,42) these investigators claimed that the extent of adsorption and retention was substantially greater with acetylene than with ethylene. The conclusions reached were that the adsorbed states of acetylene which participated in retention and hydrogenation were different and that the sites for acetylene adsorption were distinctly different from those involved in ethylene adsorption. It is important to note that there is a growing body of evidence in the literature emphasising that the adsorption of acetylene is always accompanied by deposition of carbon leading to the formation of surface carbide (31,47-49). These carbonaceous species have been suggested by many workers (36-39) to have an important

role as a source of sites in hydrogenation reactions. Indeed, the recent studies by Webb and co-workers (56-59) have demonstrated the phenomena of hydrocarbonaceous overlayer formation. Their results for the adsorption of [14-C]acetylene and [14-C]ethylene on Group VIII metals, supported on silica and alumina at room temperature, have shown that these adsorptions occurred in two distinct regions, a non-linear primary region and a secondary linear region. The primary region on each catalyst was suggested to correspond to mono-layer coverage and characteristic of a self-hydrogenation process and the secondary region was related to the formation of a secondary layer in which hydrogenation reactions occur.

1.5.3 Adsorbed States of Butenes and Butadienes

By comparison with the number of studies relating to ethylene and acetylene adsorption on metal surfaces, much less work has been reported on higher alkenes and alkadienes. Hence, information regarding the adsorbed states of this class of molecules has been deduced from the reactions that they undergo (31). From the studies of the hydrogenation of propadiene (60), buta-1,2-diene, buta-1,3-diene (43,44) and higher conjugated dienes (45), it has been confirmed that these hydrocarbons are more strongly adsorbed than the mono-olefins formed by their hydrogenation. Therefore, the strong adsorption of buta-1,3-diene relative to but-1-ene may suggest that both the olefinic linkages interact with the surface. By analogy with the adsorbed states of ethylene and acetylene (sections 1.5.1, 1.5.1), the two possible structures of the adsorbed buta-1,3-diene can be depicted as the structures,

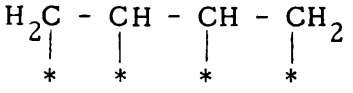

(u)

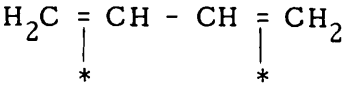

(v)

Structure (u) represents a strongly adsorbed molecule containing four carbon-metal σ-bonds, one from each of the four carbon atoms which exhibit sp^3 hybridization. However, due to the fact that surfaces are inhomogeneous from geometrical considerations and due to the induced internal strain within the carbon atoms, adsorbed species in this form would be unstable and hence is unlikely. Structure (v) requires two π-bonds between the olefinic linkages of the butadiene and the surface. Since the sp^2 hybridization of the free molecule is not likely to be greatly disturbed by the interaction with the surface, little strain will be present in the adsorbate. Most of the studies on buta-1,3-diene hydrogenation (60-64) have shown that all three isomers (but-1-ene, trans-but-2-ene, cis but-2-ene) were formed. This again reinforces the idea that buta-1,3-diene must have been adsorbed in a way similar to structure (v) with the molecule undergoing conformational interconversion to yield the isomeric hydrocarbons. The relative proportions of these conformations (structures w and x) determines the ratio of the isomeric butenes. Addition of a hydrogen to each of the terminal

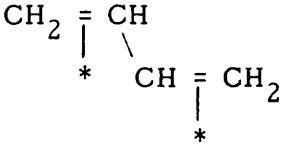

anti (w)

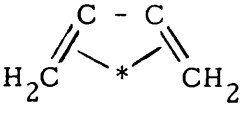

syn (x))

carbon atoms of the anti-buta-1,3-diene (structure w) is expected to give trans-but-2-ene, whereas addition of hydrogen to the adsorbed syn-conformation (structure x) will produce cis-but-2-ene. It should be noted, however, that there is, as yet, no direct evidence for these structures (u, v, w and x). Such structures were used as a basis for the proposed mechanisms of buta-1,3-diene hydrogenation on Group VIII metals in the earliest studies by the group at Hull University (60-64) and subsequently reported.

Traditional infrared spectroscopy has played a major role in the study of the adsorbed states of the dienes compounds on various supported metal catalysts. For example, Avery (65) has found when buta-1,3-diene was adsorbed at 20°C on a clean Pd/SiO_2 surface, no IR spectrum was observed. Subsequent addition of hydrogen yielded an intense spectrum containing bands similar to those observed in the adsorption of mono-olefins on hydrogen-covered surfaces (2960 cm^{-1}, 2912 cm^{-1}, 2874 cm^{-1} and 2855 cm^{-1}). It was also observed that subsequent heating of the adsorbed species in the presence of H_2 to 300°C did not remove the adsorbed hydrocarbons. These observations were interpreted in terms of the formation of C_{4n} species which were multiply bonded to the surface. Similar observations were made on linear and branched higher olefins. Eischens and Pliskin (66), in their early investigation of the adsorption of isomeric-butenes, pentenes and hexenes at 35°C on Ni/SiO_2 precovered with H_2, discovered species adsorbed to the surface via three or more carbon atoms with a structure of the type $-\underset{*}{\underset{|}{CH}}-$ or $-\underset{*}{\underset{|}{CH}}CH_2$ with the adsorbed species being suggested

to be independent of the position of the C=C double bond in the starting olefin. If hydrogen was admitted to the surface following the adsorption, surface 1-alkyl radicals of the type $-\underset{*}{CH_2}(CH_2)_nCH_3$ were predominantly formed. However, IR studies of the adsorption of propene, trans-but-2-ene and 1-pentene on Pt/SiO_2 and Ir/SiO_2 (67) demonstrated the existence of both π-bonded $C\underset{*}{=}C$ and σ-bonded $-\underset{*}{C}-\underset{*}{C}-$ species, and surface alkyl groups were formed by the action of H_2.

There is IR evidence that, of the dienes examined, allene formed the surface species $H_2=\underset{*}{C}-\underset{*}{CH_2}$ on Group VIII metals (68).

$$CH_2 = CH - CH = CH_2 \qquad CH_2 = CH - \underset{*}{CH} - CH_3$$

(y) (z)

The π-adsorbed species (structures x and y) were obtained from buta-1,3-diene adsorption at low temperatures, -80° to 0°C on Pd, Ni and Co supported on γ-alumina. These π-species were found to undergo transformation at room temperature to give di-σ-adsorbed species (structure z) (69).

From a study by LEED, the adsorption of cyclohexene and cyclo-1,3-hexadiene on Pt(111) surface at 20°C, π-adsorbed structures have been suggested. There was no adsorption on Au(111) surface under similar conditions (70). Very recently, Oudar et al. (71-73), using LEED and AES techniques have proposed that in the temperature range 27°-427°C and at low coverages (6×10^{-9} Torr), buta-1,3-diene adsorbs flat via the two olefinic linkages in the valleys of the Pt-(110)

and (100) surfaces (as structure w). As the pressure of the diene was increased (6×10^{-2} Torr), the molecule was adsorbed on the topmost layer of the Pt atoms as butadienyl or butylidyne species via one carbon atom only which can be represented as follows:

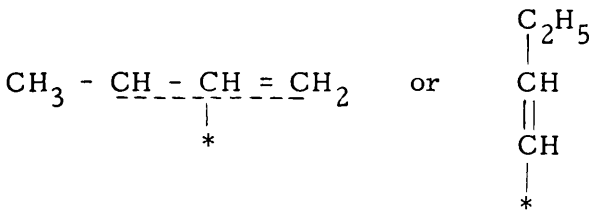

Comprehensive studies of the dependence of the adsorption states on metal structure have been made by Touroude, Gault and Ledoux (74-76), for Group VIII metals. Investigations of the isomerisation and exchange reactions of 1,2- and 2,3-diMe-cyclopentenes and of various straight and branched chain olefins have demonstrated that the transformations occurring via the olefins adsorbed in various ways proceed in parallel as competing reactions. The ratios of these transformations were found to depend on the metal used and its pretreatment procedure. These authors proved that it is possible to obtain a correlation between the various crystal faces and the different types of adsorption. Isomerisation reactions which took place via the associative mechanism occurred on the edge atoms, while the atoms on faces with high coordination numbers catalysed the direct cis-trans isomerisation via double bond migration (structure I) and π-alkyl complexes (structure II). The latter processes were always initiated by π-olefin adsorption.

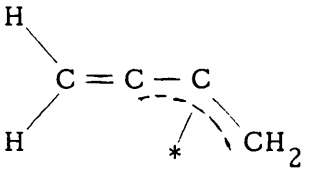

(I)

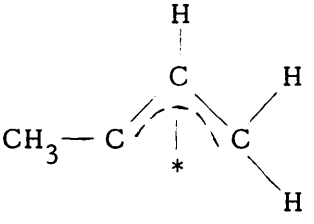

(II)

1.6 The Adsorption of Carbon Monoxide on Metal Surfaces

A wealth of work has been done in recent years to try to understand the interaction of carbon monoxide with metal surfaces. Primarily this is because CO chemisorption is an important step in various industrially important reactions, such as, methanol synthesis, the Fisher-Tropsch process and the formation of alcohols. Secondly, CO has been used widely as a probe for catalyst surface areas and as a test molecule to distinguish the active centres in the catalytic reactions.

The adsorption of carbon monoxide on transition metals has been the subject of a survey by Ford (77) and another review concerning the use of infrared spectroscopy in the studies of CO adsorption on supported Group VIII metals has been made by Sheppard and Nguyen (78). Indeed, much of the evidence for the nature of the adsorbed states of carbon monoxide on metal surfaces has come from infrared spectroscopic studies, though the recently established techniques such as, LEED, TPD, and AES, have been employed in the past few years and have yielded useful information which will inevitably enable the understanding of the CO-metal interactions to be improved.

The current knowledge of the spectroscopy of adsorbed molecules on catalyst systems originated from the pioneering work of

Eischens and his co-workers (79,80) and was based on the data of organometallic chemistry. The C-O streching frequency of gaseous CO is at 2143 cm^{-1} and this band was observed to shift to between 2000 cm^{-1} and 2100 cm^{-1} after monodentate ligand formation with transition-metal compounds of Ni, Fe, Co, Mn and Re. The formation of bi-dentate ligands caused a greater shift in frequency to below 2000 cm^{-1}. In view of this analogy, Eischens et al. (79) attributed the bands at above 2000 cm^{-1} to a "linear" CO group on the surface (Type A) and those below

Type A

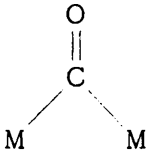

Type B

2000 cm^{-1} to a "bridged" CO species (Type B). However, although these assignments still find acceptance among surface scientists, there is uncertainty concerning the low frequency band. Blyholder (81) cautioned the interpretation of the low frequency band as being due to the bridged carbonyl form, pointing out that significant back-donation of electrons from the metal to the adsorbed carbon monoxide may disturb the linear forms. He also suggested that surface atoms at the edges and corners may be favourably positioned to produce such back donation. Other workers, however, ascribed the appearance of the low frequency band to changes in surface topography (82), sintering (83), support effect or O_2 contamination (84). In view of this, some care is required

in relating CO adsorption directly to the free-metal surface area.

The CO-Rh/Al_2O_3 system was studied by Yang and Garland (85), who suggested a species consisting of two linear CO molecules bonded to a single rhodium atom (Type C or D), which showed two peaks as doublets at 2095 and 2027 cm^{-1}

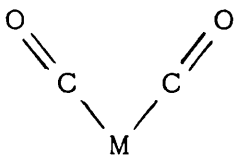

Type C

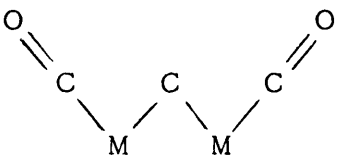

Type D

The single band which occurred at 2062 cm^{-1} was ascribed to a linear species with one CO per Rh atom (type A). Similar species were assigned for CO adsorption on Pd/SiO_2 (82) and Ni/SiO_2 (79) at room temperature. The IR spectra of carbon monoxide chemisorbed on Ru supported on both Al_2O_3 and SiO_2 was reported by Lynds (86). For the Ru/Al_2O_3 bands were observed at 2125 cm^{-1} and 2060 cm^{-1}, whereas for Ru/SiO_2 sample, bands occurred at 2151 cm^{-1} and 2083 cm^{-1}. In contrast, Ru/MgO showed only one strong band at 2030 cm^{-1} and has been characterised as due to multiple CO adsorption on one single Ru arom (Type C) (84). For CO adsorption on Ir, only one band has also been observed (86); this occurred at 2070 cm^{-1} when an alumina support was used and at 2074 cm^{-1} when a silica support sample was employed.

The infrared spectrum of carbon monoxide adsorbed on a platinum surface was first determined by Eischens et al. (79). Adsorption of CO on silica-supported Pt led to the appearance of only one adsorbed

species with a band at 2073 cm^{-1} (Type A). Adsorption on the alumina-supported sample gave rise to two bands at 2040 cm^{-1} and 1820 cm^{-1}.

Tanaka and White (87) reported the IR of the system CO-Pt/TiO_2. On a reduced catalyst (at 200°C), two types of linear species were observed and assigned to Pt-terrace sites (2094 cm^{-1}) and Pt-step sites (2077 cm^{-1}) with a band appearing at 1854 cm^{-1} which was attributed to the bridged species (Type B). When the catalyst was reduced at 400°C, the bridged and terrace species were remarkably reduced. On oxidized samples, the IR bands of these species were shifted to the high frequency region, terraces to 2130 cm^{-1}, steps to 2101 cm^{-1} and bridged to 1880 cm^{-1}. In addition, these authors have also observed weak bands at 2060 cm^{-1} and 1942 cm^{-1}, which were thought to be due to a dicarbonyl species (Type C). Similar assignments have been made by Haaland (88) on Pt/Al_2O_3. His IR spectrum showed three CO bands, 2094 cm^{-1} (linear-terraces), 2045 cm^{-1} (linear steps) and 1850 cm^{-1} (bridged CO). These bands were shifted ($\Delta\tilde{\nu} \sim 25$ cm^{-1}) to lower energy as the adsorption temperature was increased from 27° to 187°C. However, during temperature programmed desorption (TPD) of the adsorbed CO in the range 27°-527°C, the bridged (1850 cm^{-1}) band split into two bands. These bands were attributed to CO species adsorbed in 2-Pt (Type D) and 3-Pt (Types E, F or G) sites.

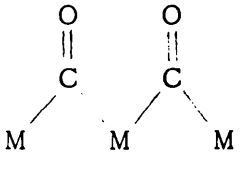

Type (E)

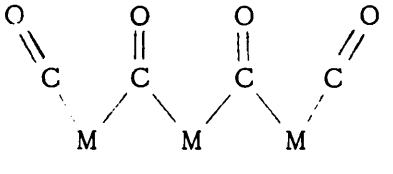

Type (F)

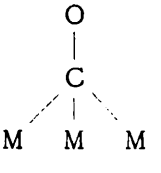

Type (G)

The above results, observed on supported catalysts, show a general agreement with the CO adsorption data obtained on Pt(111) single crystals. This indeed provides some assurance that observations made on single crystal surfaces at low pressures and temperatures are applicable to real catalysts under working conditions. For example, Hayden and Bradshaw (89), in a study using a combination of IR-reflection-absorption spectroscopy (IRAS), TPD and LEED techniques, confirmed the presence of both the linear (2094 cm^{-1} and 2040 cm^{-1}) and bridging (1840 cm^{-1} and 1857 cm^{-1}) adsorbed CO on a Pt(111) surface. The linear CO bands were insensitive to the adsorption temperature (-178 to 27°C). On the other hand, a pronounced grow-in to the bridging bands occurred as the temperature was increased. However, these bridging bands were pressure dependent and appeared only at $\Theta_{CO} > 0.33$, whereas the linear species developed at coverages as low as $\Theta_{CO} \sim 0.01$.

The adsorption of carbon monoxide on Pt(111) in the presence of alkali metal atoms, such as potassium, has been reported (90,91). The adsorption characteristics of CO enhanced considerably as the amount of K was increased ($\Delta H_{ads.}$ incr. from 104.7 to 150.5 kJ mol^{-1}). This effect was explained as being due to charge transfer from K to Pt and an increase in the back-donation from Pt to CO. Whilst dissociation to C and O has not been ruled out in these studies, it has been reported to occur on Al_2O_3 (92).

Although many papers have dealt with CO adsorption on supported Pt catalysts, the only study concerned with the measurements of heat of adsorption of this molecule on these surfaces has recently been

reported by Vannice et al. (93). The observed $\Delta H_{ads.}$ of carbon monoxide adsorption on Pt supported on SiO_2, SiO_2-Al_2O_3, Al_2O_3 and TiO_2 were in the range 87.8-133.8 kJ mol^{-1} at the adsorption temperature 27°C (reduction in H_2 at 450°C). In contrast, adsorption at -58°C gave values between 87.8 and 133.8 kJ mol^{-1}. The authors claimed that this variation in $\Delta H_{ads.}$ was a function of crystallite size; the bigger the crystallite, the higher $\Delta H_{ads.}$, with the weaker Pt-CO bond occurring as the Pt dispersion was increased.

Despite the fact that radiotracer techniques provide no information about the chemical identity of adsorbed species, nevertheless its sensitivity of detection can reveal the extent of adsorption and desorption for a molecule such as CO. For example, Thomson and co-workers (94), studied the interactions of [14-C]-carbon monoxide with Pt/Al_2O_3 and Pt/SiO_2. On both catalysts two forms of CO were identified, one was weakly adsorbed (~ 35%) removable by N_2 flashing, the other was strongly bound to the surface and could only be removed by thermal treatment at 210°C. The thermal desorption produced a mixture of CO_2 and CO with the ratio of the former to the latter being 7.07 for the alumina- and 0.70 for the silica-Pt catalysts. Webb and co-workers (56-59, 95-97) have used [14-C]-CO adsorption as a probe to distinguish between the active sites in acetylene (56-59), propylene (95) hydrogenations on Group VIII supported metals and in methanol synthesis reactions on $Cu/ZnO/Al_2O_3$ catalysts (96,97).

Finally, the ensuing paragraph is a summary of the findings reported by many workers (98) on CO adsorption on EUROPT-1 catalyst which is one of the catalysts explored in this study.

The adsorption of CO on EUROPT-1 at room temperature using the volumetric method in four laboratories employing various reduction, evacuation schedules and CO pressures, produced isotherms which showed that considerable adsorption occurred at low pressures with the high coverage being achieved at an equilibrium pressure of 1 Torr. The isotherms displayed positive gradients as the pressure was increased. Extrapolation of the isotherms to zero pressure yielded a value of 190 ± 10 μ mol CO g^{-1} which corresponded to 1.14 ± 0.06 x 10^{20} CO molecules g^{-1}. Each gram of EUROPT-1 contained 1.95 x 10^{20} Pt atoms, hence, the CO:Pt ratio was calculated to be 0.6:1.0. The IR spectra of adsorbed CO on H_2-depleted surface showed a strong band at 2070 cm^{-1} and two weak bands at 1854 cm^{-1} and 1715 cm^{-1} with the majority of chemisorbed CO present in the linear form.

1.7 The Adsorption of Hydrogen on Pt-Metal Surfaces

Despite the simplicity of the hydrogen molecule, H_2, and the vast number of studies reported in the literature, its interaction and fate on metal surfaces is far from understood (99).

The adsorption of H_2 on Pt surfaces has been reported to exist in different forms. For example, Tsuchinya et al. (100), using a temperature programmed desorption (TPD) technique, studied the chemisorption of H_2 on Pt-black in the temperature range -196°C to 397°C. Four peaks appeared in the TPD spectrum at -103°, -23°, 77° and 297°C and these have been designated by these authors as hydrogen adsorbed in the α, β, γ and σ states:

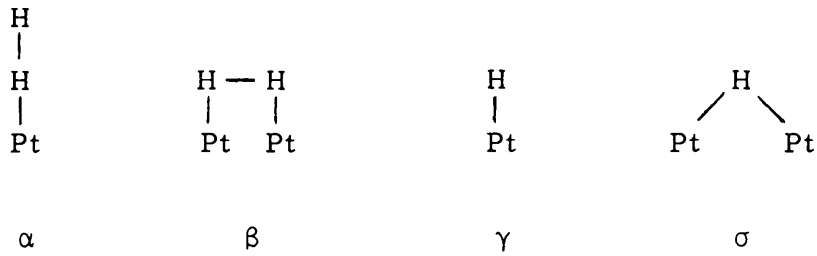

Nagy and co-workers (101) observed an additional hydrogen peak at 217°C which they called the ε-peak. They also found an inhibiting effect of the ε and γ hydrogen on the hydrogenation of the C=C double bond (cyclohexene, ethylene, but-1-ene). Pt-black catalysts containing the σ-hydrogen only hydrogenated olefins about six times more rapidly than those which contained any of the other H-forms of hydrogen. For Pt-films, Stephen et al. (102) found three states of hydrogen with desorption maxima at -153°, -73° and 75°C (called γ, β_1, β_2) and they evaluated their respective energies of adsorption ($\Delta H_{ads.}$) as 34, 50, 88 kJ mol^{-1}.

Candy and his colleagues (103) studied the adsorption and thermal desorption of H_2 on Pt/SiO_2 (EUROPT-1), Pt/Al_2O_3 and Pt/Y-zeolite. Two types of surface species could be formed on adsorption of H_2 (β_1, β_2) with TPD peaks appearing at 27° and 427°C, respectively. These authors proposed an on top (direct on Pt) adsorption for β_1 and interstitial (interatomic holes) adsorption for the β_2 state when hydrogen was adsorbed on the supported Pt catalysts at 627°C, which was attributed to Si-O-H-Pt or Al-O-H-Pt bridged species and showed a TPD signal at 477°-527°C. Menon and Froment (104,105) reported the TPD of H_2 from Pt/SiO_2, Pt/Al_2O_3 and Pt/TiO_2 catalysts reduced at 197°-497°C and cooled to 20°C. For samples reduced at 197°C, the desorption of H_2 was

complete by about 350°C, with the spectrum consisting of two overlapped peaks with their maxima at approximately 97° and 197°C. When the catalysts were reduced at 300°, 400°, and 500°C, these two peaks became smaller with simultaneous desorption of H_2 at higher temperature at about 497°C. This interestingly shows that the hydrogen adsorbed at the higher temperature of reduction can be desorbed only at higher temperature.

Konvalinka and co-workers (106,107) studied the TPD of hydrogen from supported and unsupported Pd, Ni, Ir and Pt catalysts. They identified three types of adsorbed hydrogens, named as "weak", "strong" and "very strong" chemisorptions. They also found that the heat of adsorption, $\Delta H_{ads.}$, of these types of hydrogen were close to each other for the different catalysts. The values of $\Delta H_{ads.}$ were found as approximately (19) weak, 25 (strong) and 30 kJ mol^{-1} (very strong). These authors concluded that catalytic differences between these metals should be ascribed mainly to differences in interaction with the substrates under hydrogenation conditions and not to differences in the hydrogen interaction with catalyst surfaces.

The adsorption of H_2 on Pt(111) at -123°C has been reported by Christmann et al. (108). It also gave rise to two adsorbed states, called β_1 and β_2 with a temperature of maximum desorption between -83° and -43°C for β_1 and 47°-67°C for β_2.

Paal and Thomson (109,110) utilized the radiotracer technique to examine the possibility of retention of H_2 by a Pt-black catalyst using tritium (^3H) as a tracer. Using gas proportional- and scintillation-counters, they were able to monitor the ^3H gas phase by the former and

and estimated the adsorption and retention by the latter counter. These authors results showed that tritium adsorption occurred at 20° and 360°C and its removal could be achieved either by exposure to air (96%), by vacuum (100%), or by exchange with non-radioactive H_2 at 360°C (98%). They also identified two classes of hydrogen on the surface, H_I, which was stable even at 360°C and which they proposed resembled both the γ and σ types of Tsuchiya et al. (100), and another form denoted as, H_{II}, which they suggested to correspond to absorbed hydrogen. Earlier, Thomson and colleagues (111) had investigated the retention of H_2 on Pt, Rh and Pd supported on Al_2O_3 catalysts, using ethylene as a test molecule. They found that the amount of reactive H_2 was distinguishable on these catalysts, in the order Pd $\approx$ Rd $>$ Pt, although the total amount of retained hydrogen was in the order Pt $\approx$ Rh $>$ Pd.

Lang et al. (112) demonstrated that on Pt(111) single crystals, H_2 could form sub-surface layers. The adsorbed hydrogen disappeared as the crystal was heated in vacuum. However, upon O_2 treatment, the H_2 species reappeared again on the surface. This cycle was reproducible several times.

Wells (113) studied the retention of hydrogen by Pt-black catalysts after their reduction in H_2. Using butene hydrogenation and H_2-D_2 exchange reactions as a titrant for the adsorbed H_2, it was found that a proportion of H_2 could be titrated rapidly, whereas the remainder exchanged over a length of time. Wells proposed that the latter type of hydrogen could be contained in microscopic and even sub-microscopic

cavities of the Pt-Crystallite structure. This phenomenon was termed Occlusion

The phenomenon of migration of chemisorbed H_2 atoms from the metal to its support is known as hydrogen spillover. For instance, Taylor et al. (42) studied tritium (H^3) retention by Rh, Pd and Pt supported on Al_2O_3. They found the ratio of H:Pt-surfaces to be 23.6 (Rh), 5.7 (Pd) and 97.1 (Pt). In contrast, the ratio of H:total metal was about 0.7 for Rh and Pd and 1.4 for Pt. With increasing dispersion the H:Pt-surface ratio increased from 1 for 5% Pt/Al_2O_3 to 64 for a 0.1% Pt/Al_2O_3 catalyst. These authors concluded, therefore, that the retention must be attributed to H_2-spillover to the support and was thought to be associated with the OH groups of the alumina support. Similar conclusions were reached by Altham and Webb (43) for Pt/Al_2O_3 and Pt/SiO_2. The phenomenon of H_2-spillover was found to be more pronounced on the former than on the latter catalyst.

Bianchi et al. (114) conducted a systematic study to investigate the H_2-spillover phenomenon. A Pt/Al_2O_3 catalyst was initially kept in a glass bucket above inert oxides (MgO and SiO_2). After exposure to H_2 in the temperature range 197°-397°C, the catalyst bucket was removed from the system and the oxide materials were then studied separately. These materials surprisingly acquired entirely new catalytic properties for catalyzing various reactions, such as, hydrogenation, dehydrogenation, hydrogenolysis and even cracking of hydrocarbons at mild temperatures in the range 167°-267°C. These authors extended their investigation to the $C_2H_4/H_2/Pt/Al_2O_3$ system. They found the amount of ethane formed was always much higher than the amount of initially adsorbed H_2 and

suggested a chain mechanism for ethylene hydrogenation, that is, once hydrogen atoms formed on Pt and migrated to Al_2O_3, they were able to maintain the hydrogenation process.

Parera and co-workers (115) studied H_2-spillover on Pt/Al_2O_3 catalysts containing varying amounts of Cl^-, using n-heptane as a model molecule. They found a significant correlation between Cl^- content and H_2 spillover. Pt/Al_2O_3 catalysts containing ~ 0.9% wt/wt Cl showed a higher tendency for H_2-spillover. Moreover, this catalyst displayed the most stable catalytic activity and minimum coke deposition in reforming of n-heptane at 467°C. It is interesting to note that the optimum low coke formation encountered in this study as a function of Cl^- content and the amount of spillover H_2 must arise from the fact that a reasonable proportion (~ 1/2) of the hydroxyls of Al_2O_3 are substituted by Cl^- and the spillover hydrogen minimized the carbide precursors (fragmented hydrocarbons) from deposition on the support surface which, for such reactions (cracking, reforming), acts as a second catalytic phase. Enrichment of catalyst materials with Cl^- is, nowadays, a well-recognised advantage for the industrially used catalysts.

The other phenomenon which is quite often blamed for loss of catalyst activity when catalysts are subjected to H_2 at high temperature (> ~ 250°C) or when a decrease in H_2 or CO chemisorption capacity is observed, is known as Sintering. This effect has been recognised since the advent of the use of transmission electron microscopy (TEM) for the study of catalyst materials (116). Baird et al. (117), using TEM, investigated the extent of sintering of a Pt-black catalyst under different conditions. The fresh catalyst showed a crystallite size of

8 nm. This was found to increase to 12.5 nm (under He or air), 14 nm (in vacuo), 18 nm (under C_2H_4 pulses) and 50-60 nm (under H_2 at 297°-397°C). Chu and Ruckenstein (118) studied the sintering and redispersion of Pt on Al_2O_3. The change in size, shape and position of the Pt crystallite was followed by examining the specimen after each step by TEM. Several cycles of heating the sample in 1 Torr of O_2 and H_2 at 747°C were required before Pt-crystallites started to redisperse. The authors concluded that heating in H_2 produces sintering because metallic Pt cannot wet (stick on) the surface and hence has no strong interaction with it. Fiderow et al. (119) have also studied the changes in dispersion of Al_2O_3-supported Pt, Ir and Rh catalysts. Their results showed that thermal treatment at 247°-797°C in O_2 gave a stability order of Rh > Pt > Ir, whereas in H_2, the sequence was Ir > Rh > Pt.

Finally, nine laboratories have investigated H_2-adsorption on EUROPT-1 catalyst using conventional volumetric procedures (120). After being evacuated the sample was reduced between 155°-400°C and then evacuated again at 300°-500°C. The amount of chemisorbed hydrogen at 40 Torr equilibrium pressure lay between 163 and 190 μ mol g^{-1}. The adsorption isotherms did not show a plateau region up to ~ 300 Torr equilibrium pressure. The temperature programmed desorption (TPD) of H_2 over the range -173° to 627°C showed four overlapping peaks with their maxima at -155°, 109°, 237° and 470°C. Based on a study (121) by extended X-ray absorption fine structure (EXAFS), using the same hydrogen reduction procedure and evacuation at 250°C, the Pt particles were found to consist of PtO_x units ($x \leqslant 6$). Thus a change in Pt character occurred resulting in Pt-O bond formation. Therefore, H_2

adsorption on this catalyst will first involve the hydrogenolysis of the Pt-O bond, as shown in equations (1) and (2).

$$2(\equiv Si\text{-}O\text{-}Pt\text{-}) + H_2 \longrightarrow 2(\equiv Si\text{-}OH) + \text{-}Pt\text{-}Pt\text{-} \quad (1)$$

$$\equiv Si\text{-}O\text{-}Pt\text{-} + H_2 \longrightarrow \equiv Si\text{-}OH + H\text{-}Pt\text{-} \quad (2)$$

It has been proposed (120) that the amount of desorbed hydrogen at 237°C corresponded to the amount of H_2 required to reverse the character change revealed by EXAFS (equations 1,2). The -155°C peak was suggested as being due to weakly chemisorbed hydrogen on Pt atoms of low coordination number. The band at 109°C has been assigned to hydrogen adsorbed strongly on the Pt-atoms and that at 470°C attributed to the spillover H_2.

1.8 The Hydrogenation of Alkynes and Dienes

The hydrogenation of alkynes and alkadi ns has been discussed in some detail by Bond and Wells (31) and by Webb (45). It is generally considered that, before undergoing hydrogenation, an unsaturated hydrocarbon must be adsorbed on to the metal surface. The adsorbed states of ethylene (structure e, section 1.5.1), acetylene (structure l, section 1.5.2) and buta-1,3-diene (structure v, section 1.5.3) are generally accepted as the catalytically active forms of these hydrocarbons on catalyst surfaces.

It is well known that the hydrogenation of multiply unsaturated hydrocarbons over metal surfaces is a much more complex system than

that of the mono-olefins (31). This is mainly because of the various parallel reactions involved, leading to the formation of a variety of different product (mono-olefins, isomeric olefins, paraffins) with a degree of preference for one of these products. The extent to which an alkyne or an alkadiene would favour to yield a mono-olefin as opposed to paraffin is expressed by the selectivity of the reaction. This selectivity (5), which is defined as

$$S = \frac{(P_{C_nH_{2n}})}{(P_{C_nH_{2n}} + P_{C_nH_{2n+2}}}$$

where P is the respective hydrocarbon pressure, is dependent upon two factors. First, a thermodynamic factor which is based on the fact that the same surface sites are responsible for both alkene and alkyne adsorption, respectively, i.e., it takes into consideration the difference in strengths of adsorption between the alkyne and the alkene hydrocarbons. Second, a mechanistic factor which takes into account the parallel reactions of alkene and alkyne hydrocarbons to form the respective alkane, i.e., it depends on the specific properties of the catalyst (metal morphology, support) (31,45).

1.8.1 The Hydrogenation of Acetylene

The reaction was first studied by Sheridan et al. (122,123) on pumice-supported metals), by Bond and colleagues (124,125) using various supported VIII metals, and by Webb and co-workers (55-59) using alumina- and silica-supported Pd, Rh, Ir and Ni catalysts. The

general features which have emerged from these studies can be summarised as follows: The shape of the pressure against time curves was dependent upon the initial hydrogen:acetylene ratio and upon the catalyst used. Catalysts with high selectivity display pressure time curves of two proportionally equal regions, whereas those catalysts which exhibit a low selectivity show second regions which either appear very late in the reaction or not at all. Moreover, in addition to ethylene and ethane, hydrocarbons containing more than two carbon atoms were frequently observed.

From the early studies of the kinetics of acetylene hydrogenation, Bond and Wells (31) have proposed the following hydrogenation mechanism:

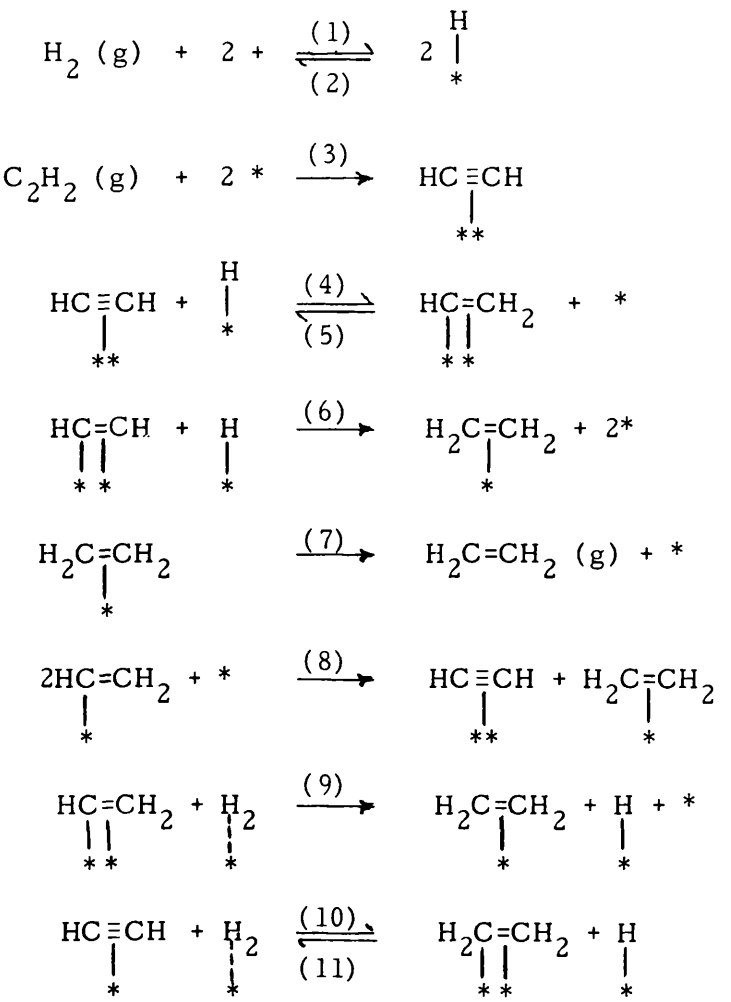

The hydrogen atom involved in step (6) may arise from either step (1) or step (5). If step (5) dominates, ethylene is being formed via the disproportionation of two adsorbed vinyl species (step 8). This mechanism was observed to operate on Ru, Os, Ir, Rh, Pd and Ni, which exhibited an order of unity in hydrogen and zero or negative order with respect to acetylene. In cases where the possibility of a hydrogen molecule is being adsorbed, as reported for Pt/Al_2O_3 catalyst (124), it was assumed that in such a situation, step (8) was accompanied by step (10) and a higher order with respect to hydrogen is then expected.

From the recent studies of Kemball et al. (126) and Al-Ammar and Webb (59), using alumina- and silica-supported Pd, Rh and Ir catalysts, the mechanism in steps (12) and (13) has been proposed for

$$HC{=}CH_2 + H \xrightarrow{(12)} HC - CH_3 + *$$

$$HC{-}CH_3 + 2H \xrightarrow{(13)} H_3C - CH_3(g) + *$$

the direct ethane formation. The latter workers showed that three different types of sites were involved in the hydrogenation of acetylene on these catalysts. Type I sites were active for the hydrogenation of acetylene to ethylene, type II sites were active for the direct conversion of acetylene to ethane via an α,α-diadsorbed species, but inactive for ethylene hydrogenation, and type III sites were active for ethylene hydrogenation, but not active for acetylene hydrogenation (Figure 5).

Most of the investigations on acetylene hydrogenation have indicated that the reaction is frequently accompanied by the formation

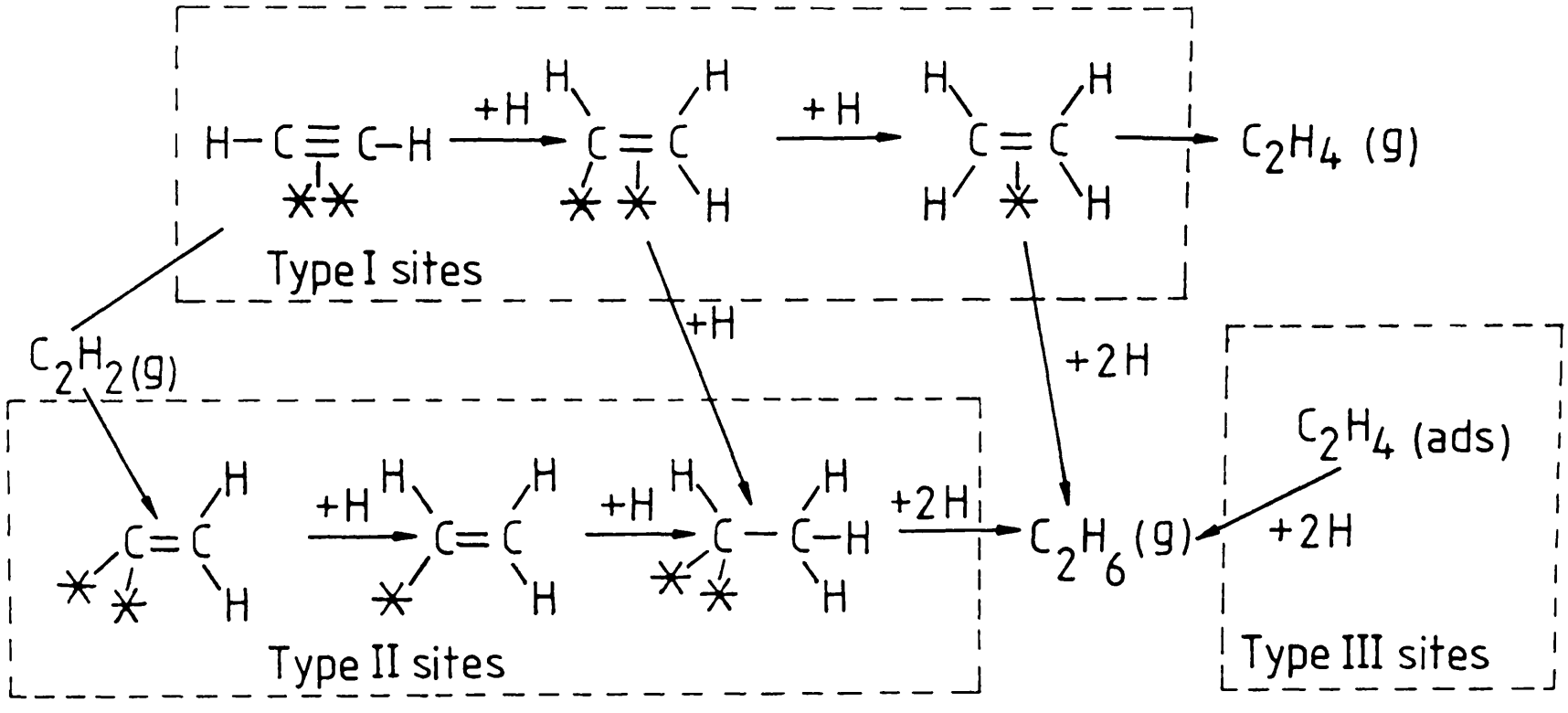

Figure 5. Reaction scheme for acetylene hydrogenation proposed by Al-Ammar and Webb (59).

of small amounts of hydrocarbons containing more than two carbon atoms. The mechanism for such side reactions has been proposed (124) to involve the interaction of an adsorbed vinyl radical with an adsorbed acetylene or a normal vinyl species

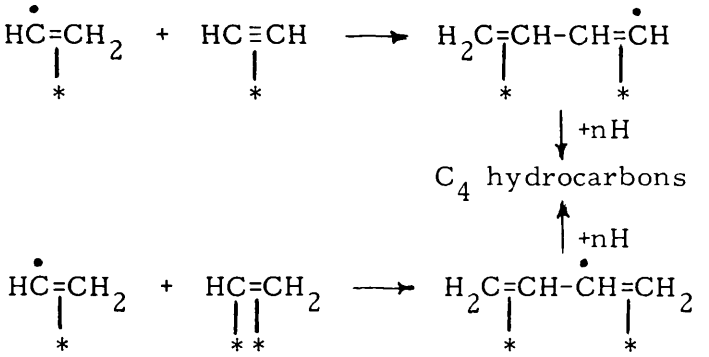

1.8.2 The Hydrogenation of Buta-1,3-diene

The gas phase hydrogenation of buta-1,3-diene with hydrogen was first studied extensively by Wells and co-workers (62,127,128) over Group VIII metals and, more recently, Oudar and colleagues (71-73) have investigated the reaction on Pt-(111) and -(110) single crystals. The kinetics of the reaction over the metals reported by Wells et al. (62,127, 128) showed that the reaction was positive in H_2 and negative or zero in C_4H_6. Over all the metals studied (except Ir and Os), the selectivities and olefin distributions were almost constant until most of the buta-1,3-diene had been removed, which was indicative evidence that the thermodynamic factor was high, that is, the presence of butadiene effectively prevented the readsorption of butenes from the gas phase and also aided the desorption of these butenes. Such an observation makes the assumption that the same sites were involved in the diene and the olefin adsorption.

The early studies of Wells et al. (62,127,128) were and are still used as a basis for the interpretation of buta-1,3-diene hydrogenation results subsequently reported (71-73). The proposed mechanisms are shown in Figure 6. In mechanism A, gaseous buta-1,3-diene was considered to chemisorb as a mono-π-bonded (species II) and as a di-π-bonded species which could exist in two conformational forms (I and III) Addition of a hydrogen atom to these chemisorbed species would give the half-hydrogenated species (IV, V, VI and VII). Further addition a hydrogen atom to these species leads to the formation of but-1-ene. This process was termed 1:2-addition of hydrogen and was assigned to those metals (Ir, Pt, Ru, Os, Cu and Ni) which exhibited a high but-1-ene yield (50-90%) with a trans-:cis-but-2-ene ratio of ~ 1.

Mechanism B, was proposed for the metals which displayed a high trans:cis ratio $>$ 1 (~ 10). In this mechanism conformational interconversion of the adsorbed species does not occur and the trans:cis ratio is a direct reflection of the relative surface concentrations of the anti- (species I) and syn- (species III) di-adsorbed buta-1,3-diene and these are dependent upon the nature of the sites available at the surface and the relative stabilities of the two conformers. This mechanism was found to operate on Co and Pd metals. However, the isomeric trans and cis-but-2-ene could be produced indirectly by the isomerization of but-1-ene after its formation on the surface by the 1:2-addition process and this was found to occur on the metals in the sequence Ni $\approx$ Rh ($\gtrsim$ 80°C) $>$ Ru $>$ Os $>$ Pt $>$ Ir $\approx$ Cu.

Mechanism A

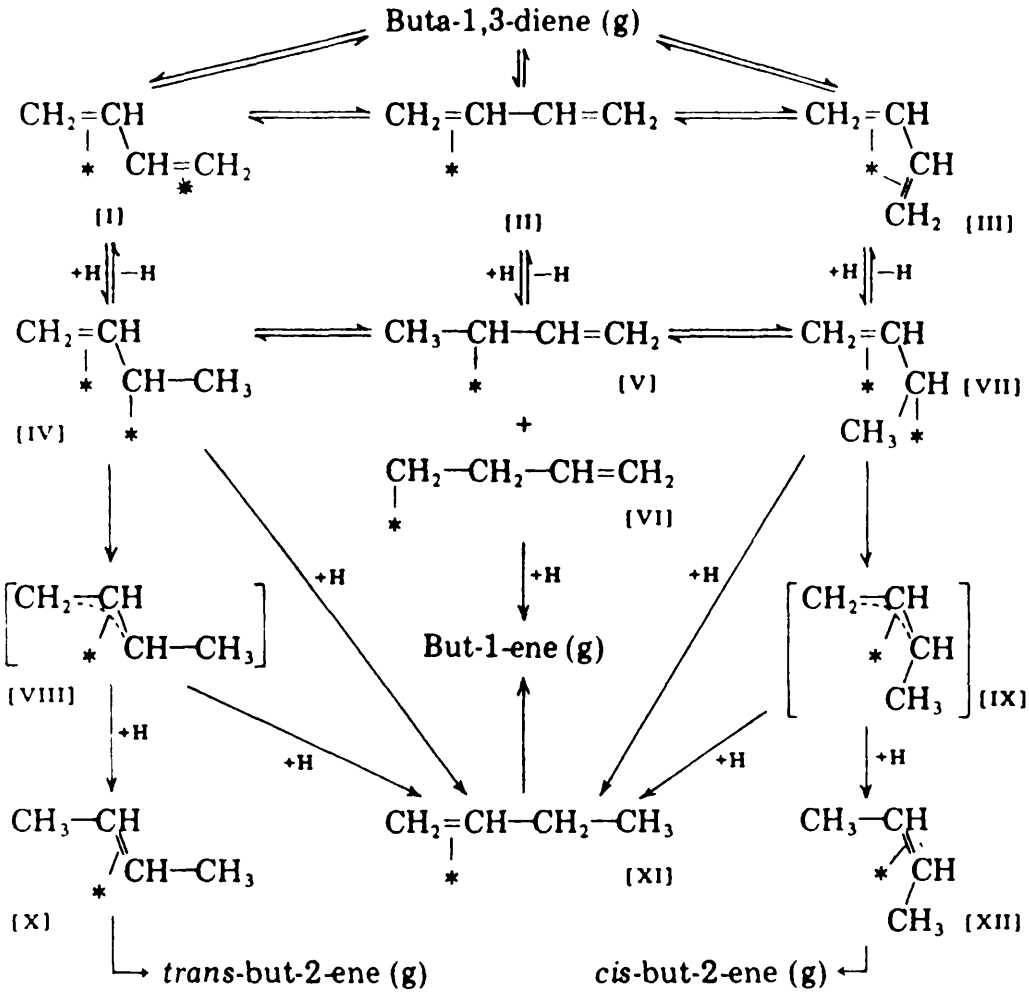

Mechanism B

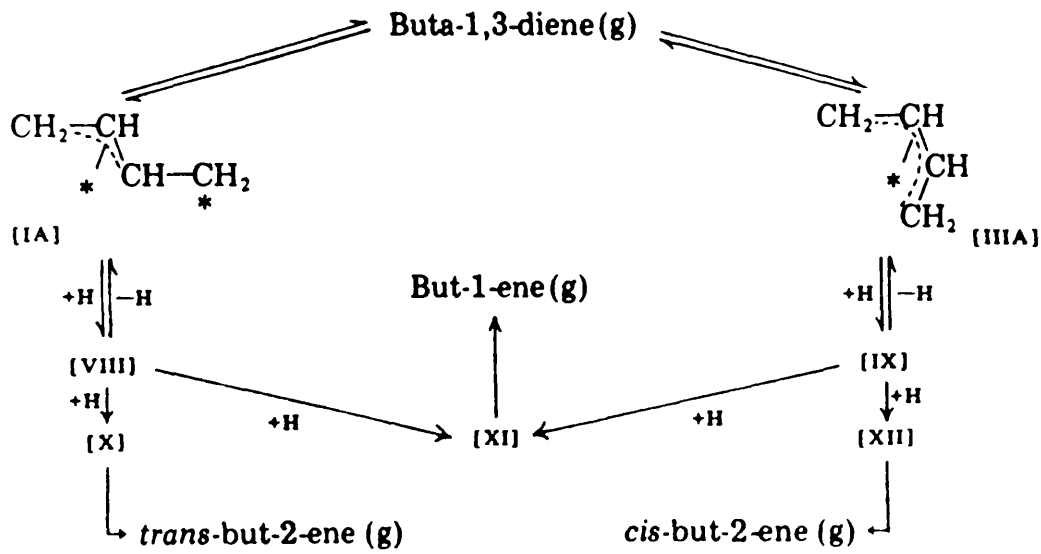

Figure 6. Reaction schemes for the hydrogenation of buta-1,3-diene proposed by Wells et al. (62, 127, 128).

1.9 Sulphur Poisoning of Platinum Catalysts

The phenomenon of catalyst poisoning is one of the most serious problems associated with the industrial application of supported metal catalysts in numerous catalytic reactions, especially those involving hydrogen, such as, methanation of coal ($CO + H_2$) and its conversion to fuels and chemicals, reforming of naphthas or hydrocarbon hydrogenation reactions. The extremely harsh poisoning encountered in these catalytic systems is that induced by sulphur, mainly because of the fact that the feedstocks of these reactions usually contain significant amounts of sulphur-containing compounds, such as, H_2S, COS, SO_2, CS_2, or organic sulphides. Sulphur apparently bonds so strongly to metal surfaces that a marked reduction in the catalyst activity may occur even at extremely low concentrations (p.p.b. quantities). Hence, for example, the life of a commercial catalyst may be reduced to only a few months or weeks, instead of years, and its regeneration process is impossible or impractical. On the other hand, the chemisorption of sulphur on metal catalysts may cause beneficial effects on the selectivity by a partial and well controlled poisoning.

The possible mechanisms by which sulphur poisoning may bring about a positive or a negative effect, with respect to the selectivity of metallic catalysts, are numerous, and can be summarised as follows. The catalytic surface is composed of different active sites with different coordination numbers of atoms, which are capable of catalysing different reactions in different ways. Sulphur may adsorb preferentially on certain sites, thus inhibiting reactions occuring on them.

This type of selective blocking of sites by sulphur can change the distribution of products and hence the selectivity. Sulphur could poison the catalyst to reduce the activity sufficiently, so the yields of desirable products may be unfavourably affected by transport processes, such as diffusion. Sulphur may interact with the metal so strongly that the stability of the metal-metal bonds could be changed and, in consequence, an increase in the mobility of surface atoms may occur.

The topic of sulphur poisoning of metallic catalysts was reviewed comprehensively by Maxted in 1951 (129), by Oudar in 1980 (130), by Bartholomew and colleagues in 1982 (131) and by Barbier in 1985 (132). The following is a summary of the literature in which the main features of sulphur adsorption are considered, together with its effects on the adsorption of other molecules, such as, H_2, CO and hydrocarbons, and its impact on the activity and selectivity of the catalytic reactions on platinum single crystals and supported catalysts.

It is generally considered from LEED studies (130,133-137) that, during the initial stages of sulphur adsorption on clean Pt(110), (100) and (111) single crystal surfaces at room temperature, sulphur atoms reside in the high coordination sites (structures a, b and c) forming an ordered p (2 x 2 overlayer (structure (d)). This has been confirmed up to a sulphur coverage of Θ = 1/4.

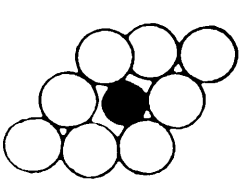

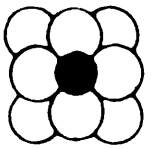

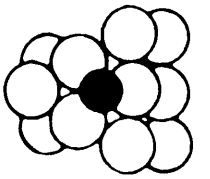

Top view

(110) (100) (111)

surface/structure

(a) (b) (c)

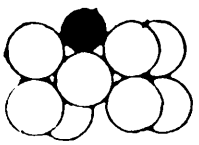

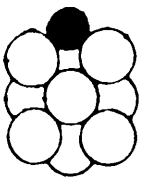

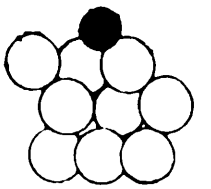

Side view

At higher coverages (up to Θ = 1/2), sulphur is adsorbed with an ordered c (2 x 2) overlayer with a sulphur atom bonded to two Pt atoms (structure (e)).

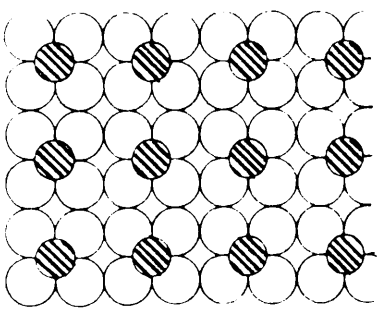

structure d p(2 x 2)

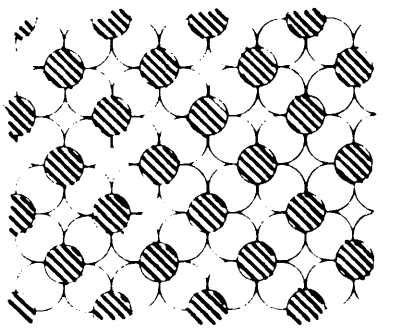

structure e c (2 x 2)

For coverages above Θ = 1/2, a compact arrangement of sulphur atoms with a coincidence lattice in relation to the platinum surface atoms has been observed forming a p (2 x 2, $\sqrt{3}$ x $\sqrt{3}$ or p (5 x 5 structure (structures f,g and h, respectively).

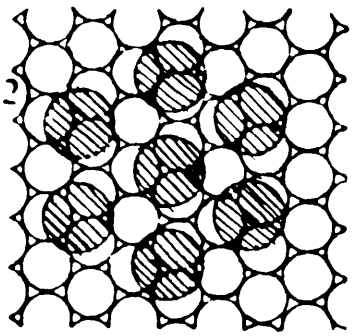

P(2x2)
(Structure f)

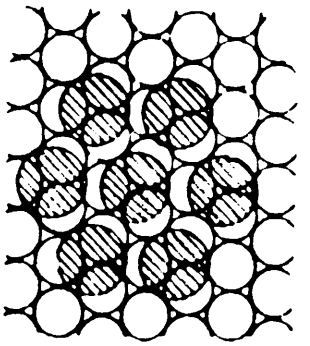

($\sqrt{3}$x$\sqrt{3}$)
(Structure g)

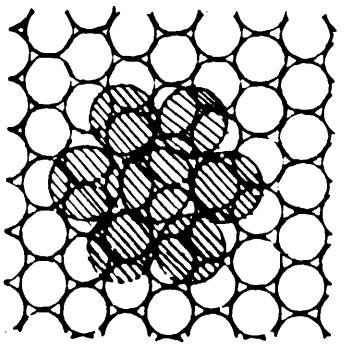

P(5x5)
(Structure h)

A number of investigators (138-140) have examined the nature of sulphur compounds adsorbed on metal films, foils and supported catalysts, employing a variety of techniques. The results suggested that H_2S chemisorbs dissociatively on various metals including platinum. However, there is disagreement regarding the number of surface metal atoms involved per sulphur atom. For example, Saleh et al. (138, 139) suggested a three-site model for H_2S chemisorption in the temperature range -80° to 100°C (structure (i)),

$$H_2S\ (g) + -M - M - M- \longrightarrow \begin{matrix} H & S & H \\ | & | & | \\ -M & - M & - M- \end{matrix}$$

(i)

However, Den Besten and Selwood (140), from their magnetic measurements at 0° - 120°C, suggested that H_2S formed four bonds upon adsorption on the metal surface of Ni (structure (j)),

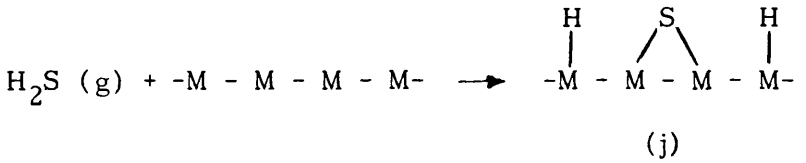

(j)

Similar observations were made by Contractor and Lal (141) for H_2S and SO_2 adsorption on a polycrystalline Pt surface at 80°C. They suggested that sulphur atoms are either adsorbed with one S atom strongly bonded to two Pt atoms, or with one S atom weakly bonded to only one Pt atom (as predicted in structures (i) and (j), respectively).

Kinetic studies of the rate of sulphur adsorption (134,135,142) revealed that the rates of H_2S adsorption on platinum were generally very rapid. Two adsorption regimes were observed. At $\theta < 0.25$-0.3, sulphur adsorption occurred with a high sticking coefficient ($\simeq 1.0$) and at $\theta > 0.3$, sulphur adsorbed slowly due to a decrease in the sticking coefficient ($\simeq 0.03$). However, at low temperature, -80°C, less than monolayer sulphur coverage was observed and the process was partially reversible (139). In contrast, the adsorption of CS_2 and SO_2 on Pt was weak and completely reversible in the temperature range -80° to 250°C (139).

The effect of sulphur on hydrogen adsorption on platinum (110) single crystal has been studied by Oudar and colleagues (143), using a [35-S] radiotracer technique. They found that sulphur has only a minor effect on the reactivity of the sites which were active for hydrogen adsorption. In another study, Oudar et al. (143) studied the reaction $H_2 + C_4H_6$ on Pt-(110) and -(100). Their results demonstrated that on Pt(110) sulphur was displaced by butadiene from

the most energetic sites to the sites which were responsible for hydrogen dissociation (bridged sites in the first layer of Pt atoms). Different behaviour was observed with Pt(100) on which sulphur settled in 4-fold symmetry sites, inducing significant electronic effects. It was suggested that these sites, which were well-suited for sulphur adsorption, did not have the geometrical and/or electronic requirements for a strong adsorption of the butadiene molecule. A similar study of the co-adsorption of sulphur and hydrogen on the Pt(111) face has been reported by Protopopoff and Marcus (144). The main feature emerging from their results was that the surface was totally poisoned for the adsorption of hydrogen when it was saturated by sulphur, with the number of hydrogen adsorption sites blocked by one sulphur atom calculated as 8 ± 1.

Carbon monoxide, CO, adsorption on Pt(110) precovered with varied amounts of sulphur , H_2S, has been investigated by Bonzel and Ku (142) using LEED and flash desorption techniques. Their results showed that the higher the coverage in sulphur, the lower were the temperatures at which the desorption of CO occurred. The authors suggested that, due to the heterogeneity of the surface, sulphur would be adsorbed preferentially on the highly energetic sites which were capable of forming the strongest CO-metal bond, and this was likely to cause the desorption peak to disappear from the high temperature region. Using the reaction $CO + 1/2 \rightleftharpoons CO_2$ as a model in this study, these workers observed that the formation of CO_2 was virtually stopped as soon as the sulphur coverage reached a third of a monolayer, while the adsorption of CO continued to take place up to a coverage of 0.75 of a monolayer. The poisoning of the reaction was

presumed as likely to be due to the prevention of the dissociation of the O_2 molecule on the metal surface. The conclusion reached was that the dissociation site for O_2 consisted of two surface metal atoms in closest neighbour position, with a requisite that on either side of this pair of metal atoms a pair of vacant sites were available to receive the dissociated oxygen atoms. In other words, a cluster of six adsorbent vacancies was necessary for the oxygen dissociation. Neither of these sites should be in contact with a site occupied with sulphur. This study has demonstrated a good example of the crucial electronic effect that could be superimposed by sulphur on blocking the catalytically active sites and consequently paralysing their activities. On Pt(100) a systematic study of the adsorption of CO, NO, C_2H_2 and C_6H_6 and the oxidation reaction $CO + NO \rightarrow CO_2 + 1/2\ N_2$ as a function of sulphur uptake has been carried out by Fisher and Kelemen (133). From this study three mechanisms dependent on sulphur coverage were proposed. At low S coverage ($\Theta < 0.15$), the strong Pt-S bond formed weakened the interaction of other molecules with Pt surface and virtually all the CO and NO that could adsorb reacted to form CO_2 and N_2. At $\Theta \simeq 0.25$, a p (2 x 2) sulphur layer (structure (d)) was formed thus restricting the adsorption of other adsorbates within the cages of adsorbed sulphur, leading to a total suppression of CO formation. When the Pt surface was covered with a saturation layer, the catalyst became chemically inert.

Argano et al. (145) conducted an I.R. investigation to determine the effect of H_2S poisoning on CO-adsorption on a Pt/Al_2O_3 catalyst. H_2S adsorption on a CO-covered surface caused a drastic

decrease in the intensity of the 2080 cm^{-1} band, which was detected during the chemisorption of CO on a clean catalyst, with a new weak band appearing at 2170 cm^{-1}. When CO was adsorbed on a S-covered catalyst, bands at 2170 cm^{-1}, 2080 cm^{-1} and 2060 cm^{-1} were formed. The 2170 cm^{-1} band disappeared with evacuation and was attributed to weakly adsorbed CO on sulphur-poisoned sites.

From their I.R. spectroscopic characterisation of adsorbed CO, Besoukhanova et al. (146) reported that, Pt supported on KL zeolite was less susceptible to sulphur than Pt supported on NaY zeolite. The authors interpreted the effect as being due to the excess of electrons displayed on the Pt/KL-surface by the basic sites which Pt/NaY did not possess. Yao and colleagues (147) studied the effects of SO_2 on the oxidation of CO, and of saturated and unsaturated hydrocarbons over Pt/Al_2O_3 catalysts, using propane and propylene as representatives of saturated and unsaturated hydrocarbons, respectively. Their results, using a flow reactor system and I.R. spectrophotometer, showed that the presence of SO_2 in the feed gas enhanced propane oxidation, but remarkably suppressed both propylene and CO oxidation. It was suggested that the surface sulphate on γ-Al_2O_3 enhanced C_3H_8 desorption on Pt and suppressed both CO and C_3H_6 adsorptions on Pt surfaces.

Examples of the influence of metal dispersion and the nature of support on the toxicity of sulphur poisoning have been reported for hydrogenation and hydrogenolysis reactions. Gallezot et al. (148) have shown that the toxicities of sulphur on Pt, measured using the hydrogenation of benzene passed from 6.2 to 10 when the size of Pt

particles grew from 10Å to 20Å. The greater resistance to sulphur adsorption by the smaller particles has been explained by these authors as being due to their electronic properties, that is, when the size of the crystallites decreases, electron deficient characteristics appear, which could explain the reduced ability of these particles to adsorb an electron acceptor such as sulphur. Gallezot et al. (148) have also shown, on zeolite-supported Pt catalysts, that the toxicities of sulphur compounds were not only a function of metal dispersion, but could also vary with the nature of the support. Using X-ray photoelectron spectroscopy (XPS), the same authors found that as the electronic density of the metal increased, the possibility of the adsorption of S also increased in the sequence $Pt/Y > Pt/SiO_2 > Pt/CeY > Pt/MoY$. Barbier and co-workers (132) using samples of Pt/Al_2O_3 of variable dispersions, through varying metal loading, examined benzene hydrogenation as a function of poisoning with thiophene. They showed that the toxicity of thiophene increased with Pt dispersion. It is important to emphasize that in numerous cases, sulphur could adsorb not only on the metal, but also on the support. For example, Oliphant et al. (136) reported that only 4% of H_2S adsorbed on Al_2O_3 at 452°C compared to that adsorbed on Ni/Al_2O_3. Fitzharris et al. (137) observed negligible amounts of H_2S to adsorb on Al_2O_3 and SiO_2 at 380°-390°C in the H_2S concentration range 13-100 ppb. However, Erekson et al. (149) found that, at lower temperatures (~ 227°C), the amount of H_2S adsorbed on Al_2O_3 was quite significant compared to that on the metal (Ni).

The action of sulphur on exchange reactions of benzene with deuterium and on the hydrogenolysis of cyclopentane on Pt/Al_2O_3 has

been studied by Maurel et al. (150). They found that SO_2 and H_2S were non-selective poisons in the hydrogenation of benzene and benzene-D_2 exchange on Pt, that is, they did not affect the ratio of exchange/hydrogenation rates. However, elemental sulphur was a selective poison causing the ratios of the rates for exchange/hydrogenation to increase by a factor of two. They concluded that H_2S and SO_2 were adsorbed indifferently on all catalytic sites, whereas elemental sulphur adsorbed on sites responsible for hydrogenolysis. This is in accordance with the proposal of Somorjai (151) that facile reactions, such as hydrogenation or dehydrogenation, should be less affected by sulphur poisoning than demanding reactions, such as hydrogenolysis, because sulphur could, by restructuring the surface, thereby affect the deactivation of more than one site for the structure-sensitive reactions. The phenomenon of "facetting" by the action of H_2S has recently been reported for the first time for Pt/Al_2O_3 by Harris (152).

Barbouth and Salame (153) have reported the effect of adsorbed sulphur on the catalytic activity of polycrystalline Pt for ethylene hydrogenation. Their results suggested that sulphur could play a double role during hydrogenation reactions. It can act as a promoter at low coverages and as an inhibitor at higher coverages of sulphur.

In a kinetic study by Apesteguia and Barbier (154) for the hydrogenolysis of cyclopentane on sulphided and unsulphided Pt/Al_2O_3 catalysts, sulphur was found to inhibit the adsorption of cyclopentane in preference to that of hydrogen. For the sulphided catalyst, the reaction order in relation to cyclopentane was positive and

close to 0.6. Conversely, on clean Pt/Al_2O_3, the order was much weaker and close to 0.1. On the other hand, the reaction rate with respect to hydrogen displayed a convex curve as the pressure of hydrogen was varied. The sulphided catalyst displaced a maximum in the curve towards the low hydrogen pressure end as compared to the unsulphided catalyst. These authors also showed that the adsorption of sulphur on Pt caused an increase in the activation energy, E_a, which rose from 25 k cal mol^{-1} on the sulphur free catalyst to 34 k cal mol^{-1} on the S-poisoned catalyst. The increase in activation energy tends to show that sulphur is likely to inhibit the most active sites on the surface. If this is the case, the toxicity of any poison should depend on the heterogeneity of the surface, which has also been suggested by Bonzel and Ku (142).

The role of sulphur poisoning on another class of reactions, namely, hydrocarbon reforming, has received the attention of many workers because of its major importance to the petrochemical industries. On Pt/Al_2O_3 and $Pt\text{-}Re/Al_2O_3$ catalysts, Menon and Prasad (155) found that at 500°C the pre-adsorbed sulphur suppressed all the metal reforming reactions including hexane and cyclohexane dehydrogenation, dehydroisomerisation of methyl cyclopentane, dehydrocyclisation of benzene and hydrocarcking. On $Pt\text{-}Re/Al_2O_3$, the extent of hydrocracking was reduced to a much greater extent than the other reactions studied. Sulphur was ascribed to being responsible for less coke formation on this catalyst than on Pt/Al_2O_3. The hydrogenation, dehydrogenation and isomerisation of cyclohexane has also been investigated by Sterba and Haensel (156). Their results showed that the

addition of low levels of sulphur (50 ppm) caused a drastic change in the activity and selectivity. It decreased the conversion of cyclohexane to benzene from 97 to 0% and conversions to methylcyclopentane and methylcyclopropane from 0.9 and 0% to 44 and 35%, respectively. Wilde et al. (157) reported more recently the effects of sulphur on Pt/Al_2O_3, $Pt-Re/Al_2O_3$, $Pt-Re-Cr/Al_2O_3$ and $Pt-Ir/Al_2O_3$ reforming catalysts for the conversions of n-hexane, n-heptane and methylcyclopentane. Their findings showed that, in each case, presulphidation affected the formation of methane, lowered the dealkylation activity of n-heptane and enhanced the yield of aromatics. This positive effect of sulphur poisoning with respect to selectivity has been suggested by this group to be due to a retardation of the self-poisoning of the metal surface by coke and a more effective dilution of the metal ensembles by sulphur than by coke. It is important to mention that this effect is commonly used in industry in order to "cool" the catalyst for which an appropriate treatment by sulphur can have a beneficial effect on the catalyst activity, minimising excessive hydrocracking which leads to the formation of coke.

It is well known that the adsorption and desorption of a poison are regulated by the energies of the metal-poison bonds, hence it is apparent that the nature of the metal will determine its sensitivity to a given poison. This has been investigated by Simpson (158), who measured the desulphurising temperature of various metals in the presence of 20 ppm H_2S. The results obtained showed that sulphur desorbed from these metals in the sequence Ni, Pd, Pt, Ir (371°C); Co (427°C); Pb, Ru (482°C); Mo (538°C); Cu and Fe (649°C). This clearly shows

the advantage of using the noble metals as catalysts.

The only studies reported in the literature regarding regeneration of sulphur-poisoned Pt catalysts were those of Mathieu and Primet (159) and Bonzel and Ku (142). The former workers investigated H_2S sulphurization and regeneration of Pt/Al_2O_3, using benzene hydrogenation and n-butane hydrogenolysis as the test reactions. The optimal conditions for restoring the original catalyst activity was by O_2 treatment of the catalyst at 300°C, followed by H_2 reduction at 200°C. The latter investigators also indicated that on Pt(110), sulphur could be removed as SO_2 by low pressures (1.4×10^{-8}-7×10^{-6} Torr) of O_2 at 160° 0 397°C.

1.10 Methods for Catalyst Characterisation

A variety of methods have been developed and utilized to correlate catalyst behaviour with its physical and chemical structure. Some of these methods are well-established and have reached the point of standardization. Such methods include the determination of total surface area by the Brunauer-Emmet-Teller (BET) method, pore size distribution using the Kelvin method and the measurement of specific metal areas by selective chemisorption (e.g. CO, H_2). Other methods are solely instrumental, some of which have been available for some time and others which have been more recently developed.

Modern surface physics methods are based on bombarding the catalyst with an incident beam of electrons which will scatter and hence can reveal information about the structure and chemical composition of the working catalyst surface on the atomic scale. These techniques

include low energy electron diffraction (LEED), which can determine the atomic surface structure of the top-most layers of the clean catalyst or of the adsorbed intermediates. Others, such as, Auger electron spectroscopy (AES), X-ray photoelectron spectroscopy (XPS), ultra-violet photoelectron spectroscopy (UPES), electron loss spectroscopy (ELS), can be used to determine the chemical composition of the surface layer.

Transmission electron microscopy (TEM) can reveal information regarding the size, shape and position of crystallites of the catalyst after its use or the light probe can be focused on a small area to yield a picture of the mobility of the small particles and the growth of carbon filaments on metal surfaces in the scanning electron microscopy (SEM).

The role and value of infrared spectroscopy (IR) in the surface chemistry of solids has been recognised for a long time since it was adapted by Eischens and Sheppard for studying supported catalysts (66). However, the advent of laser beams and computers has advanced the way by which the IR spectra can be recorded. Fourier transform infrared (FTIR) is capable of dealing with intensely coloured solids and providing a continuous picture of the change in band intensities accompanying various surface processes.

Other techniques, such as, electron spin resonance (ESR), nuclear magnetic resonance (NMR), Raman spectroscopy (RS) and the methods based on neutron scattering are, however, still in their infancy and their application to catalysis is certainly promising.

Temperature programmed reduction (TPR) and desorption (TPD) techniques are very useful systems for obtaining information on the

nature of the interaction between adsorbed species and a catalyst system.

Radioisotope methods have long served as valuable tools for elucidating mechanisms of chemical conversions at solid surfaces. Indeed, the application of radioactive tracer techniques in the study of catalysis was first recognised as early as 1922 by Paneth and Vorwerk (160), who used [212-Pb] to determine the surface area of the solid $PbSO_4$ by the exchange reaction between the surface Pb and the [212-Pb] in solution. Since then, the method has been adapted and used by several investigators to study a variety of interesting phenomena which are of great importance in surface science or, more specifically, in heterogeneous catalysis. Many reviews have appeared in the literature describing the use of radioactivity in studying adsorption and catalysis (161-163). The topic has been reviewed, most recently, by Berndt (164).

The main attraction of using radioactive tracer methods in the investigation of processes which take place on surfaces, lies in the sensitivity of detection. With this sensitivity it is possible to trace interactions occurring between a small number of atoms or molecules on surfaces with areas as low as 1 cm^2 ($\sim 10^{15}$ sites) using radiotracers with specific activity of $\sim$ 1 mCi m mol^{-1}. Additionally, it allows the observer to directly monitor surfaces and changes occurring on them. For this reason, Thomson and Wishlade (165) developed a direct observation method for use in the study of adsorptions of a variety of active species on metal surfaces. The technique was modified and used by Cormack, Thomson and Webb (166) to study such processes on supported metal catalysts. The method has many advantages; it can be

used in a long pressure range (0-760 Torr); it can be used to study the behaviour of one kind of molecule in the presence of another, with no disturbance to the system during the observation, and it also allows the possibility of adsorption and catalysis to be studied independently. However, the technique has certain disadvantages - it cannot give information about the host species in which the label is incorporated; it cannot identify the composition of the products formed and it is limited to a temperature range over which the Geiger-Müller counters can operate (-10° to + 100°C). However, the former disadvantages can be overcome by using a combination of direct monitoring, spectroscopic and gas chromatography techniques which, together, form a powerful tool for use in the study of catalysis.

The use of radioactive tracers to follow reactions in terms of gaining some insight into their mechanisms has been widely used. This can be accomplished if the gas chromatographic separation of the reaction products is accompanied by a simultaneous determination of the radioactivity contents of these products. From these measurements, reaction mechanisms can be deduced. Gas-flow proportional counters are usually employed in such studies with methane or argon-methane as the quenching agent. Unlike Geiger-Müller counters, proportional counters can be operated at high temperatures (250° - 300°C) with high efficiencies (~ 100% c.f. GM counters < 5%).

Radiotracer methods have also been used in catalyst surface area determinations. Aylmore and Jepson (167) developed a technique for surface area measurement using Krypton-85 as a tracer. The technique is based on the Brunauer, Emmett and Teller (BEM) method,

in which the amount of [85-Kr] adsorbed is measured by its disappearance from the gas phase. Another technique was developed by Hughes et al. (168), where [14-C]-carbon monoxide was used as the adsorbate. These authors used a gas-flow system in which the labelled [14-C]-CO was injected into a helium carrier gas stream at constant rate and hence on to the catalyst. The amount of unadsorbed carbon monoxide was monitored in a chamber viewed by a Geiger-Müller counter. It is important to notice that surface areas measured by the former method can be correlated with the total surface area of the catalyst, whereas measurements made by the latter method reveal the metal adsorption sites as a result of a specific chemisorption.

The tracer method has also contributed to the studies of surface heterogeneity. For example, Roginskii and Keir (169) developed a method by which the degree of the heterogeneity of the surface can be determined. The method is based on the fact that the catalyst surface is partially covered with one kind of adsorbate followed by a complete coverage with another kind of different isotopic composition. If the surface is heterogeneous, on thermal desorption, the last adsorbate which reached the catalyst would be the first to desorb, that is, "First on, Last off". However, although this method has been applied by several workers, it suffers from the drawback that, on heating the catalyst, a surface migration of atoms may occur and hence the surface heterogeneity may be misunderstood. Thomson and Cranstoun (170) used a displacement method in which the surface was partially covered by hydrogen followed by the adsorption of tritrated hydrogen (^{3}H). When the more strongly adsorbed [203-Hg] or [197-Hg]

was admitted to the catalyst surface, the displaced hydrogen gas was examined for radioactivity. Their results on nickel films at 25°C obeyed the "First on, Last off" rule.

Much information concerning catalyst poisoning effects has been obtained with the aid of radioactive tracers. For example, Campbell and Thomson (171) studied the effect of nickel catalyst poisoning on the cyclopropane and propylene hydrogenation, using [203-Hg]. Their results showed that the Hg poison was active in cyclopropane hydrogenation, but not in propylene hydrogenation. The observations were interpreted as being due to the displacement of hydrogen by mercury in the case of cyclopropane hydrogenation, whereas, due to the steric interactions of propylene molecules, the poison did not inhibit its hydrogenation reaction. [203-Hg] was also used by Webb and MacNab (172) to investigate the effect of catalyst poisoning on the hydrogenation and isomerisation of but-1-ene over supported Rh catalysts. It was found that the hydrogenation and isomerisation processes occurred independently of each other and the isomerisation activity was mainly governed by the support. Al-Ammar and Webb (59) used [14-C]-CO to study the effect of carbon monoxide poisoning on supported Rh, Ir and Pd catalysts which were used for acetylene hydrogenation. The authors concluded that the poisoning effects of carbon monoxide are not due simply to hydrocarbon "site-blocking" effect but rather involve a selective hydrogen "site-blocking" process.

CHAPTER TWO

OBJECTIVES OF THE PRESENT WORK

The work described in this thesis is a detailed investigation of the hydrogenation of acetylene and buta-1,3-diene on the standard catalysts, EUROPT-1 (6% Pt/SiO_2) and EUROPT-3 (0.3% Pt/Al_2O_3) which have been designed by the Council of Europe Catalysis Group (EUROCAT), to be used by the academic and industrial communities as reference catalysts. These, in addition to another three Pt catalysts supported on silica, alumina and molybdena prepared at Glasgow University by Dr. G. McLellan, were studied with the aim of gaining information concerning:

1 - The adsorptions of [14-C]-acetylene, [14-C]-ethylene, and [14-C]-carbon monoxide on these catalysts.

2 - The evaluation of the effects of various treatments such as, evacuation, molecular exchange, and hydrogenation upon the adsorbed [14-C] species.

3 - The hydrogenation of acetylene and buta-1,3-diene on these catalysts.

4 - The nature of the active sites involved in the adsorption and hydrogenation reactions.

5 - The effects of support on the adsorptions and hydrogenation reactions.

6 - Mechanisms for these reactions using [14-C]-ethylene, the factors which determine the selectivity exhibited by these catalysts.

7 - The effects of H_2S-poisoning on the adsorption of hydrocarbons and carbon monoxide and on the activity and selectivity of these catalysts towards the hydrogenation reactions.

SECTION TWO

EXPERIMENTAL

CHAPTER THREE

APPARATUS AND EXPERIMENTAL PROCEDURES

3.1 The Vacuum Systems:

3.1.1 Acetylene Hydrogenation System

The apparatus which was used for the reaction of acetylene with hydrogen consisted of a conventional vacuum system (Figure 7). The system, which was maintained at a pressure of $< 10^{-4}$ Torr by using a mercury diffusion pump (D) backed by an oil rotary pump (R), incorporated four two litre bulbs (G) for the storage of hydrogen and reactant hydrocarbons (acetylene, ethylene and ethane) and three 250 ml bulbs (g) for the storage of diluted [14-C]-radioactive gases. These storage bulbs were connected directly to a secondary manifold via 2 mm taps to allow ease of filling or evacuation and via 2 mm taps to a part of the vacuum system close to the reaction vessel (R.V.). A [14-C]-carbon dioxide converter (C) was attached to the apparatus for the conversion of [14-C]-carbon dioxide to [14-C]-carbon monoxide. A 250 ml bulb of [35-S]-H_2S (S) was connected adjacent to the reaction vessel and the pressure transducer to control the expansion of the H_2S to the reaction vessel. Reaction mixtures of the required compositions for use in the hydrogenation reactions were pre-mixed and stored in a 500 ml vessel (MV) fitted with a cold finger. Another 250 ml standard vessel (SV) was connected to the vacuum line in which a standard mixture of ethane, ethylene and acetylene could be stored and used for

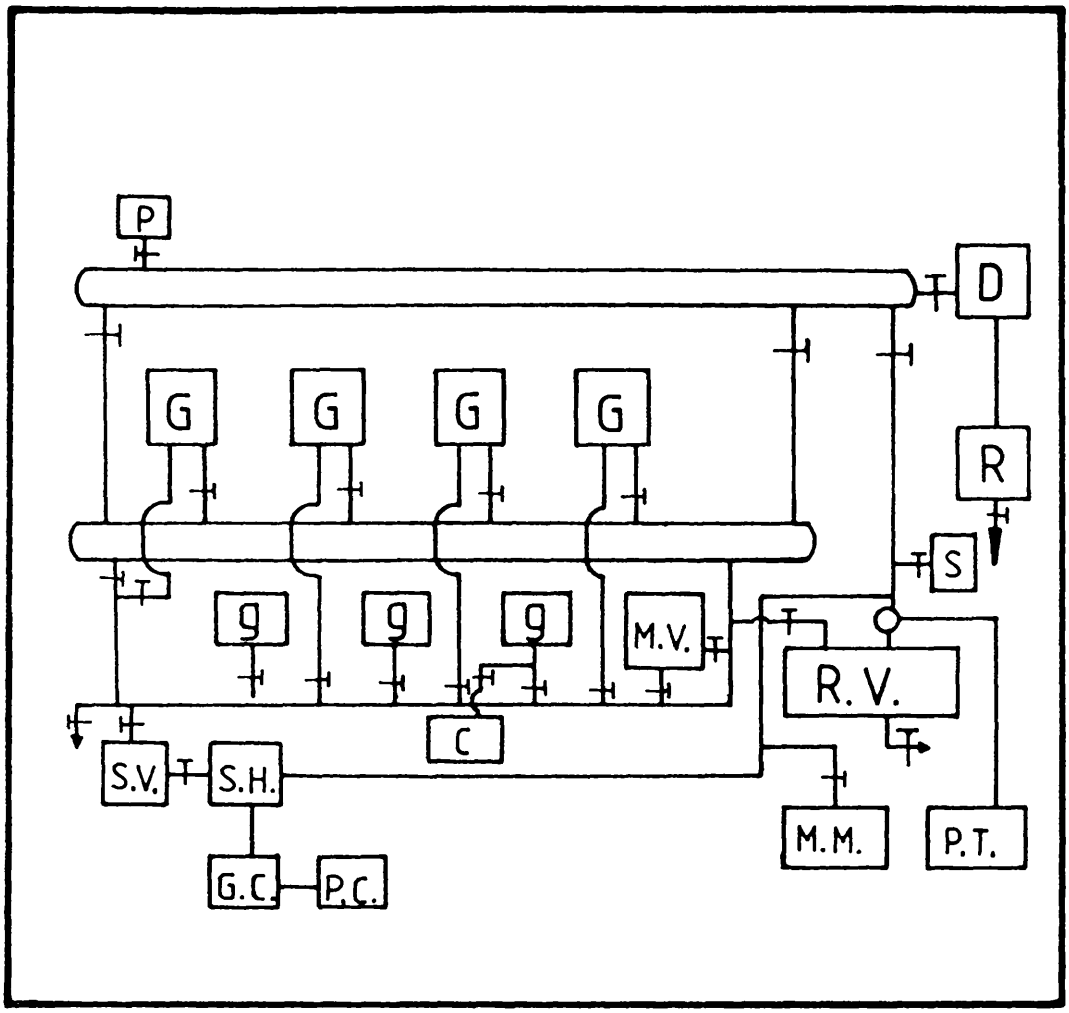

Figure 7. Vacuum line diagram for adsorptions and acetylene hydrogenation.

G	=	inactive gases storage bulbs
g	=	radioactive gases storage bulbs
S	=	sulphur bulb
R.V.	=	reaction vessel
M.V.	=	mixing vessel
P.T.	=	pressure transducer
M.M.	=	mercury manometer
S.H.	=	sample handling unit
S.V.	=	standard vessel for gas chromatography
G.C.	=	gas chromatography
P.C.	=	proportional counter
D	=	diffusion pump
R	=	rotary pump
C	=	carbon dioxide converter
P	=	Pirani gauge
⊢	=	stopcock
O	=	three-way stopcock

calibration of the gas chromatographic system prior to hydrogenation experiments, without it entering the reaction vessel.

The pressures in the system were measured using a mercury manometer (MM), a calibrated differential pressure transducer (PT) (section 3.1.1.4), and a Pirani vacuum gauge (P) (Edwards high vacuum, model 812). Pressures in the reaction vessel were measured using the pressure transducer, rather than using the mercury manometer, in order to avoid catalyst contamination by mercury vapour and to measure accurately the small pressure changes involved. The mercury manometer was mainly used to measure pressures in the gas storage bulbs during filling. The Pirani gauge was used to monitor the pressure of the vacuum line.

Using a vessel of known volume, filled with air, the volumes of the various parts of the vacuum line were measured. The closest three measurements were used to evaluate the mean volume $\bar{x}$ which defined as $\frac{\Sigma x}{n}$ and the deviation in these measurements σ_n which defined as

$$\sqrt{\frac{\Sigma x^2 - \Sigma x^2/n}{n}}$$

Reaction vessel	416.80 ± 2.84 cm^3
Primary manifold	610.80 ± 1.68 cm^3
Secondary manifold	252.42 ± 0.96 cm^3
Hydrogen bulb	3260.05 ± 3.77 cm^3
Acetylene bulb + cold finger	2621.61 ± 2.02 cm^3
Ethylene bulb + cold finger	2533.26 ± 1.44 cm^3
Ethane bulb + cold finger	2533.76 ± 1.94 cm^3

[35-S]-H_2S bulb	+	cold finger	334.28 ± 5.20 cm^3
[14-C]-C_2H_2 bulb	+	cold finger	335.90 ± 4.03 cm^3
[14-C]-C_2H_4 bulb	+	cold finger	382.11 ± 2.91 cm^3
Mixing vessel	+	cold finger	698.39 ± 3.09 cm^3
Standard vessel	+	cold finger	420.05 ± 2.45 cm^3

3.1.1.1 The Reaction Vessel

The reaction vessel (Figure 8) was designed in such a way that it allowed the simultaneous determination of the surface and gas phase count rates during (i) the adsorption of [14-C]-labelled hydrocarbons at ambient temperature and (ii) the hydrogenation reactions. It also contained the facility for the in situ reduction of the catalysts at elevated temperatures using a coil furnace (F). It was situated in a position to make it possible to measure directly the pressure changes occurring within the reaction vessel by using a differential pressure transducer (section 3.1.1.4) and to extract samples for analysis by gas chromatography (section 3.2) and gas-proportional counting (section 3.1.1.5). It was of a similar design to that originally developed by Cormack et al. (166) and subsequently modified by Reid et al. (173).

The reaction vessel was connected to the vacuum line via (T_1) tap, to the pressure transducer via (T_2) tap, and to the sample handling unit via tap (T_3). The catalyst was always spread on the walls of a glass boat (X), which was divided into two compartments by a glass wall. Compartment (b) was identical to compartment (a), but did not contain any catalyst. The catalyst boat could be moved from position (1) to position (2) by the use of an external magnet applied to

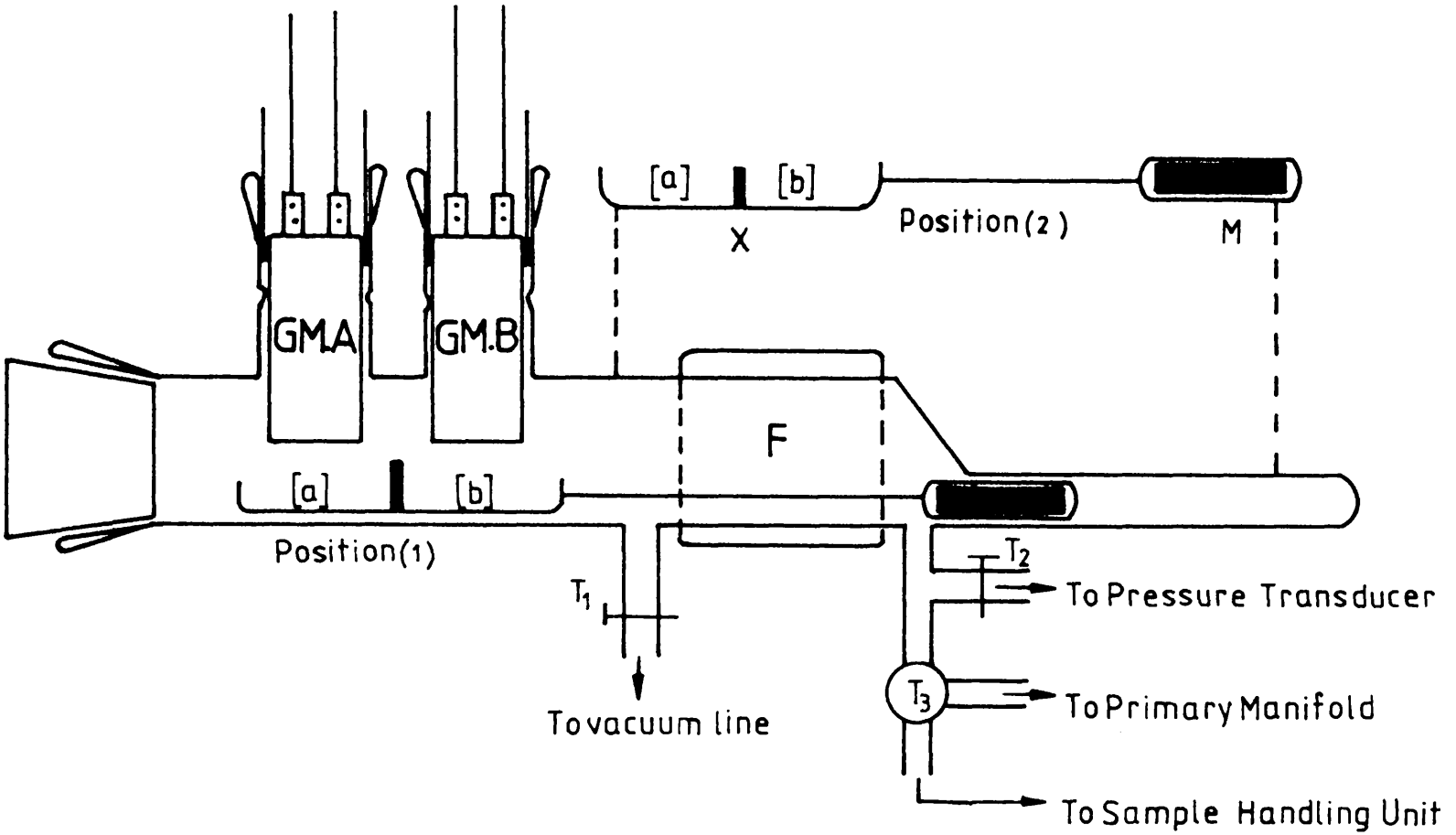

Figure 8. The reaction vessel and the Geiger-Müller counters.

the glass-enclosed metal bar (M). During the experiments the catalyst boat was always at position (1) and it was only moved to position (2) when catalyst reduction was required. The high temperatures required for the reduction of the catalysts up to 400°C were maintained by the use of an electric furnace (F), which was controlled by a Variac transducer (Type - V6 HMTF). Temperatures in the furnace region were measured using a thermocouple wire connected to a Comark electronic thermometer (Electronics Ltd. 1602 Cr/Al). The catalyst boat could be removed from the reaction vessel via a B34 joint.

The reaction vessel was fitted with two Geiger-Müller counters, GM(A) and GM(B), which were held in position by using extended B34 cones into which the counters were sealed with an adhesive (Araldite).

3.1.1.2 The Geiger-Müller System

The Geiger-Müller tubes used in this study were of type Mullard ZP1481 end window counters filled with a mixture of neon, argon, and hydrogen gases. Each counter was connected to a scaler ratemeter (Nuclear Enterprises Ltd., model S.R.5). The working voltage (plateau region) of the counters, where the count rate is nearly independent of the applied voltage, was determined for each Geiger-Müller tube using a [60-Co] source. A typical plateau is shown in Figure 9. The voltage in the middle of the plateau was chosen as the working voltage for the Geiger-Müller counter during the experiments.

Since the efficiencies of the two Geiger-Müller tubes were found to be slightly different (Figure 10), it was necessary to inter-calibrate them in order that the count rates recorded by the two

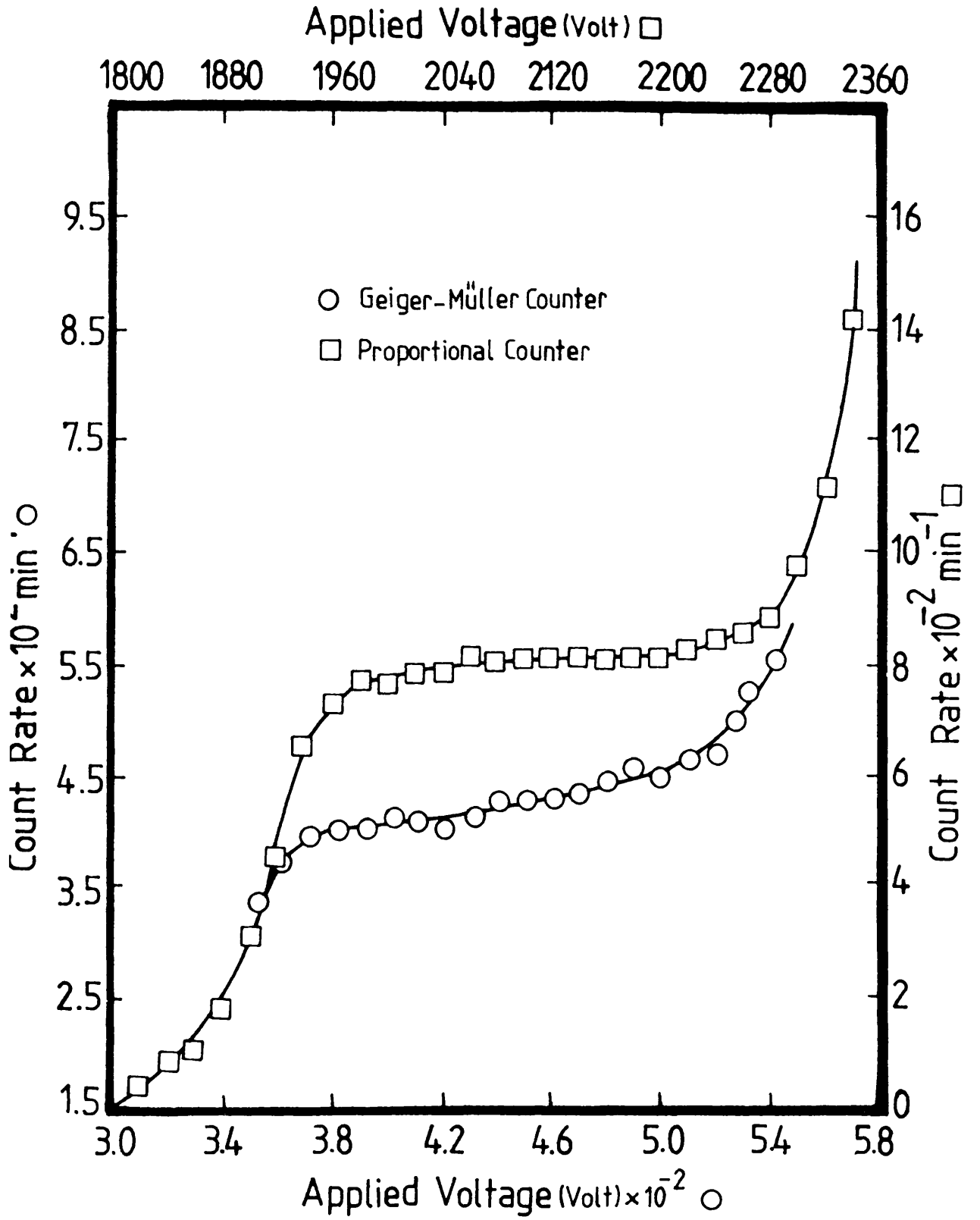

Figure 9. Geiger-Müller and proportional counters plateau.

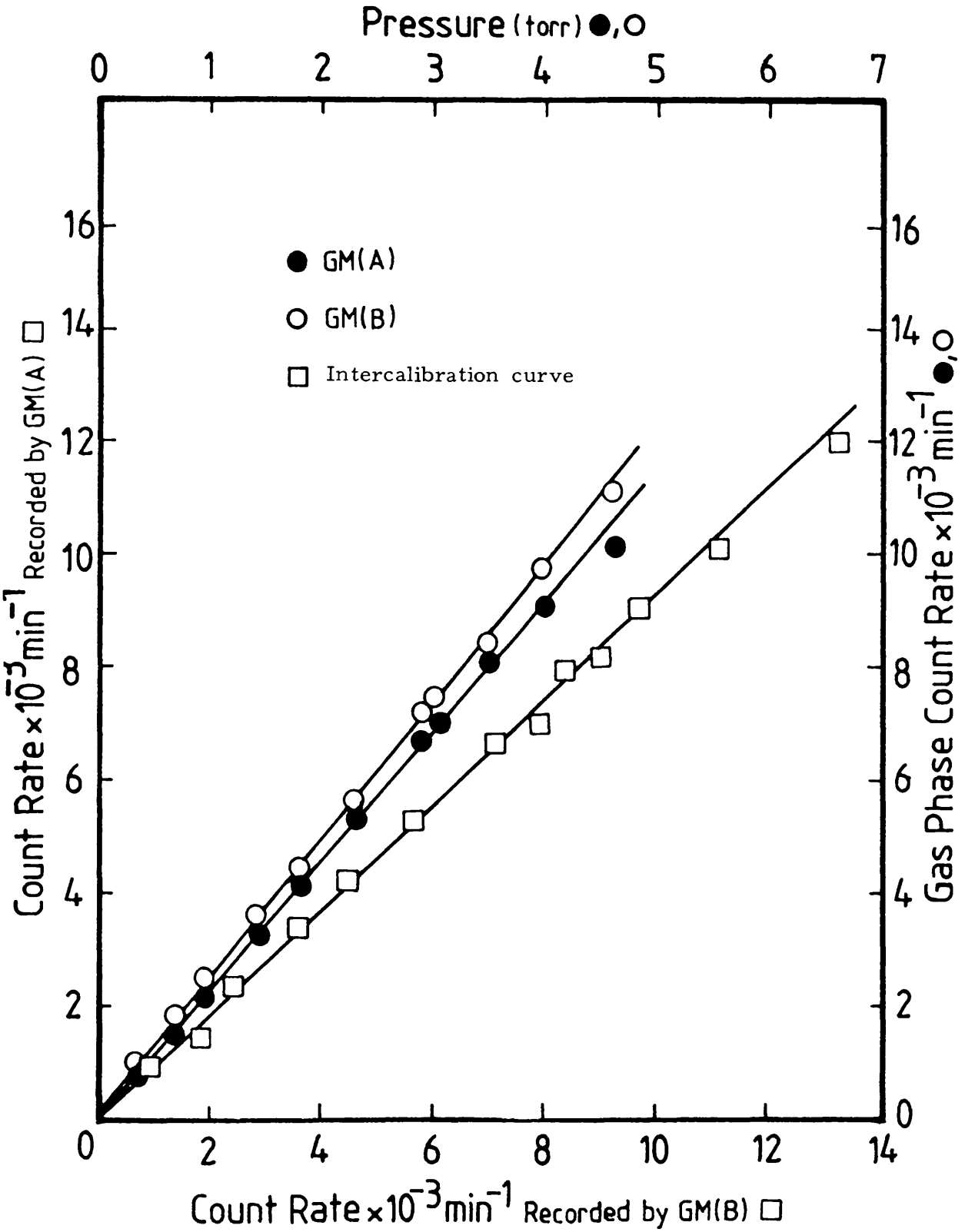

Figure 10. Gas phase count rate recorded by GM(A) and GM(B) against pressure of radioactive gas; the intercalibration curve of the counters.

counters could be directly compared. The intercalibration was performed by admitting small aliquots of a radioactive gas (e.g. [14-C]-C_2H_4) to the reaction vessel in the absence of any catalyst with the boat in position (1). Twelve separate two-minute counts of the radioactive gas were made and the count rates were corrected for dead time and background. The intercalibration factor was determined from a plot of the count rate recorded by Geiger-Müller (GM.A) against the count rate recorded by Geiger-Müller (GM.B). From the resulting plot (Figure 10), it was found that:

$$1.035 \times \text{count rate (GM.A)} = \text{count rate (GM.B)}$$

Hence all the count rates recorded by the Geiger-Müller (GM.A) were multiplied by the intercalibration factor (1.035) before subtraction from the count rates recorded by Geiger-Müller (GM.B).

Due to the fact that after a particle has been detected, the counter is unable to detect another for a period of time. The observed count rates must be corrected for this dead time of the detector, which is specified by the manufacturer to be 500 μ seconds for the ZP1481 counters. Hence, all count rates recorded by GM.A and GM.B tubes were corrected for the dead-time losses according to the relation

$$N_T = \frac{N_o}{1-N_o t}$$

where N_o = the counts per second recorded on the SR5 scaler

N_T = the true count rate

t = dead time in seconds (5×10^{-4} s.)

The correction for the background activity (activity due to external radiation) was made by counting several two-minute counts before each experiment. The average of these count rates was used as the background activity. Thus

$$N_C = N_T - N_B$$

where N_T = the true count rate

N_B = the background activity

N_C = the actual number of counts after correction

In order to examine the adsorption effects on the amount of radioactive emissions reaching the Geiger-Müller counters, two effects of concern were considered. The phenomena of self-absorption (losses in count rate detected from the gas phase with increasing gas pressure) was investigated by determining the count rate as a function of [14-C]-carbon monoxide pressure (Figure 10). It can be seen within the gas pressures used in this study (5 Torr) that the effect was negligible. Absorption of β' radiation from the surface by the gas phase was probed by placing a ^{60}Co source under GM(B) and pressures of air were admitted to the reaction vessel which was evacuated after each admission. It was found that at pressures less than 100 Torr the effect was negligible.

3.1.1.3 Technical Consideration

It is important to note that the height of the Geiger-Müller tubes (Mullard Mx168/01) was found to affect the count rates which were recorded by the counter (GM.A). In an attempt to study the adsorption isotherm of [14-C]-carbon monoxide with the counters at a height of 30.74 mm from the internal bottom of the glass boat, initially, the amount of [14-C]-carbon monoxide adsorbed on the catalyst surface was found to increase progressively. After a pressure of about 1 Torr, the count rate adsorbed on the catalyst surface was found to decrease rapidly, although a pressure in excess of 5 Torr was used. It was believed that this behaviour is likely to be the result of a chemical reaction.

When the [14-C]-acetylene adsorption isotherm was studied with the counters at the same height, a similar behaviour was observed (Figure 11) and the count rate recorded on the catalyst surface dropped to the background activity. However, when the catalyst was evacuated for a period of 45 min, the count rate recorded by (GM.B) was found to be 1478 cpm. This indicated that a reasonable amount of [14-C]-acetylene had been adsorbed on the catalyst surface.

When the height of the Geiger-Müller counters was changed to 17.85 mm from the internal bottom of the glass boat, a different behaviour was observed and the count rate on the catalyst was found to increase with the amount of [14-C]-acetylene admitted. After the reaction vessel had been evacuated for 45 min, the amount of the radio-activity recorded by (GM.B) was found to be slightly different from that adsorbed on the catalyst surface before evacuation. This phenomenon

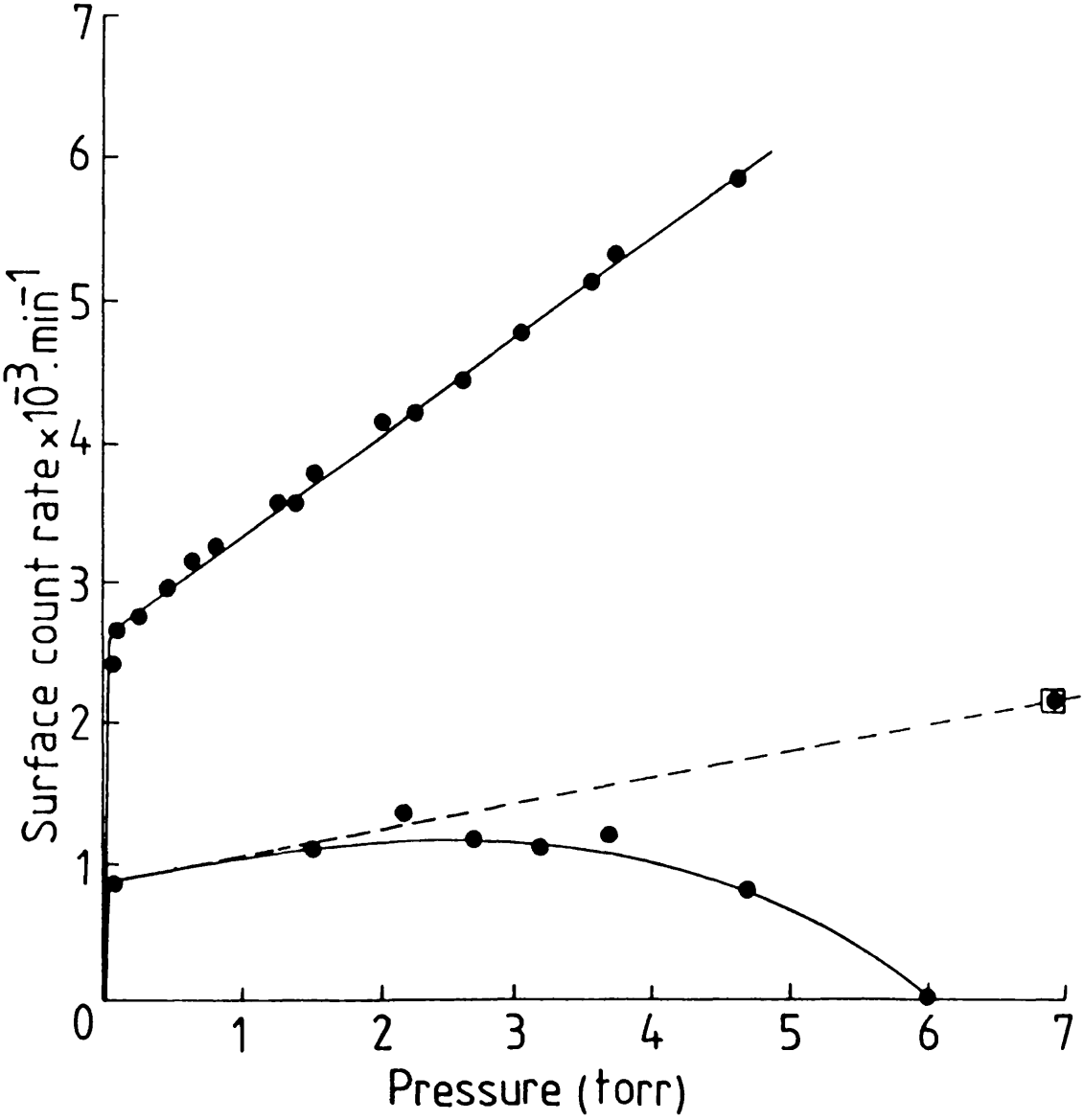

Figure 11. The effect of Geiger Müller counters height on the adsorption isotherm plot.

can be explained by the fact that some of the adsorbed radioactivity on the catalyst scattered and was detected by the Geiger-Müller (GM.A) and it would increase as the pressure of the radioactive gas increased. All the experiments described in this thesis were carried out with the Geiger-Müller counters at the second height.

3.1.1.4 The Pressure Transducer

The pressure in the reaction vessel was measured using a differential pressure transducer (E.S. Laboratories (E.M.I.) Ltd., model SE21/V/10D). The use of the pressure transducer allowed the possibility of measuring the pressure of small aliquots of the hydrocarbons, which were introduced to the catalyst during the adsorption isotherm experiments. It was also used to continuously record the pressure fall during the course of hydrogenation reactions by connecting the output from the transducer directly into a Servoscribe (model R.E.511.20) chart recorder. The pressure transducer was calibrated over the range 0-100 Torr using a mercury manometer. A linear relationship was found between the applied pressure and the output response from the pressure transducer (Figure 12). An output deflection of 1 mV corresponded to a pressure of 0.47 Torr.

3.1.1.5 The Proportional Counter

To identify the radioactive content of each component of the products during the hydrogenation of acetylene, a gas-flow proportional counter was coupled to the gas chromatography system (Figure 13). The counter (Figure 14) was constructed using a design similar to that

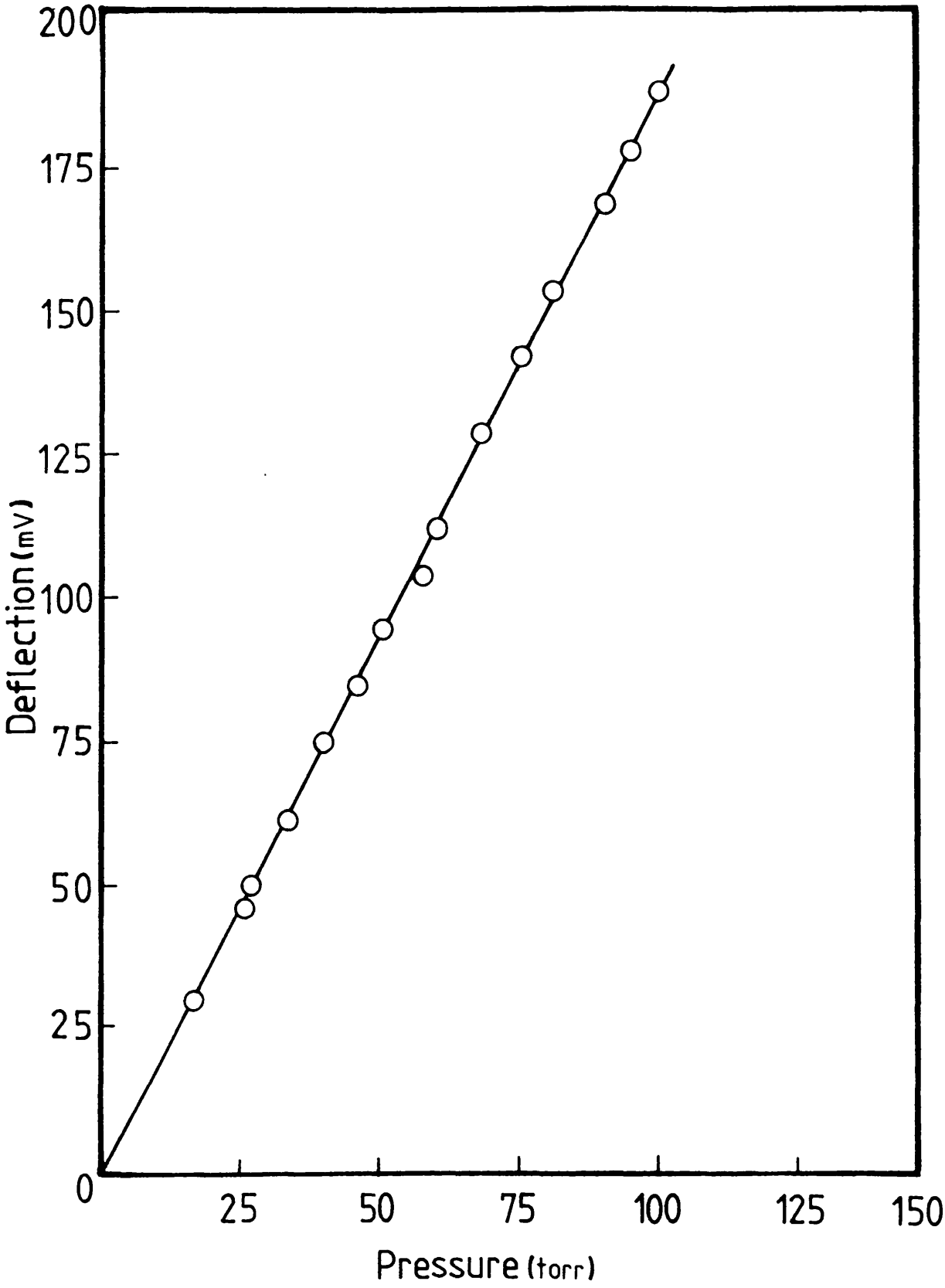

Figure 12. Calibration of pressure transducer.

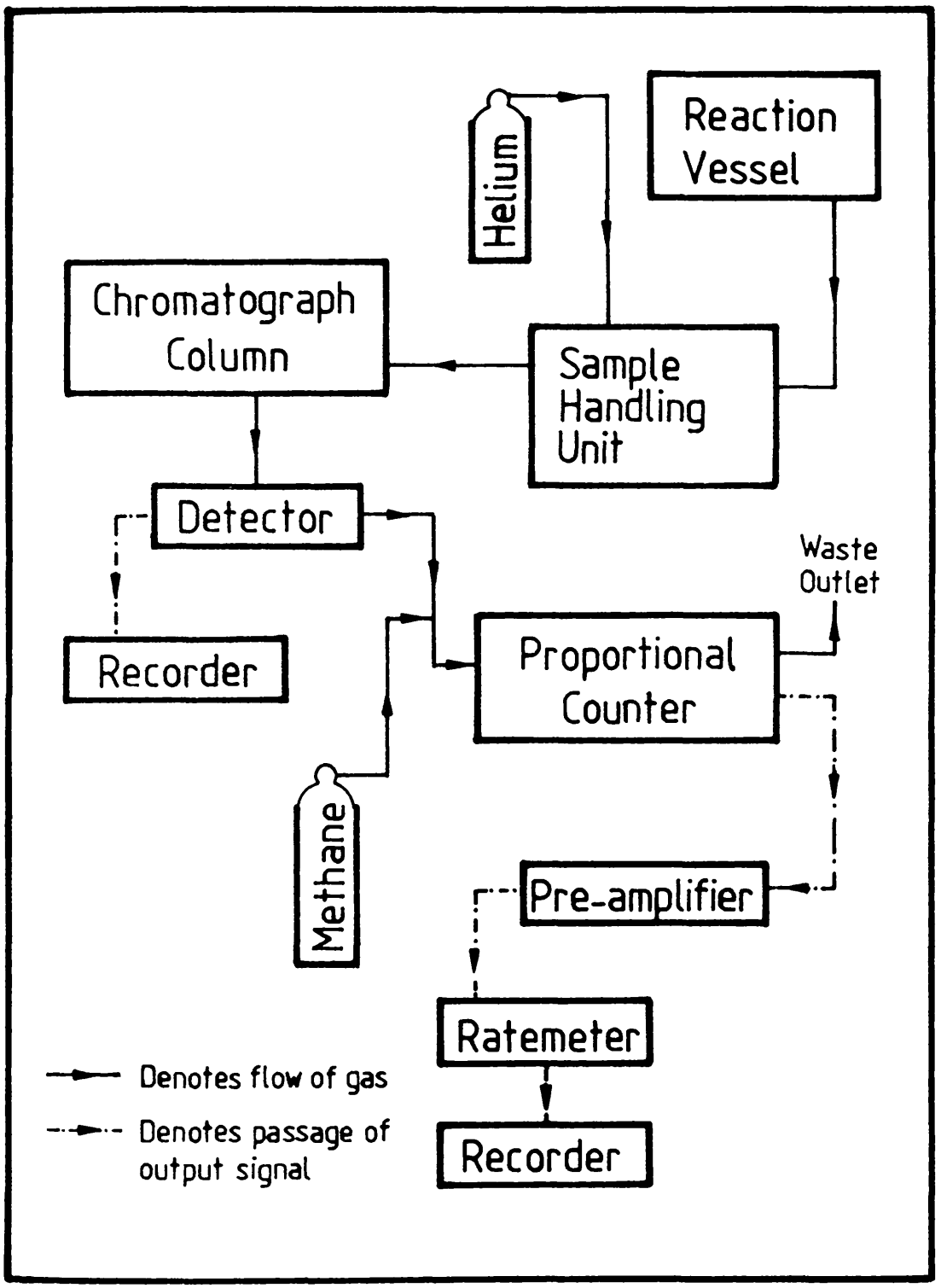

Figure 13. Block diagram of gas chromatographic and proportional counter system.

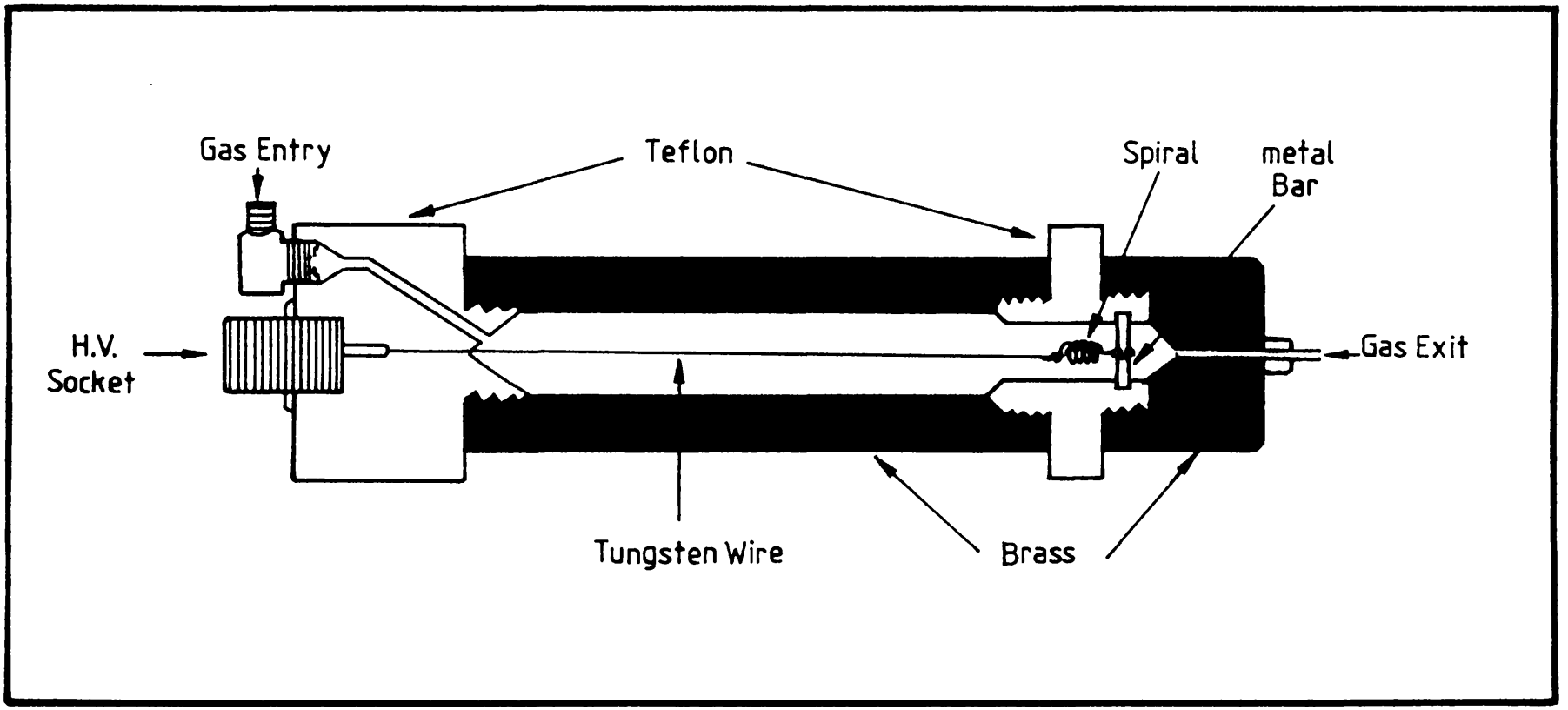

Figure 14. The proportional counter

developed by Schmidt, Bleeck and Rowland (174). It was constructed from brass and Teflon and had an internal volume of approximately 36 cm^3. The anode was a stainless steel wire of diameter 0.01 mm. The proportional counter was connected to a pre-amplifier (ESI 425), which was in turn connected to a scaler ratemeter (Model - SR5). The output from the scaler ratemeter was connected into one channel of the two-channel Servoscribe potentiometric chart recorder (type R.E.520.20). The other channel was connected to the output of the detector of the gas chromatography system, in which a direct comparison of the radioactivity contents of the products can be made on the same chart paper. The proportional counter was operated with a helium-methane mixture. A helium flow rate of 60 ml min^{-1} was required for efficient chromatographic separation. Methane was introduced into the helium carrier gas stream at the exit from the chromatographic system and its flow rate was controlled by using a Nupro (L series) fine needle valve which was connected to a Negretti Zambra valve.

Using a [60-Co] external source placed adjacent to the counter, it was found that the location and length of the plateau of the counter was dependent on the composition of the helium-methane ratio. The optimum helium to methane ratio was found to be 10:1, provided that the flow rate of helium was maintained at 60 ml^{-1}. Thus, the flow rate of methane was 6 ml min^{-1}.

Under these conditions a plateau length in excess of 80 volts with a variation of less than 5% in the count rate over the length of the plateau was obtained (Figure 9). The counter plateau region was checked before each experiment using the [60-Co] source under the above mentioned conditions.

When [14-C]-hydrocarbon samples were passed through the proportional counter, the output from the scaler ratemeter was recorded as a peak on the chart recorder. These peaks were used as an indication of when to start and to stop counting. The total radioactivity in the hydrocarbon gas was obtained by subtracting the background activity from the counts, determined during the passage of the sample through the counter. In order to investigate whether the passage of an inactive hydrocarbon gas through the proportional counter would have any quenching effect, which in turn may cause an alteration to the count rate, several pulses (10-20 Torr) from the standard mixture of inactive ethane, ethylene, and acetylene were admitted to the gas chromatography system and then through the gas proportional counter with the external [60-Co] source in position. No quenching to the count rate was observed in the pressure range used.

3.1.2 Buta-1,3-diene Hydrogenation System

The reaction of buta-1,3-diene with hydrogen was carried out in a static conventional vacuum system (Figure 15). It contained three bulbs for the storage of hydrogen (H), buta-1,3-diene (B), and the reaction mixture (M). Each bulb was connected through a 2 mm tap to a secondary manifold for evacuation and filling with gases and, via another 2 mm tap to a part of the vacuum line close to the reaction vessel (R.V.) and the pressure transducer (P.T.). The apparatus was maintained at a pressure of 10^{-4} Torr or, better, by means of a mercury diffusion pump (P) backed by a rotary oil pump (R). The higher pressures (> 200 Torr) were usually measured using a mercury

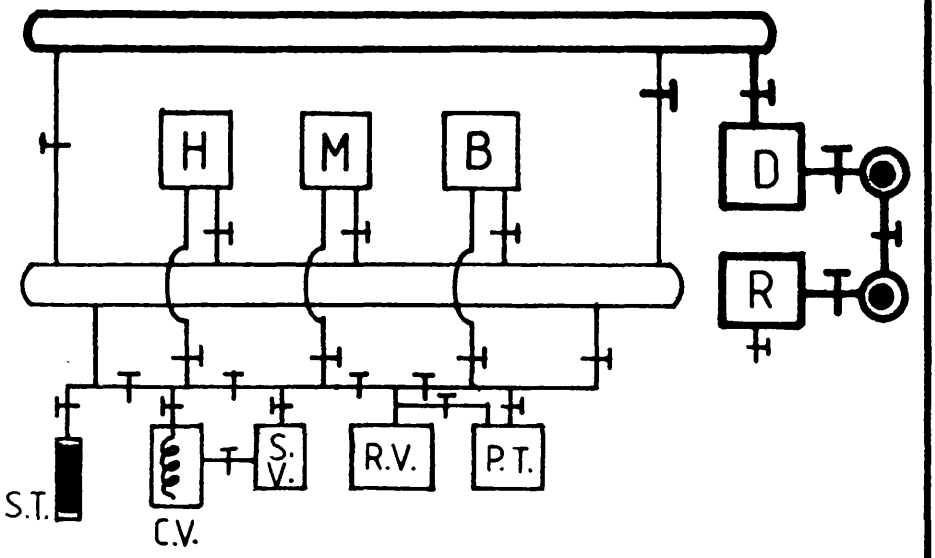

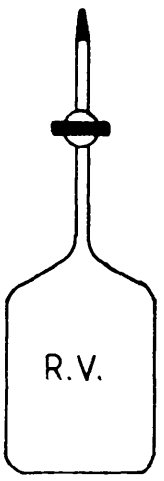

H = hydrogen bulb
M = reaction mixture bulb
B = buta-1,3-diene bulb
D = diffusion pump
R = oil rotary pump
P.T. = pressure transducer
R.V. = reaction vessel
S.V. = sampling vessel
C.V. = cold vessel
S.T. = sampling tube
◉ = liquid N_2 traps
⊢ = stopcock

Figure 15. Butadiene hydrogenation vacuum system.

manometer, whereas the pressures in the reaction vessel were measured using a calibrated pressure transducer (S.E. type SE/V/10D) (section 3.1.1.4), capable of accurately recording pressure changes of 0.01 Torr. The reaction vessel (Figure 15) which was approximately 80 cm^3 was loaded with the catalyst and attached to the vacuum line through a B10 joint. To facilitate analysis of the reaction products, the reaction vessel was coupled to a sampling vessel (S.V.) which was in turn joined to a vessel containing a glass spiral tubing (C.V.) which was maintained at -196°C using liquid N_2, for removal of hydrogen from the reaction products. The products were then transferred to an evacuated sampling tube connected to the system.

The volume of the different parts of the vacuum system were measured using the method described in section 3.1.1 and were as follows:

Reaction vessel	89.12 ± 0.02 cm^3
Primary manifold	487.24 ± 4.76 cm^3
Secondary manifold	408.89 ± 2.69 cm^3
Hydrogen bulb	2452.23 ± 6.00 cm^3
Butadiene bulb + cold finger	1081.35 ± 4.00 cm^3
Butadiene + H_2 bulb + cold finger	2509.61 ± 8.49 cm^3
Sampling vessel	515.11 ± 4.28 cm^3
Cold vessel	115.89 ± 1.50 cm^2
Sampling tubes	7.46 ± 0.01 cm^3

3.2 The Gas Chromatography Systems

Analysis of the reaction products was performed by gas chromatography using a thermal conductivity (Gow-Mac model 10-285) chromatographic detector, operated at a filament current of 200 mA. The output from the detector was fed to a Servoscribe chart recorder (type R.E.520.20). The sensitivity, S_A, of the detector to each component of the hydrocarbon mixture was determined by admitting a known pressure of a mixture of accurately known composition to the gas chromatograph and the sensitivity was calculated according to the relation

$$S_A = \frac{\text{Peak area}}{\text{Partial pressure of hydrocarbon}}$$

After four samples of the mixture had been analyzed by the gas chromatograph, the average of the closest three sensitivities was taken as the sensitivity of the detector for that particular hydrocarbon component. This was then used to determine the partial pressures of that hydrocarbon component in the reaction products and hence the percentage composition of the product mixture could be deduced.

In the separation of the products of the hydrogenation of acetylene, a column containing 40-60 mesh activated silica gel was used. The column was 1 metre long, 2 mm internal diameter, packed with activated silica gel, and operated at 40°C, using helium as the carrier gas at a flow rate of 60 ml min^{-1}. The inlet of the column was connected to a sample handling unit (Figure 16) which was connected

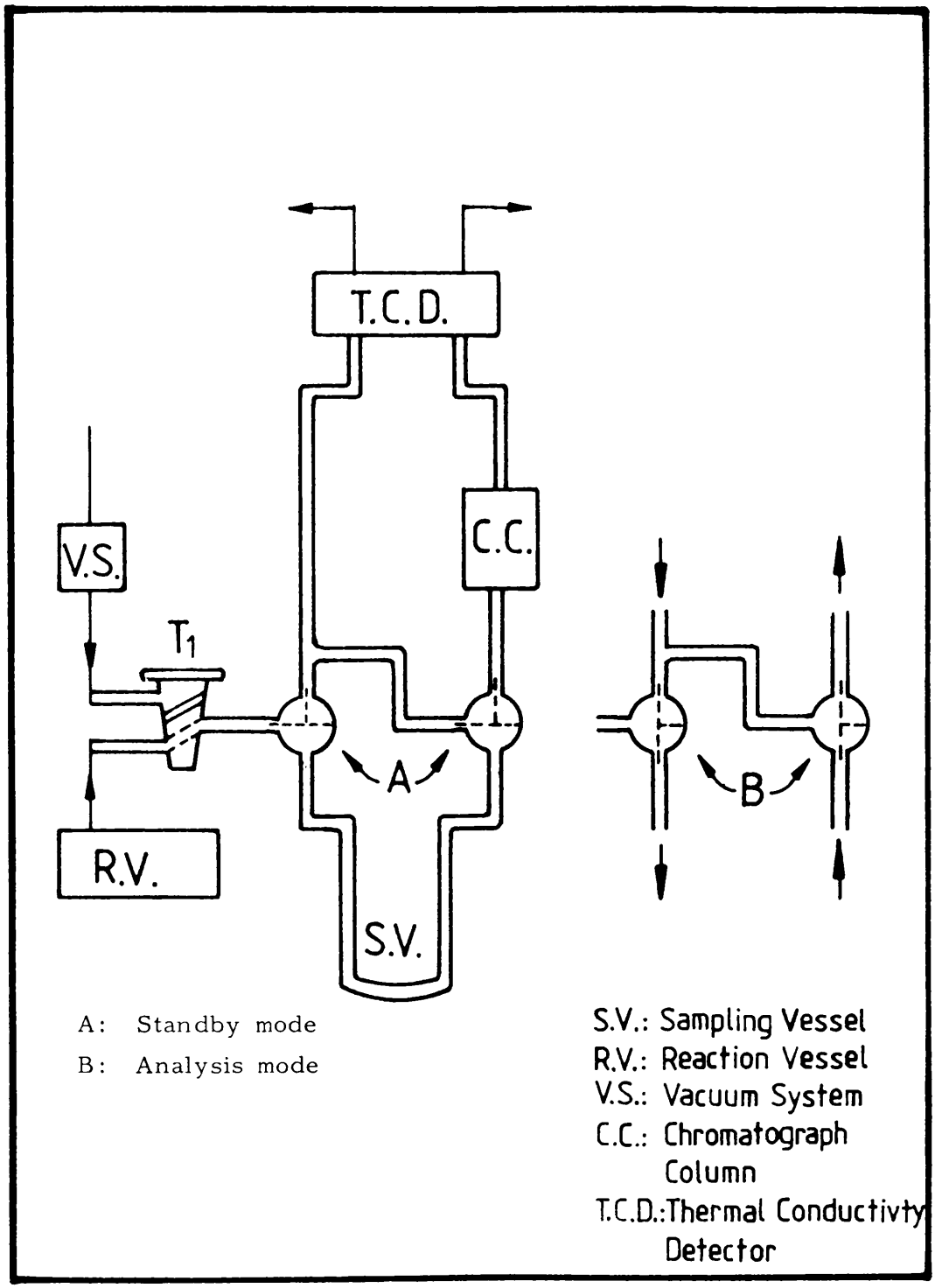

Figure 16. Sample handling unit

directly to the reaction vessel in which samples from the reaction products can be analyzed during the course of the reaction. A typical separation of a hydrocarbon mixture of ethane, ethylene, and acetylene is shown in Figure 17. The retention time of each component of the hydrocarbon mixture on the column measured from the injection point were as follows:

Hydrocarbon	Retention time (min.)
Ethane	1.30
Ethylene	2.40
Acetylene	7.80
C_4-Hydrocarbons	18.20

Peak areas were determined by direct measurement of the peaks using a fixed arm planimeter.

In the case of buta-1,3-diene hydrogenation, reaction products were collected in sampling vessels which in turn connected to a micro vacuum line attached to the gas chromatograph. The products then passed through a U-tube similar to that shown in Figure 16. The column employed was 12 metres in length, and 6 mm external diameter, packed with 33% dimethyl sulpholane supported on 40-60 mesh chromosorb-P. It was operated at room temperature with helium as the carrier gas at a flow rate of 60 ml min^{-1}. The retention time of the hydrogenation products was measured prior to each experiment by pulsing a known pressure of a pre-mixed mixture of n-butane, but-1-ene, trans-but-2-ene, cis-but-2-ene and buta,1,3-diene in to the gas chromatograph.

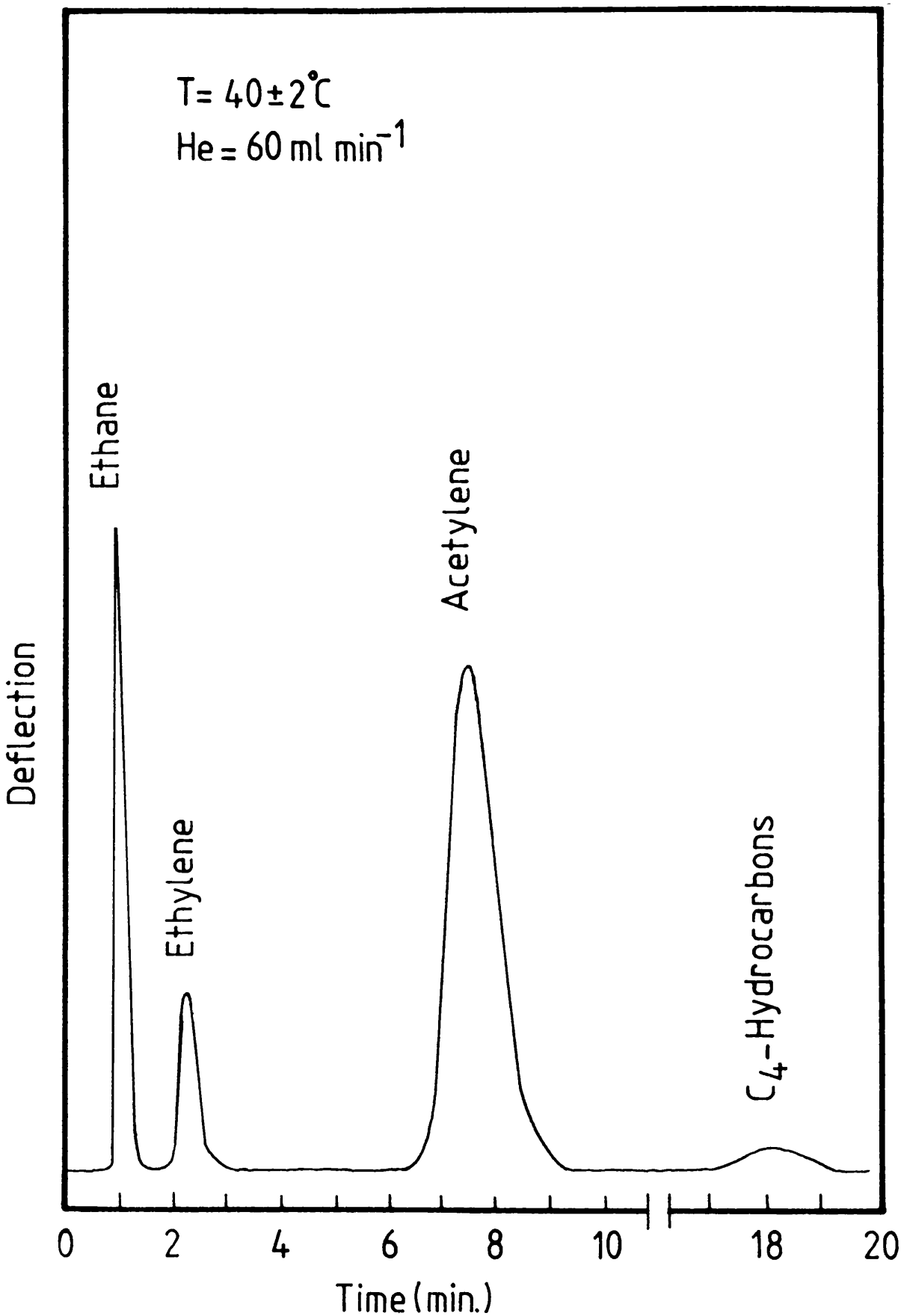

Figure 17. A typical gas chromatograph trace from a mixture of ethane, ethylene and acetylene.

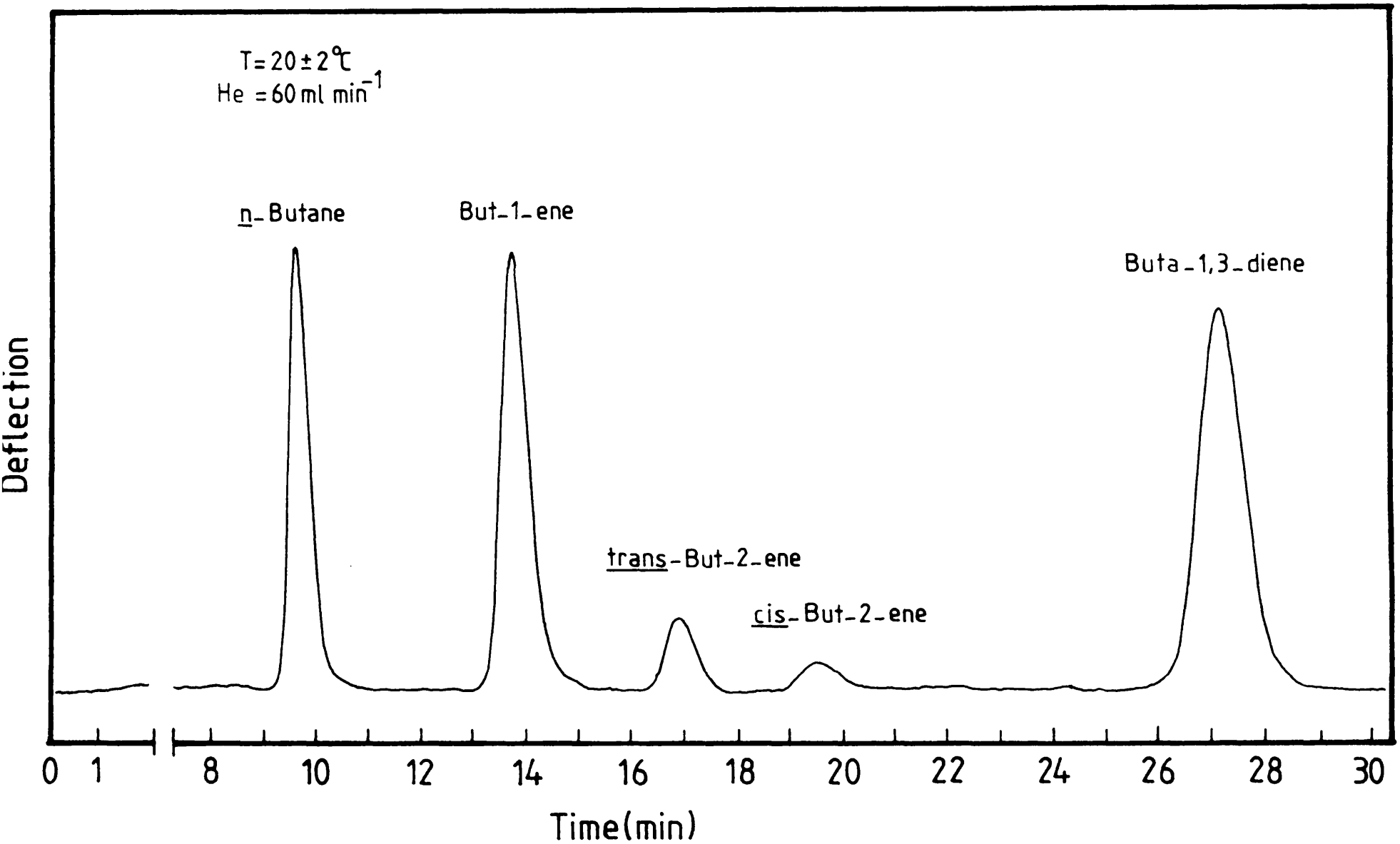

Figure 18. A typical gas chromatograph trace from buta-1,3-diene hydrogenation products.

A typical trace of the chromatogram obtained is shown in Figure 18 and the retention time of each hydrocarbon was as tabulated below:

Hydrocarbon	Retention Time (min.)
n-Butane	9.70
But-1-ene	13.70
trans-But-2-ene	16.89
cis-But-2-ene	19.35
Buta-1,3-diene	27.34

3.3 Preparation of [14-C]-Carbon Monoxide

[14-C]-Carbon monoxide was prepared by the reduction of [14-C]-carbon dioxide (1 mCi batches, specific activity 59.9 mCi m mol^{-1} , supplied by the Radiochemical Centre, Amersham) with metallic zinc. The apparatus, which was used for the reduction process, is shown in Figure 19. It contained small pellets, each of about 5 mm diameter, which were made from a moistened mixture composed of 95% (w/w) zinc mixed with Aerosil silica, the silica being used to increase the porosity and to prevent clogging. The zinc pellets were dried at 120°C in an air oven for about 24 hours before being introduced into the converter. With the [14-C]-carbon dioxide sample attached to the B14 joint, the converter was degassed for 24 hours at 320°C. The temperature was provided by surrounding the part of the converter containing the zinc pellets with an electric furnace and the current was controlled by a Variac transformer.

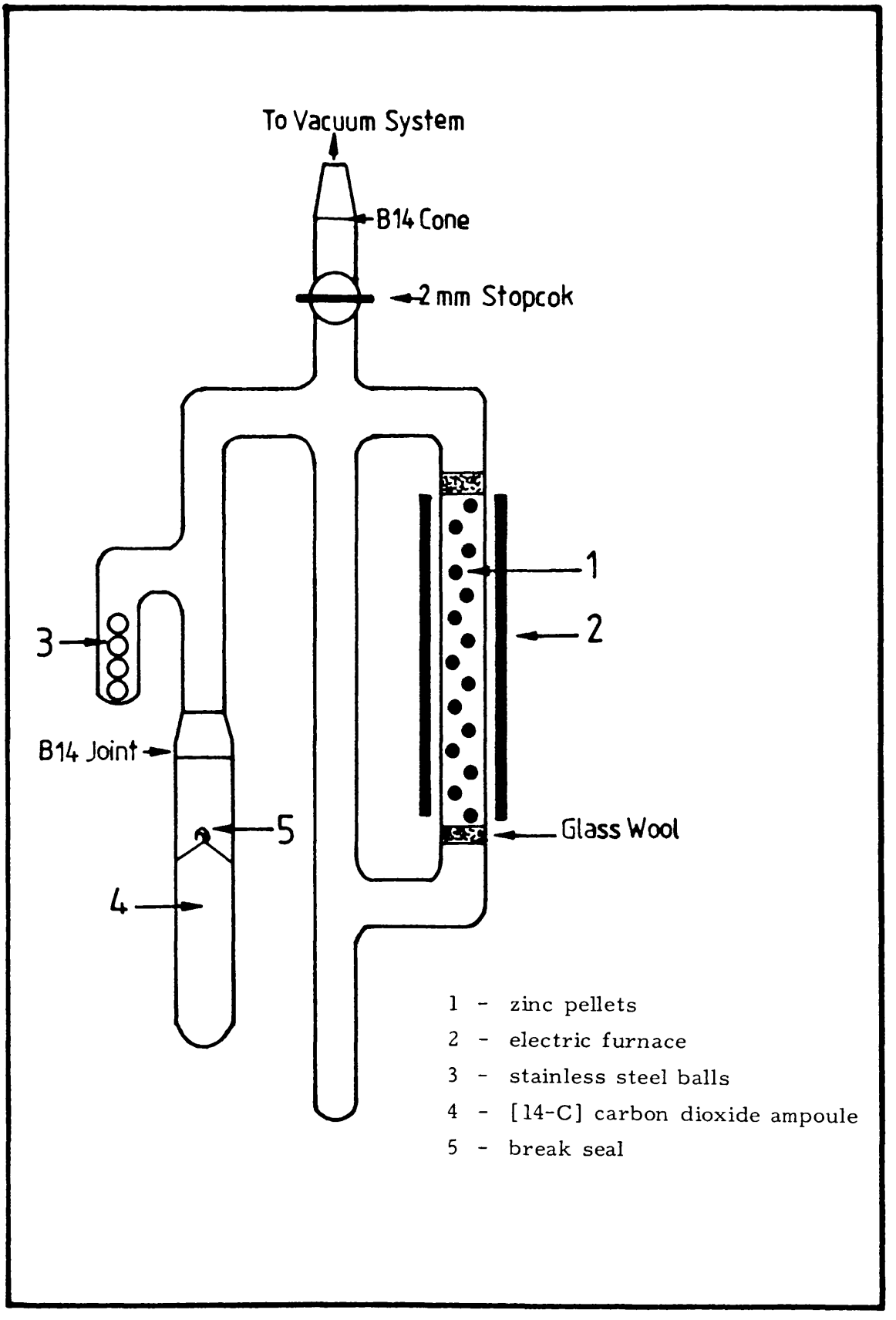

Figure 19. Apparatus for the conversion of [14-C] carbon dioxide to [14-c] carbon monoxide.

The temperature was measured using a Comark electronic thermometer with the hot end of the thermocouple attached to the side of the converter. The [14-C]-carbon dioxide was then introduced into the converter by rupturing the break seal of the ampoule using the stainless steel balls and an external magnet. The conversion of [14-C]-CO_2 with zinc pellets at ~ 380°C was completed in about 72 hours. The [14-C]-CO was allowed to expand into a 250 ml storage bulb and diluted with non-radioactive carbon monoxide (Air Products Ltd.) to the required specific activity.

3.4 Preparation of [35-S]-Hydrogen Sulphide

The apparatus used in the preparation of the radioactive [35-S]-H_2S is shown in Figure 20. It consisted of a standard vacuum line, constructed from capillary glass tubing (2 mm i.d.) to minimize the loss of sulphur material during its synthesis. The vacuum in the system was achieved by using an oil rotary pump (R.P.) situated behind two liquid N_2 traps (LN_2). Pressures were measured using a mercury manometer (M.M.) attached to the main manifold. Two P_2O_5 + liquid N_2 traps (5 cm^3) were incorporated into the system for the purification of [35-S]-H_2S, and four B14 joints permitted the transfer of the radioactive gas into storage ampoules. The gas was generated in a 50 cm^3 rounded flask (B) fitted with a double-limbed separatory funnel (S) containing the decomposing acid.

[35-S]-H_2S was prepared according to the equation

$$Na_2S.9H_2O + H_3PO_4 \rightleftharpoons H_2S + Na_2HPO_4 + 9H_2O$$

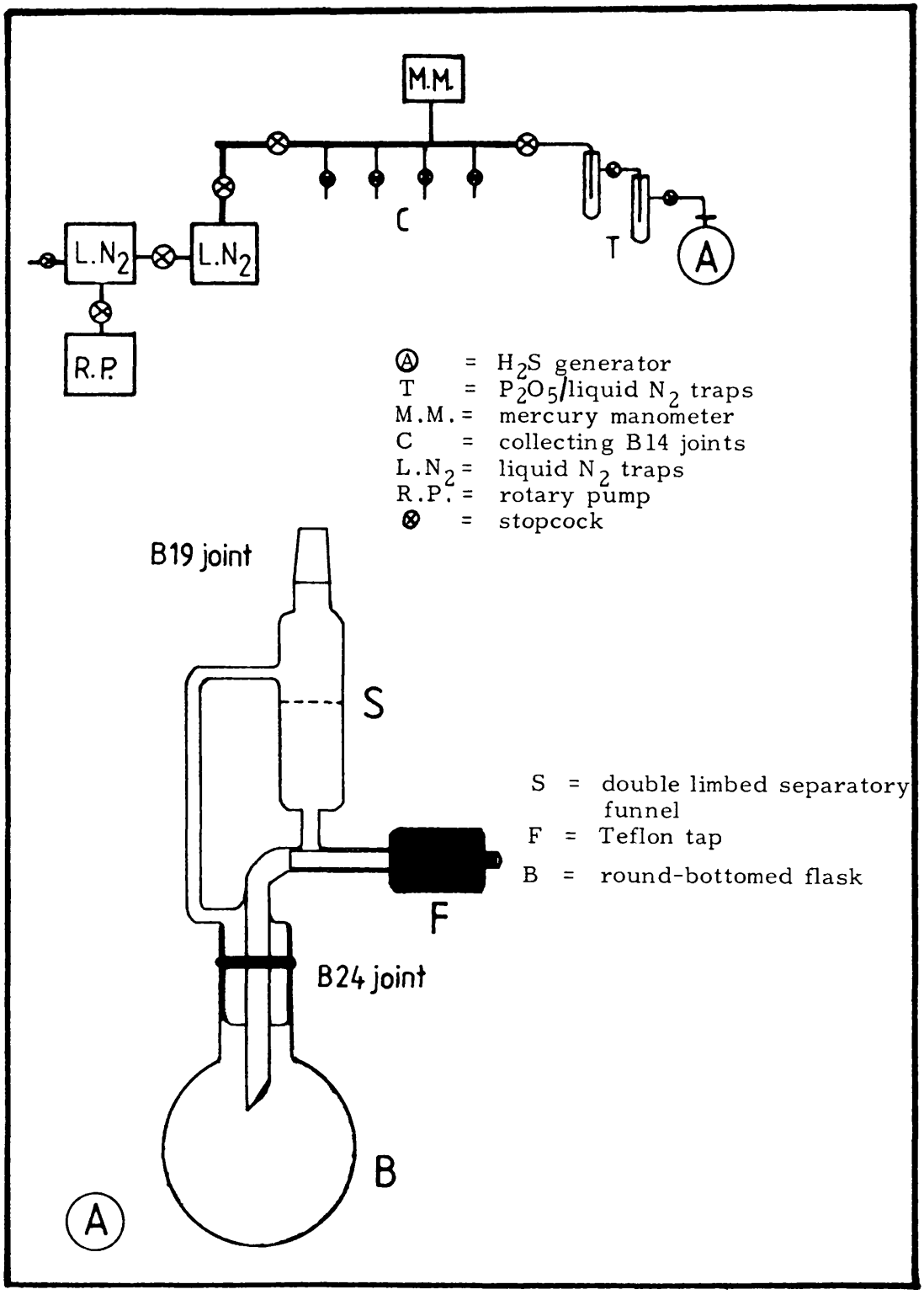

Figure 20. [35-S]-Hydrogen sulphide preparation line.

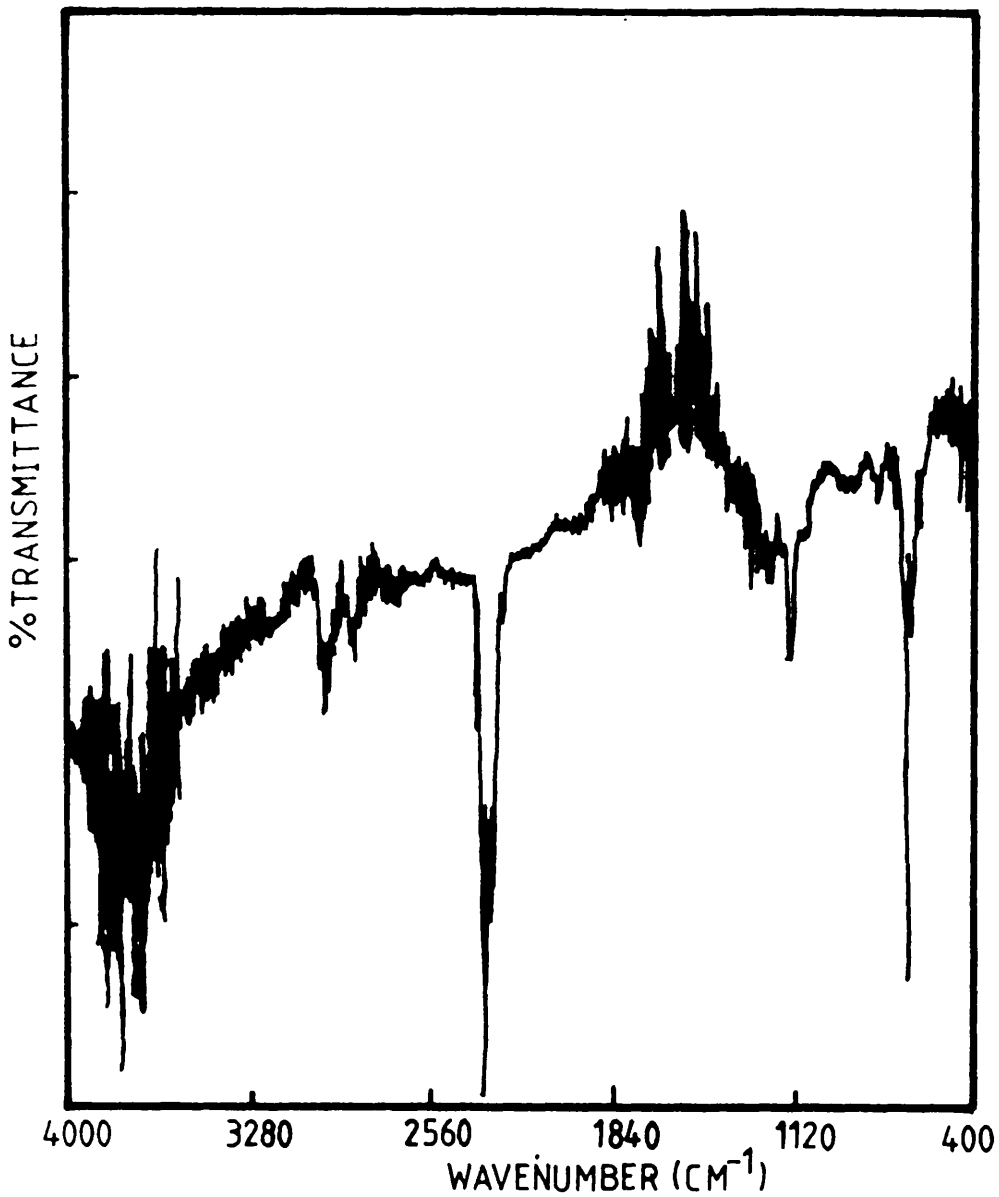

Figure 21. Infrared spectra of H_2S (gas).

5.9 mg [35-S]-Na_2S, (Sigma Radiochemicals), of specific activity 186.5 mCi g^{-1} was loaded into the rounded flask and diluted with 508.2 mg inactive $Na_2S.9H_2O$, 5 ml of 20-30% phosphoric acid, H_3PO_4, was allowed to drip slowly from the separatory funnel into the sodium sulphide solution. The evolved gas was dried over P_2O_5 + liquid N_2 traps, transferred into storage ampoules and used as required. Analysis of the [35-S]-H_2S thus produced by infrared spectroscopy showed bands at 2992 cm^{-1}, 2848 cm^{-1}, 2358 cm^{-1}, 2329 cm^{-1} and 1134 cm^{-1} (Figure 21).

3.5 Materials and Catalysts

Hydrogen (B.O.C., commercial grade) was used in the catalyst reduction and hydrogenations without further purification.

Acetylene (Air Products Ltd.) contained both air and acetone as the main impurities. The air was removed by cooling the mixture in the cold finger at -196°C using liquid nitrogen and then pumping for about 15 minutes. Acetone was removed by three bulb-to-bulb distillations. The acetone was trapped in the cold finger at -78°C using methylene chloride + solid CO_2 mixture, whereas acetylene was trapped at liquid N_2 temperature in the other cold finger bulb. The gas chromatography analysis of the purified acetylene did not show any impurities.

Helium (B.O.C. Ltd., grade A), for use as the carrier gas for the gas chromatography system, was used directly without any further purification.

Methane (Air Products Ltd., c.p. grade), for use as a quenching gas in the proportional counter, was used as supplied (> 99% pure).

Ethane and ethylene (Air Products Ltd. c.p. grade) were used in the calibration of the gas chromatography system after degassing at liquid N_2 temperature (-196°C).

Buta-1,3-diene was used in the hydrogenation experiments and but-1-ene, trans-but-2-ene, cis-but-2-ene and n-butene which were used for the gas chromatography calibrations, were obtained from B.D.H. Ltd. and found to contain no impurities detectable by gas chromatography and were merely degassed before use.

Carbon monoxide and 6% v/v hydrogen in nitrogen, used in the temperature programmed reduction (TPR) experiments were supplied by British Oxygen Co. (B.O.C.) and were found to contain no impurities detectable by gas chromatograph, were used as supplied.

[14-C]-Ethylene, 1.06 mCi (The Radiochemical Centre, Amersham) with a specific activity of 5.8 mCi $mmol^{-1}$ was diluted with non-radioactive ethylene to give a count rate of about 3000 count min^{-1} $Torr^{-1}$.

[14-C]-Acetylene, 500 μCi (The Radiochemical Centre, Amersham) with a specific activity of 1.08 mCi $mmol^{-1}$ was diluted with non-radioactive acetylene to give a count rate of about 3000 count min^{-1} $Torr^{-1}$.

[14-C]-Carbon monoxide was prepared by the reduction of [14-C]-carbon dioxide (see section 3.3), which was obtained as the gas, or was prepared from barium [14-C]-carbonate, both obtained from the Radiochemical Centre, Amersham.

The precursor [35-S]-Na_2S for the preparation of [S-35]-H_2S was supplied by Sigma Radiochemicals (see section 3.4).

Catalysts

In order to achieve a better understanding of catalysts and reactions occurring on them, the Council of Europe Catalysis Group (EUROCAT) designed a series of catalysts to be used as standard catalysts by the academic and industrial scientific communities. These catalysts are currently the subject of a comprehensive characterisation at various laboratories in Europe, using a variety of methods.

A 6% (w/w) Pt/SiO_2 catalyst designated as EUROPT-1 was prepared by Johnson Matthey Chemicals plc. 6 kg dry weight of SiO_2 (Sorbosil grade AQ U30 silica gel, supplied by Crossfield Chemicals) was stirred with 60 litres of 0.01M $Pt(NH_3)_4Cl_2$ solution until thoroughly wetted. The slurry was adjusted to pH 8.9 by careful dropwise addition of a basic reagent consisting of 0.01M $Pt(NH_3)_4Cl_2$ and 0.1M $Pt(NH_3)_4(OH)_2$. The slurry was maintained at this pH for 1h by further addition of the basic reagent. The slurry was then filtered and washed with demineralised water to free the silica from the chloride ion and then dried for 16h in a circulating-air oven at 105°C. The reduction of the material was carried out in a tube furnace under flowing H_2 at 400°C for 0.5h. The platinum content of the catalyst was found to be 6.3 ± 0.1% by weight using atomic absorption spectrophotometry and proton induced X-ray emission (177).

A 0.3% (w/w) Pt/Al_2O_3-0.82% Cl catalyst designated as EUROPT-3 was also prepared and distributed by the Council of Europe

Catalysis Group (EUROCAT) to the participating groups. This catalyst is currently being used as a commercial industrial catalyst and coded as KETJEN-CK303 with a BET surface area of 184 $m^2 g^{-1}$ and a pore volume of 0.49 $cm^3 g^{-1}$ (178).

Another series of platinum catalysts, supported on silica (Cab-O-Sil), γ-alumina (Degusa Ltd.) and molybdenum trioxide (Koch-Light Ltd.) of 99.9% purity, were prepared by Dr. G. McLellan, Glasgow University, by adding the aqueous solution of the metal chloride (H_2PtCl_6) containing the required weight of the metal, to an aqueous suspension of the support. The excess water was evaporated using a rotary evaporator and the materials were then dried in an air oven at 150°C. These catalysts were characterised as 0.8% (w/w) Pt/SiO_2, 0.8% (w/w) Pt/Al_2O_3, and 0.5% (w/w) Pt/MoO_3 and were referred to as impregnated catalysts and were used in this study for comparison of the results obtained with those obtained on the EUROPT-catalysts.

3.6 The Experimental Procedure

In the studies discussed in this thesis, catalysts when employed for adsorption of [14-C]-labelled gases or acetylene hydrogenation, were weighed, placed in the boat, slurried with H_2O, spread evenly at the boat walls, and were then dried using a hair dryer. After the catalyst had been evacuated briefly, the reaction vessel was isolated from the vacuum system, hydrogen was introduced to the catalyst with the glass boat at position (2) at a flow rate of 30 ml min^{-1} and the temperature was then raised gradually to 250°C and maintained

at this value for 2h. The catalyst was then evacuated at 250°C for 30 min. and cooled in vacuo to room temperature. It was assumed that, under these conditions, catalysts were almost free from adsorbed hydrogen, as has been reported by Altham and Webb (43).

The adsorption isotherms were determined by admitting accurately known pressures of the radioactive gas measured, using the pressure transducer, to the catalyst sample in compartment (b) of the glass boat situated at position (1). After each aliquot had been admitted, an interval of approximately 20 minutes was allowed for equilibration to take place. With the boat at position (1), Geiger-Müller (GM.A) recorded only the gas phase radioactivity and Geiger-Müller (GM.B) recorded the gas phase radioactivity of a similar volume of gas to that sensed by (GM.A) plus the radioactivity arising from the material adsorbed on the catalyst surface. Hence, the amount of radioactive material adsorbed on the surface could be determined by subtracting the counts recorded by (GM.A) from those recorded by (GM.B), after each individual count rate had been corrected for dead-time and background, as described in section 3.1.1.2. This procedure was repeated several times and a plot of the adsorption isotherm obtained.

Before each hydrogenation, a mixture of acetylene and hydrogen was prepared by admitting an accurately measured pressure of acetylene into the mixing vessel and condensing it at liquid nitrogen temperature (-196°C) in the cold finger. A known pressure of hydrogen was then admitted until the required ratio of acetylene: hydrogen was obtained. The two gases were allowed to mix for at least one hour before use.

Acetylene hydrogenation reactions were carried out by introducing 50 Torr of the reaction mixture (3:1, hydrogen:acetylene) into the reaction vessel with the boat containing the catalyst at position (1). The reaction was followed by monitoring the pressure fall using the pressure transducer. Samples from the reaction mixture were extracted into the sample handling unit (Figure 16) with the taps in position (A), and then introduced to the radio-gas chromatographic system for analysis with the taps in position (B). In a typical hydrogenation reaction six samples were analyzed during the course of the reaction.

When catalysts were used for buta-1,3-diene hydrogenation, they were weighed, placed inside the reaction vessel (Figure 15) which was then attached via a 2mm stopcock and B10 joint to the vacuum system. The vessel was evacuated for ~ 20 min. before a pressure of 200 Torr H_2 was introduced. The reaction vessel was then isolated from the vacuum system via the 2 mm taps, surrounded by an electric furnace, and gradually heated to 250°C. After 2h the catalyst was evacuated for 30 min. at 250°C and then cooled *in vacuo* to room temperature.

The reaction mixture (3:1, buta-1,3-diene:hydrogen) was prepared before each series of hydrogenation experiments, by admitting a known pressure of the butadiene into the mixture vessel, followed by hydrogen until the required ratio was obtained. The two gases were allowed to mix for 2-3h before use.

Buta-1,3-diene hydrogenation reactions were performed by introducing 50 Torr of the reaction mixture (3:1, H_2:diene) into the

reaction vessel and monitoring the reaction pressure fall by using the pressure transducer (section 3.1.1.4). Samples from the reaction products were extracted at various stages of the reaction and analyzed by the gas chromatograph (section 3.2).

In the [35-S]-hydrogen sulphide poisoning experiments, catalysts were prepared and reduced as described above. When [14-C]-hydrocarbons, [14-C]-carbon monoxide adsorption or C_2H_2/H_2 hydrogenation experiments were required, an aliquot (0-5 Torr) of the radioactive-H_2S was admitted into the reaction vessel (section 3.1.1.1), kept in contact with the catalyst for 15 min, the radioactivity content was counted, the reaction vessel was then evacuated for 15 min to remove any gas phase H_2S, and three successive count rates, which represent the sulphur-uptake by the catalyst (see section 4.6.1.), were recorded. The adsorption or hydrogenation (C_2H_2/H_2) experiments were then performed in the way described above.

Poisoning experiments for buta-1,3-diene hydrogenation were carried out in a reaction vessel similar to that shown in Figure 15. After each catalyst had been reduced and treated, as described above, it was subjected to a pulse of [35-S]-H_2S. The reaction vessel was then evacuated for 15 min before the hydrogenation reaction was carried out in the manner described above. The amount of H_2S adsorbed on the catalyst was determined from the pressure of H_2S admitted to the reaction vessel.

3.7 Temperature Programmed Reduction (TPR)

The basic idea of characterising catalyst materials by monitoring the extent of their reducibility was adapted from the H_2-chemisorption experiments of Benesi et al. (175). McNicol and co-workers (176) were the first to report the development of the TPR technique. The technique, as shown in Figure 22, involves the use of a series of valving arrangements (V_1-V_5, V_a and V_b) which allows various gases to be directed over the sample, a thermal conductivity detection system (D) to measure the sample effluent gas composition, sample cell (C), sample heating furance (F), linear temperature programmer (TP) which allows the sample temperature to be ramped at specified and adjustable rate, recorder, traps (T_1 filled with molecular sieve, T_2 cooled to -80°C) using dry ice/$CHCl_3$ to remove reduction products, and mass spectrometer to detect the desorbed species. Basically, the same apparatus can be used for the temperature programmed desorption/oxidation (TPD and TPO) and surface area determination.

When the system was used for TPR, the catalyst sample was weighed and contained in a fused silica glass cell (C), positioned inside the furnace, and flushed with helium gas at a flow rate of 30 ml min^{-1} to remove the physically adsorbed impurities. The gas flow over the sample was then changed to 6% H_2/N_2 with V_b at position 1 and the flow adjusted to 30 ml min^{-1}. After allowing a short period (typically 20 min.) for the detector system to stabilize, the sample temperature was then ramped at a linear rate of 10°C min^{-1} up to the required temperature (up to 500°C in this work) depending on the cell fabrication material (Pyrex glass 500°C, fused silica glass 750°C, stainless

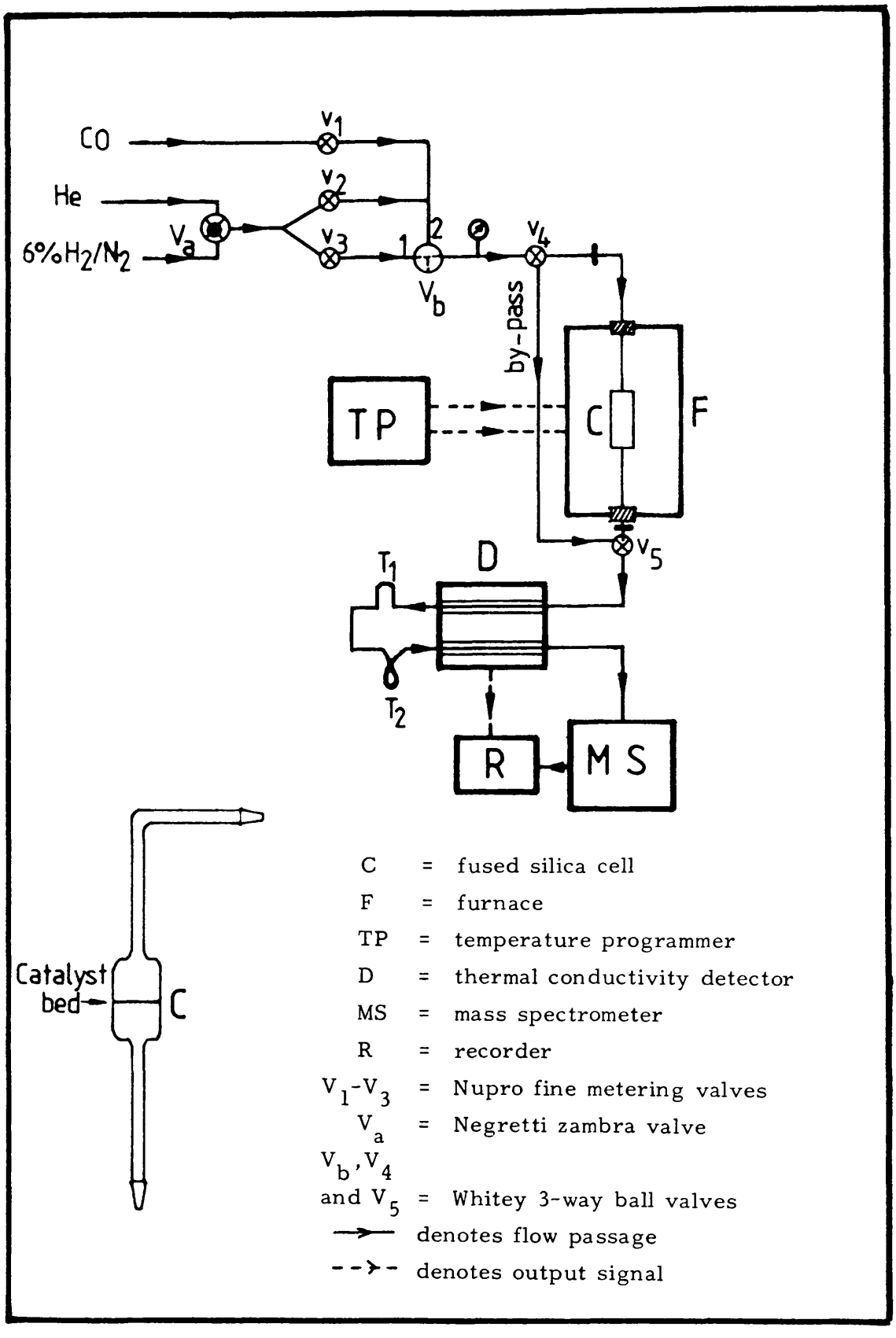

Figure 22. Block diagram of the TPR apparatus.

steel > 750°C), and the hydrogen concentration in the effluent gas stream recorded as a function of sample temperature. At the end of a TPR experiment the catalyst sample was cooled to the required temperature (to room temperature in this work). A subsequent temperature-programmed desorption (TPD) experiment could then be carried out by changing the gas stream to helium (V_b at position 2) at a flow rate of 30 ml min^{-1}. After allowing sufficient time for the detector base line to become constant (~ 15 minutes), the sample temperature was then ramped at a linear rate of 10°C min^{-1} and the hydrogen concentration in the effluent stream recorded as a function of sample temperature.

When a carbon monoxide adsorption was required, the catalyst was reduced in the same manner as described above, the temperature held ~ 500°-600°C for 20 min with the gas stream switched to helium (V_b at position 2) at flow rate of 30 cm^3 min^{-1}. The sample was then cooled to room temperature and the catalyst was subjected to a series of pulses of CO. When the catalyst had reached a saturation point, the amount of CO chemisorbed by the catalyst could be deduced by subtracting the peak areas of the CO recorded for pulses over the catalyst from those of a standard CO pulse, that is, (P.A. (standard)-P.A. (sample)). From the amount of CO adsorbed on the catalyst, information relating to the catalyst metal surface area could be obtained.

3.8 The Preparation of Catalysts for Electron Microscopy

Samples of catalysts pre-deactivated by hydrocarbon adsorption, hydrogenation reactions, or carbon monoxide adsorption were examined by Transmission Electron Microscopy (TEM) and Scanning Electron Microscopy (SEM) to investigate the effects of these processes on the catalyst's morphology.

When catalysts were probed by TEM, the microscope employed was a JEOL 1200 EX instrument, operated with an accelerating voltage of 120 kV. Catalyst samples were ground manually or the fines were used directly. The fine materials were then added to H_2O and mounted onto standard 3 mm copper grids, covered with carbon films and then fired.

When the catalysts were investigated by SEM (model, Philips EM420), they were prepared by embedding the samples in a methyl methacrylate-butyl methacrylate mixture, followed by an ultrathin sectioning using a diamond knife. (for EUROPT-1).

3.9 The Preparation of Catalysts for Infrared Investigations

Catalyst samples which were employed for the adsorption of [14-C]-hydrocarbons or [14-C]-carbon monoxide, or for hydrogenation reactions, were examined by FTIR-infrared spectroscopy, using a Nicolet 5-DXC instrument to identify the surface species formed during the adsorptions or surface interactions and also to examine the effects of various treatments on these species, such as, heating or flushing with carrier gases such as He. The in situ I.R. cell used for this purpose is shown in Figure 23. This cell contained a catalyst wafer

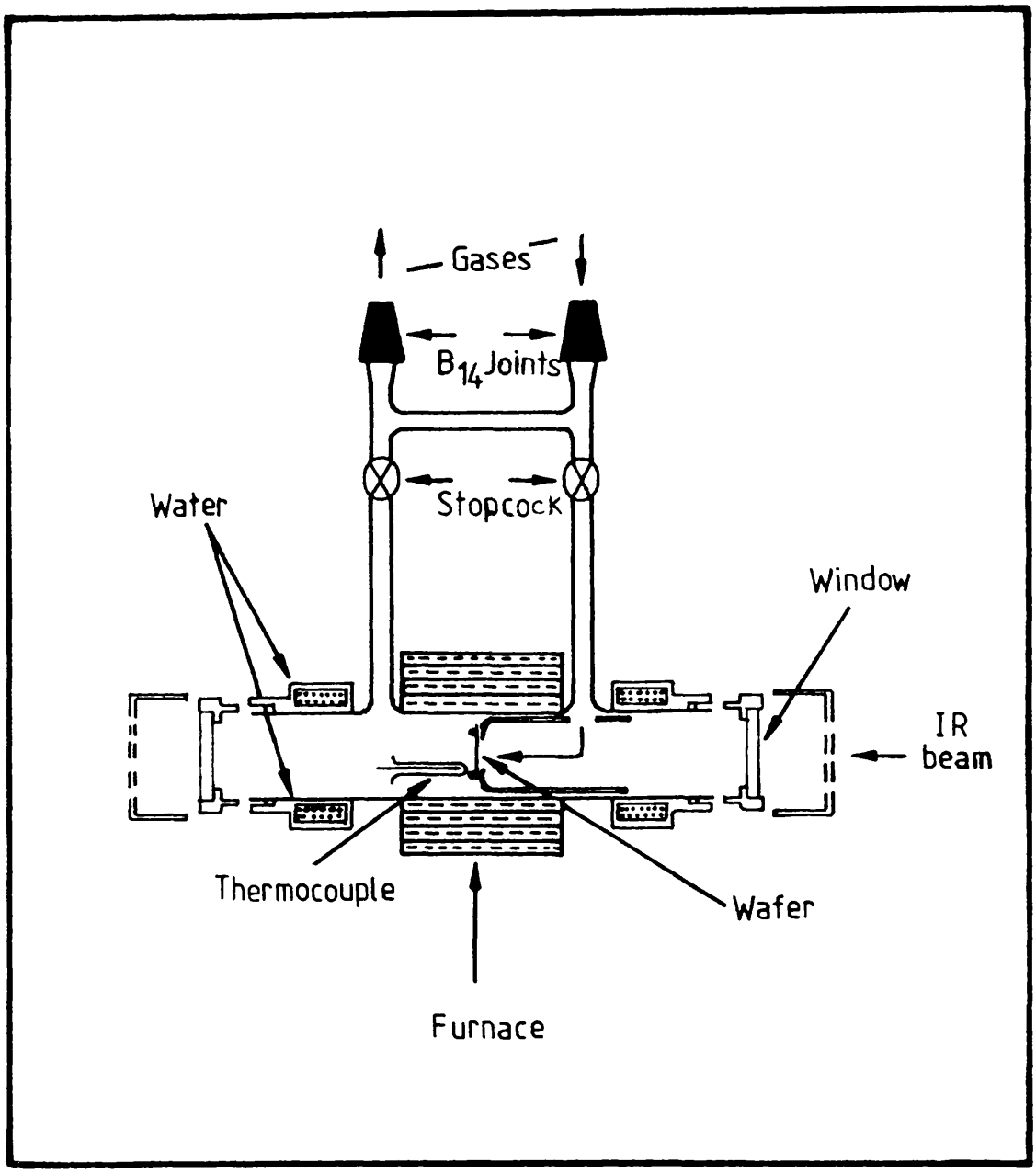

Figure 23. The in-situ IR cell

specimen holder. A Nichrome-wire furnace surrounding the outer body of the quartz cell was capable of heating the wafer sample to 800°C. The temperature in the I.R. cell was monitored by an electronic thermometer (Electronics Ltd. - 1602 Cr/Al) coupled to a chromel-alumel thermocouple located in a thermowell close to the sample. Two KBr windows (25 x 4 mm Barns), sealed in stainless steel rings with Araldite adhesive, were fitted to the two ends of the I.R. cell by stainless steel threaded jackets and sleeves surrounded by a water coolant system to prevent thermal shock to the KBr windows. The cell could be pumped to 10^{-4} Torr using a vacuum line fitted with a mercury diffusion pump backed with an oil rotary pump. The catalyst powders (~ 0.05g) were pressed in to wafer discs in air (~ 7 tonnes pressure). The wafers were placed in the I.R. cell and about 500-1000 scans were recorded. This was usually followed by I.R. measurements of the sample after a brief evacuation (~ 10 minutes), flushing with He (25 ml min^{-1}), or heating to an elevated temperature.

When direct adsorption of carbon monoxide or hydrocarbons was required, a diffuse reflectance collector (type DRIFT - Spectra-Tech Inc.) was used. The design of the collector employs 4 flat and 2 aspherical reflectors, plus an alignment mirror (Figure 24). The aspherics are off-axis ellipsoids which focus and collect infrared energy with a 6x condensation of the beam. A typical FTIR-spectrophotometer beam has from a 3 mm to 18 mm spot size at the focus, so the spot size with the DRIFT cell will be between 0.5-3.0 mm. The sample cup (13 mm, i.d.) could be removed (for emptying and filling) from the top of the collector, by sliding the ellipsoids out of the way. The collector

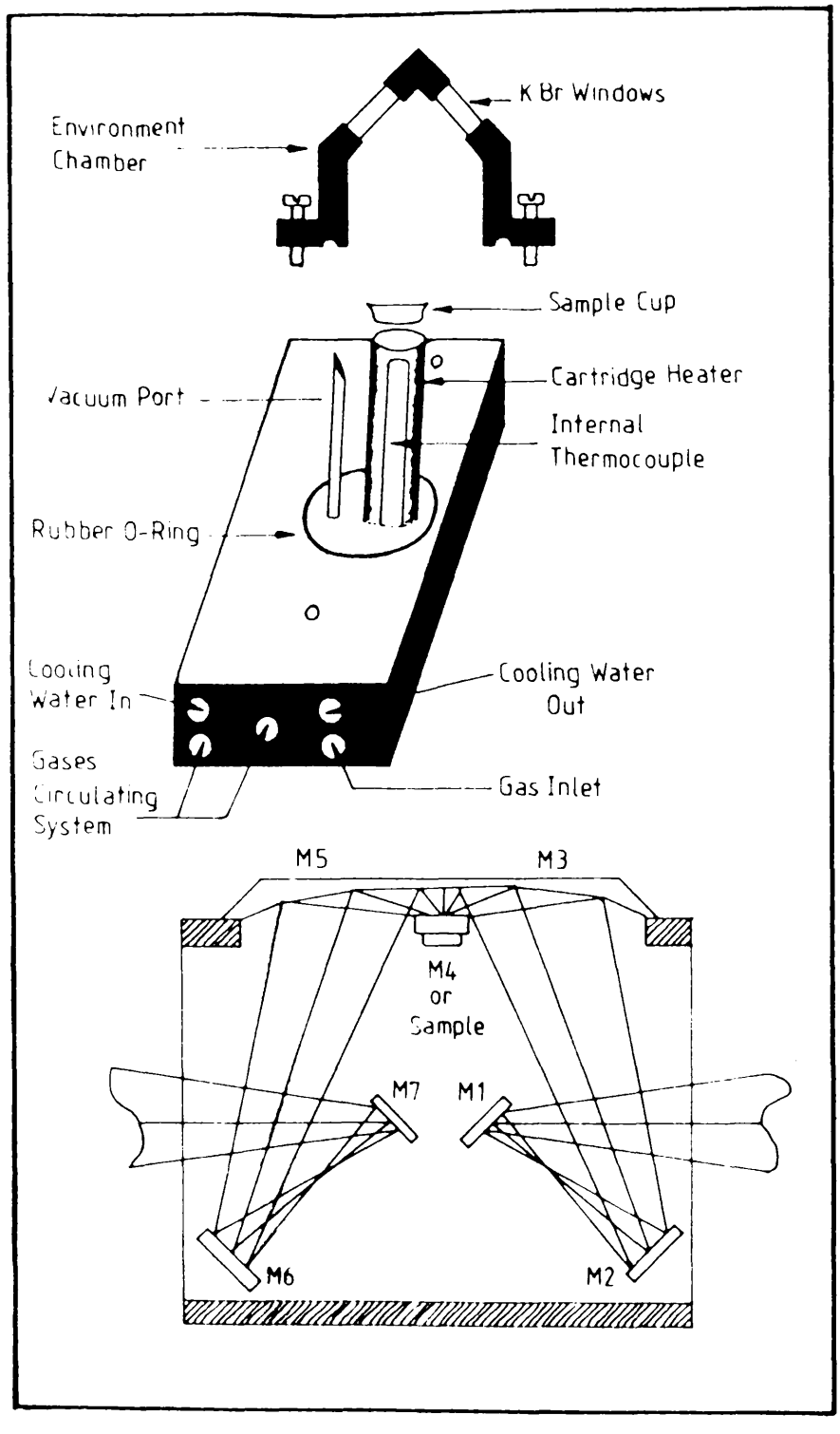

Figure 24. Diffuse reflectance IR cell (DRIFTS).

was connected to a vacuum system fitted with a series of bulbs for handling the adsorbate gases and was capable of producing a vacuum of $\sim 10^{-4}$ Torr in the collector. The catalyst samples were heated to the required temperature by an internal cartridge heater (Figure 24), the current to this was controlled by a Variac controller, and the temperature of the catalyst was monitored with a chromel-alumel thermocouple touching the centre of the catalyst cup.

The procedure used in the 'DRIFTS' experiments was as follows: a background spectra was acquired using KBr as a diffuse reflector in the Nicolet 5-DXC spectrophotometer at 4 cm^{-1} resolution. A catalyst sample was loaded in the cup of the collector and was reduced in flowing H_2 (30 ml min^{-1}) at 250°C for 1h, evacuated briefly ($\sim$ 10 min) at this temperature and then cooled to room temperature. The catalyst was then pulsed with the required adsorbate and after recording the I.R. spectra, the catalyst was subjected to various treatments, such as, evacuation, flushing with He, or heating at elevated temperatures.

3.10 Regeneration of the Catalysts

When the catalysts had been used for [14-C]-acetylene or ethylene adsorptions, or for hydrogenation of acetylene with hydrogen, it was found possible to regenerate them under the following conditions. Heating at 300°C in flowing H_2 (30 ml min^{-1}) for 2h, evacuation at 300°C for 0.5h, followed by cooling to ambient temperature in vacuo. This procedure was efficient in removing about 95 ± 5% of the carbonaceous deposits chemisorbed on the catalysts. However, with catalysts poisoned with H_2S, it was not found possible to remove all of the sulphur

material using the above procedure. Only 18% could be removed, although the regeneration temperature was increased to 350°C. During the regeneration of carbon-deactivated catalysts, the only hydrocarbon product detected in the gas phase over the catalyst, was methane. However, because of the small quantities involved and the fact that this was continuously produced under a hydrogen stream, quantitative determination of the actual amount formed was not possible.

SECTION THREE

RESULTS

CHAPTER FOUR

THE ADSORPTIONS OF ACETYLENE, ETHYLENE AND CARBON MONOXIDE ON Pt CATALYSTS

4.1 ACETYLENE ADSORPTIONS

4.1.1 [14-C]-Acetylene Adsorption on Freshly Reduced 6% Pt/SiO_2 (EUROPT-1) Catalyst

A 0.054g sample of EUROPT-1 catalyst which had been reduced was evacuated at 250°C for 0.5h and allowed to cool *in vacuo* to room temperature. A typical adsorption isotherm for [14-C]-labelled acetylene on freshly reduced catalyst is shown in Figure 25. The shape of the isotherm consisted of a steep primary non-linear region followed by a linear secondary region. In the former region, surface count rate rose rapidly at low pressures below ca. 1 Torr, whereas in the latter region it increased with a gentler slope. The turning point between the two regions was obtained by extrapolating the linear secondary region to zero pressure. The uptake of [14-C]-acetylene was continued up to a gas pressure of about 5 Torr, which was the maximum pressure used. The amount of adsorbed [14C]-acetylene removed from the surface of the catalyst by evacuation of the reaction vessel for about 30 min. was found to be approximately 22.3 ± 1% of the total adsorbed species.

Readsorption of [14-C]-acetylene on the same catalyst sample after evacuation, showed no primary region with much reduced capacity for [14-C]-acetylene adsorption compared to the amount adsorbed on a

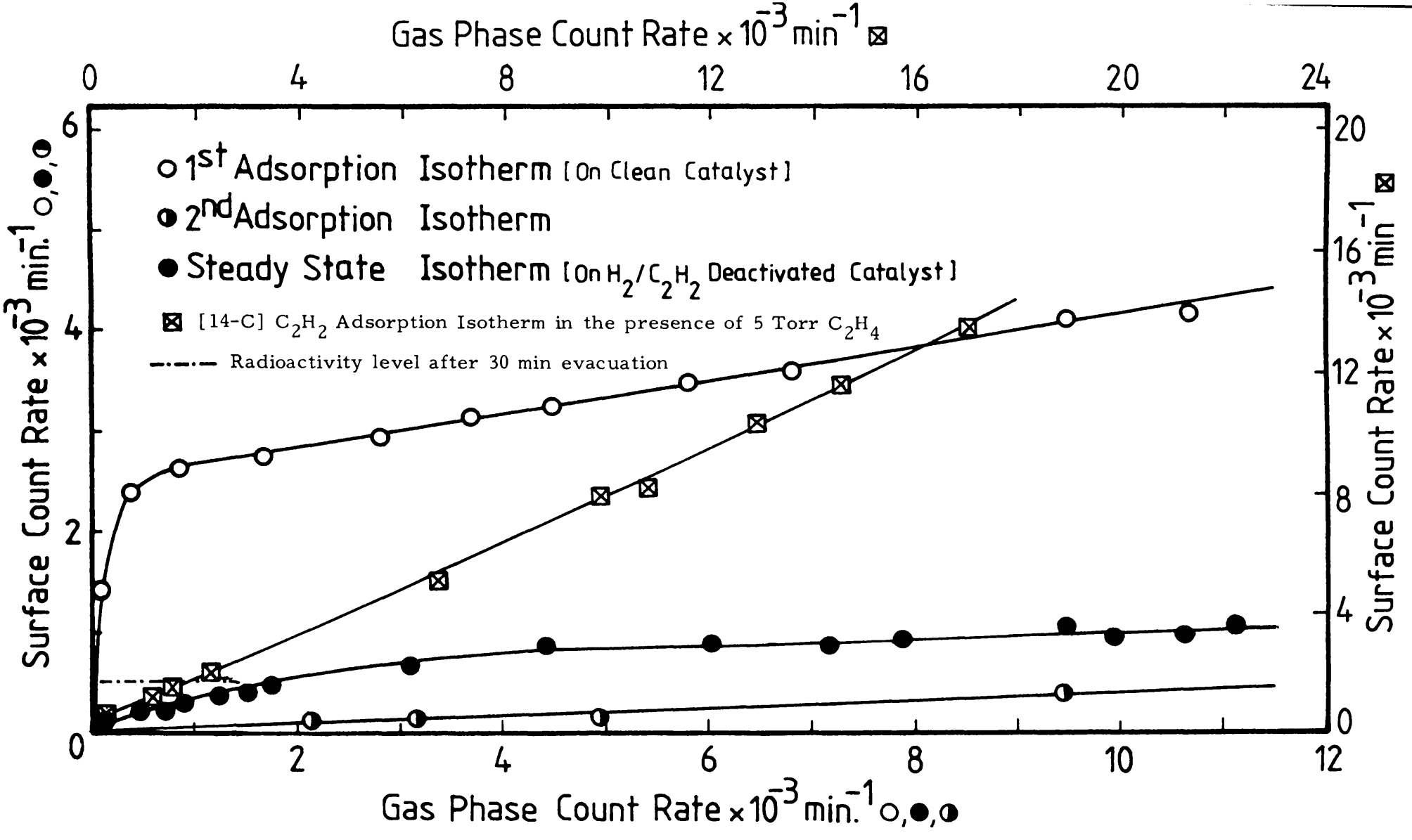

Figure 25. Adsorption isotherms of [14-C] acetylene on EUROPT-1.

freshly reduced catalyst (2nd adsorption, Figure 25).

4.1.1.1 Reactivity of [14-C]-Acetylene Species Adsorbed in Primary Region

In order to investigate the identity of the acetylenic species adsorbed in the primary region and the extent of its participation in the hydrogenation reactions, 0.08g EUROPT-1 catalyst was reduced and treated in the standard manner (see section 3.6). The [14-C]-acetylene adsorption was built up on the catalyst to a point corresponding to the turning point of the primary region (ca. 0.85 Torr). The gas phase hydrocarbon that had been in contact with the surface was then analyzed by radio-gas chromatography. The profiles of the analysis showed a product composition of 87.2 ± 0.5% ethylene and 12.7 ± 0.4% ethane.

In another experiment, 0.095g catalyst was reduced and the [14-C]-acetylene adsorption covering the primary region was built up as described above. After 15 min, the reaction vessel was evacuated for 15 min and a pre-mixed sample of 12.5 Torr acetylene and 37.5 Torr hydrogen was introduced to the reaction vessel. The radioactivity content of the adsorbed acetylene was monitored during the course of the hydrogenation reaction. Several hydrogenation reactions (5 reactions) were carried out on the same catalyst, with the hydrocarbon products of each reaction being evacuated for 20 min between reactions. As shown in Figure 26a, during the course of hydrogenation, the surface count rate fell in two distinct stages. First, the radioactivity level decreased substantially up to a point where a plateau

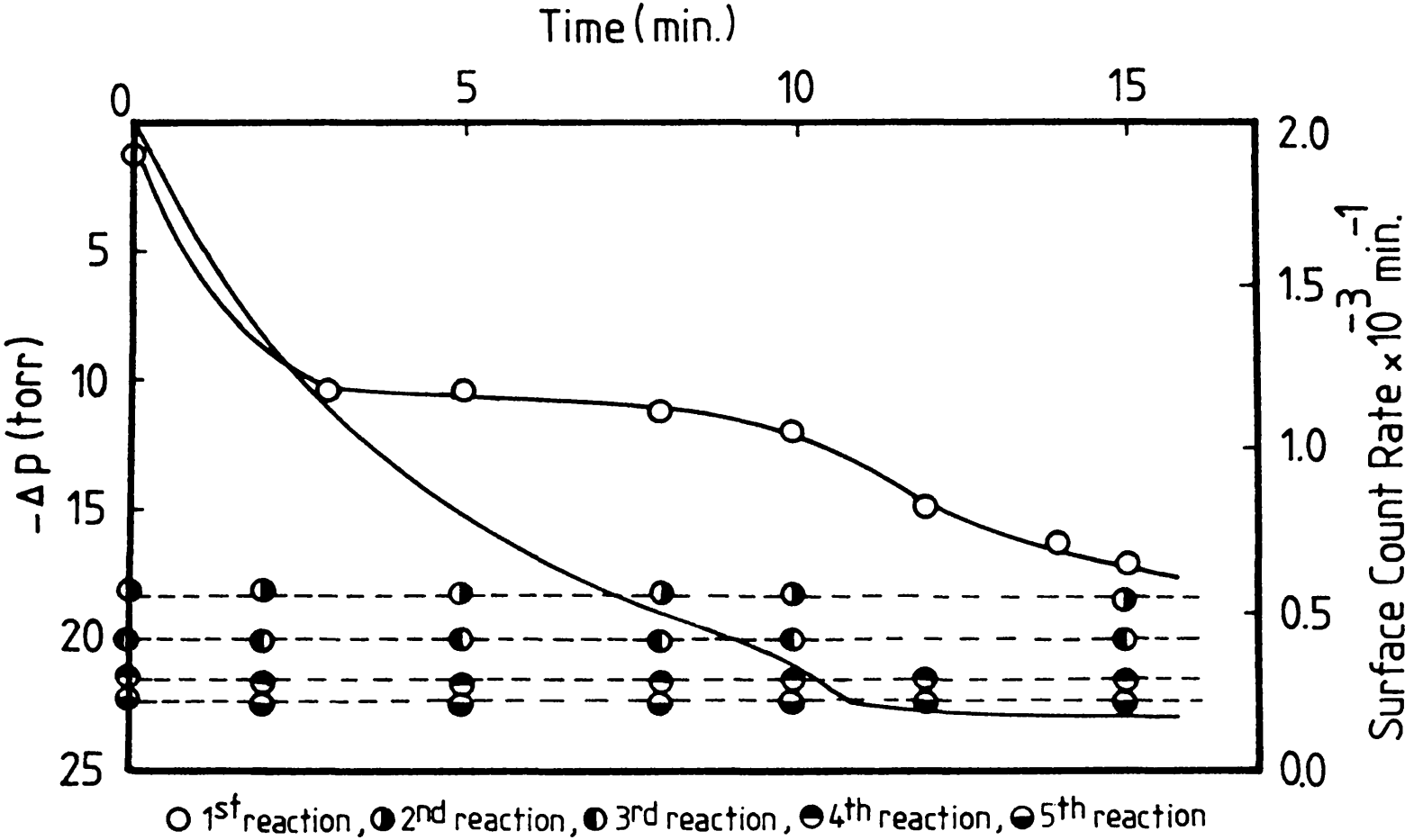

Figure 26a. Reactivity of [14-C] acetylene species adsorbed in primary region.

region was reached. This was then followed by a second stage which showed a more pronounced drop in the surface radioactivity content. From this experiment, a reasonable amount (ca. 68%) of the acetylenic species adsorbed in the primary region was removed from the catalyst surface during the first hydrogenation reaction, plus a further ca. 22% was removed by successive hydrogenations with ca. 10% of the acetylene being retained by the catalyst as a strongly bound species.

4.1.1.2 Effects of Various Treatments on Adsorbed [14-C]-Acetylene Species

The effects of various treatments on the pre-adsorbed [14-C]-acetylene were investigated in order to examine the reactivity of the adsorbed species under similar conditions to those pertaining in acetylene hydrogenation. On a 0.08g of freshly reduced EUROPT-1 catalyst a [14-C]-acetylene adsorption isotherm was built up and various treatments, as shown in Figure 26b, were carried out. From these, it can be seen that as a result of evacuation, ca. 21.2% of the adsorbed [14-C]-acetylene was removed. A further ca. 32% was removable by a series of hydrogenation reactions (6 reactions) using a 3:1, hydrogen:acetylene mixture; the remainder, ca. 47%, was strongly bound on the catalyst surface. The amount removed could not be increased by further hydrogenation.

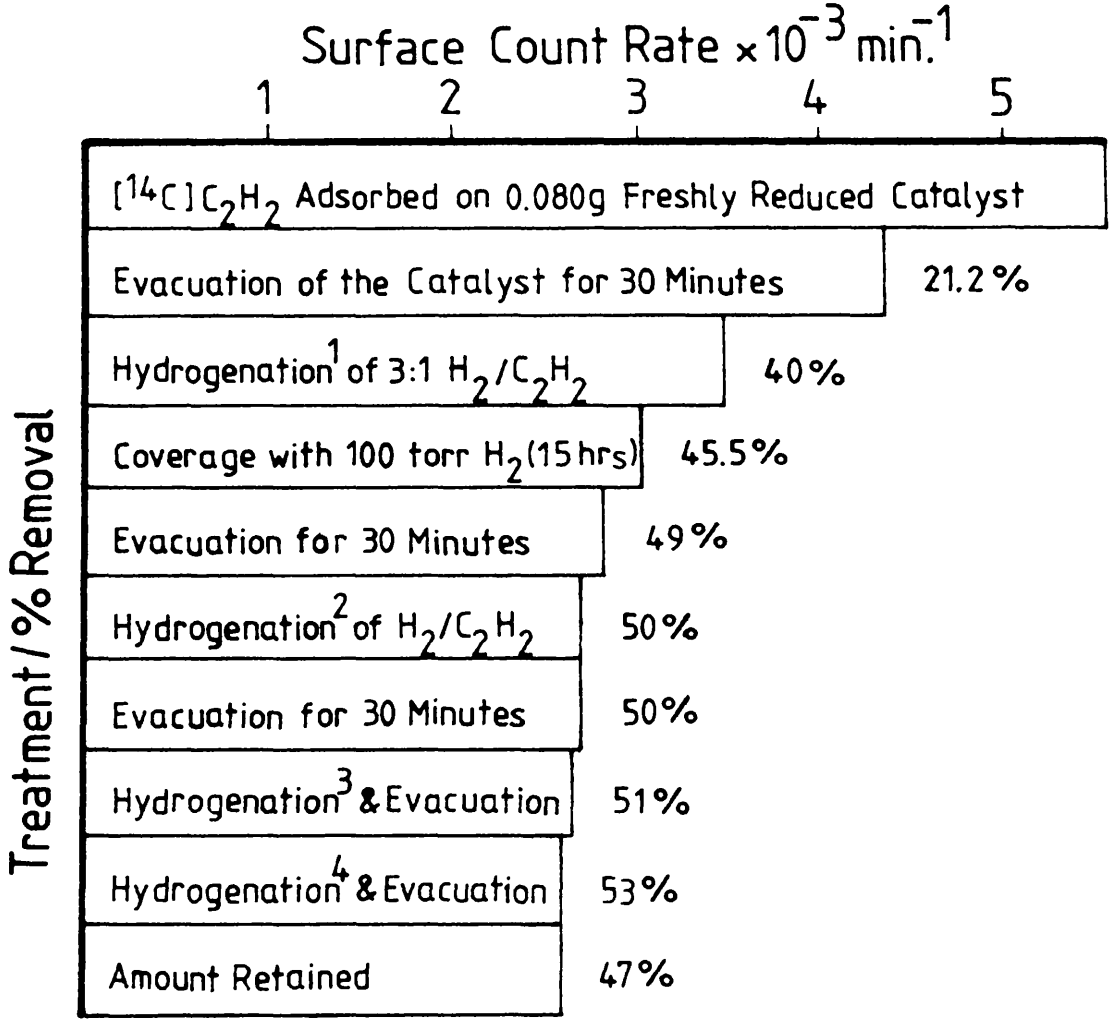

Figure 26b. The effect of various treatments on adsorbed [14-C] acetylene species.

4.1.1.3 Adsorption of [14-C]-Acetylene on Steady State Catalysts

An investigation was made of the behaviour of adsorbed [14-C]-acetylene on the surface of a catalyst deactivated to a steady state by acetylene hydrogenation. A sample of a 0.0947g catalyst was reduced and allowed to cool to ambient temperature in vacuo. A series of 37 reactions of 3:1, hydrogen:acetylene were performed on the catalyst. Before each hydrogenation reaction, the catalyst was evacuated for 20-30 mins. to remove the gas phase hydrocarbon products in the reaction vessel. The catalyst activity (the first order rate constant, K min^{-1}, Figure 41) was determined. Figure 25 shows that the effect of catalyst deactivation by C_2H_2/H_2 decreased the extent of the primary adsorption region and the capacity of the secondary region for [14-C]-acetylene adsorption was reduced considerably, with only a very slight increase in the gradient of the isotherm.

4.1.1.4 Co-adsorption of [14-C]-Acetylene and -Ethylene

The effect of the presence of ethylene on the adsorption of [14-C]-acetylene and vice versa was investigated in order to gain some knowledge about the extent of the possible existence of the thermodynamic factor in the hydrogenation of acetylene on this catalyst.

A 0.10g sample of EUROPT-1 was reduced and treated as described in section 3.6 before being cooled to ambient temperature. A pressure, ca. 5 Torr, of non-radioactive ethylene was admitted to the catalyst and left to equilibrate for 10 min. This was subsequently followed by the adsorption of [14-C]-acetylene on the catalyst in the

manner described in section 4.1.1. The adsorption isotherm obtained is shown in Figure 25. The isotherm showed a significantly different shape from that obtained on the fresh and steady state catalysts. When the catalyst was evacuated for 30 min, a substantial amount, ca. 90%, of the adsorbed species was removed, compared with only ca. 21% from the freshly reduced catalyst.

When aliquots of [14-C]-ethylene were introduced to a freshly reduced catalyst in the presence of ca. 5 Torr non-radioactive acetylene, no adsorption was observed to take place, although a pressure in excess of 8 Torr was used.

4.1.2 [14-C]-Acetylene Adsorption on Freshly Reduced 0.3% Pt/Al_2O_3 (EUROPT-3) Catalyst

A 0.2682g sample of EUROPT-3 catalyst was cleaned with hydrogen for 2h at 250°C, evacuated at this temperature for 0.5h and then allowed to cool to ambient temperature in vacuo. The adsorption isotherm (Figure 27) was obtained by admitting successive aliquots of [14-C]-acetylene to the freshly reduced catalyst. The isotherm showed general behaviour, similar to that observed in the adsorption of acetylene on the EUROPT-1 catalyst. This showed a non-linear primary region and a linear secondary region. The extent of the adsorption in the linear secondary region continued to increase with increasing pressure but no plateau was reached even though a gas pressure in excess of 4 Torr was used. However, in comparison with the adsorption isotherm of acetylene on EUROPT-1, this isotherm showed a less steep primary region with a much more positive gradient in the secondary

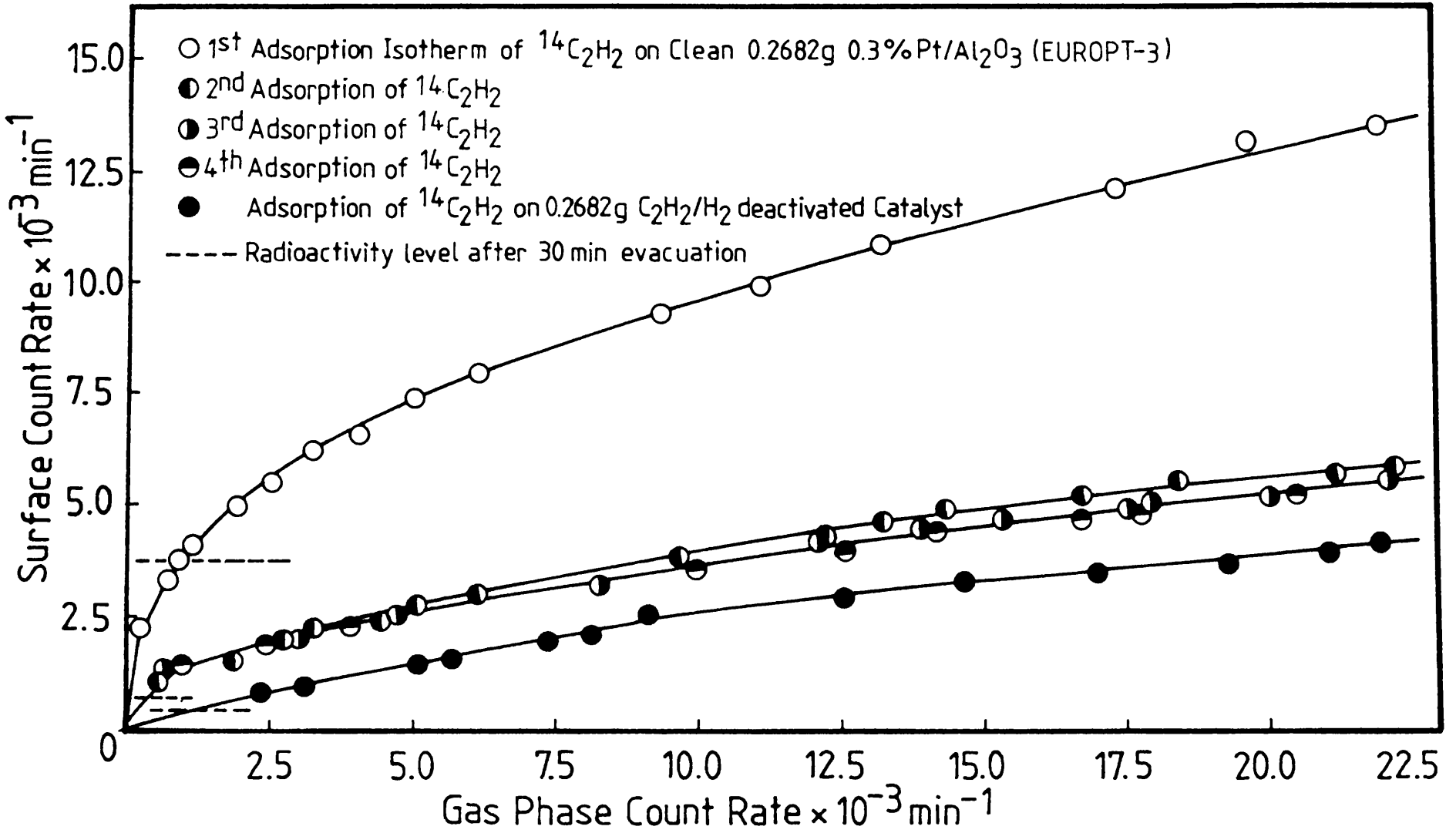

Figure 27. Adsorption isotherms of [14-C] acetylene on EUROPT-3.

region as the pressure was increased.

When the catalyst used above was evacuated for 30 min, ca. 73% of the adsorbed acetylene was removed. This removable [14-C]-acetylene could be restored by successive adsorption and evacuation cycles (adsorptions 2-4, Figure 27).

4.1.2.1 Effects of Various Treatments on Adsorbed [14-C]-Acetylene

To establish an understanding of the nature and identity of the acetylenic species adsorbed on EUROPT-3 catalyst, an adsorption isotherm of [14-C]-acetylene was built up on 0.2682g of catalyst which had been reduced and treated as described in section 3.6. This was followed by a series of treatments which are summarised in Figure 28. From these results it is interesting to note that evacuation of the acetylene pre-covered surface for 30 min. resulted in a decrease in the surface count rate by 46.8%, whilst treatment of the catalyst with H_2 for 45h resulted in a total removal of 13.6% compared with a value of 7.6% which was removed as a result of 6 hydrogenation reactions of C_2H_2/H_2. The amount of the acetylenic species held strongly on the catalyst was ca. 33.4%.

4.1.2.2 Adsorption of [14-C]-Acetylene on a Steady State Catalyst

After reduction and treatment of a sample of 0.2632g EUROPT-3 catalyst, as previously described, the catalyst was "run-in" to its steady state by performing ten reactions using a (1:3), $C_2H_2:H_2$ mixture. The reaction vessel was evacuated for 30 min after each

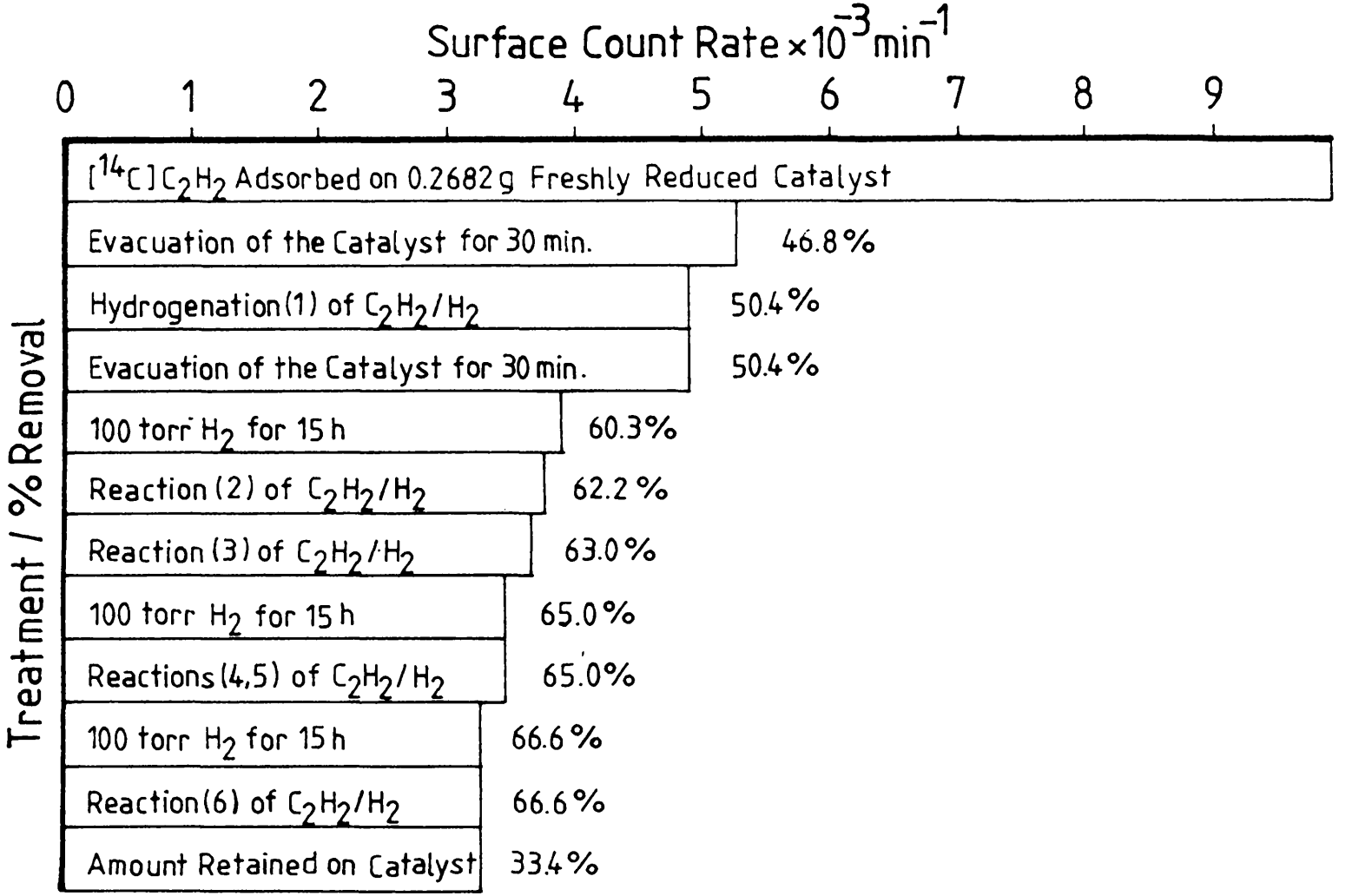

Figure 28. Effects of various treatments on adsorbed [14-C] acetylene.

reaction to remove the gas phase hydrocarbon products. The adsorption of [14-C]-acetylene was then followed using the direct monitoring technique, as described in section 4.12. Figure 27 shows an adsorption isotherm for [14-C]-acetylene adsorbed on a steady state catalyst. It can be seen that the isotherm showed almost no primary region with the capacity and gradient of the secondary region being significantly reduced.

4.1.3 [14-C]-Acetylene Adsorption on Freshly Reduced 0.5% Pt/MoO_3, 0.8% Pt/SiO_2, and 0.8% Pt/Al_2O_3 (Impregnated Catalysts)

3.7109g of Pt/MoO_3, 2.0598g of Pt/SiO_2 and 3.7109g of Pt/Al_2O_3 catalysts were reduced under flowing H_2 (30 ml min^{-1}) at either 250°C (Pt/SiO_2, Pt/Al_2O_3) or 350°C (Pt/MoO_3) for 2h, evacuated at these temperatures for 0.5h and then cooled in vacuo to ambient temperature. The adsorption of [14-C]-acetylene on each of these catalysts was then carried out. As shown in Figure 29, with the exception of the Pt/MoO_3 catalyst, the adsorption of acetylene on the Pt/SiO_2 and Pt/Al_2O_3 catalysts occurred in two stages, a non-linear "primary" process followed by a linear "secondary" process. The extent of acetylene adsorption on Pt/MoO_3 showed a distinctly different behaviour. It showed a steep primary region followed by a non-linear secondary region with a sharp slope which subsequently rose rapidly as the pressure was increased. No plateau region was observed on these catalysts, although gas pressures in excess of 5 Torr were used.

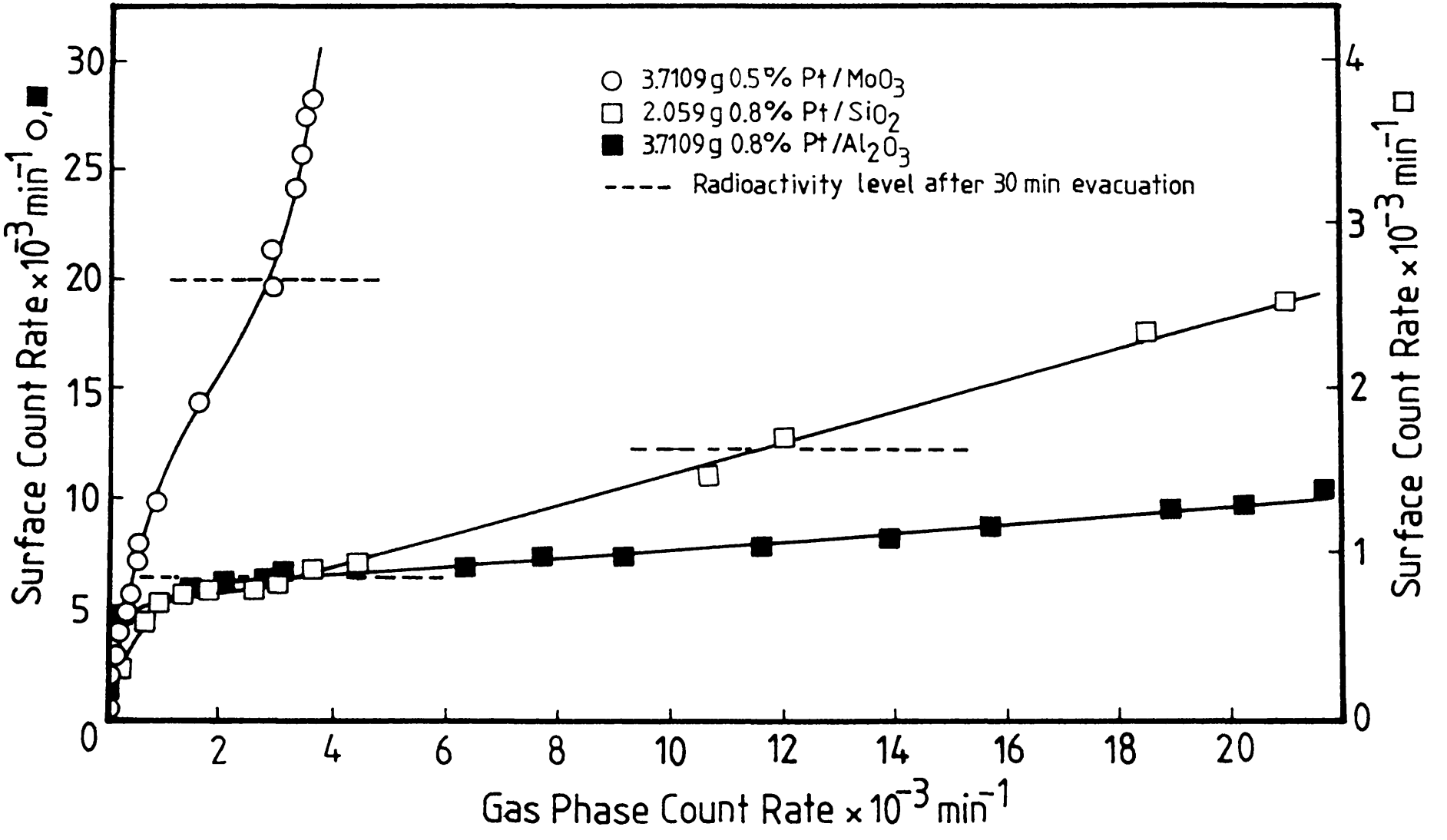

Figure 29. Adsorption isotherms of [14-C] acetylene on 0.5% Pt/MoO_3, 0.8% Pt/SiO_2 and 0.8% Pt/Al_2O_3.

Table 1. Effects of evacuation and molecular exchange on acetylene adsorbed on Pt catalysts.

Procedure	Surface count rate (counts min^{-1})	Total change %
Catalyst = 3.7109g Pt/MoO_3		
(a) build-up of [14-C]acetylene adsorption (gas pressure = 5 Torr)	28157	-
(b) evacuation for 30 min.	19907	-29.3
(c) admission of 5 Torr [12-C]-C_2H_2/15h	18330	-34.9
Catalyst = 2.0598g Pt/SiO_2		
(a) build-up of [14-C]-acetylene adsorption (gas pressure = 4.5 Torr)	2513	-
(b) evacuation for 30 min.	1633	-35
(c) admission of 5 Torr [12-C]-C_2H_2/15h	1532	-39
Catalyst = 3.710g Pt/Al_2O_3		
(a) build-up of [14-C]-acetylene adsorption (gas pressure = 4.6 Torr)	10300	-
(b) evacuation for 30 min.	6488	-37
(c) admission of 5 Torr [12-C]-C_2H_2/15h	6084	-41

4.1.3.1 Effects of Evacuation and Molecular Exchange on [14-C]-Acetylene Adsorbed Species

The catalysts which were used in section 4.1.3 were used here. After the build-up of adsorbed [14-C]-acetylene, the catalysts were evacuated for 30 min. A pressure of 5 Torr of non-radioactive acetylene was then introduced into the reaction vessel. The surface and gas phase radioactivities were determined. Table 1 and Figure 29 show that approximately 30-37% of the adsorbed acetylene was removed by evacuation for 30 min, with a further 8.7% on Pt/MoO_3, 4% on Pt/SiO_2, and 5% on Pt/Al_2O_3 being displaced by $[12\text{-C}]\text{-}C_2H_2$. It is also interesting to note that a large fraction, 65% on Pt/MoO_3, 61% on Pt/SiO_2, and 59% on Pt/Al_2O_3 of the adsorbed acetylene was retained by the catalyst as a strongly bound species.

4.2 ETHYLENE ADSORPTIONS

4.2.1 [14-C]-Ethylene Adsorption on Freshly Reduced 6% Pt/SiO_2 (EUROPT-1) Catalyst

The adsorption of [14-C]-ethylene on 0.0752g of freshly reduced EUROPT-1 catalyst was followed by the direct observation technique. After the catalyst had been activated in H_2 for 2h at 250°C and cooled *in vacuo* to ambient temperature, small aliquots of the labelled adsorbate were admitted to the reaction vessel and the surface and gas phase count rates were determined after each addition. A typical isotherm (Figure 30) revealed similar behaviour to that observed previously (sections 4.1.1 and 4.1.2, with acetylene) on the EUROPT

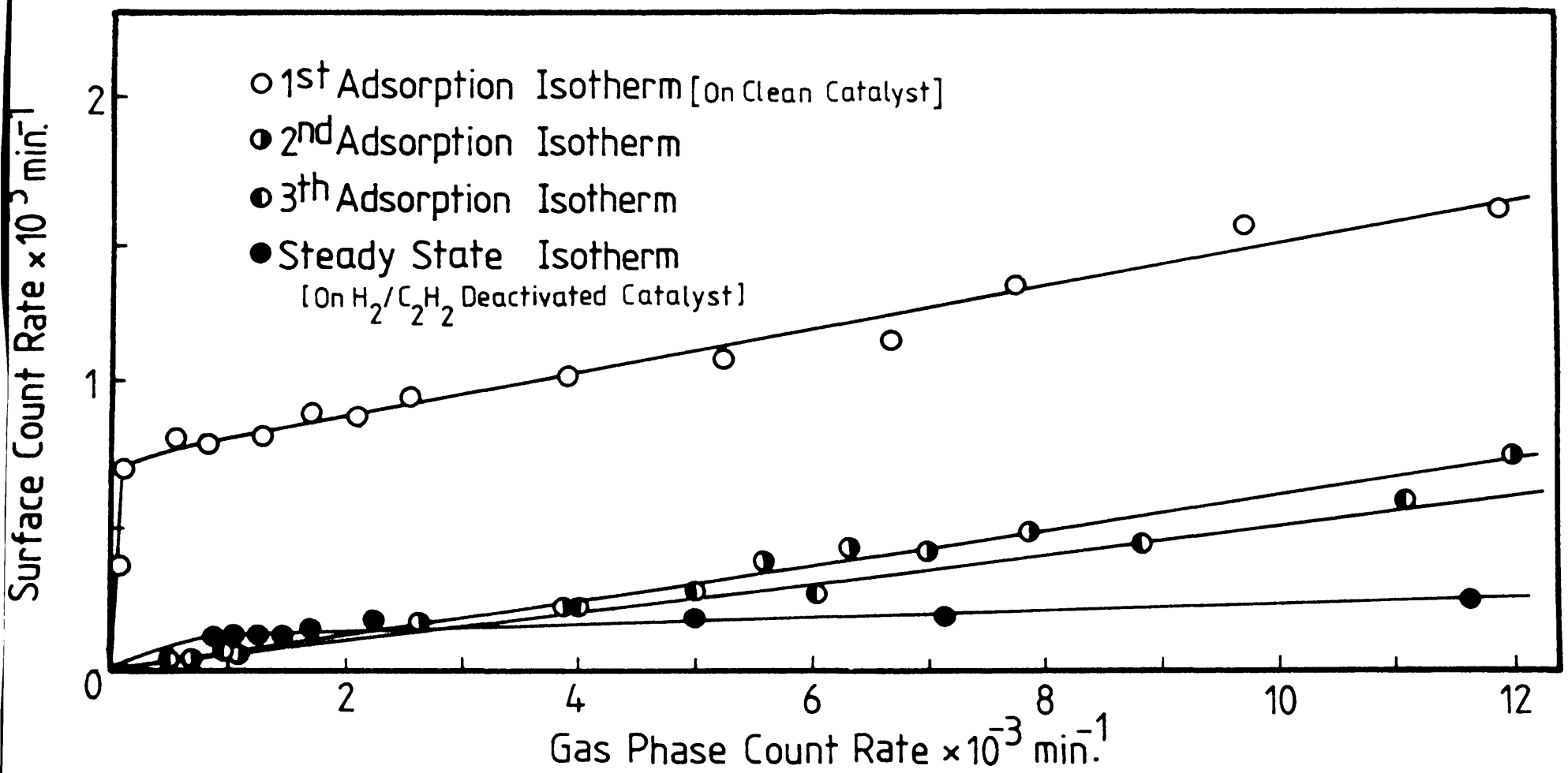

Figure 30. Adsorption isotherms of [14-C] ethylene on EUROPT-1.

catalysts. The isotherm had primary and secondary regions. The extent of the primary region showed less adsorption capacity than was found with [14-C]-acetylene (about 1/4 of that of acetylene). The secondary region continued to increase linearly up to a gas pressure of 5 Torr, which was the maximum pressure studied.

After evacuation of the reaction vessel for 30 min, approximately 10.7% of the surface radioactivity had been removed. Re-adsorption of [14-C]-ethylene on the evacuated catalyst showed an adsorption of ethylene equivalent to the amount removed as a result of evacuation (2nd and 3rd adsorption, Figure 30).

4.2.1.1 Effects of Various Treatments on Adsorbed [14-C]-Ethylene Species

The effects of various treatments, such as, evacuation and molecular exchange, were investigated on a catalyst with a pre-adsorbed ethylene, in order to gather information regarding the nature of the adsorbed species and their behaviour during the acetylene hydrogenation process. A sample of 0.075g EUROPT-1 was reduced and treated in the standard manner described previously, then an adsorption isotherm of [14-C]-ethylene was built up, followed by a cycle of evacuations and hydrogenations of $3:1::H_2:C_2H_2$ (Figure 31). The total amount of the pre-adsorbed ethylene removable by evacuation was ca. 19.7% with a large proportion, ca. 61.7%, removed by the hydrogenation of C_2H_2/H_2 on the catalyst. From these, a value of 18.8% was calculated for the amount of the initially adsorbed material, which was retained on the catalyst as carbonaceous deposits.

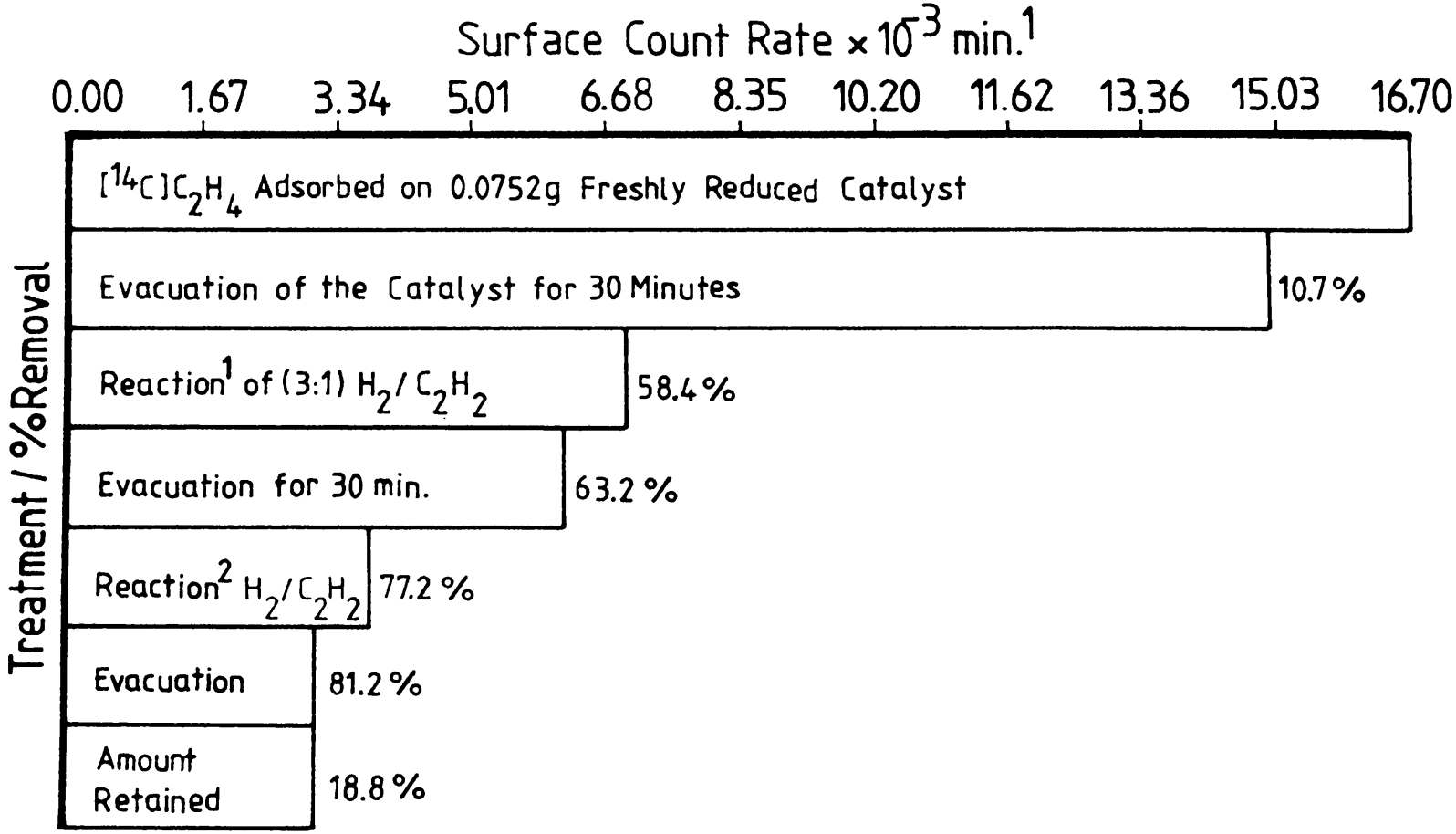

Figure 31. Effects of various treatments on adsorbed [14-C] ethylene species.

When a sample of freshly reduced EUROPT-1 catalyst was pre-covered with carbon monoxide, followed by the admission of [14-C]-ethylene, no adsorption of [14-C]-ethylene was observed, although a gas pressure in excess of 5 Torr was used.

4.2.1.2 [14-C]-Ethylene Adsorption on a Steady State Catalyst

0.097g of EUROPT-1 was activated by hydrogen and a number of acetylene hydrogenation reactions (39 reactions) were carried out to bring the catalyst to its steady state. A [14-C]-ethylene adsorption isotherm was then built-up (Figure 30). It was found that the primary adsorption region almost disappeared, with the uptake capacity of ethylene in the secondary region being substantially suppressed compared with the amount adsorbed on a freshly reduced catalyst.

4.2.2 [14-C]-Ethylene Adsorption on a Freshly Reduced 0.3% Pt/Al_2O_3 (EUROPT-3) Catalyst

The adsorption of [14-C]-ethylene on a freshly reduced EUROPT-3 catalyst was investigated to look at the scope of its adsorption, to compare it with ethylene adsorption on Pt/SiO_2 (EUROPT-1), and to gain some insight into the behaviour of this adsorbate during the hydrogenation of acetylene on the EUROPT-3 catalyst.

A sample of the catalyst (0.2397g) was reduced in H_2 at 250°C for 2h, evacuated for 30 min at 250°C, and then left to cool *in vacuo* at ambient temperature. Successive pulses of [14-C]-ethylene were allowed to expand into the reaction vessel and the surface radio-

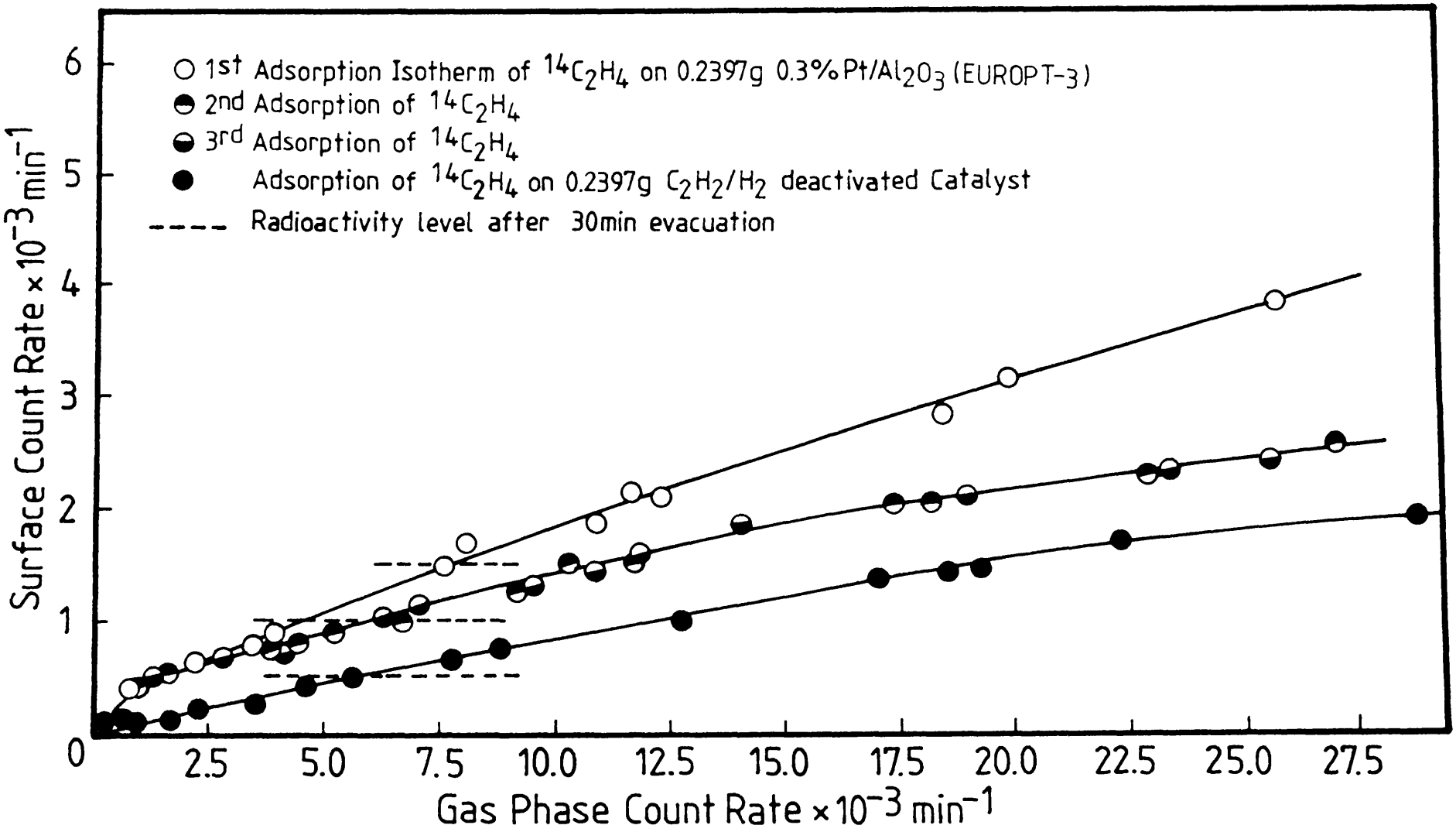

Figure 32. Adsorption isotherms of [14-C] ethylene on EUROPT-3.

activity was measured after each pulse, as described in section 4.1.1. The adsorption isotherm (Figure 32), showed a shape different from those observed with acetylene and ethylene on EUROPT-1 and of acetylene on EUROPT-3 in the sense that it showed almost no primary region. However, as further gas was admitted to the reaction vessel, a steady increase in the surface count rate was observed. This behaviour was continued up to a pressure of 7 Torr, which was the maximum pressure studied.

When aliquots of [14-C]-ethylene were introduced to a sample of 2.74g freshly reduced catalyst in the presence of ca. 5 Torr non-radioactive acetylene, no adsorption was observed to take place, although a gas pressure in excess of 10 Torr was used.

4.2.2.1 Effects of Various Treatments on Adsorbed Species

The effects of various treatments on the pre-adsorbed [14-C]-ethylene were investigated in an attempt to gain some knowledge about the reactivity of these adsorbed species, their role in conditioning the catalyst surface, and the possible participation of these species in C_2H_2/H_2 hydrogenation under similar conditions.

0.2397g of EUROPT-3 catalyst was reduced in H_2 and treated as in the normal procedure. A [14-C]-ethylene adsorption isotherm was then built-up. As the results presented in Figure 33 show, evacuation of the catalyst for 30 min removed 31% of the [14-C]-ethylene adsorbed species. When a total static pressure of 200 Torr H_2 was left in contact with the catalyst for 87h, about 15% of the pre-adsorbed ethylene was removed. Another 18.6% of the surface

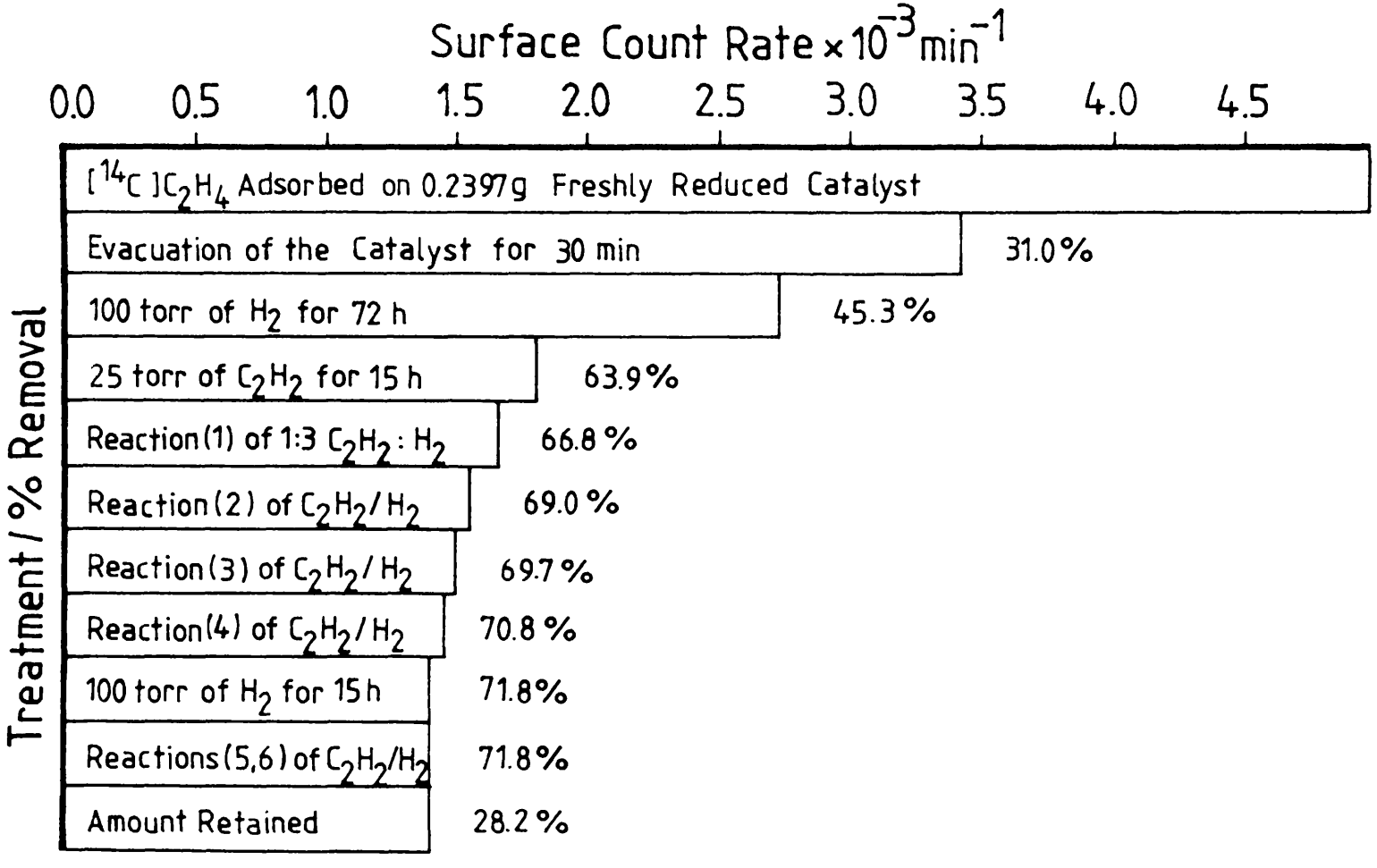

Figure 33. Effects of various treatments on adsorbed species.

species was displaced by 25 Torr [12-C]-C_2H_2, with a further 7% being removed as a result of four hydrogenation reactions of C_2H_2/H_2. The amount retained on the catalyst was calculated to be approximately 28%.

4.2.2.2 Adsorption of [14-C]-Ethylene on Steady State Catalysts

The effect of catalyst deactivation by C_2H_2/H_2 on its adsorptive ability for [14-C]-ethylene was also studied. A 0.2397g sample of EUROPT-3 catalyst was reduced and treated as above. Twelve acetylene hydrogenation reactions ($3:1::H_2:C_2H_2$) were carried out on the catalyst, which was evacuated after each reaction to remove the gaseous hydrocarbon products from the reaction vessel. Subsequently, an adsorption isotherm of [14-C]- ethylene was determined. The adsorption isotherm (Figure 32) showed no primary adsorption region with a slight positive gradient of the secondary region. The total amount of [14-C]-ethylene adsorbed on the deactivated catalyst was 50% less than that adsorbed on a freshly reduced catalyst.

4.3 CARBON MONOXIDE ADSORPTIONS

4.3.1 [14-C]-Carbon Monoxide Adsorption on Freshly Reduced 6% Pt/SiO_2 (EUROPT-1) Catalyst

The adsorption of [14-C]-carbon monoxide was examined for 0.0522g of EUROPT-1 catalyst which was reduced in a stream of hydrogen (30 ml min^{-1}) for 2h at 250°C, then evacuated for 0.5h at 250°C. The catalyst was then allowed to cool *in vacuo* to room temper-

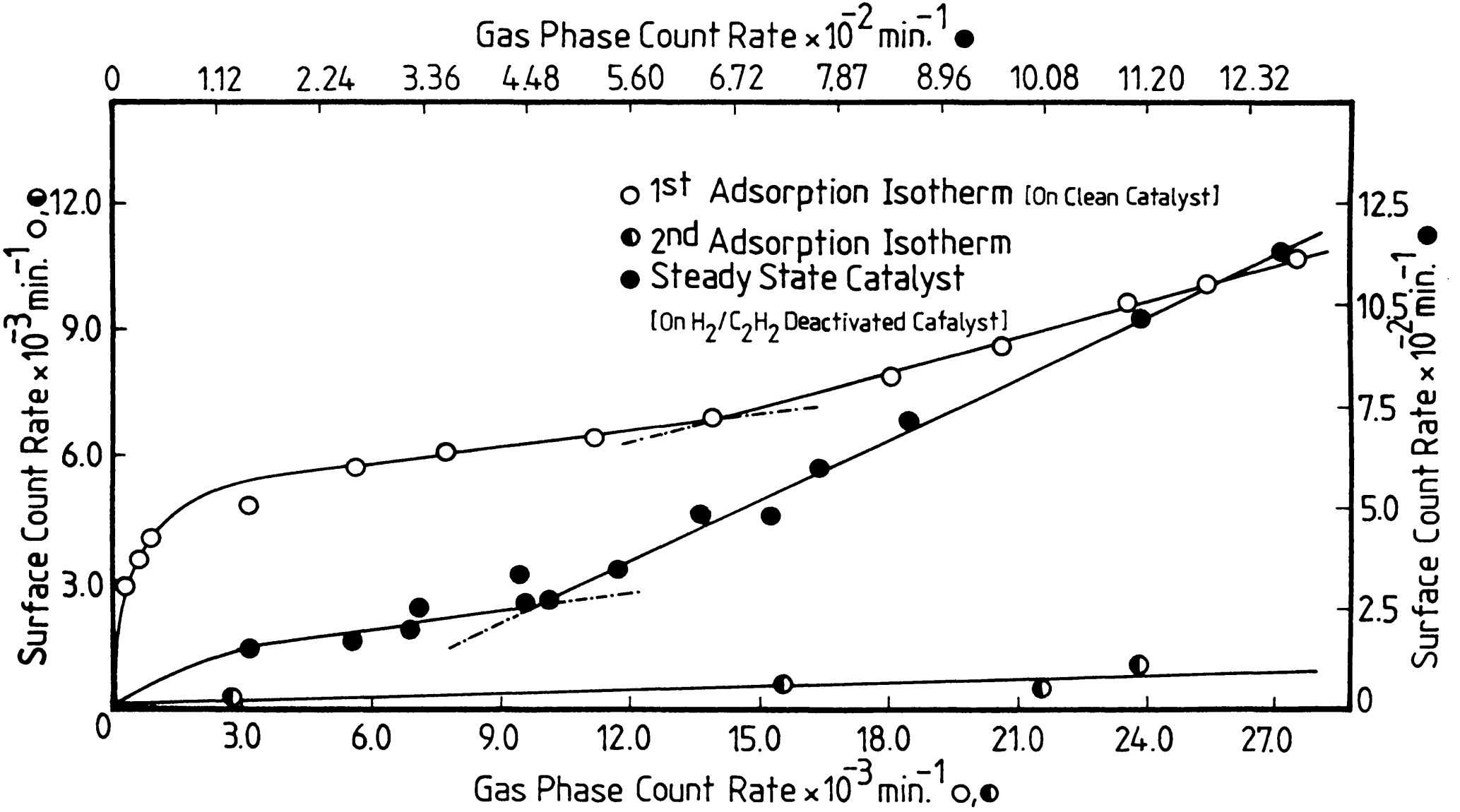

Figure 34. Adsorption isotherms of [14-C] Carbon monoxide on EUROPT-1.

ature and the [14-C]-CO adsorption isotherm was determined. A typical [14-C]-carbon monoxide adsorption isotherm is shown in Figure 34. The shape of the isotherm was significantly different from those observed with [14-C]-acetylene and [14-C]-ethylene on EUROPT and the platinum-impregnated catalysts. It was also surprisingly unlike the expected Langmuir-type CO behaviour observed on supported rhodium, iridium, palladium and nickel catalysts (55,58). The surface count rate rose sharply with increasing gas pressure until a turning point was attained, which was then followed by a linear build-up in the surface radioactivity. This was subsequently followed by a greater positive gradient of a second linear region. No plateau region was observed up to the 6 Torr limit studied.

The catalyst was evacuated at room temperature for 30 min to determine the amount of [14-C]-carbon monoxide which could be removed by evacuation. As a result of evacuation, only 2.5% of the pre-adsorbed [14-C]-carbon monoxide was removed. Re-adsorption of CO on the evacuated catalyst showed that [14-C]-CO adsorption continued to take place with a slight positive gradient as the pressure was increased (2nd adsorption, Figure 34).

When aliquots of [14-C]-ethylene were admitted to the reaction vessel containing a 0.0593g sample of EUROPT-1 pre-covered with CO, no adsorption was observed, although a gas pressure in excess of 5 Torr was used. However, when [14-C]-carbon monoxide adsorption was studied over a [14-C]-ethylene pre-covered surface, the adsorption took place and the isotherm had the same shape as that obtained on a freshly reduced catalyst.

4.3.1.1 Effects of Various Treatments on CO Adsorbed Species

The pre-adsorbed [14-C]-carbon monoxide was subjected to various treatments, such as, evacuation, a C_2H_2/H_2 mixture and non-radioactive carbon monoxide, to examine the extent of removal and displacement of the pre-adsorbed species.

0.0522g of catalyst was reduced and activated in the standard manner. A [14-C]-CO adsorption isotherm was built-up on the freshly reduced catalyst, which was then subjected to cycles of evacuation and acetylene hydrogenation reactions. The results of these experiments (Figure 35) showed that during catalyst evacuation, a total of 5% of the CO species was removed, whilst 13.3% was displaced by C_2H_2/H_2 reactions on the catalyst.

In another experiment, 0.150g of catalyst was reduced and pre-covered with [14-C]-CO. A 5 Torr non-labelled CO was then admitted to the reaction vessel and allowed to remain in contact with the catalyst for 15h. After a brief evacuation of the catalyst, the surface count rate decreased from 3062 cpm to 1141 cpm, corresponding to a removal of 62.7% of the adsorbed carbon monoxide.

4.3.1.2 Adsorption of [14-C]-Carbon Monoxide on Steady State Catalysts

A 0.0522g EUROPT-1 catalyst was reduced and treated according to the standard procedure. A pre-mixed sample of 12.5 Torr C_2H_2 and 37.5 Torr H_2 was introduced to the reaction vessel. This process was repeated several times until a steady state constant activity was reached. A [14-C]-CO adsorption isotherm was built-up

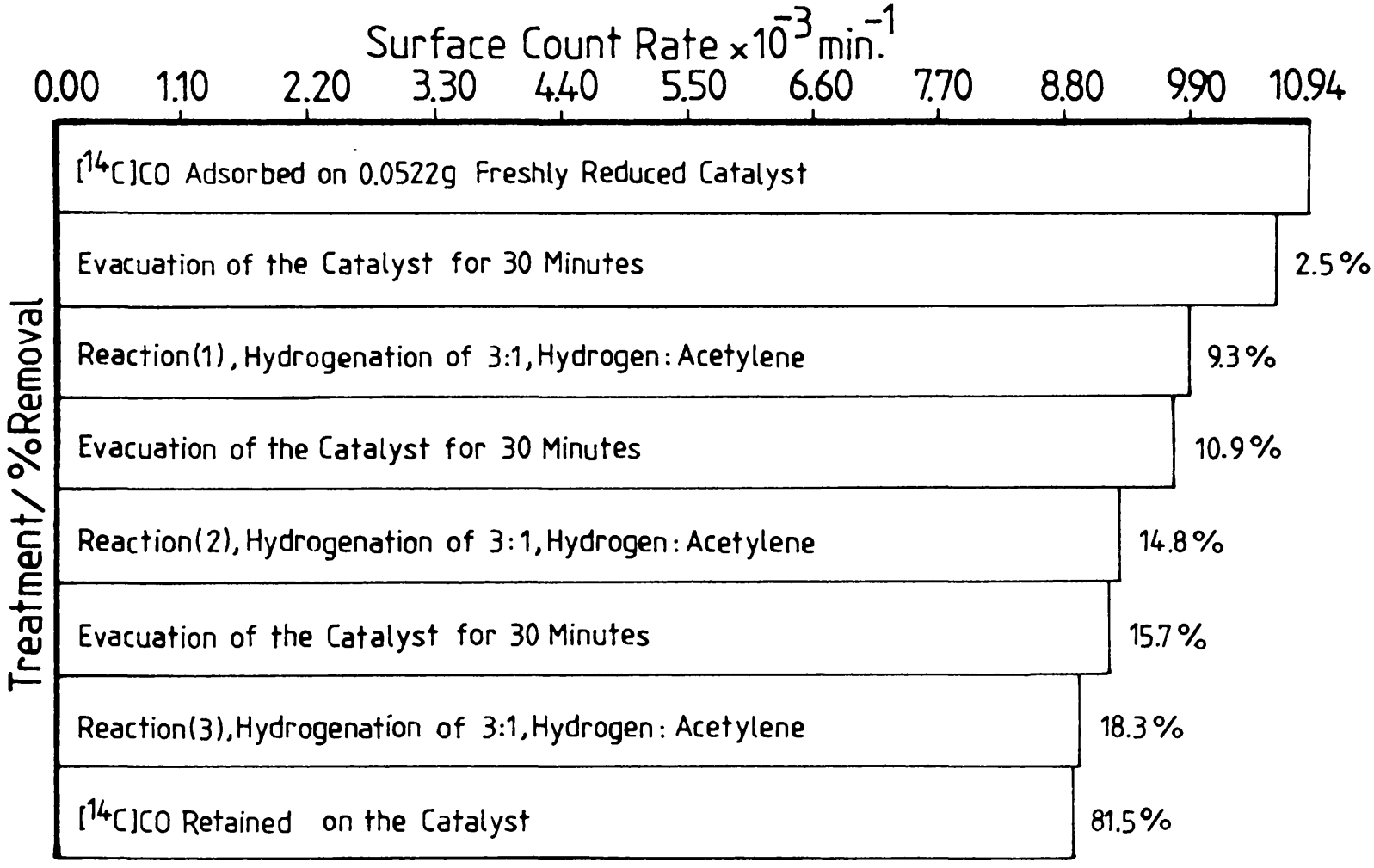

Figure 35. Effects of various treatments on CO adsorbed species.

(Figure 34) which showed that on a catalyst in the steady state, carbon monoxide adsorption took place with the adsorption isotherm similar in shape to that obtained using a clean catalyst, except that the amount of [14-C]-CO adsorbed was substantially reduced.

4.3.2 Carbon Monoxide Adsorption on Freshly Reduced 0.3% Pt/Al_2O_3 (EUROPT-3) Catalyst

The adsorption of [14-C]-carbon monoxide on freshly reduced EUROPT-3 was investigated using a 0.2763g sample of catalyst. After reduction at 250°C for 0.5h, evacuation at 250°C for 0.5h and cooling in vacuo, the catalyst was pulsed with successive aliquots of [14-C]-CO and the adsorption isotherm was determined. The adsorption isotherm (Figure 36) showed a different shape from that for the CO adsorption on EUROPT-1 and was similar "in general" behaviour to that found for the adsorption of [14-C]-labelled hydrocarbons on EUROPT-1 and EUROPT-3 catalysts. It showed two distinct regions, a steep primary region followed by a secondary region, which showed a slight positive gradient as the gas pressure was increased. Similar behaviour has been observed with carbon monoxide adsorption on partially oxidised copper surfaces (96,97).

The catalyst was evacuated for 30 min to determine the quantity of [14-C]-CO which could be removed by evacuation. The results (Figure 36) showed that about 23% of the adsorbed CO was removed. This removable amount, however, could be restored by the re-admission of [14-C]-CO into the catalyst (2nd adsorption, Figure 36).

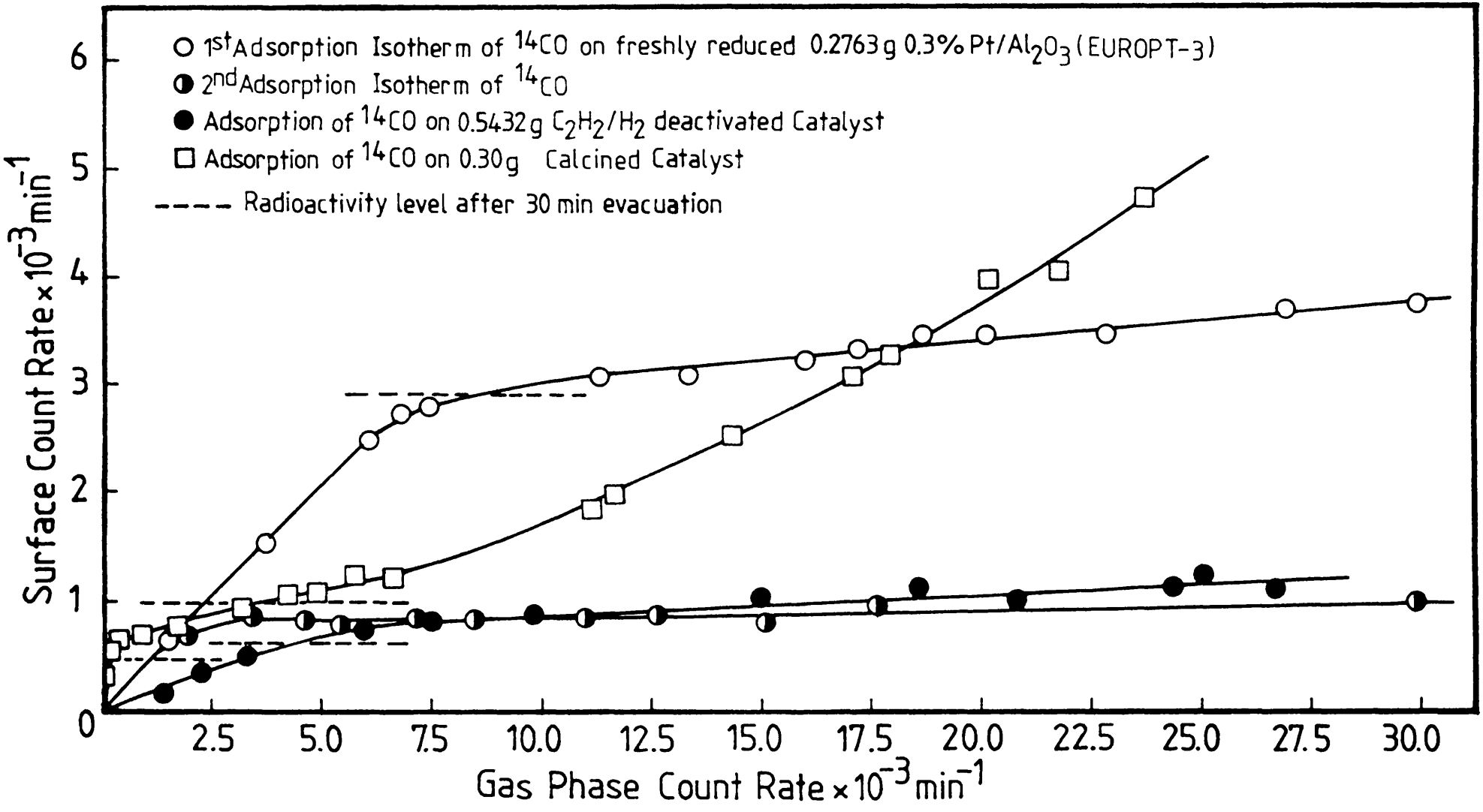

Figure 36. Adsorption isotherms of [14-C] Carbon monoxide on EUROPT-3.

In another experiment, 0.30g of EUROPT-3 catalyst was calcined in air at 500°C for 18h and was then reduced in flowing H_2 (30 ml min^{-1}) at 400°C for 4h, followed by evacuation at 400°C for 0.5h and the catalyst was then cooled down to room temperature in vacuo. Figure 36 shows the adsorption isotherm obtained by admitting successive aliquots of [14-C]-CO to this calcined and reduced catalyst. It showed a drastically different shape from that observed with freshly reduced uncalcined catalyst, in that, after the turning point of the primary process, the CO uptake increased remarkably as the pressure was increased (up to ~ 6 Torr). It is also noticeable from Figure 36 that the adsorptive capacity for carbon monoxide in the primary region was approximately one-third of that found on the uncalcined catalyst. Evacuation of the catalyst for 30 min removed about 90% of the adsorbed species.

4.3.2.1 Effects of Various Treatments on Adsorbed CO Species

A 0.2763g sample of EUROPT-3 catalyst was reduced and covered with pulses of [14-C]-CO, sufficient to build up an adsorption isotherm similar to that obtained on a freshly reduced catalyst. Figure 37 presents the results of various treatments performed on this [14-C]-CO pre-covered surface. From this it can be seen that 23.1% of the adsorbed species were removed by a 30 min evacuation, with a further 2% being removed when the catalyst was treated with either H_2 or C_2H_2/H_2. However, covering the catalyst with 100 Torr C_2H_2 alone for 72h resulted in 19.4% removal of the pre-adsorbed CO. The amount

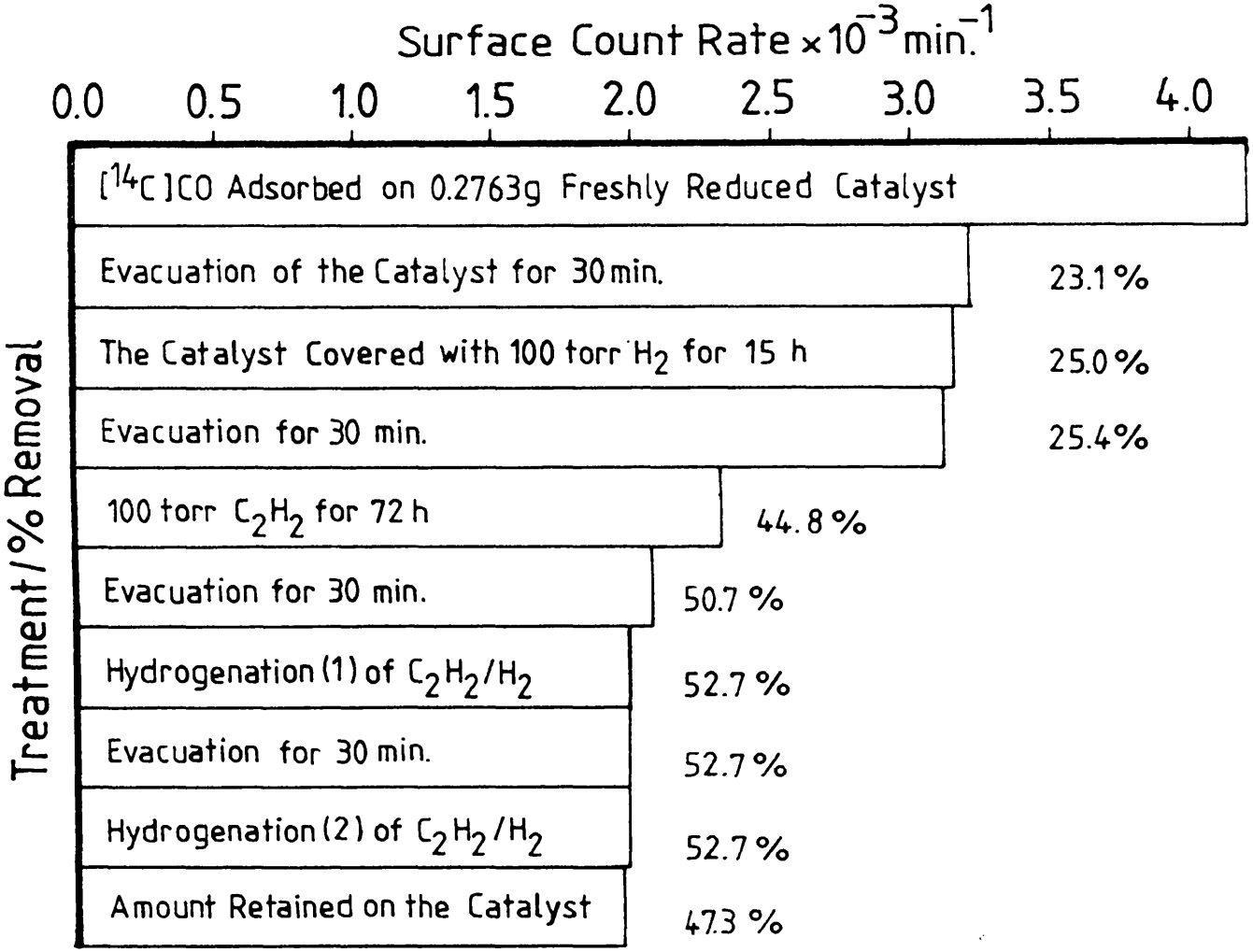

Figure 37. Effects of various treatments on CO adsorbed species.

of [14-C]-CO retained permanently on the catalyst was ca. 47.3% of that initially adsorbed.

A fraction, ca. 24%, of the pre-adsorbed [14-C]-CO could be exchanged with non-labelled CO.

4.3.2.2 [14-C]-Carbon Monoxide Adsorption on Steady State Catalysts

0.5432g of EUROPT-3 catalyst was reduced and treated by the standard procedure. Sufficient acetylene hydrogenation reactions were carried out to reach a steady state constant activity. A [14-C]-carbon monoxide isotherm was built-up. As can be seen from comparison of this adsorption isotherm with that obtained with a freshly reduced catalyst (Figure 36), it was of a similar shape to that found with the freshly reduced catalyst, although the amount of adsorption on a steady state catalyst was substantially less.

4.3.3 [14-C]-Carbon Monoxide Adsorption on Freshly Reduced 0.8% Pt/SiO_2, 0.8% Pt/Al_2O_3, and 0.5% Pt/MoO_3 Catalysts

0.6281g Pt/SiO_2, Pt/Al_2O_3, and Pt/MoO_3 were reduced and treated, as described in section 3.6. Figure 38 shows the adsorption isotherms obtained by introducing successive aliquots of [14-C]-CO to the freshly reduced catalyst samples. The shapes of the carbon monoxide isotherms on Pt/SiO_2 and Pt/Al_2O_3 are of a similar form to those observed with the EUROPT-1 catalyst. They showed a primary adsorption region followed by a secondary region which displayed a progressively increasing CO uptake as the gas pressure was increased.

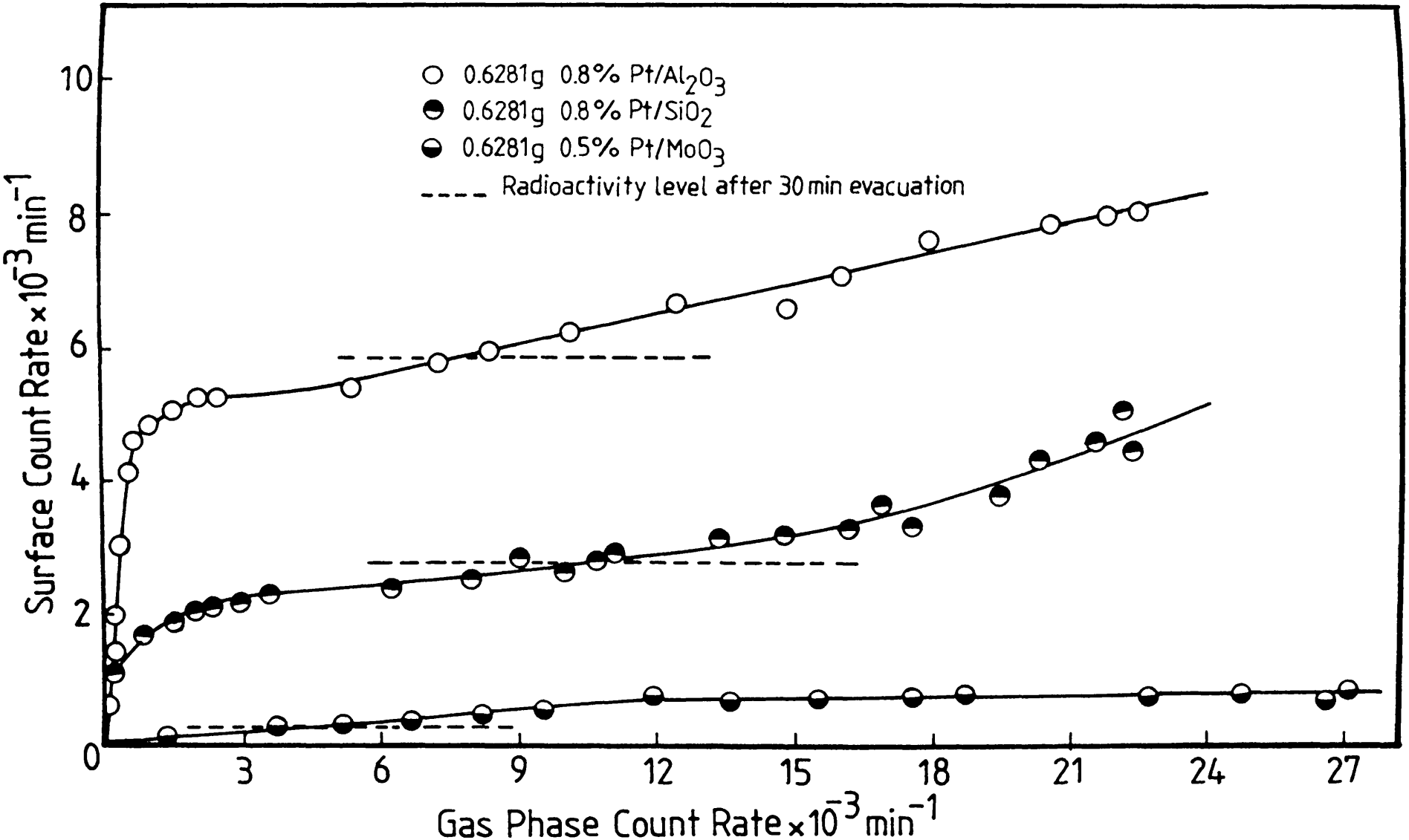

Figure 38. Adsorption isotherms of [14-C] carbon monoxide on 0.8% Pt/SiO_2, 0.8% Pt/Al_2O_3 and 0.5% Pt/MoO_3.

No plateau region was observed up to a pressure of 5 Torr. The adsorption of [14-C]-CO on Pt/MoO_3 showed the expected behaviour, in that the surface count rate increased slowly as the pressure was increased until a plateau was reached. The shape of the isotherm suggests that carbon monoxide adsorption reaches a saturation level which confirms the completion of a monolayer of adsorbed species (Langmuir-type adsorption).

The catalysts were evacuated for 30 min to determine the amount of [14-C]-carbon monoxide which could be removed by evacuation. After evacuation the surface count rates were decreased to a point corresponding to a removal of 47.4% (Pt/SiO_2), 26.4% (Pt/Al_2O_3), and 68% (Pt/MoO_3) of the adsorbed [14-C]-CO. Subsequent treatment of these catalysts with 5 Torr of non-radioactive carbon monoxide for 15h displaced ~ 1% (Pt/MoO_3), 90% (Pt/SiO_2), and 84% (Pt/Al_2O_3) of the species which could not be removed by evacuation.

CHAPTER FIVE

THE REACTION OF ACETYLENE WITH HYDROGEN OVER 6% Pt/SiO_2 (EUROPT-1) CATALYSTS

5.1 DEACTIVATION CURVES

The reaction of 12.5 Torr of acetylene with 37.5 Torr of hydrogen was studied using 0.095g of the catalyst. Reactions were carried out by admitting a sample of pre-mixed gases into the reaction vessel containing the freshly reduced catalyst (see section 3.6) at room temperature. The progress of the hydrogenation reaction was monitored by measuring the fall in the total pressure using a pressure transducer (section 3.1.1.4). Figure 39 shows a typical pressure fall against time curves. From this it can be seen that the reaction took place in two recognizable stages. Analysis of the reaction products by gas chromatography during the course of the hydrogenation revealed that in the first stage, ethane and ethylene were produced. The second stage was accompanied with an acceleration to the reaction rate. The acceleration point denoted as $(-\Delta P_a)$, was obtained by extrapolating the first and second stages of the reaction and was found to occur at a pressure fall of 21.9 ± 0.1 Torr. After the commencement of the second stage, the major process occurring was the further hydrogenation of ethylene to ethane. At the later stages of the reaction, tracers of C_4-hydrocarbons (identified as butane) were also observed. The pressure against time curves show that the reaction was first order in

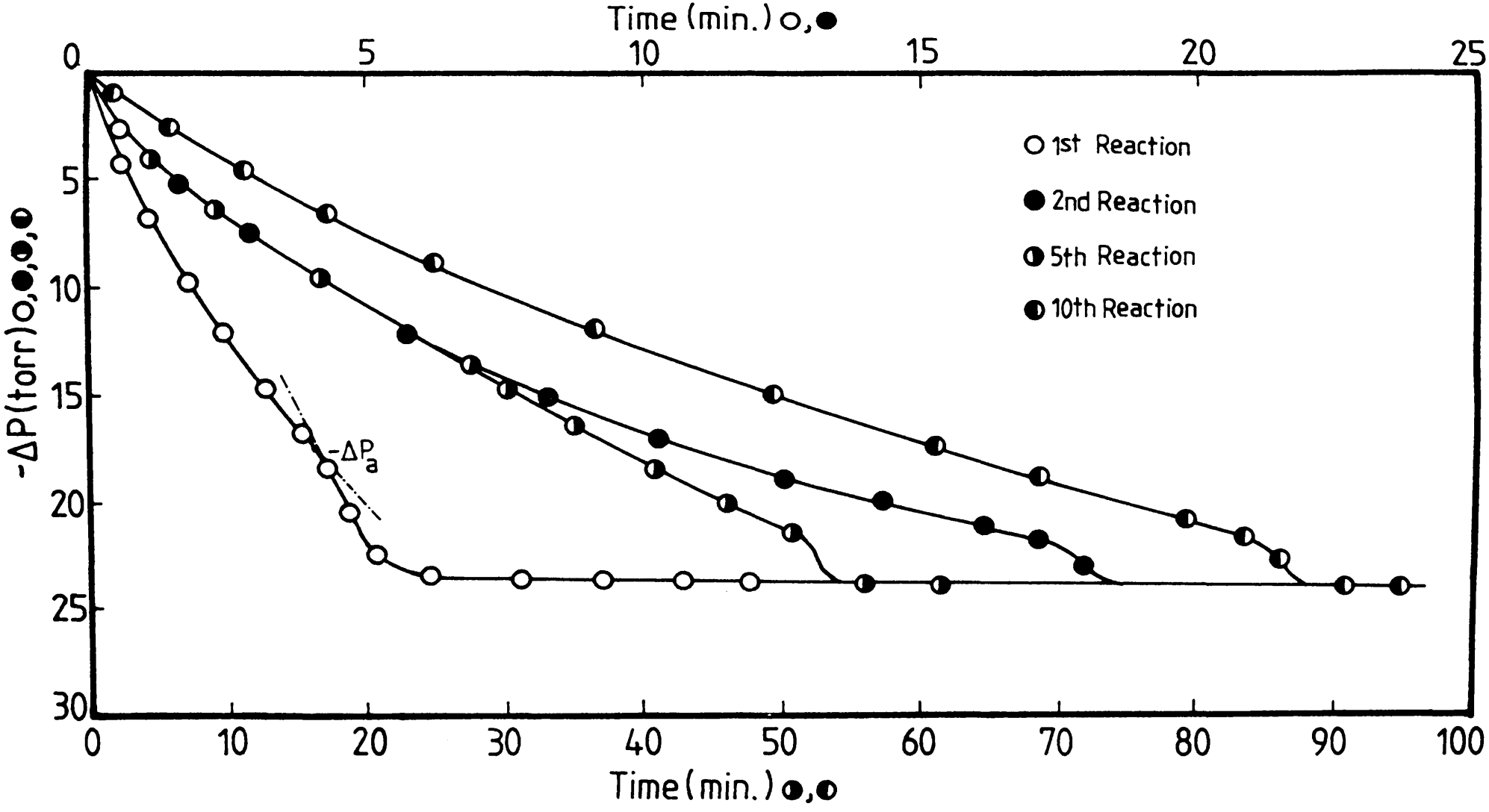

Figure 39. Pressure fall-time curve of acetylene hydrogenation on EUROPT-1.

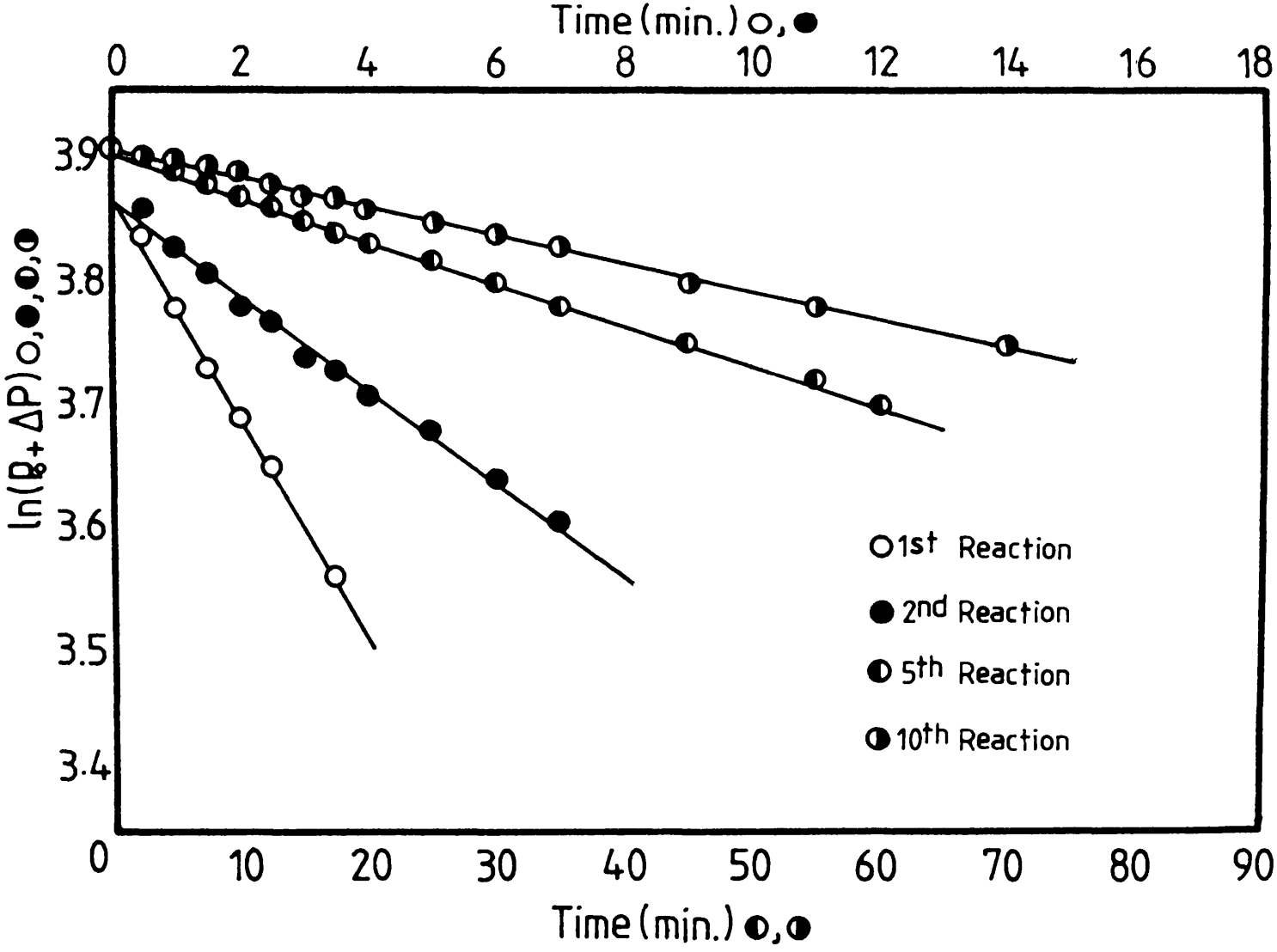

Figure 40. First order plots of acetylene hydrogenation on EUROPT-1.

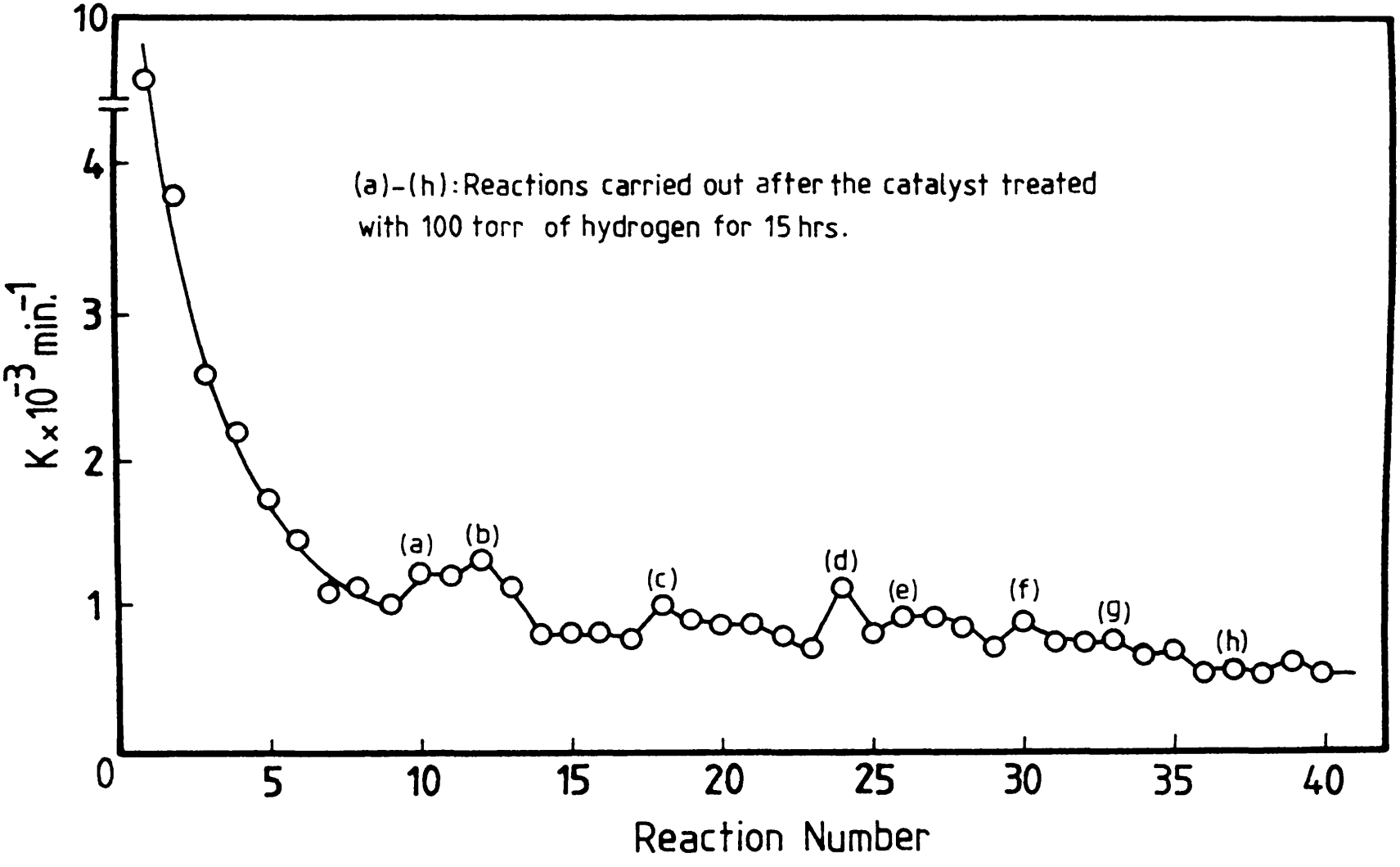

Figure 41. Variation of the first order rate constant with reaction number on EUROPT-1.

total pressure. Plots of $\ell n\ (P_o + \Delta P)$ against time (Figure 40) were found to be straight lines and from the gradients of these, the values of the first-order rate constants (K min^{-1}) were calculated.

The catalysts could be deactivated by performing a series (> 10 reactions) of acetylene hydrogenations at room temperature using a 3:1::H_2:C_2H_2 mixture. Figure 41 shows that the rate of the hydrogenation as determined from the linear part of the first-order plots, decreased with successive reactions until a steady state activity was attained. From Figure 41, it can also be seen that during the early stages of the deactivation process, the activity could be partially restored when the catalyst was kept in contact with 100 Torr H_2 for 15h.

When a freshly reduced EUROPT-1 catalyst was kept in contact with ~ 10 Torr acetylene or ethylene for 12-15h and then used for acetylene hydrogenation, the reaction rates were very similar to those produced with a freshly reduced catalyst under comparable conditions.

5.2 PRODUCT DISTRIBUTION ON FRESHLY REDUCED AND STEADY STATE CATALYSTS

0.095g of EUROPT-1 catalyst was activated and treated under standard conditions. A pre-mixed mixture of 3:1::H_2:C_2H_2 was then introduced to the catalyst. The progress of the reaction was monitored by the pressure transducer and samples of the reaction products were extracted and analysed by gas chromatography (section 3.2) to follow changes occurring in the product distribution. Figure 42 shows a

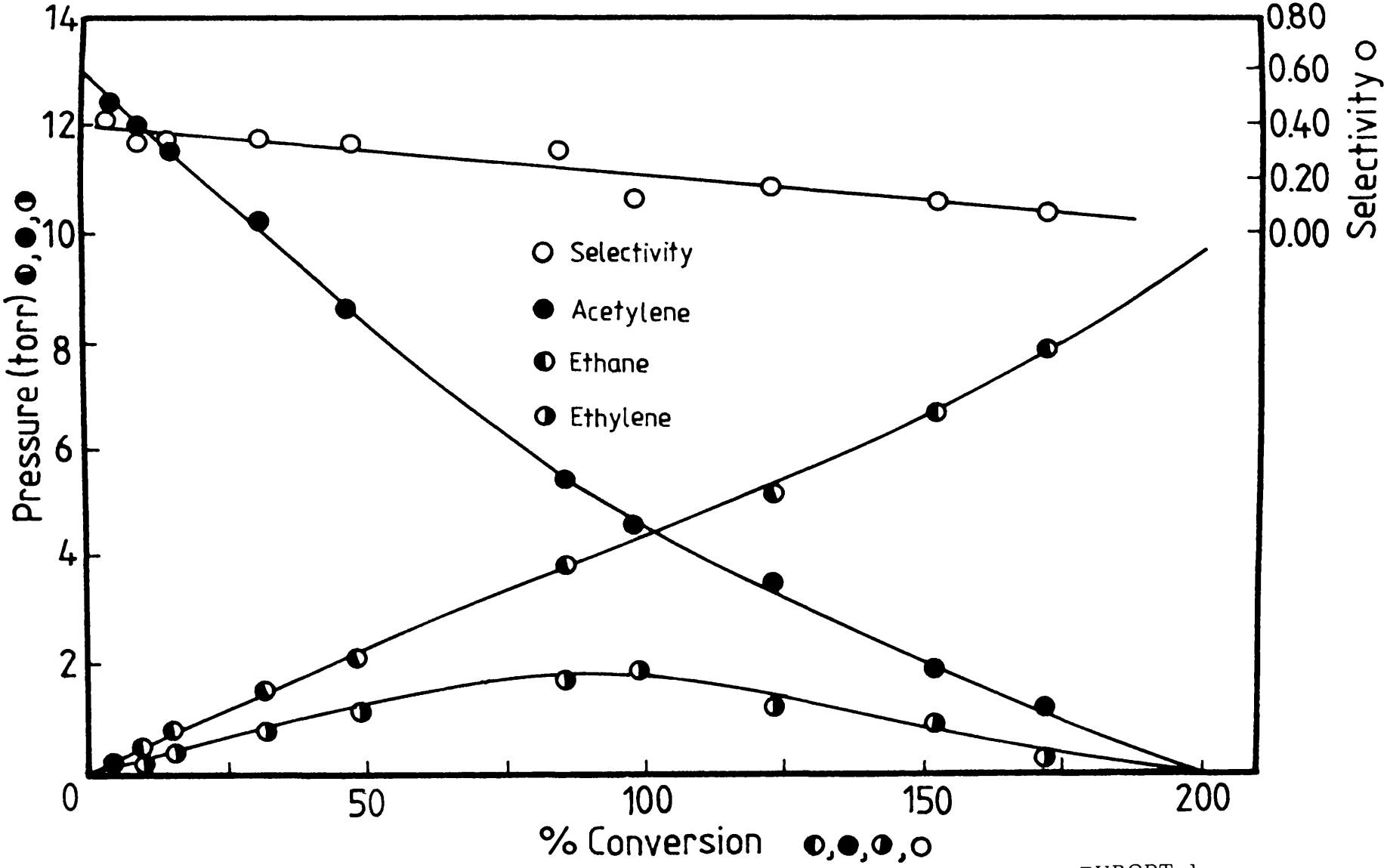

Figure 42. Product distribution curves of acetylene hydrogenation on freshly reduced EUROPT-1.

typical trace of the product distribution curves of acetylene hydrogenation on a freshly reduced catalyst. The percentage conversion was calculated from the gas chromatography analysis profiles as the number of moles of hydrogen consumed per mole of hydrocarbon present in the reaction mixture. Accordingly, the formation of a mole of ethane requires two moles of hydrogen and the formation of a mole of ethylene requires one mole of hydrogen, therefore,

$$\% \text{ conversion} = \frac{(2 \times \text{ethane yield}) + (1 \times \text{ethylene yield})}{\text{total yield of hydrocarbons}}$$

The results in Figure 42 show that, at conversions lower than 100%, the production of ethane and ethylene increased linearly with % conversion with the ratio of the former to the latter being approximately 2. However, after 100% conversion and as the partial pressure of acetylene diminished towards zero, the ethylene yield decreased with a simultaneous increase in the ethane yield. Acetylene hydrogenation continued to take place up to the 200% conversion.

The variation in selectivity with increasing percentage conversion for acetylene hydrogenation on EUROPT-1 is also shown in Figure 42. The selectivity (S) for ethylene production, which is defined as,

$$S = \frac{P_{C_2H_4}}{P_{C_2H_4} + P_{C_2H_6}}$$

where $P_{C_2H_4}$ and $P_{C_2H_6}$ represent the partial pressures of ethylene and ethane, decreased steadily as the reaction progressed from a value of

about 0.380 at approximately 10% conversion to a value of 0.200 at approximately 100% conversion.

In order to investigate the product distribution on a steady state catalyst, a sample of 0.0947g of the catalyst was reduced and treated in the standard manner (section 3.6) and then deactivated by a series of 40 hydrogenation reactions. Samples from the products were extrated and analysed several times during the reaction to follow the changes in product distribution throughout the reaction. Figure 43, which corresponds to reaction 27, shows that both ethane and ethylene were produced. The yield of ethylene showed a reduction of ~ 50%, compared with that on the freshly reduced catalyst. The variation of selectivity with respect to conversion on a steady state catalyst (Figure 43) showed an initial value of 0.300 at approximately 1% conversion, which then decreased rapidly to a value of 0.140 at approximately 100% conversion. This value was maintained until almost all the acetylene had reacted.

A set of hydrogenation reactions carried out on the above catalyst after it had been regenerated to its original activity (section 3.10), to examine the effect of reaction number on the selectivity for ethylene formation. Samples were extracted from the reaction mixture after a pressure drop of ~ 15 Torr, which was equivalent to approximately 99 ± 10% conversion. It was found that the deactivation with C_2H_2/H_2 had a minor effect on selectivity (Table 2).

It was observed that treatment of the steady state catalyst with 100 Torr H_2 for up to 20h at room temperature produced a 20% improvement to the selectivity value from 0.175 to 0.203.

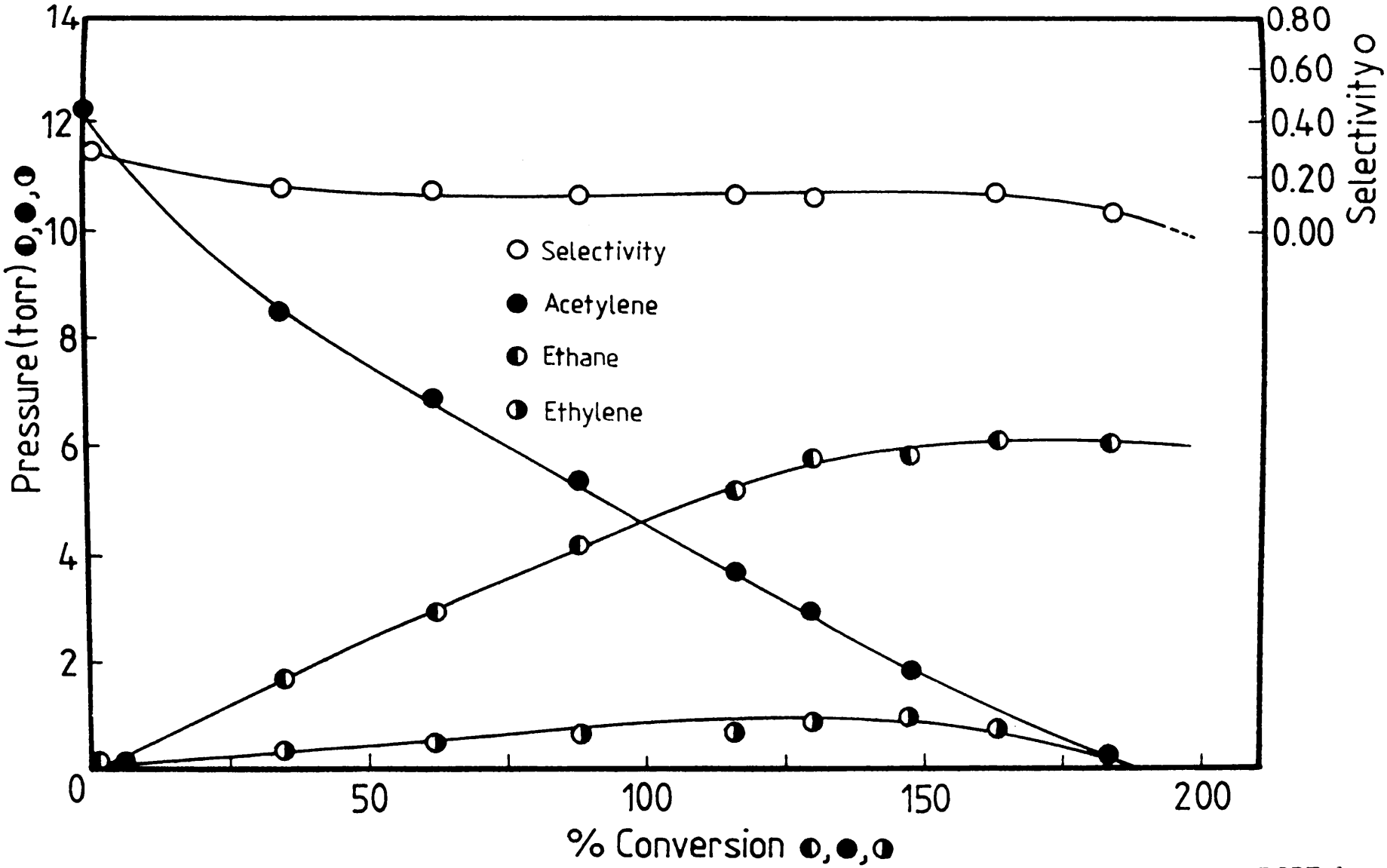

Figure 43. Product distribution curves of acetylene hydrogenation on a steady state (reaction 27) EUROPT-1.

Table 2. Effect of Reaction Number on Selectivity

Reaction No.	% Conversion	Selectivity
3	115.60	0.179
6	104.95	0.173
32	96.07	0.172
33	87.10	0.176
35	91.41	0.177

5.3 THE REACTION ORDER WITH RESPECT TO HYDROGEN AND ACETYLENE

Because of variations in catalytic activity from reaction to reaction, it was not possible to obtain meaningful measurements for the variations in initial rate with reactants pressures and hence determine the orders of reaction with respect to each reactant.

In a series of reactions, the effect of variation of reactants pressure on the selectivity was studied using a constant pressure of one reactant (acetylene = 12.5 Torr and hydrogen = 37.5 Torr), while the pressure of the other reactant was varied. Products were analysed by the gas chromatograph at a fixed pressure fall of 10 Torr. As shown in Figure 44, the selectivity towards ethylene production increased with increasing hydrogen pressure with a limiting value of selectivity of 0.065 as the plot was extrapolated to zero hydrogen pressure. Figure 44 also shows that the selectivity decreased with

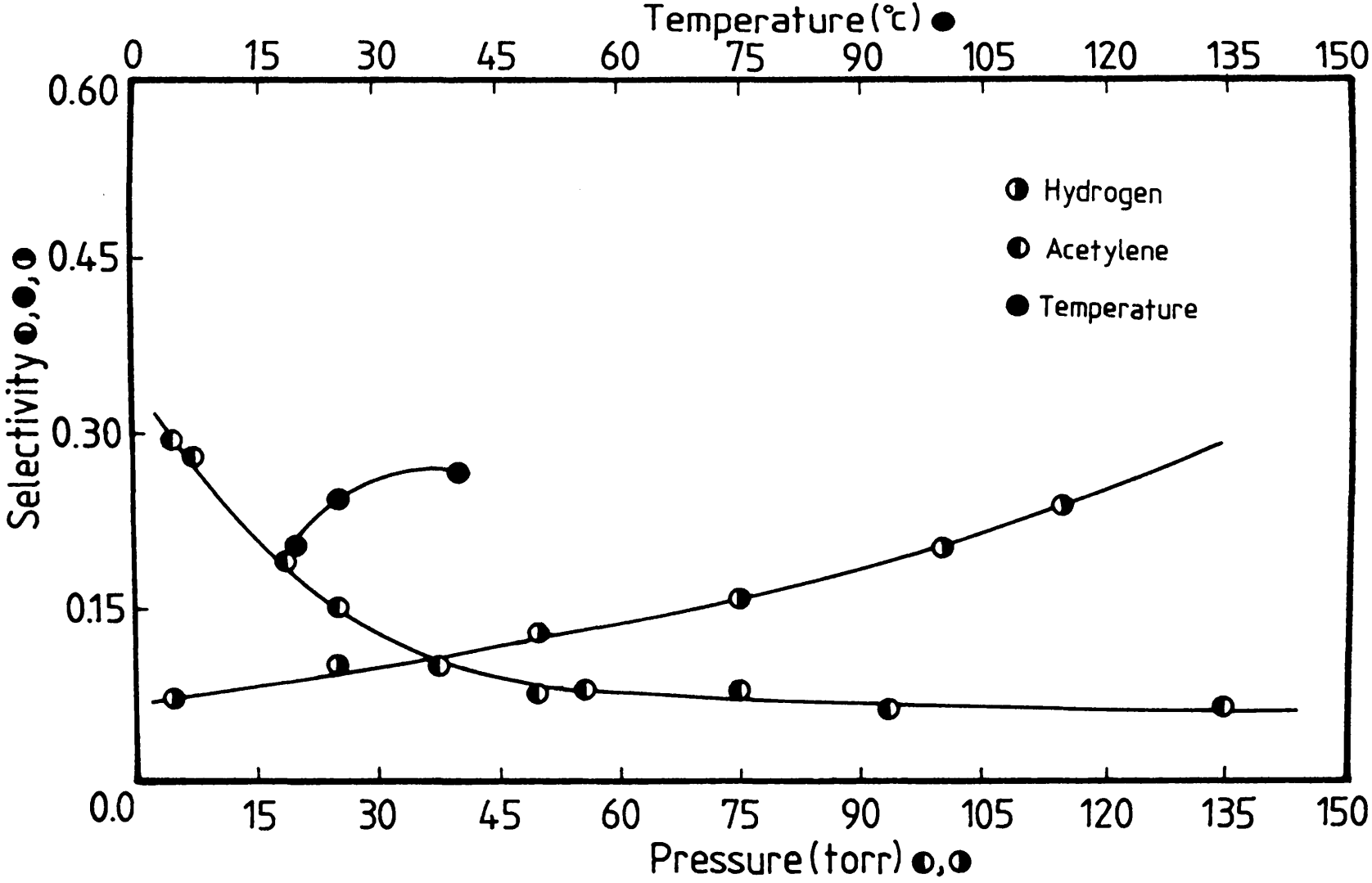

Figure 44. The variation of selectivity with experimental variables of acetylene hydrogenation on EUROPT-1.

increasing acetylene pressure up to a point corresponding to a pressure of ~60 Torr when no significant variation of selectivity with initial acetylene pressure was observed.

5.4 THE TEMPERATURE DEPENDENCE OF THE PRODUCT DISTRIBUTION AND THE ACTIVATION ENERGY OF THE REACTION

A 0.10g sample of EUROPT-1 was reduced, treated and run to the steady state, as described in the preceding section. In a series of reactions in the temperature range 20-60°C, using a hydrogen: acetylene ratio of 3:1, the variation of initial reaction rate was studied as a function of temperature. All the reactions were analysed after a pressure fall of 10 Torr. The plot of $\log_{10}$ (initial rate) against the reciprocal of absolute temperature (Figure 45) was a straight line from which an activation energy of 45.15 ± 0.05 kJ mol^{-1} was obtained. The variation of selectivity as a function of temperature is shown in Figure 44. From this, it can be seen that the selectivity increased slightly as the temperature was raised. However, it is important to mention that, at temperatures > 60°C, a diffusion control effect was observed to operate.

5.5 THE DEPENDENCE OF ACCELERATION POINT UPON EXPERIMENTAL VARIABLES

0.10g of Catalysts were activated, treated and run to the steady state activity using the standard procedure, and were used to investigate the effects of increasing hydrogen and acetylene pressures and temperatures on the acceleration point ($-\Delta P_a$) observed in the

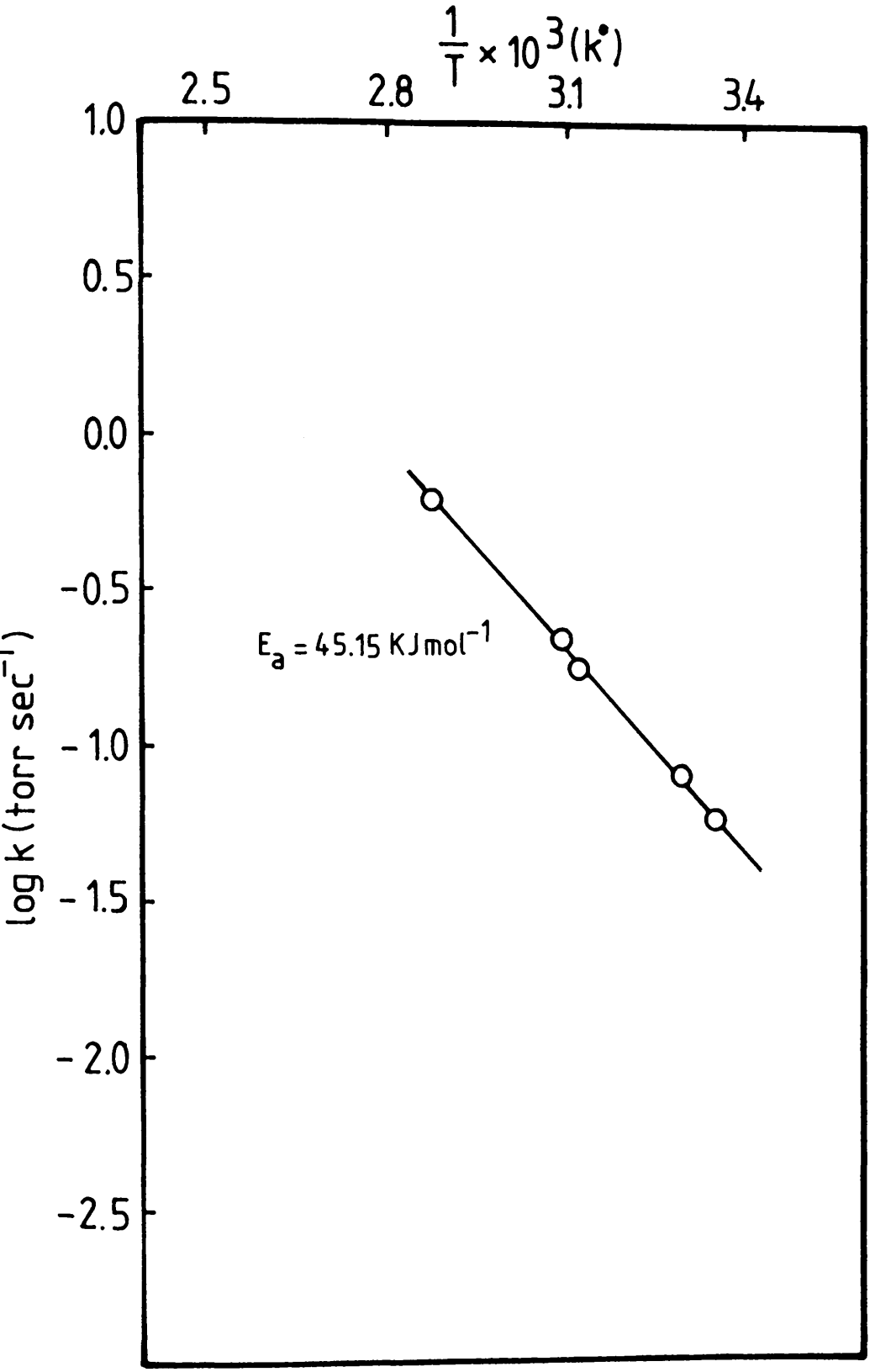

Figure 45. The variation of $\log_{10}$ (initial rate) with reciprocal of the absolute temperature on EUROPT-1.

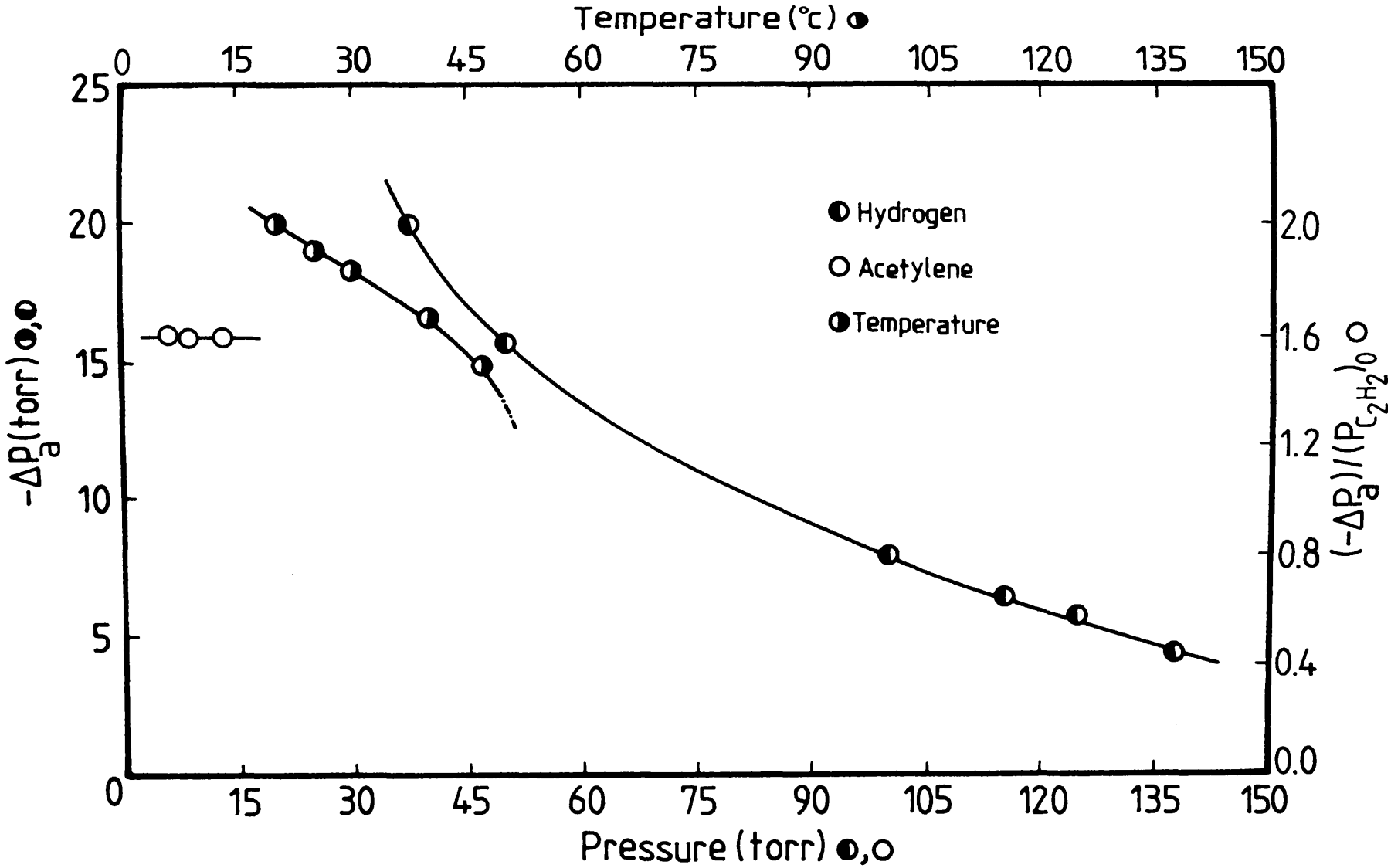

Figure 46. The dependence of acceleration point ($-\Delta P_a$) upon experimental variables.

pressure fall curves (Figure 39). Figure 46 shows that the acceleration point appeared earlier with increasing hydrogen pressure and increasing the reaction temperature, whereas the relation $(-\Delta P_a)/(P_{C_2H_2})_0$ remained unchanged as the acetylene pressure was increased.

5.6 [14-C]-DIRECT OBSERVATION STUDIES OF C_2H_2/H_2 HYDROGENATION REACTION

Three series of experiments were designed in an attempt to gain some knowledge about the behaviour of acetylene during its reaction with hydrogen, the reactivity of polymeric species formed from the adsorptions of C_2H_2 and C_2H_4 throughout the C_2H_2/H_2 hydrogenation reactions, and the amount of carbonaceous species that accumulate permanently on the catalyst surface.

Series 1

A 0.0978g of EUROPT-1 catalyst was cleaned by H_2 and treated using the standard procedure described previously. A sample of 1:3, [14-C]-acetylene:hydrogen was introduced to the reaction vessel. The quantity of [14-C]-acetylene in this sample was 5 Torr which was sufficient to build up an adsorption isotherm. The reaction was followed by minute-to-minute counting of the surface radioactivity. Figure 47 shows the variation of the surface count rate with time. According to Langmuir-Hinshelwood model of bimolecular reactions, the [14-C]-acetylene would be expected to result in an instant build up to a full coverage of surface layer of [14-C]-acetylene, which would diminish as the reaction proceeds. The behaviour observed in Figure 47

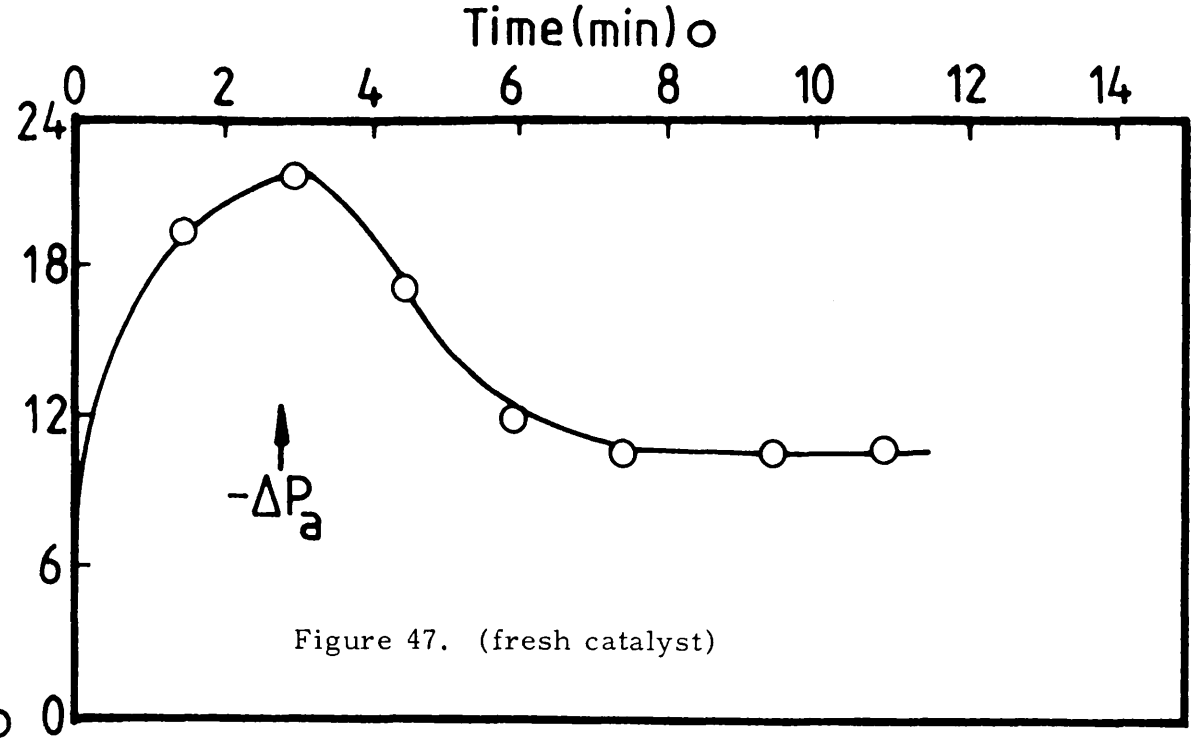

Figure 47. (fresh catalyst)

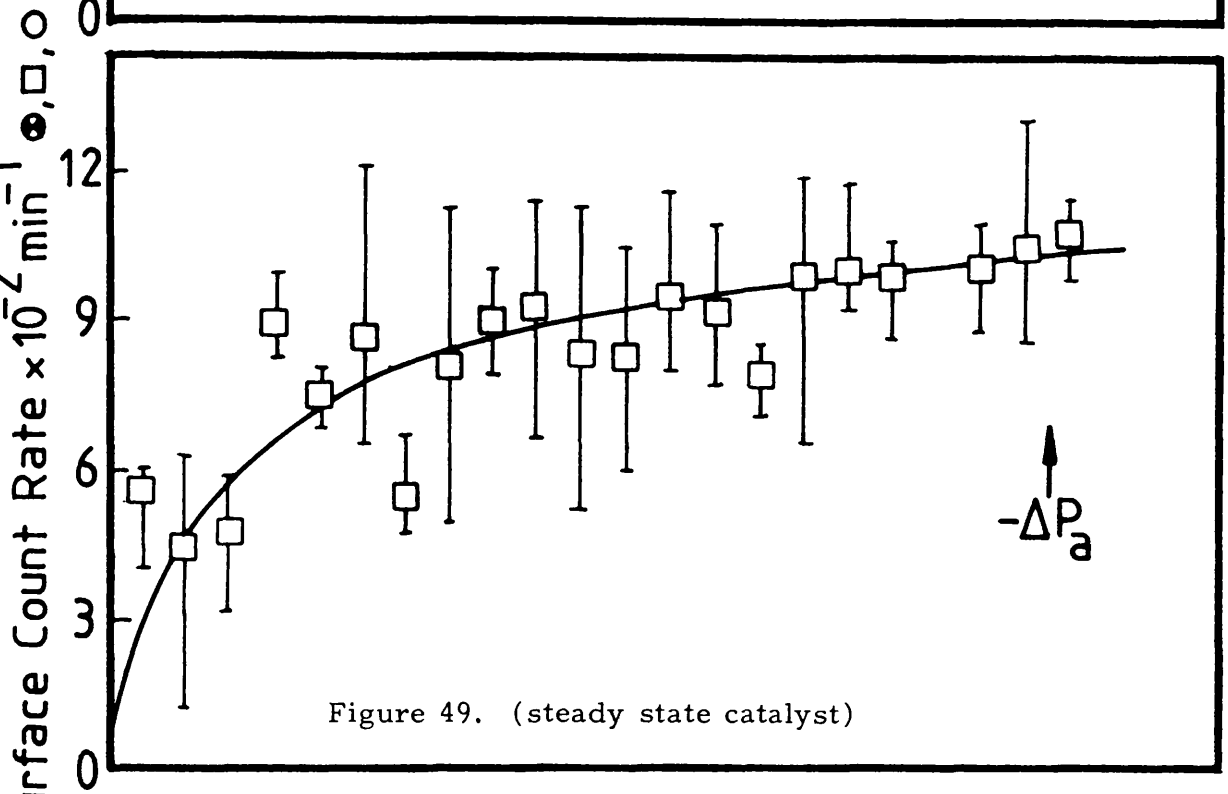

Figure 49. (steady state catalyst)

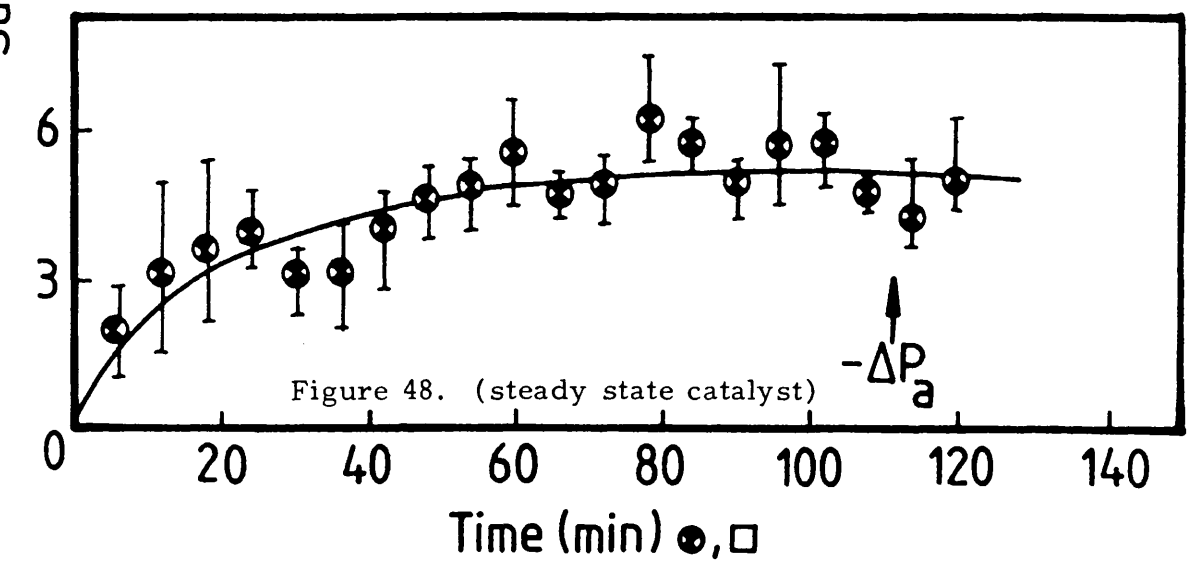

Figure 48. (steady state catalyst)

Behaviour of [14-C]C_2H_2 during its hydrogenation on EUROPT-1

on freshly reduced catalyst, represent5a reversal mechanism to the above model. This behaviour was also observed by Berndt et al. (56), using the system C_2H_2/H_2-Ni/SiO_2. The amount of [14-C] retained by the catalyst was ca. 50%.

A 0.095g catalyst was treated in the standard manner and then deactivated with 34 acetylene hydrogenations before a pre-mixed sample of 12.5 Torr [14-C]-acetylene + 37.5 Torr hydrogen (the amount of [14-C]-acetylene = 5 Torr) was admitted to the catalyst. The behaviour of the surface radioactivity is shown in Figure 48. From this, it can be seen that the behaviour of [14-C]-acetylene on a steady state catalyst is considerably more complex compared to the behaviour observed on a freshly reduced catalyst. Similar behaviour was found when the amount of [14-C]-acetylene used was increased to 12.5 Torr (Figure 49). However, it is interesting to note that the behaviour observed on a steady state catalyst is likely to exhibit oscillation cycles of adsorption-desorption which accompanied a continuous displacement of the [12-C] hydrocarbon species which are present on the catalyst.

Series 2

A freshly reduced EUROPT-1 catalyst (0.097g) was covered with 5 Torr of [14-C]-acetylene which was capable of building an adsorption isotherm. The catalyst was allowed to stand for one hour under this condition and then was evacuated for 30 min. A mixture of $3:1::H_2:C_2H_2$ was then admitted to the system and the reaction was followed by monitoring the pressure drop. The surface radioactivity was monitored at regular intervals of 1 min. Curve A (Figure 50) shows

that the surface radioactivity decreases rapidly, followed by a slower decrease. This was then followed by a second rapid decrease in the surface radioactivity. The shape of the curve suggests that the pre-adsorbed acetylene did undergo hydrogenation to ethylene which in turn underwent further hydrogenation to ethane with ca. 75% of the radio-activity staying on the catalyst.

When the above procedure was repeated on 0.098g of catalyst, deactivated to the steady state by 38 reactions of C_2H_2/H_2, the results shown in Curve B (Figure 50) indicate that the adsorbed acetylenic species did participate in the hydrogenation reaction in a manner similar to that observed on the freshly reduced catalyst. The amount of the acetylenic species which remained on the catalyst was calculated and found to be 34%.

Series 3

0.098g of EUROPT-1 was reduced and treated by the standard procedure. An adsorption isotherm of [14-C]-ethylene was built-up as described in section 4.2.1. The adsorbed ethylene was allowed to stand on the catalyst for 1h, then the reaction vessel was evacuated for 30 min. A pre-mixed sample of $3:1::H_2:C_2H_2$ was admitted to the catalyst and the surface radioactivity level was measured progressively as the hydro-genation reaction proceeded. The results of this experiment are shown in Curve C (Figure 50). The results show that about 66% of the pre-adsorbed ethylene was active to undergo hydrogenation with an amount, ca. 34%, remaining strongly adsorbed on the catalyst.

When 0.098g of EUROPT-1 in its steady state form (deactivated with 40 C_2H_2/H_2 reactions) was subjected to aliquots of [14-C]-ethylene

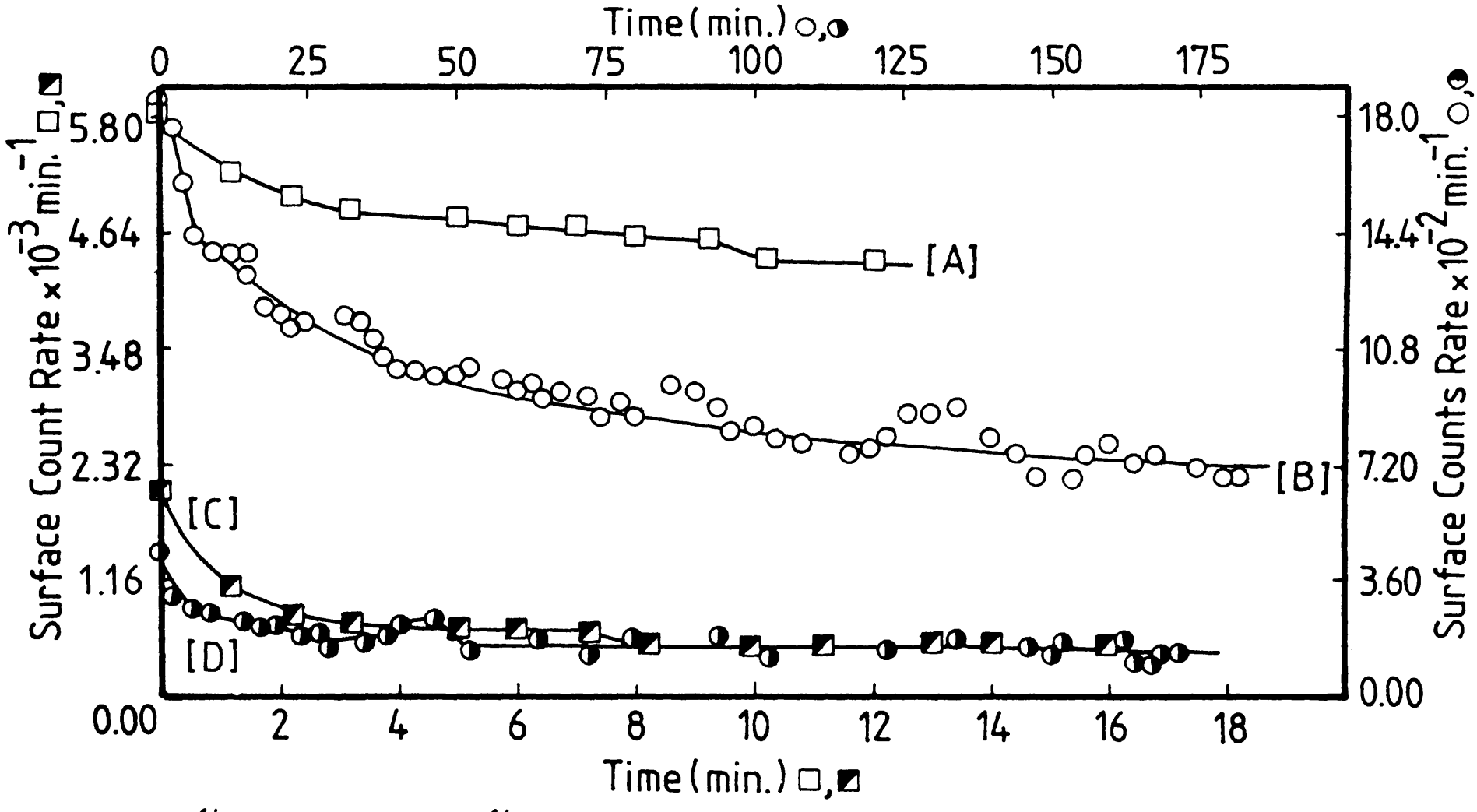

[14C]Acetylene □, and [14C]Ethylene ◪ Precovered Surface on Freshly Reduced Catalysts
[14C]Acetylene ○, and [14C]Ethylene ◑ Precovered Surface on Steady State Catalysts

Figure 50. Behaviour of pre-adsorbed hydrocarbons during C_2H_2/H_2 reaction on EUROPT-1.

and treated as described above and a hydrogenation of C_2H_2/H_2 was performed on the catalyst, similar behaviour to that observed on a freshly reduced catalyst was encountered (Curve D, Figure 50) with about 52% of the [14-C]-ethylene participating in the hydrogenation reaction and ~ 48% remaining deposited on the catalyst.

5.7 [14-C]-ETHYLENE TRACER STUDIES OF ACETYLENE HYDROGENATION

The addition of [14-C]-ethylene to the acetylene + hydrogen reaction mixture was used to gain further insight into the mechanism of the selective hydrogenation on a steady state EUROPT-1 catalyst.

0.095g of EUROPT-1 was reduced in a stream of hydrogen (30 ml min^{-1}) according to standard procedure and then cooled in vacuo to ambient temperature. The catalyst was then brought to the steady state by a self-poisoning process, using 36 hydrogenations of C_2H_2/H_2 at room temperature. A pre-mixed sample containing 12.5 Torr acetylene and 37.5 hydrogen + 1 Torr [14-C]-ethylene was introduced to the catalyst. Samples were extracted for analysis by the gas chromatograph and the amounts of radioactivity in the individual reaction products were determined using the gas proportional counter (section 3.1.1.5). The same procedure was repeated on the same catalyst using various pressures of [14-C]-ethylene (2 and 4 Torr) which were added to the reaction mixture before admission to the reaction vessel. The total ethane, ethylene and acetylene yields and the [14-C]-ethane and [14-C]-ethylene yields were determined. These are shown in Table 3.

Table 3. Distribution of C_2-products from the Hydrogenation of 12.5 torr of Acetylene in presence of Added* [^{14}C] Ethylene on 0.0947g steady state 6% Pt/SiO_2 (EUROPT-1) catalyst.

P_{H_2} = 37.5 torr temperature = 20 ± 2°C

Added* [^{14}C]C_2H_4 (torr)	(%) conversion	$P_{^{14}C_2H_6}$ (torr) x 10^{-4}	$P_{^{12}C_2H_4}$ (torr)	$P^{Total}_{^{12}C_2H_6}$ (torr)	$P^{Direct}_{^{12}C_2H_6}$ (torr)	Selectivity (S)	Inherent Selectivity (*S)
1*	19.28	7.51	0.8254	0.9593	0.9587	0.4625	0.4626
-	47.90	8.67	0.6156	1.0991	1.0986	0.3590	0.3591
-	61.50	6.58	0.5779	1.2123	1.2119	0.3228	0.3229
-	64.08	8.83	0.9741	3.0751	3.0742	0.2406	0.2406
-	87.18	19.28	1.0857	3.8871	3.8850	0.2183	0.2184
-	105.00	21.91	1.3118	5.1628	5.1599	0.2026	0.2027
-	168.50	31.82	1.5546	6.8298	6.8248	0.1854	0.1855
-	195.65	75.72	0.3536	8.3074	8.3047	0.0408	0.0408
2*	5.13	17.61	0.1209	0.2452	0.2451	0.3302	0.3303
-	41.34	226.40	0.5205	1.8794	1.8734	0.2169	0.2174

Table 3 (contd.)

Added* $[^{14}C]C_2H_4$ (torr)	(%) conversion	$P_{^{14}C_2H_6}$ (torr) x 10^{-4}	$P_{^{12}C_2H_4}$ (torr)	Total $P_{^{12}C_2H_6}$ (torr)	Direct $P_{^{12}C_2H_6}$ (torr)	Selectivity (S)	Inherent Selectivity ($^*S$)
cont. 2*	83.70	42.76	1.0154	2.5127	2.5105	0.2878	0.2879
-	120.50	228.87	1.9032	3.8631	3.8411	0.3301	0.3313
-	168.40	1051.31	1.7346	7.5849	7.4887	0.1861	0.1881
-	181.90	812.37	0.4861	8.9407	8.9201	0.0516	0.0517
4*	13.00	100.00	0.1587	0.4700	0.4696	0.2524	0.2526
-	45.70	219.70	0.6401	1.7090	1.7055	0.2725	0.2729
-	99.80	142.50	1.2669	4.5678	4.5633	0.2171	0.2173
-	180.00	944.00	0.7511	6.0705	6.0523	0.1101	0.1104
-	184.50	1388.00	0.0655	6.8382	6.8358	0.0949	0.00949

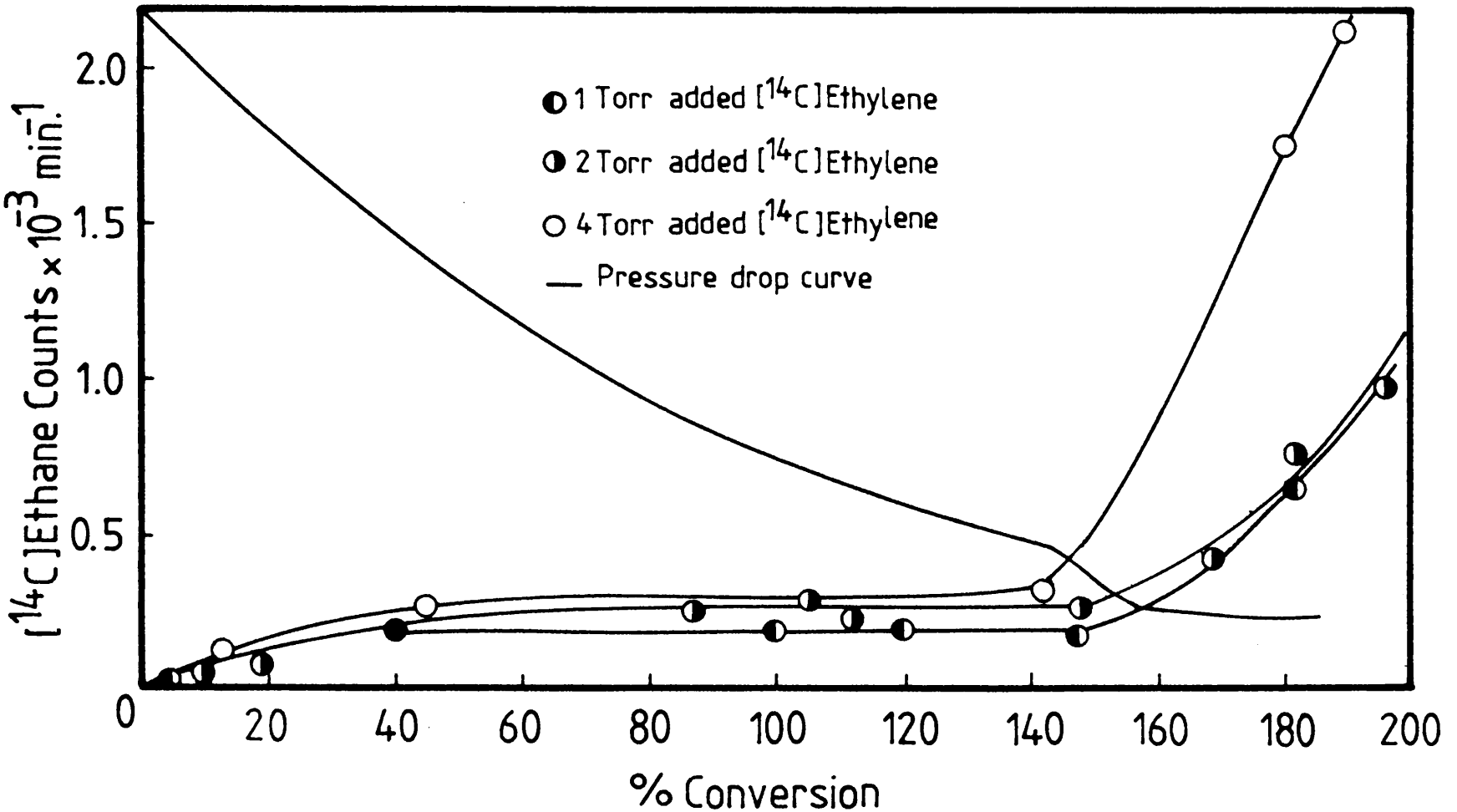

Figure 51. Variation of [14-C] ethane yield during the hydrogenation of acetylene on EUROPT-1. in the presence of added amounts of [14-C] ethylene.

Figure 51 shows the variation of the yields of [14-C]-ethane with conversion for the hydrogenation of acetylene with hydrogen in the presence of various pressures of added [14-C]-ethylene.

To further test the behaviour of [14-C]-ethylene hydrogenation in the presence of acetylene, the reaction of 12.5 Torr acetylene + 37.5 Torr hydrogen in the presence of added amounts of [14-C]-ethylene, was studied by the direct observation technique, using 0.095g of EUROPT-1. The results (Figure 52) show that during the hydrogenation of acetylene, [14-C]-ethylene behaves in a manner suggesting an oscillating process is involved, which probably could be attributed to adsorption-desorption cycles.

The amount of [14-C]-ethylene present in the reaction mixture at any stage of the reaction, as measured by radio-gas chromatography, is shown in Figure 53.

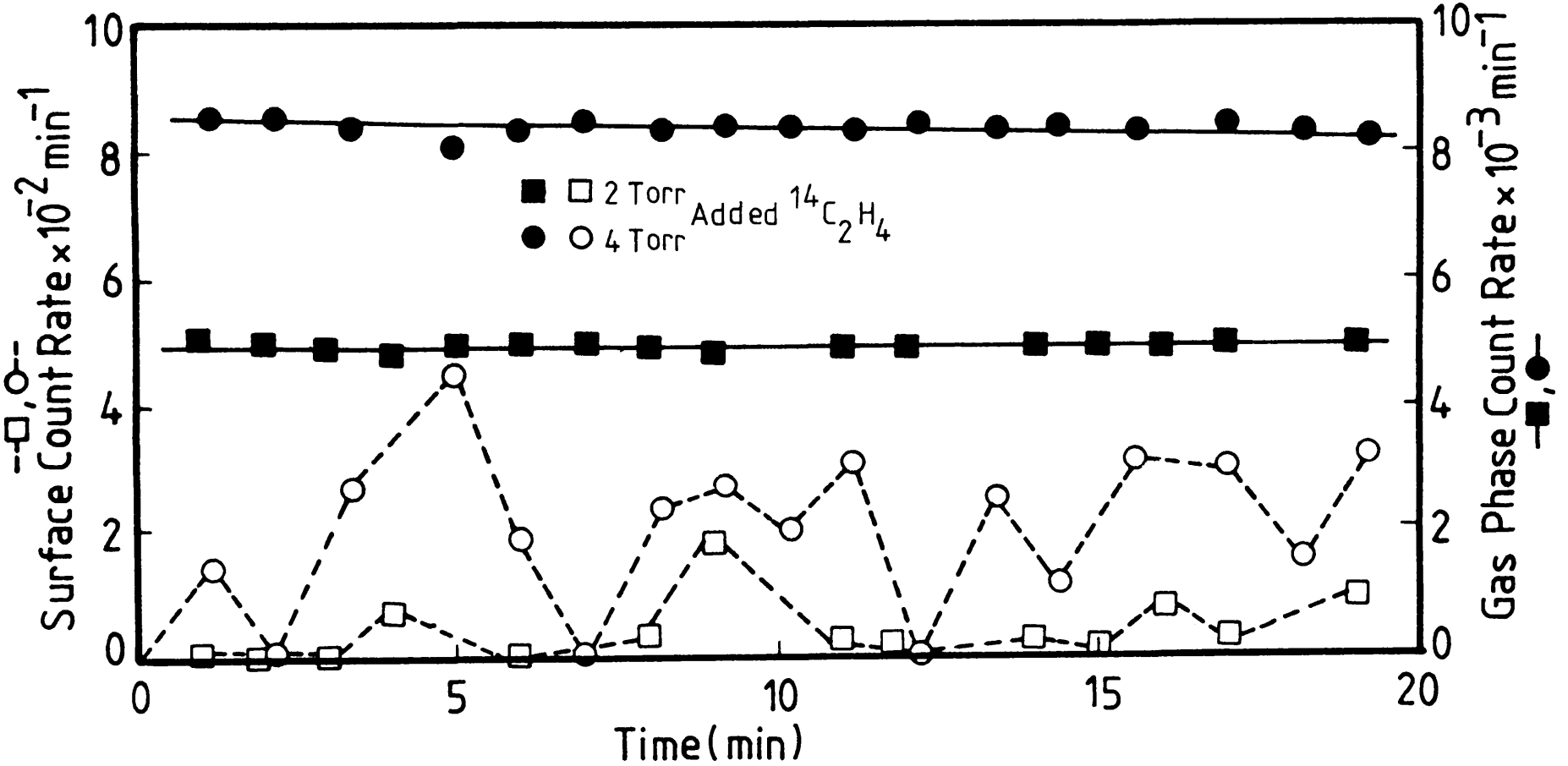

Figure 52. Behaviour of [14-C]-ethylene during the C_2H_2/H_2 hydrogenation on EUROPT-1.

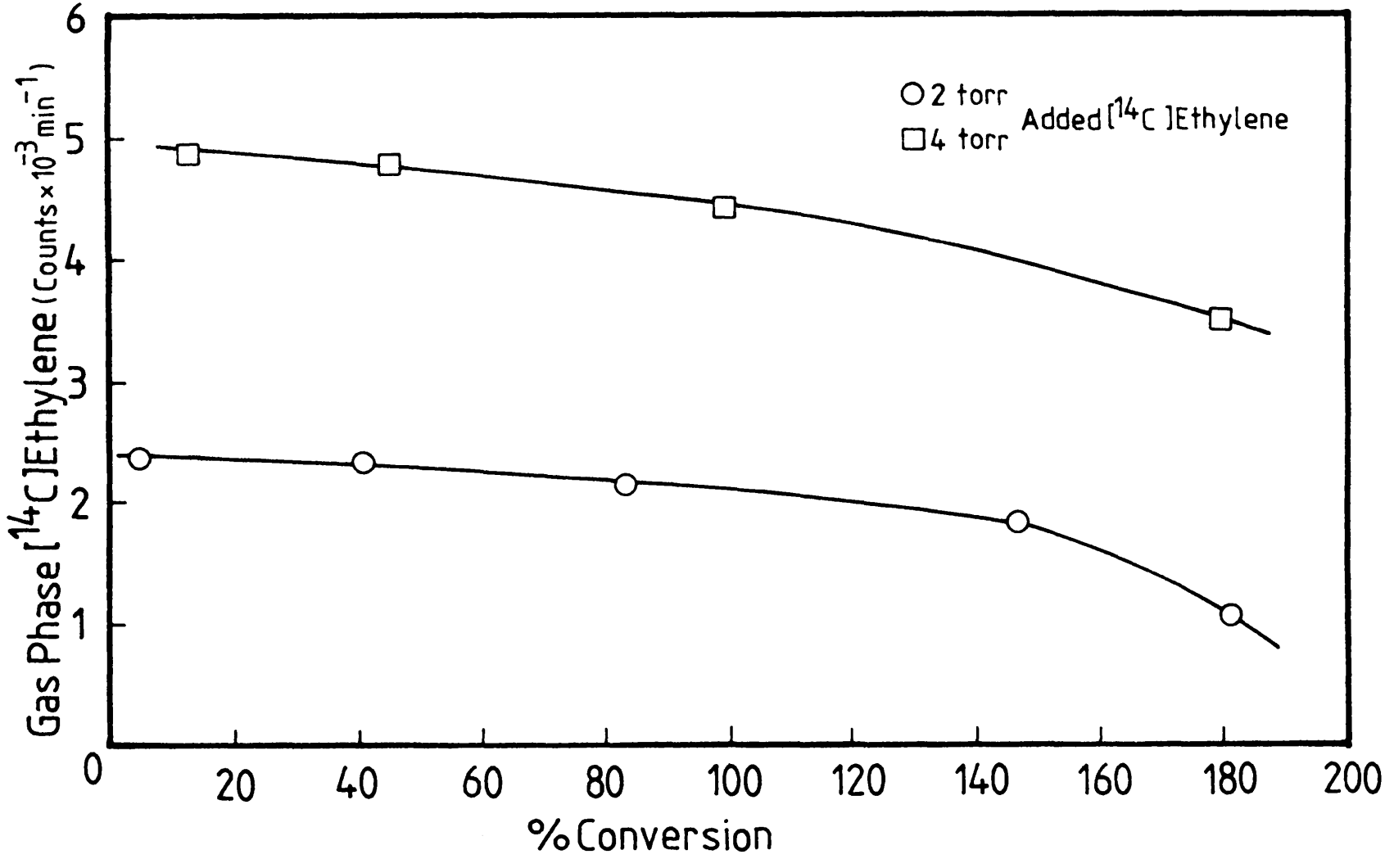

Figure 53. Variation of [14-C] ethylene count rate during the hydrogenation of acetylene on EUROPT-1.

CHAPTER SIX

THE REACTION OF ACETYLENE WITH HYDROGEN OVER 0.3% Pt/Al_2O_3 (EUROPT-3) CATALYSTS

6.1 DEACTIVATION CURVES

The hydrogenation of acetylene with hydrogen on EUROPT-3 was investigated using a 2.05g catalyst. The catalyst was reduced in a stream of hydrogen using the standard procedure (section 3.6), before being cooled to room temperature (20 ± 2°C) in vacuo.

A pre-mixed sample of 50 Torr, 3:1, hydrogen:acetylene was introduced to the reaction vessel, the progress of the reaction was monitored by the pressure transducer and the resulting pressure fall against time curve is shown in Figure 54a. This curve indicates that the hydrogenation of C_2H_2/H_2 proceeded in two stages. The acceleration point denoted by $-\Delta P_a$, which was obtained by extrapolating the first and second stages of the reaction, occurred at a pressure fall equal to 13.5 ± 0.2 Torr, that is, at a pressure fall corresponding to nearly complete removal of acetylene.

The same catalyst was subjected to a series of C_2H_2/H_2 hydrogenation reactions "consecutively" using mixtures of 12.5 Torr acetylene and 37.5 Torr hydrogen. After each hydrogenation, the reaction vessel was evacuated for 30 min to remove gaseous products formed from the preceding reaction. Figure 54a shows that the reaction rate decreased slightly between successive hydrogenations. However, both stages of the reaction remained clearly defined with the acceleration point ($-\Delta P_a$)

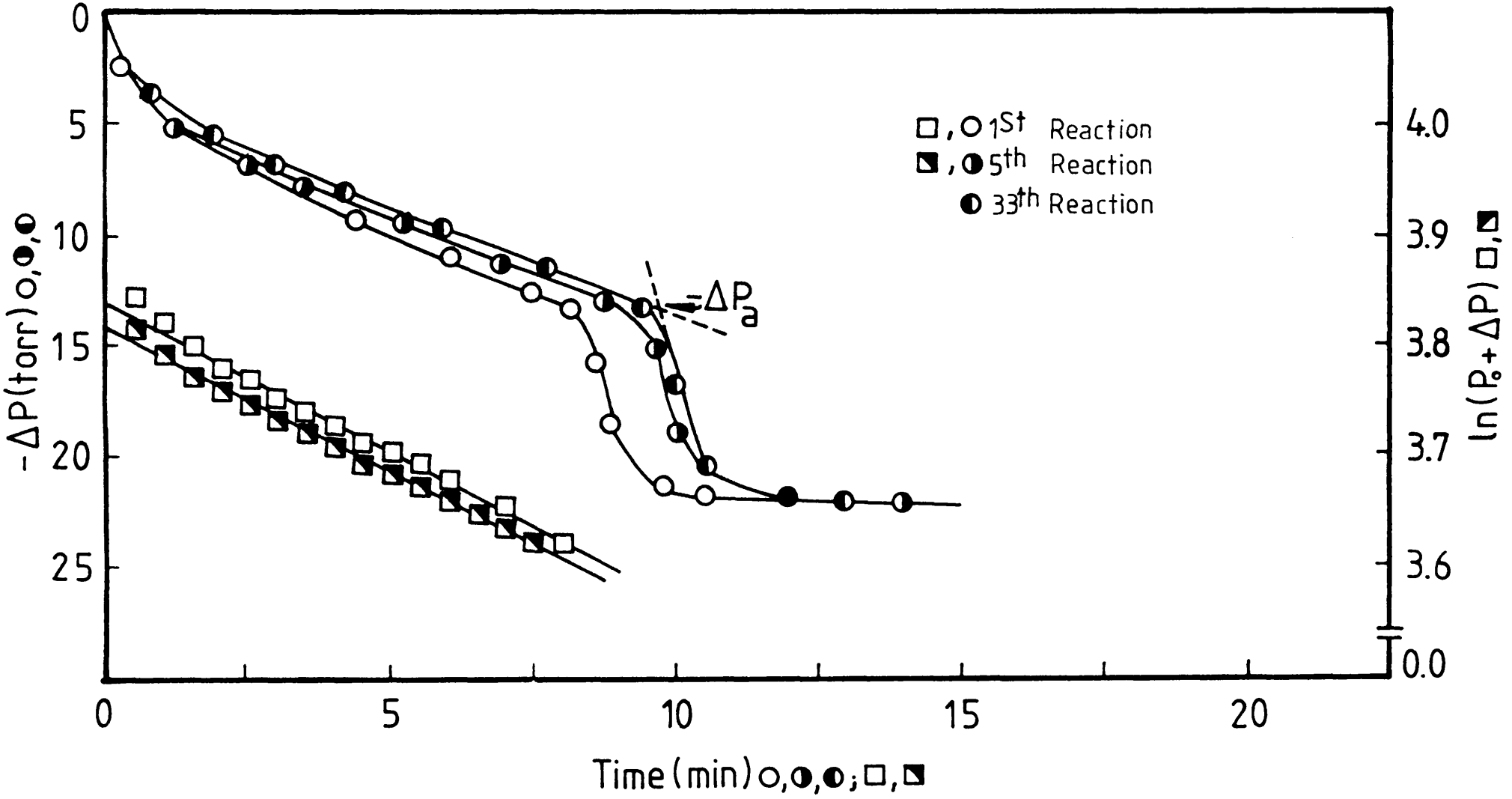

Figure 54a. Pressure fall-time curves (circles) and first order plots (squares) of acetylene hydrogenation on EUROPT-3.

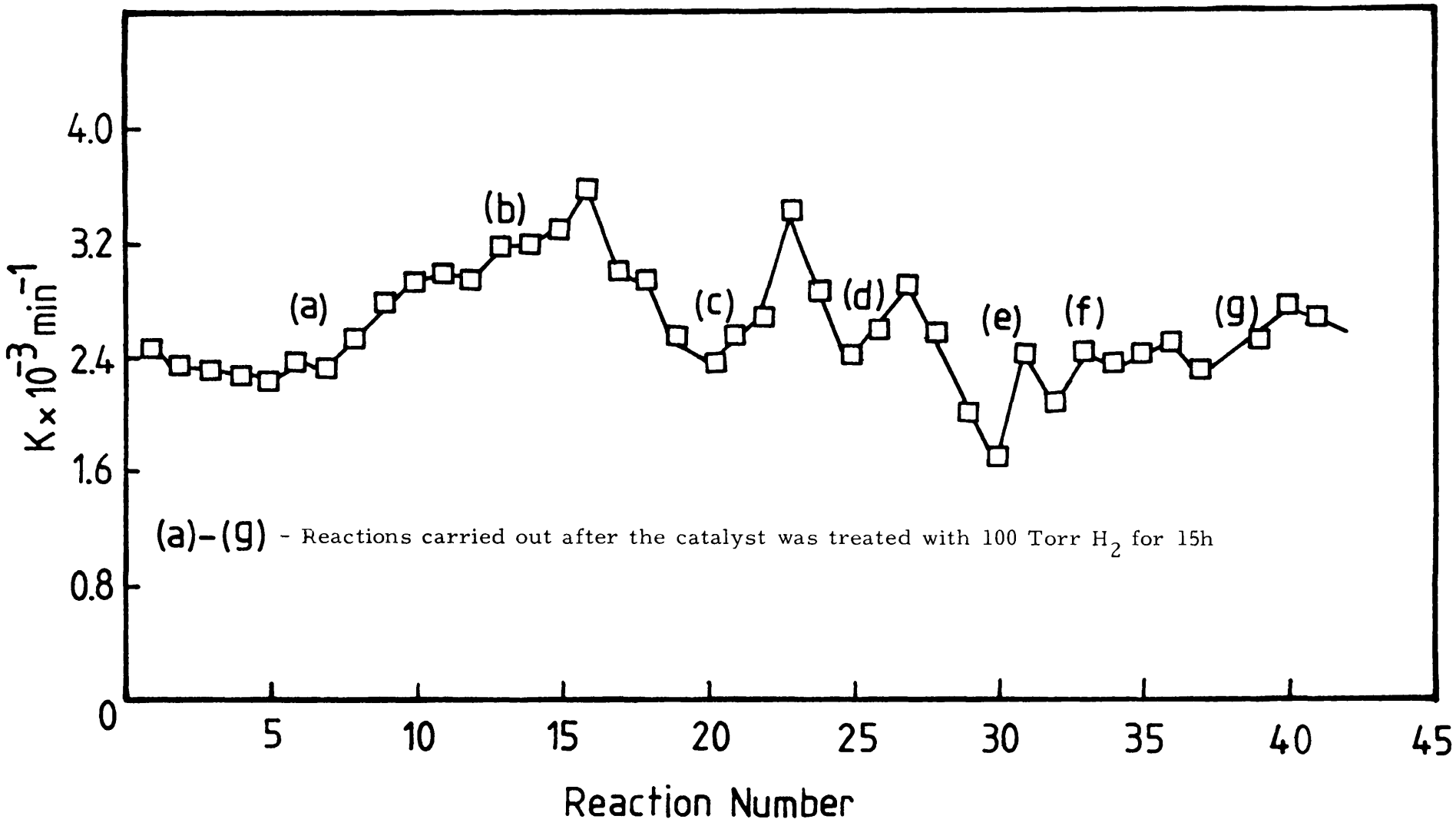

Figure 54b. Variation of the first order rate constant with reaction number on EUROPT-3.

being independent of the number of reactions carried out on the catalyst. Plots of $\ell n\ (P_o + \Delta P)$ against time (Figure 53a) produced straight lines indicating that the first stage of the reaction was first-order with respect to total pressure. The gradients of these plots gave values of the first-order rate constant ($K\ min^{-1}$). Figure 54b shows the variation of the first-order rate constant ($K\ min^{-1}$) with reaction number, from which it can be seen that, during the deactivation of the catalyst by C_2H_2/H_2 hydrogenations, the catalyst activity could be partially restored by leaving the catalyst in contact with 100 Torr H_2 for periods of $>$ 15h. The original activity could, however, be restored by regenerating the catalyst under the reduction conditions (see section 3.10). During this regeneration process, ethane and methane were produced. However, due to the small amounts involved and the fact that the regeneration process was carried out under flowing H_2, accurate quantitative analysis of the amounts of each hydrocarbon could not be achieved.

6.2 PRODUCT DISTRIBUTION ON FRESHLY REDUCED AND STEADY STATE CATALYSTS

In order to examine the possible productds which could be formed during the hydrogenation of acetylene with hydrogen on the EUROPT-3 catalyst, a 2.00g sample was reduced and treated according to the standard procedure (see section 3.6). After the catalyst had been cooled to room temperature, a hydrogenation reaction using a mixture of 12.5 Torr acetylene and 37.5 Torr hydrogen was carried out on the catalyst. Analysis of the reaction products at various stages

during the course of the reaction by gas chromatography showed (Figure 55a) that, as in the case of EUROPT-1, ethane and ethylene were produced in the early stages of the reaction. This was continued up to about 50% of the extent of the total reaction (~ 95% conversion), when the yield of ethane increased remarkably as a result of the hydrogenation of ethylene at the onset of the second stage of the reaction. The dominant feature of C_2H_2/H_2 hydrogenation on EUROPT-3 was that it showed an approximately three-fold higher selectivity when compared with EUROPT-1. The selectivity increased slightly with % conversion, from an initial value of 0.600 to 0.680 up to a point corresponding to the up-take of approximately 0.95 moles of hydrogen per mole of acetylene present (~ 95% conversion).

The hydrogenation of C_2H_2/H_2 on a steady state EUROPT-3 catalyst was also investigated. 0.95g of catalyst was reduced and treated using the standard procedure and then subjected to a series (39 reactions) of C_2H_2/H_2 hydrogenations using 3:1, hydrogen:acetylene mixtures. Samples were extracted and analysed several times during each reaction. Comparison of the results for sets of reactions on a steady state catalyst showed that the product distribution was similar from reaction to reaction. Typical product distribution curves for a steady state catalyst (reaction 46) are shown in Figure 55b. From this it can be seen that, at conversions less than ~ 100%, the yields of ethane and ethylene increased almost linearly with % conversion. Also, when about 88% of the acetylene had been reacted, the ethylene yield decreased rapidly and simultaneously the ethane yield increased rapidly. In contrast to the freshly reduced catalyst, a slight increase (about 6%)

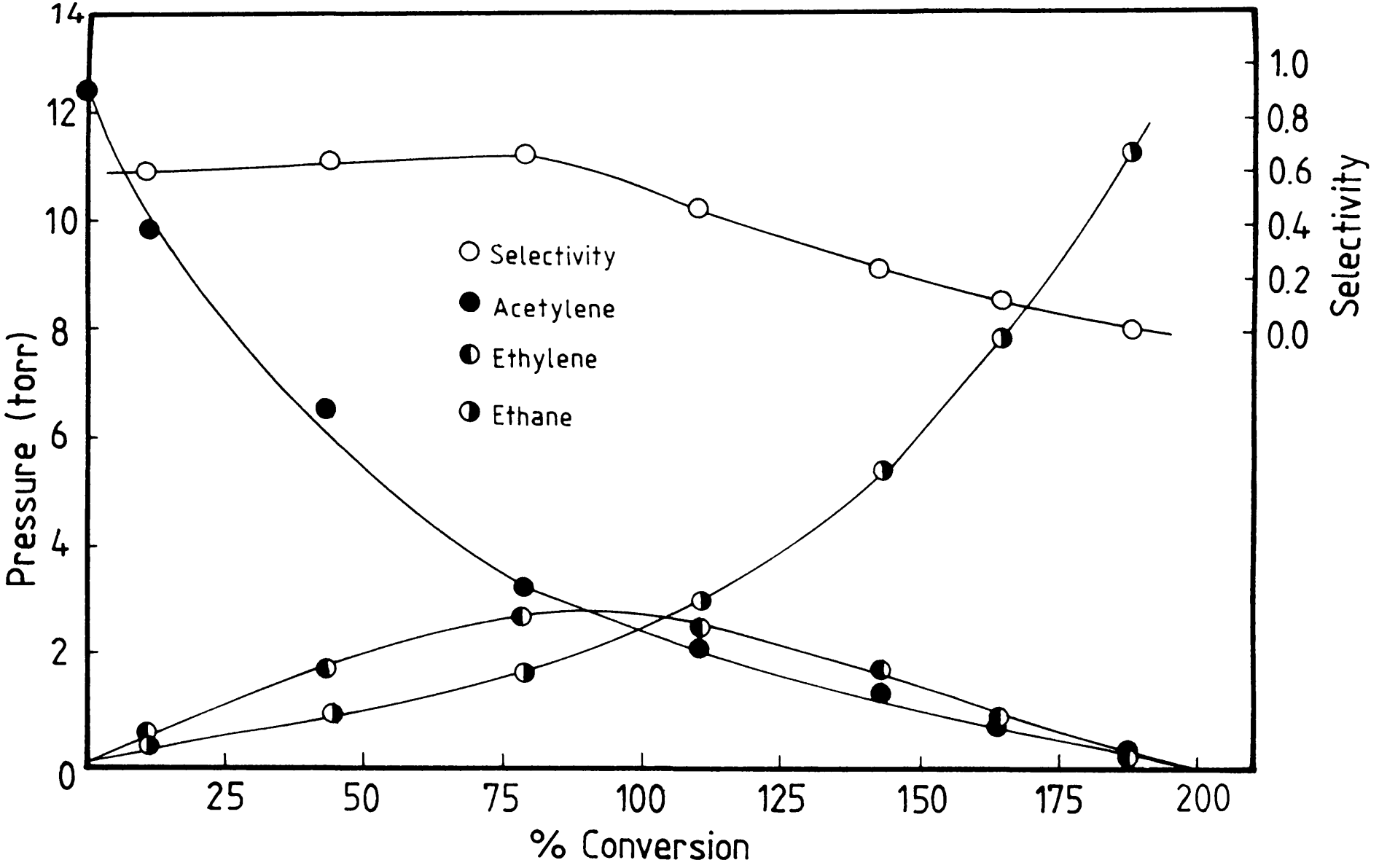

Figure 55a. Product distribution curves of acetylene hydrogenation on freshly reduced EUROPT-3.

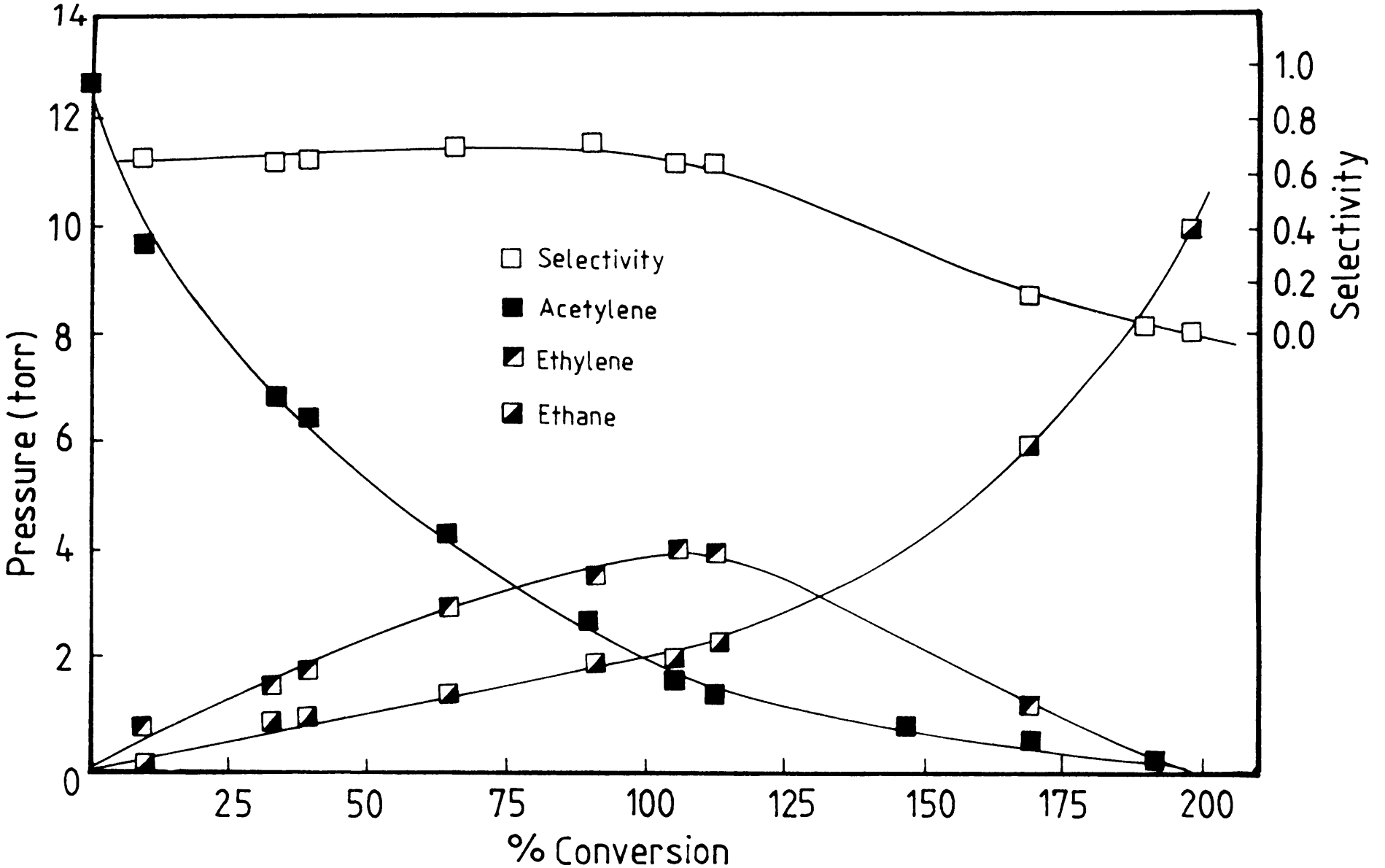

Figure 55b. Product distribution curves of acetylene hydrogenation on steady state EUROPT-3.

in the selectivity was also observed with the catalyst in its steady state (Figure 55b). At the latter stages of the reaction, tracers of polymeric hydrocarbons appeared. These were identified as C_4 products (mainly n-butane).

The variation of selectivity with increasing reaction number was also investigated in another set of reactions, using 2.0345g of catalyst. Products were analysed at a fixed pressure drop ($-\Delta P$) of ~ 10 Torr which corresponded to 46 ± 2.1 conversion. As can be seen from Table 4, the deactivation had a negligible effect on selectivity.

Table 4. Effect of Catalyst Deactivation on Selectivity

Reaction No.	% Conversion	Selectivity
7	42.8	0.675
9	44.5	0.680
15	45.9	0.696
20	47.9	0.681
24	48.1	0.658
32	47.9	0.663
35	45.4	0.683
41	46.0	0.681

6.3 THE REACTION ORDER WITH RESPECT TO HYDROGEN AND ACETYLENE

After activation, a 2.05g sample of EUROPT-3, was evacuated at 250°C for 0.5h and cooled in vacuo to ambient temperature. The catalyst was then run to its steady state by performing 30 hydrogenation reactions using 3:1 ::H_2:C_2H_2 mixtures.

In a series of experiments at room temperature, using a constant initial acetylene pressure of 12.5 Torr, the hydrogen pressure was varied between 6.25 and 75.0 torr. Products were extracted at pressure fall equal to ~ 10 Torr and analysed by gas chromatography, in order to look at the effect of increasing the H_2 pressure upon the product distribution and consequently on the selectivity. The order with respect to hydrogen was found to be 1.73 ± 0.06 (Figure 56). As shown in Figure 57, the selectivity of the catalyst for ethylene production decreased as the initial hydrogen pressure was increased. Extrapolation of this curve to zero hydrogen pressure produced a limiting value of selectivity of about 0.850.

In another set of experiments using 2.035g EUROPT-3, a series of acetylene hydrogenation reactions (3:1, hydrogen:acetylene) were carried out to bring the catalyst to its steady state. The initial pressure of hydrogen was fixed at 12.5 Torr throughout whereas the initial pressure of acetylene changed between 6.25 and 150 Torr. Products were again analysed by gas chromatography at pressure drop equal to 10 Torr in order to investigate the dependence of selectivity upon the acetylene pressure.

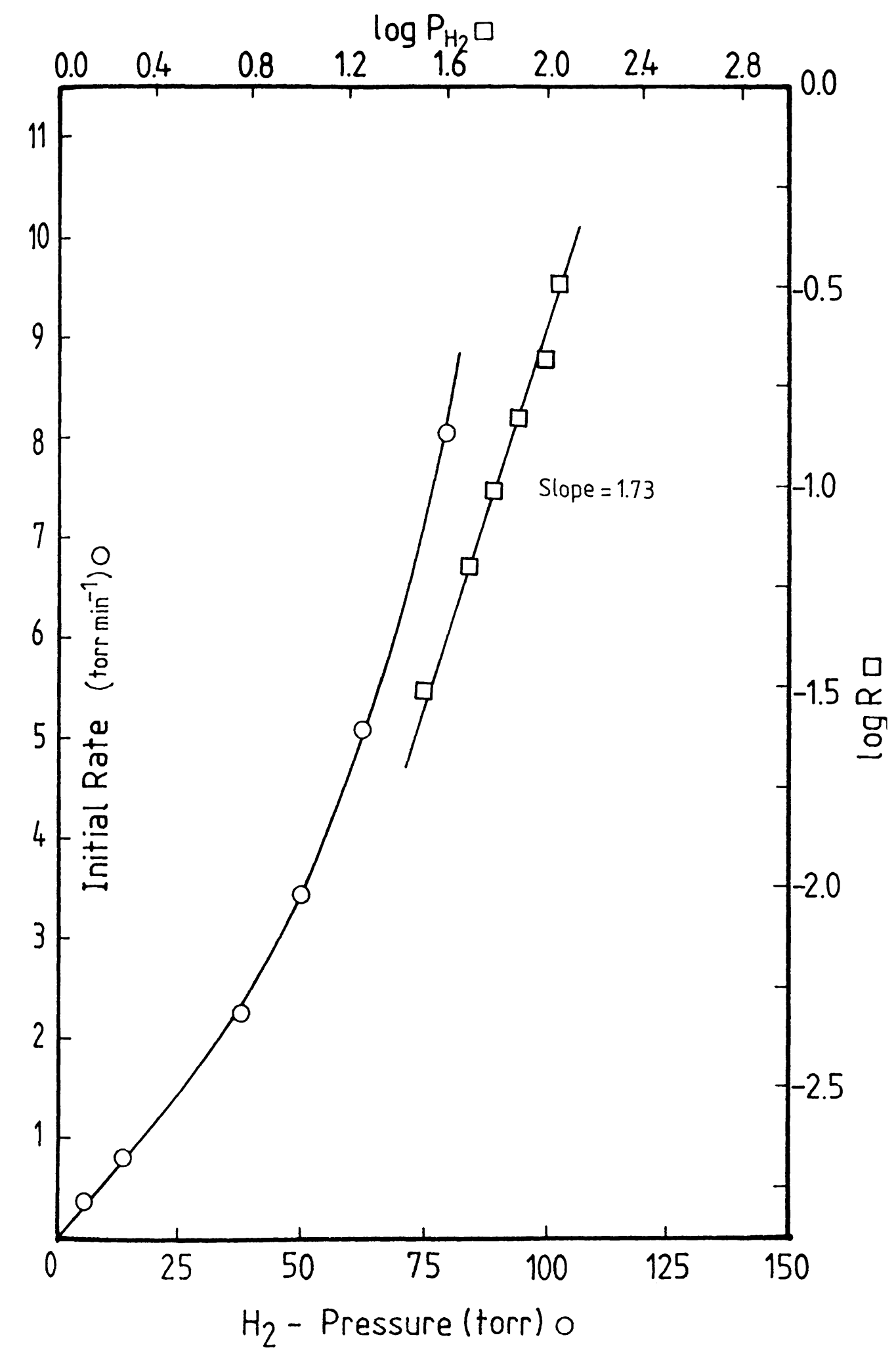

Figure 56. The variation of initial rate with H_2 pressure in acetylene hydrogenation on EUROPT-3.

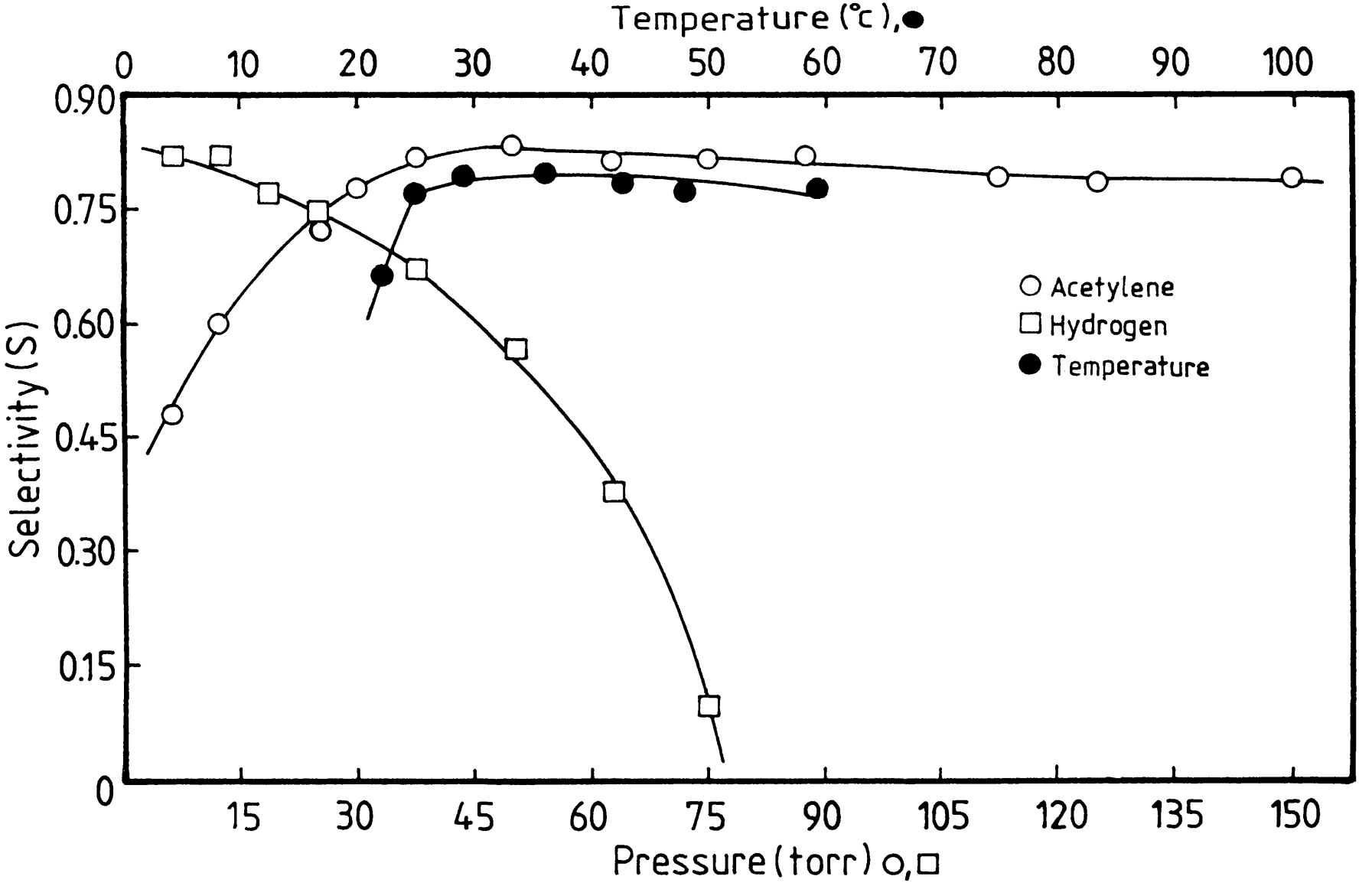

Figure 57. The variation of selectivity with experimental variables of acetylene hydrogenation on EUROPT-3.

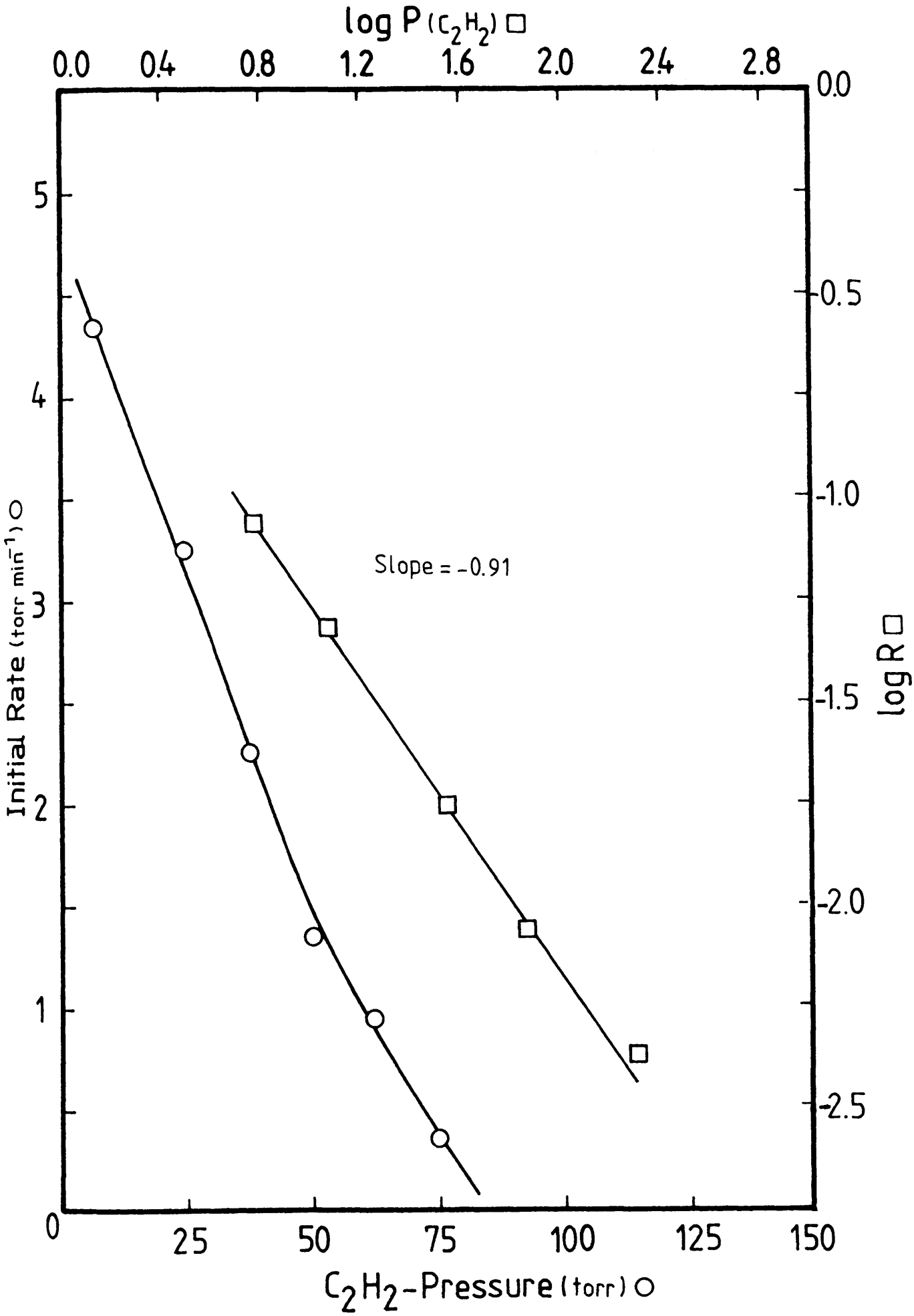

Figure 58. The variation of initial rate with C_2H_2 in acetylene hydrogenation on EUROPT-3.

The reaction order with respect to acetylene was found to be -0.95 ± 0.01 (Figure 58). As is clear from Figure 57, the selectivity increases steadily as the pressure of acetylene is increased up to a pressure ca. 38 Torr, after which no significant variation in the selectivity was observed, although pressures up to 150 Torr were used.

6.4 THE TEMPERATURE DEPENDENCE OF THE PRODUCT DISTRIBUTION AND THE ACTIVATION ENERGY OF THE REACTION

In order to examine the dependence of the selectivity upon temperature and to evaluate the activation energy of the reaction on EUROPT-3, a sample of 0.97g catalyst, after activation, was brought to the steady state, as explained in the previous sections. A series of reactions in the temperature range 22°C to 85°C, using (3:1), H_2:C_2H_2 mixtures was carried out. Each reaction was analysed after a pressure fall of ~ 10 Torr.

The plot of $\log_{10}$ (initial rate) against the reciprocal of absolute temperature (Figure 59) produced a straight line from which an activation energy of 40.66 ± 0.315 kJ mol^{-1} was obtained. The selectivity of the catalyst for the production of ethylene as a function of temperature (Figure 57) increased from a value of 0.668 to a constant value of 0.780 as the temperature was raised from 20° to 60°C. Above this temperature limit a diffusion control effect was found to operate.

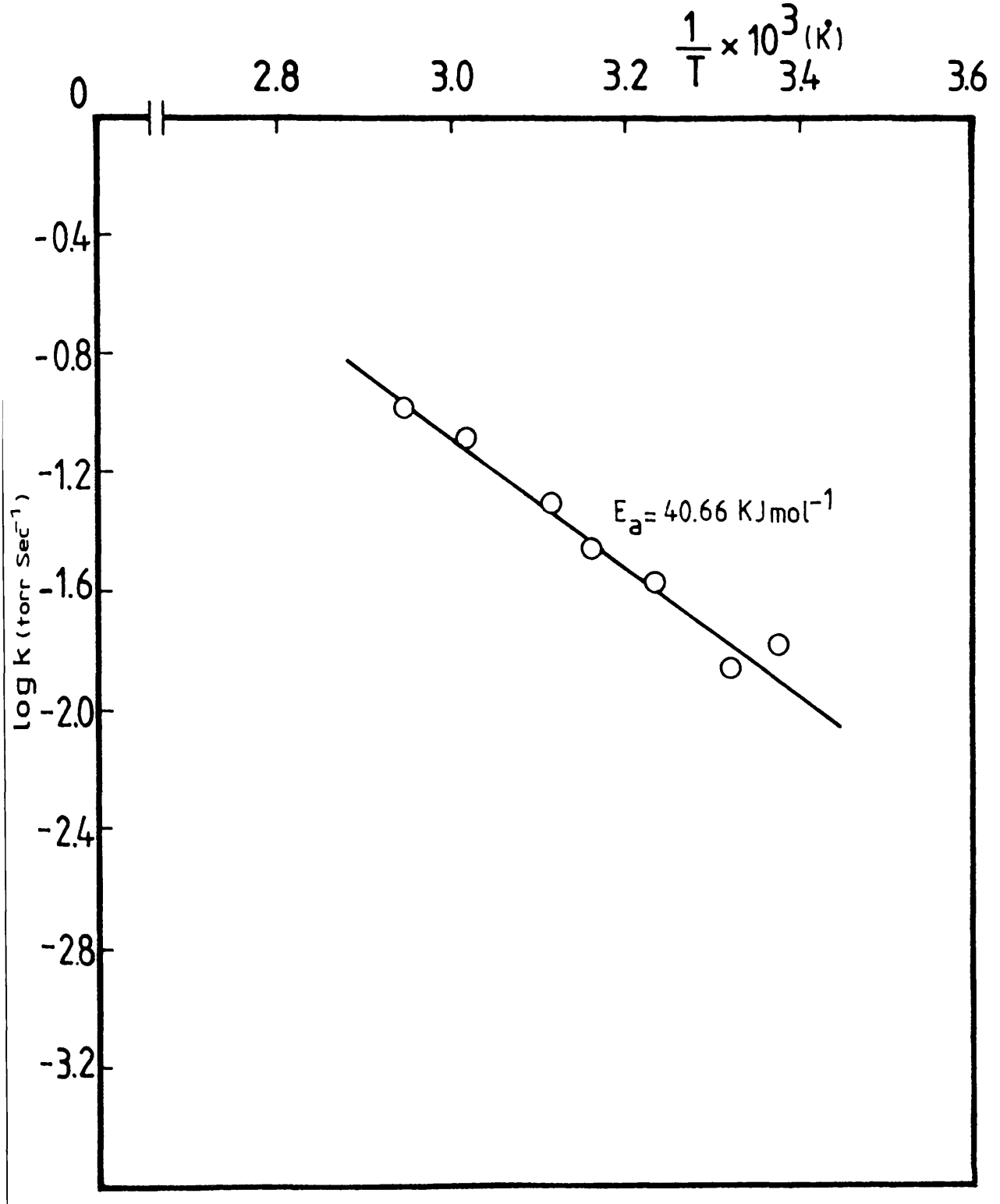

Figure 59. The variation of $\log_{10}$ (initial rate) with reciprocal of the absolute temperature of acetylene hydrogenation on EUROPT-3.

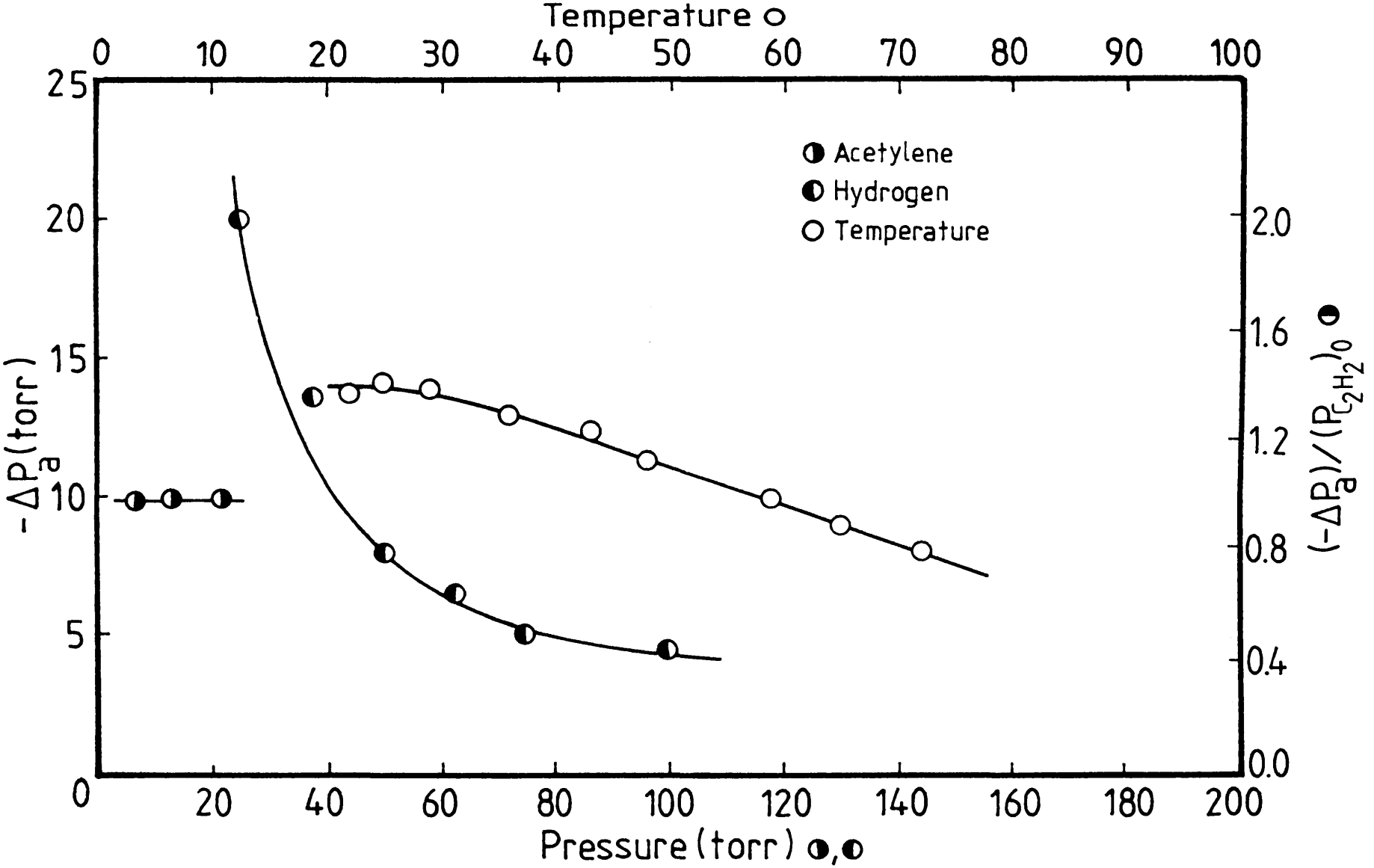

Figure 60. The dependence of acceleration point ($-\Delta P_a$) upon experimental variables.

6.5 THE DEPENDENCE OF ACCELERATION POINT UPON EXPERIMENTAL VARIABLES

The effect of acetylene and hydrogen pressures and temperature on the acceleration point ($-\Delta P_a$) was determined. The catalysts which were used in sections 6.3 and 6.4 were employed to investigate these effects.

As can be seen from Figure 60, the acceleration point ($-\Delta P_a$) appeared earlier as the initial hydrogen pressure was increased. Whereas the relation $(-\Delta P_a)/(P_{C_2H_2})_0$ remained unchanged as the pressure of acetylene was varied.

In the temperature range 30° to 70°C, the acceleration point occurred earlier as the temperature was increased.

6.6 [14-C]-DIRECT OBSERVATION STUDIES OF C_2H_2/H_2 HYDROGENATION REACTION

In an attempt to look at the behaviour of acetylene and ethylene during the C_2H_2/H_2 hydrogenation on EUROPT-3 using the corresponding [14-C]-labelled hydrocarbon, the following experiments were carried out:

Experiment 1

This experiment was designed to examine the behaviour of the acetylenic species adsorbed in the primary region of the adsorption isotherms of acetylene (section 4.12, Figure 27), during the hydrogenation reaction. It was also intended to investigate the relevance of retained carbonaceous species to the hydrogenation reaction.

0.97g of EUROPT-3 was reduced in flowing H_2 according to the standard procedure. The catalyst was then covered with ca. 0.5

Torr [14-C]-C_2H_2 to build-up the primary adsorption region. After 15 min, a sample from the gas phase in contact with the surface was analysed by the radio-gas chromatography (section 3.1.1.5). This analysis showed [14-C]-ethane as the only hydrocarbon product present in the gas phase. The reaction vessel was evacuated for 30 min to remove the gas phase radioactivity and a pre-mixed sample of 12.5 Torr acetylene and 37.5 Torr hydrogen was introduced to the reaction vessel. The reaction was followed at regular intervals of 1 min by monitoring the surface radioactivity. As shown in (Curve A), Figure 61, the surface radioactivity remained almost unchanged during the course of the reaction. However, evacuation of the reaction vessel after the completion of the reaction resulted in ca. 26% drop in the surface radioactivity.

Experiment 2

The aim of this experiment was to gain some insight into the behaviour of [14-C]-acetylene during its hydrogenation with hydrogen.

A 0.9642g catalyst was reduced in the usual manner. A sample of [14-C]-acetylene:hydrogen (1:3 reactant ratio), was introduced to the reaction vessel. The reaction was followed by continuous 1 minute counting of the radioactivity. It was found, ((Curve B), Figure 61) that, as the [14-C]-acetylene and hydrogen was admitted to the catalyst, an instant build-up to a full coverage of a surface layer of [14-C]-C_2H_2 occurred and the surface radioactivity diminished as the reaction proceeded. After the catalyst had been evacuated for 30 min, approximately 23.3% of the acetylene remained bound to the surface.

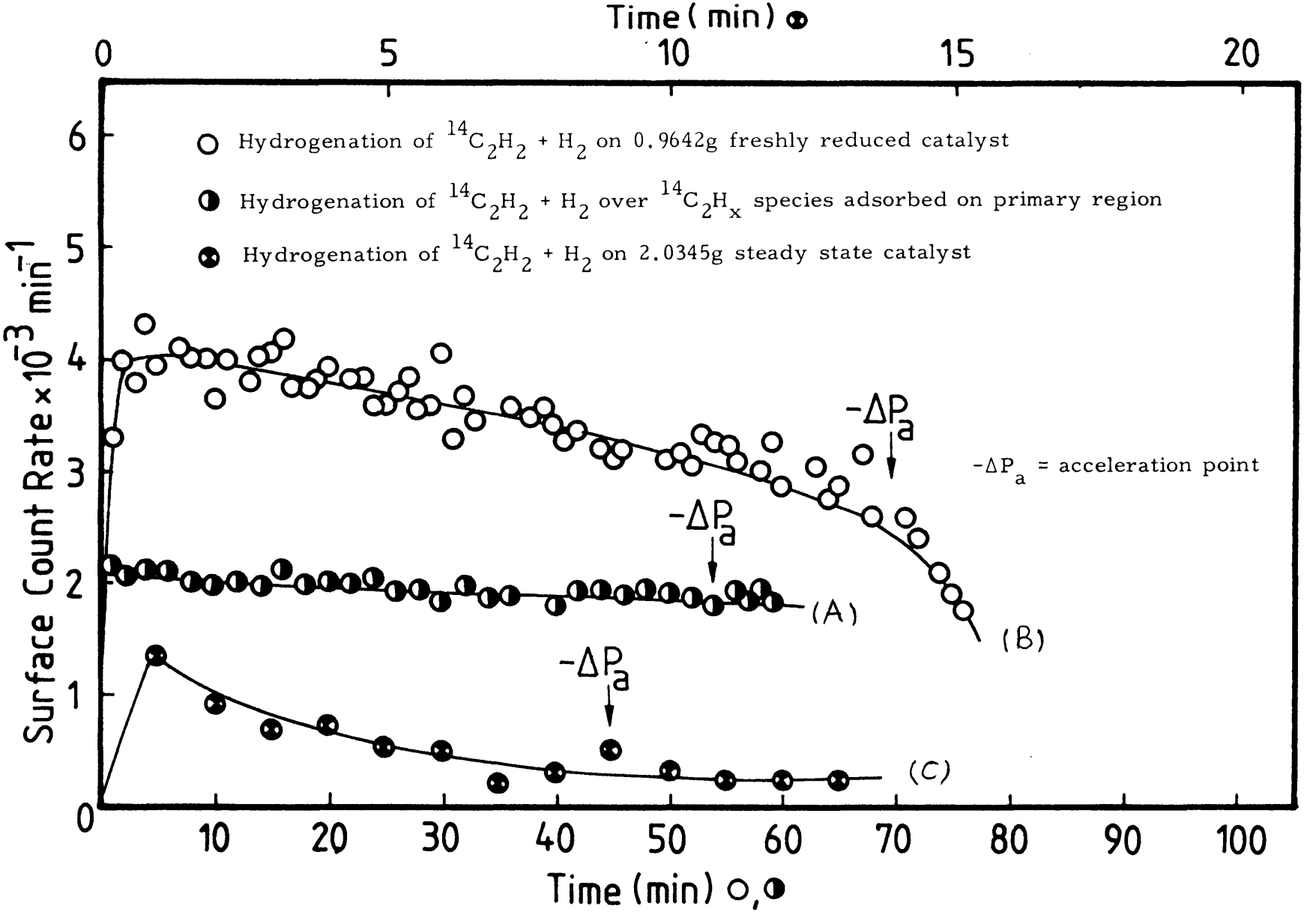

Figure 61. Direct observation of the behaviour of [14-C]-hydrocarbon during its hydrogenation on EUROPT-3.

Experiment 3

This experiment was taken with the similar objectives to those in experiment 2, but using a catalyst in its steady state. A sample of 2.0345g EUROPT-3 was reduced as usual and then deactivated to the steady state by a series of hydrogenation reactions using 3:1:: H_2:C_2H_2 mixtures. After the catalyst had been evacuated for 30 min, a pre-mixed 1:3 mixture of [14-C]-acetylene and hydrogen was admitted to the catalyst. As the reaction progressed, the count rate of the surface radioactivity was measured on a minute to minute basis. Curve C (Figure 61) shows that, as observed on a clean catalyst, the radioactivity of the surface fell steadily as the hydrogenation reaction progressed. However, about 21.7% of the admitted [14-C]-C_2H_2 remained strongly held on the catalyst even after the catalyst had been evacuated for 30 min.

6.7 [14-C]-ETHYLENE TRACER STUDIES OF ACETYLENE HYDROGENATION

The addition of [14-C]-ethylene to the reaction mixture of acetylene and hydrogen was used to gain further knowledge into the mechanism of C_2H_2/H_2 hydrogenation on EUROPT-3 and the relative importance of the thermodynamic and mechanistic factors in controlling the selectivity of the catalyst for ethylene production. This was investigated in the following series of experiments.

Experiment 1

This experiment was designed to examine the behaviour and the extent of participation of the ethylene species pre-adsorbed in the primary adsorption region during the reaction of acetylene with hydrogen. A 0.97g EUROPT-3 catalyst was reduced in flowing H_2 (30 ml min^{-1}) at 250°C according to the standard procedure, before being cooled to ambient temperature in vacuo. An amount, ca. 1 Torr of [14-C]-C_2H_4 was admitted to the catalyst, this being sufficient to cover the primary region. A hydrogenation reaction of 3:1::H_2:C_2H_2 was carried out on the catalyst with the surface radioactivity being monitored at regular 1 min intervals. The results presented in Curve A (Figure 62) suggest that the pre-adsorbed [14-C]-ethylene underwent hydrogenation as the reaction progressed. However, an amount, ca. 20%, of the pre-adsorbed ethylene remained strongly bound on the surface.

Experiment 2

In this experiment, a pre-mixed sample of 3:1::H_2:C_2H_2 + 2 Torr [14-C]-C_2H_4 was introduced to a sample of 0.97g EUROPT-3 in its freshly reduced state. The reaction progress was followed using the pressure transducer and the surface radioactivity was monitored at regular 1 min intervals throughout the reaction. Samples from the reaction products were analysed at different stages of the reaction by the radio-gas chromatography. As can be seen from Curve B (Figure 62) and Figure 63, most of the [14-C]-C_2H_4 remained in the gas phase until most of the acetylene had been consumed, after which the ethylene underwent hydrogenation to ethane. This experiment was repeated using

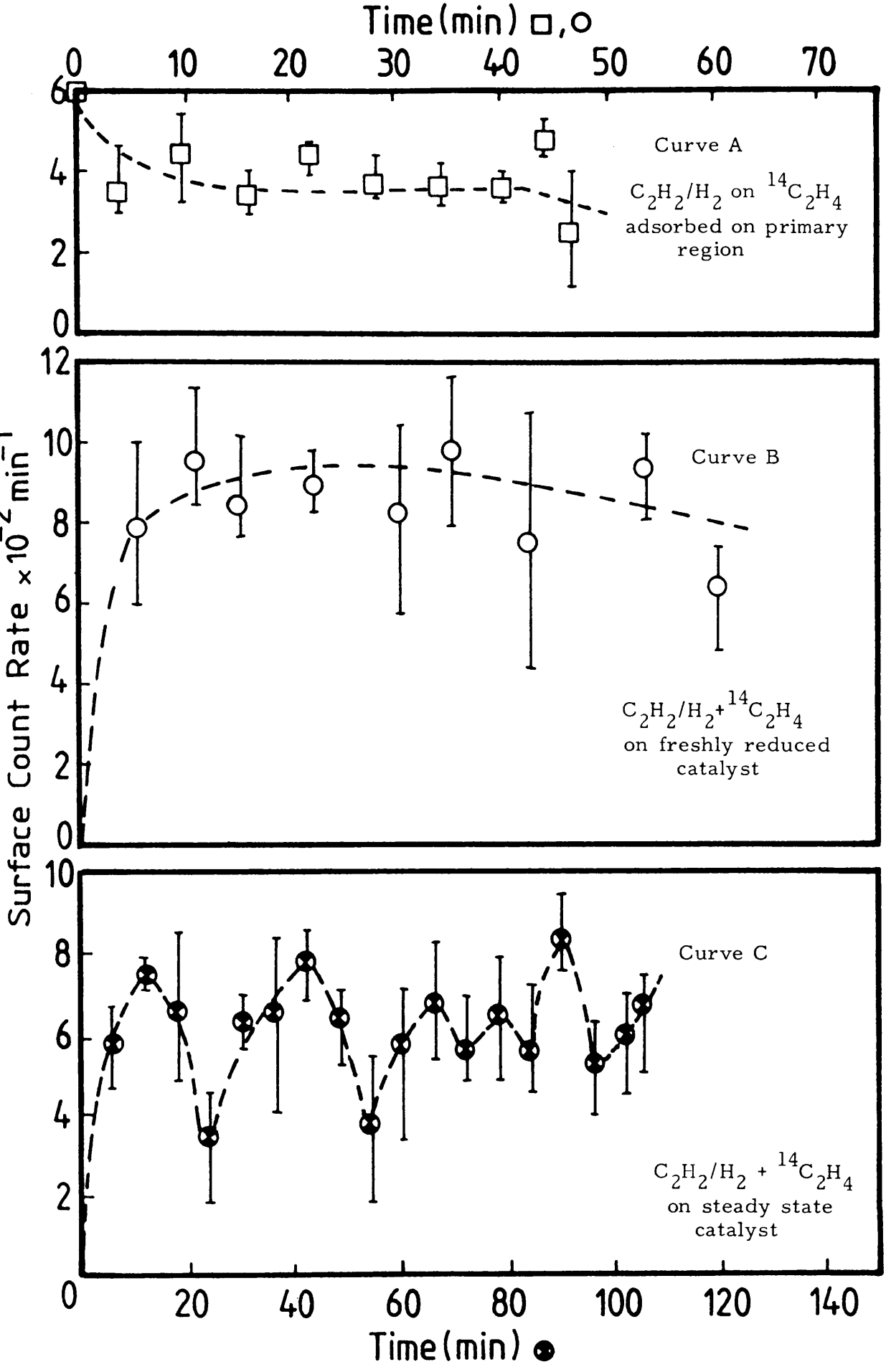

Figure 62. Behaviour of [14-C]-ethylene during the C_2H_2 hydrogenation on EUROPT-3.

larger amounts of [14-C]-C_2H_4 (5 Torr) and similar experimental conditions. The same behaviour was observed (Figure 63).

Experiment 3

This experiment was designed to look at the behaviour of [14-C]-C_2H_4 and the extent of its hydrogenation during the reaction of C_2H_2 with H_2 on a catalyst in its steady state. A 0.97g sample of EUROPT-3 was brought to the steady state by performing 30 reactions using 3:1::H_2:C_2H_2 mixtures. A pre-mixed sample of 12.5 Torr acetylene, 37.5 Torr hydrogen and 5 Torr [14-C]-ethylene was then admitted to the catalyst. The progress of the reaction and the surface radioactivity were monitored as described above. Samples from the reaction products were again analysed at different stages as the reaction progressed. The results presented in Curve C (Figure 62) showed that, [14-C]-C_2H_4 underwent cycles of adsorption-desorption as the reaction was progressed. However, the results presented in Figure 63 show similar behaviour for [14-C]-C_2H_4 on the deactivated catalyst to that observed on the freshly reduced catalyst, that is, almost all the ethylene remained in the gas phase until most of the acetylene was reacted. These experiments confirm the phenomena described in sections 4.1.1.4 and 4.2.2 in which acetylene and ethylene are competing for the same adsorption sites with the former being more strongly adsorbed.

Table 5 shows the total ethane, ethylene and acetylene yields and the [14-C]-ethane and [14-C]-ethylene yields calculated at different stages of the hydrogenation reaction. The amounts of [14-C]-ethylene present in the reaction mixture at any stage of the reaction as measured by radio-gas chromatography are shown in Figure 64.

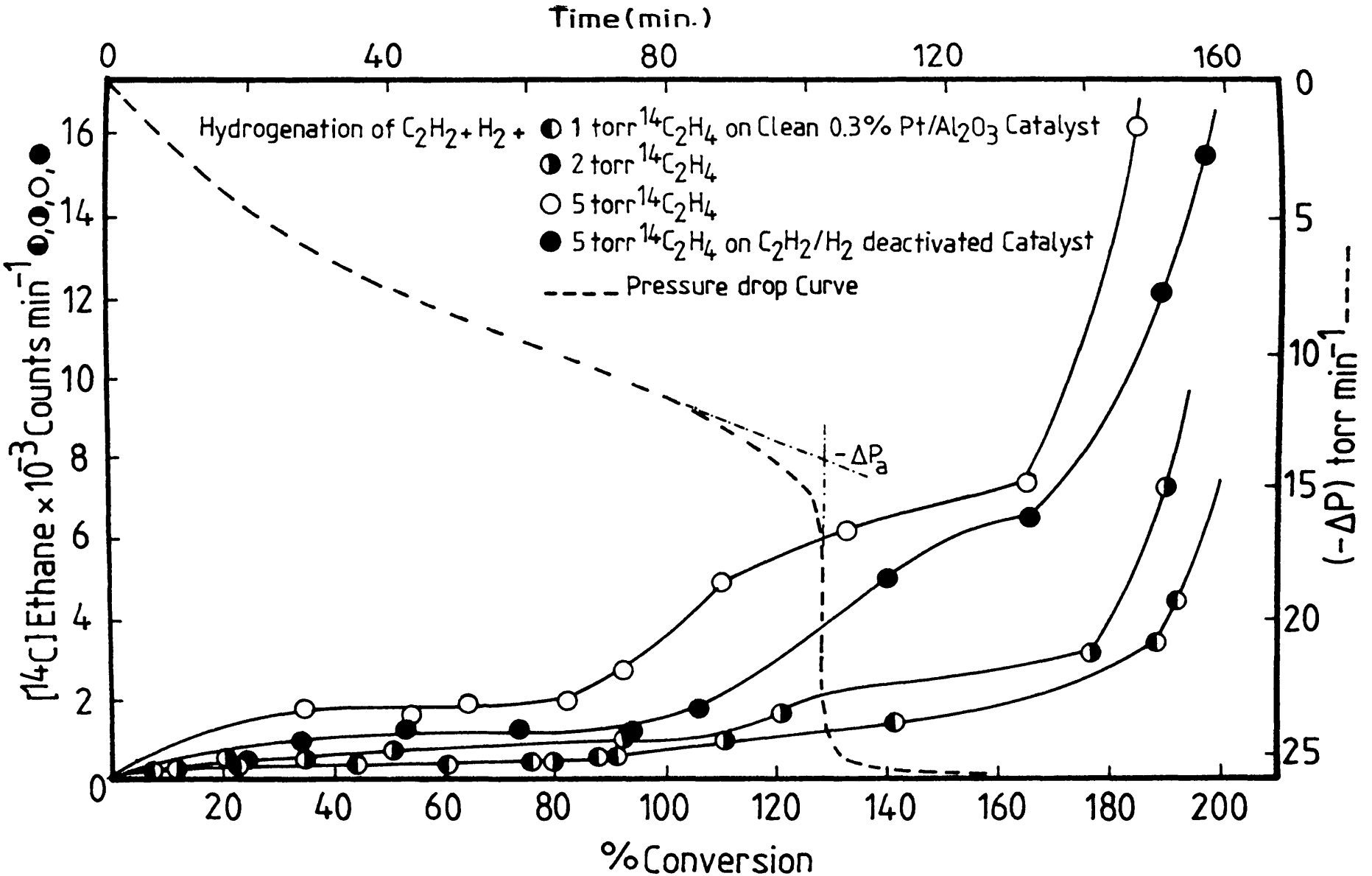

Figure 63. Variation of [14-C] ethane yield during the hydrogenation of acetylene on EUROPT-3 in the presence of added amounts of [14-C] ethylene.

Table 5. Distribution of C_2-products from the Hydrogenation of 12.5 torr of Acetylene in presence of Added* [^{14}C] Ethylene on 2.0345g steady state 0.3% Pt/Al_2O_3 (EUROPT-3) catalyst.

P_{H_2} = 37.5 torr temperature = 20 ± 2°C

Added* [^{14}C]C_2H_4 (torr)	(%) conversion	$P_{^{14}C_2H_6}$ (torr) x 10^{-4}	$P_{^{12}C_2H_4}$ (torr)	$P^{Total}_{^{12}C_2H_6}$ (torr)	$P^{Direct}_{^{12}C_2H_6}$ (torr)	Selectivity (S)	Inherent Selectivity (S')
1*	5.00	70.0	0.326	0.144	0.142	0.6936	0.6966
-	20.00	210.0	1.382	0.319	0.290	0.8125	0.8266
-	41.91	220.0	2.506	0.818	0.762	0.7539	0.7668
-	59.24	230.0	3.297	0.897	0.819	0.7861	0.8010
-	75.86	250.0	4.019	1.235	1.132	0.7649	0.7802
-	82.54	350.0	4.776	1.265	1.092	0.7906	0.8139
-	91.20	361.0	4.956	1.894	1.708	0.7235	0.7440
-	141.50	860.0	2.601	3.444	3.199	0.4303	0.4484
-	188.70	2122.0	0.602	8.028	7.866	0.0698	0.0711
-	192.60	2750.0	0.221	7.330	7.246	0.0293	0.0296

Table 5 (contd.)

Added* $[^{14}C]C_2H_4$ (torr)	(%) conversion	$P_{^{14}C_2H_6}$ (torr) x 10^{-4}	$P_{^{12}C_2H_4}$ (torr)	$P^{Total}_{^{12}C_2H_6}$ (torr)	$P^{Direct}_{^{12}C_2H_6}$ (torr)	Selectivity (S)	Inherent Selectivity (S')
2*	13.12	5350.0	0.958	0.1565	0.1302	0.8595	0.8804
-	27.71	4450.0	1.928	0.2455	0.2006	0.8870	0.9058
-	45.04	6230.0	2.794	0.3577	0.2679	0.8865	0.9125
-	93.03	8840.0	3.956	1.5916	1.4087	0.7131	0.7374
-	113.68	8280.0	4.308	1.8472	1.6611	0.6999	0.7217
-	127.11	1455.0	4.491	2.2950	1.9430	0.6618	0.6980
-	182.79	2799.0	1.2626	6.4400	6.2340	0.1684	0.1639
-	194.48	6449.0	0.3409	7.1751	7.0130	0.0454	0.0464
-	197.59	4097.0	0.0660	7.9903	7.9730	0.0082	0.0082

Table 5 (contd.)

Added* $[^{14}C]C_2H_4$ (torr)	(%) conversion	$P_{^{14}C_2H_6}$ (torr) x 10^{-4}	$P_{^{12}C_2H_4}$ (torr)	$P_{^{12}C_2H_6}$ Total (torr)	$P_{^{12}C_2H_6}$ Direct (torr)	Selectivity (S)	Inherent Selectivity (S')
5*	10.85	999.0	0.725	0.1573	0.1427	0.8217	0.8355
-	33.82	372.0	1.510	0.8030	0.7917	0.6528	0.6560
-	40.08	1303.0	1.760	0.9697	0.9226	0.6448	0.6561
-	65.35	1324.0	3.100	1.3376	1.2533	0.6986	0.7121
-	90.81	1197.0	3.640	1.9803	1.8910	0.6477	0.6581
-	105.59	1833.0	4.068	2.0870	1.9322	0.6609	0.6779
-	112.64	1299.0	4.754	2.3900	2.2632	0.6654	0.6775
-	168.91	7036.0	1.147	6.0164	5.8300	0.2052	0.1644
-	189.67	12895.0	0.3610	6.4410	6.3160	0.0531	0.0541
-	197.29	16499.0	0.0820	10.9700	10.9300	0.0074	0.0074

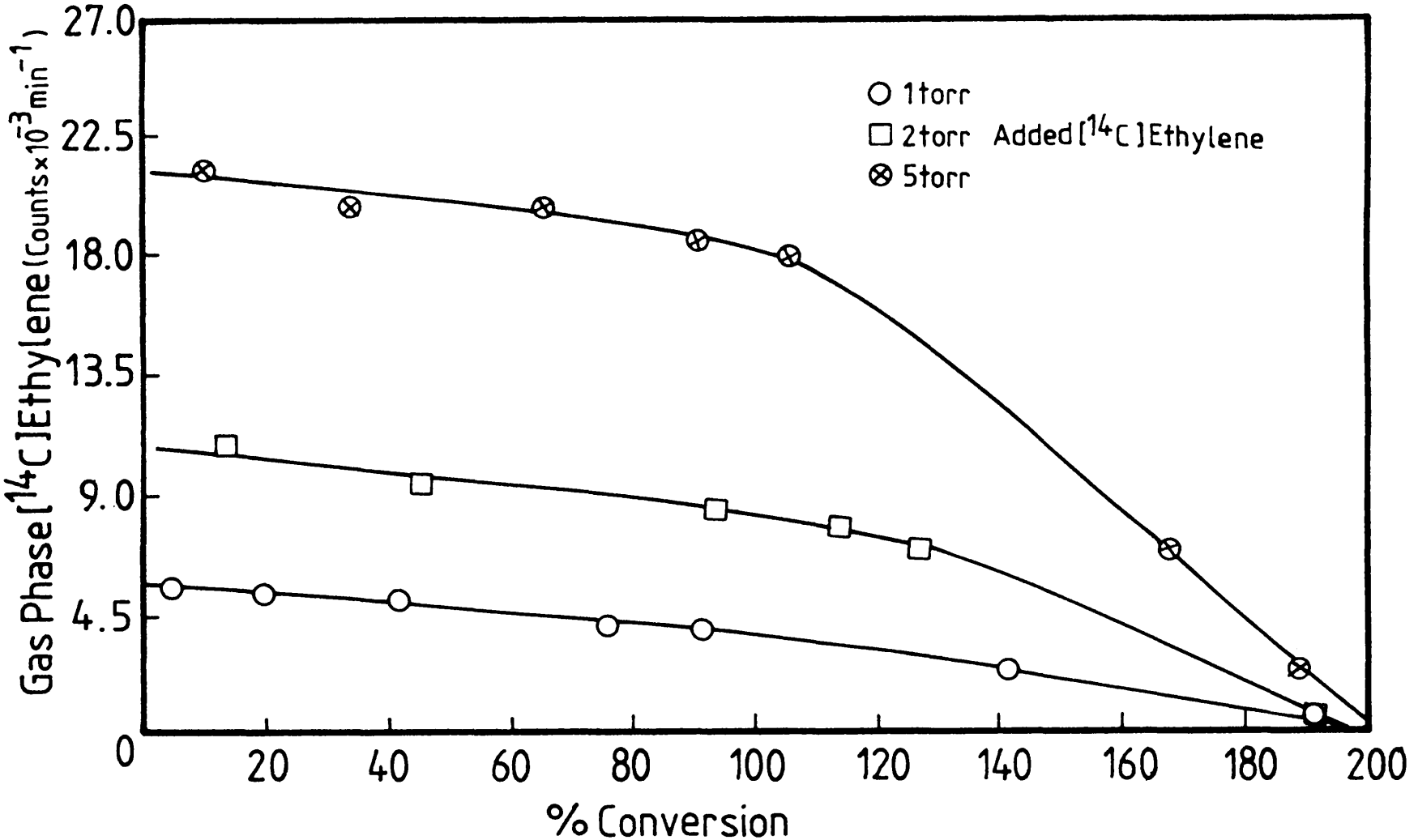

Figure 64. Variation of [14-C] ethylene count rate during the hydrogenation of acetylene on EUROPT-3.

CHAPTER SEVEN

THE REACTION OF ACETYLENE WITH HYDROGEN OVER 0.8% Pt/SiO_2, 0.8% Pt/Al_2O_3 and 0.5% Pt/MoO_3 CATALYSTS

It was decided to perform a series of acetylene hydrogenation reactions on the above catalysts with the aim of comparing their product distribution and hence, their selectivity profiles with those obtained on EUROPT-1 and EUROPT-3 catalysts (Chapters 5 and 6).

2.06g Pt/SiO_2, 3.71g Pt/Al_2O_3 and 3.71g Pt/MoO_3 catalysts were reduced and treated as described in section 3.6.

A series of hydrogenation reactions were carried out on each catalyst using pre-mixed 50 Torr samples of a (3:1), H_2:C_2H_2 mixture. After admission of the reactants to the reaction vessel, the progress of each reaction was followed using the pressure transducer (section 3.1.1.4) and by gas chromatographic analysis of the products at regular intervals throughout the reaction (section 3.2).

The pressure fall against time curve and product distribution profiles obtained with the 0.8% Pt/SiO_2 catalyst are shown in Figure 65. From these it can be seen that the reaction occurred in two stages. In the first stage (up to 100% conversion), ethylene and ethane were produced as the main products. Initially the yield of the former was about five times higher than that of the latter. The onset of the second stage was accompanied by an increase in the rate corresponding to the further hydrogenation of ethylene to ethane. The selectivity of the catalyst for ethylene production displayed a maximum value of

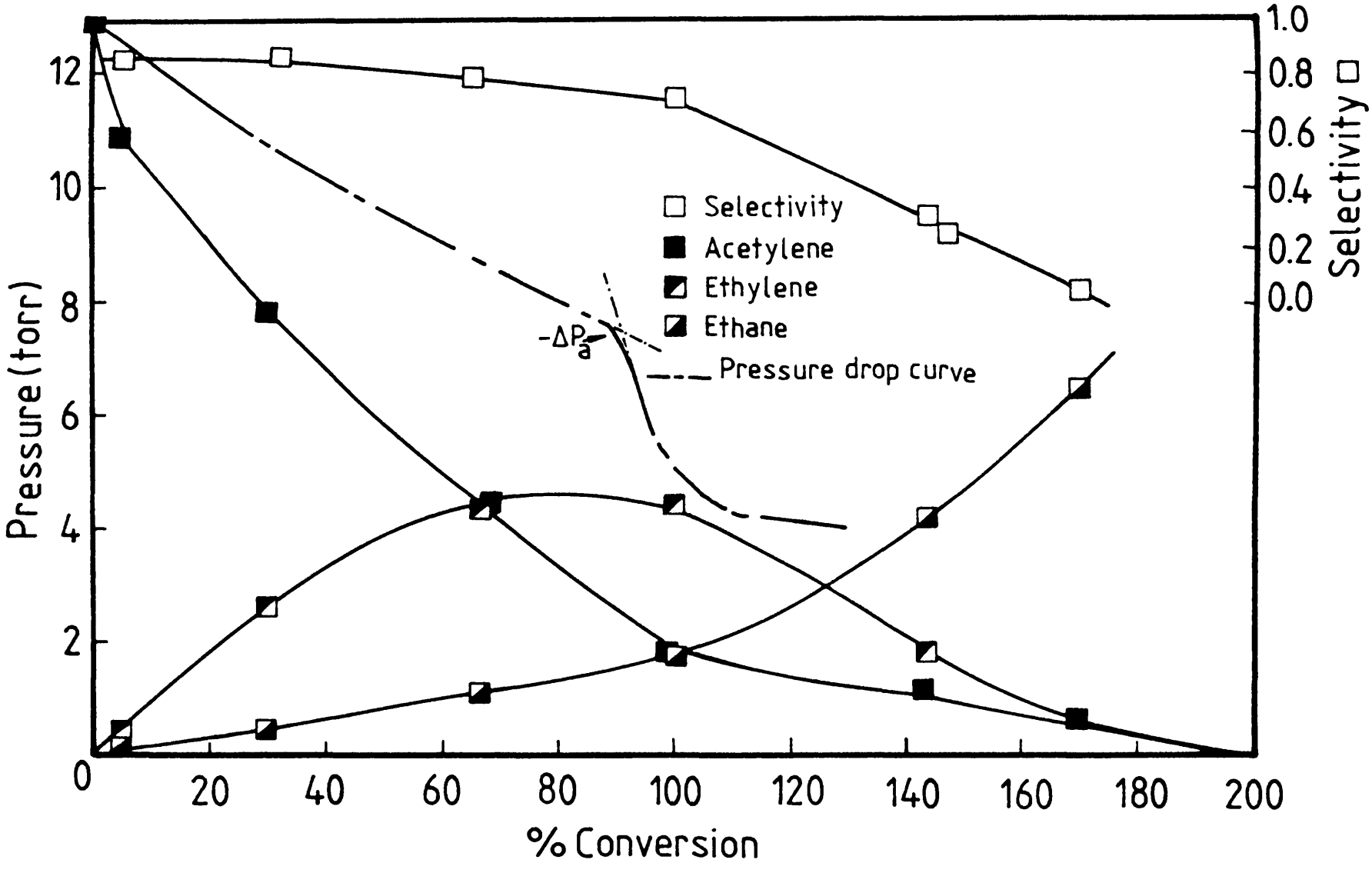

Figure 65. Product distribution curves of acetylene hydrogenation on freshly reduced 0.8% Pt/SiO_2 catalyst.

approximately 0.85 at 30% conversion which decreased as the reaction proceeded. This compares with the selectivity value of ~ 0.30 exhibited by EUROPT-1 (6% Pt/SiO_2) catalyst (Chapter 5).

Hydrogenation of acetylene over the 0.8% Pt/Al_2O_3 catalyst showed pressure fall-time and product distribution curves similar to those observed with EUROPT-3 (0.3% Pt/Al_2O_3, sections 6.1 and 6.2), though the initial selectivity was slightly lower (~ 0.40), c.f. ~ 0.60 on EUROPT-3.

No appreciable reaction between C_2H_2 and H_2 was observed to occur on the 0.5% Pt/MoO_3 catalyst, only traces of unmeasurable amounts of ethane and ethylene were detected.

CHAPTER EIGHT

THE REACTIONS OF BUTA-1,3-DIENE WITH HYDROGEN OVER EUROPT-1 AND EUROPT-3 CATALYSTS

In the ensuing sections, the terms buta-1,3-diene, but-1-ene, cis-but-2-ene, trans-but-2-ene and n-butane will be abbreviated to 1-3B, 1-B, c-2-B, t-2-B and n-B, respectively.

8.1 DEACTIVATION CURVES

Figures 66 and 67 show some typical pressure fall against time curves. From these figures it can be seen that, with 0.003g EUROPT-1 (Figure 66) and 0.249g (EUROPT-3) (Figure 67), the reaction occurred in two distinct stages. The onset of the second stage was accompanied with an increase in the reaction rate.

The "acceleration point", denoted in Figures 66 and 67 as $-\Delta P_a$, occurred at a pressure fall of 12.9 ± 0.5 Torr (EUROPT-1) and of 14.5 ± 0.3 Torr (EUROPT-3). Analysis of the reaction products by gas chromatography showed that n-B and all the butenes (1-B, c-2-B, t-2-B) were formed as the initial products. After the commencement of the second stage of the reaction the major process occurring was the isomerisation of 1-B to t-2-B and c-2-B, together with the hydrogenation of the butenes to n-B.

The first stage of the reaction was found to be first order in total pressure. Plots of $\ell n\ (P_o + \Delta P)$ against time were found to be straight lines for both catalysts (Figure 68), and their gradients can be used to determine the first order rate constants (k).

A series of hydrogenation reactions, using mixtures of 12.5 Torr 1-3B and 37.5 Torr hydrogen, were carried out consecutively on

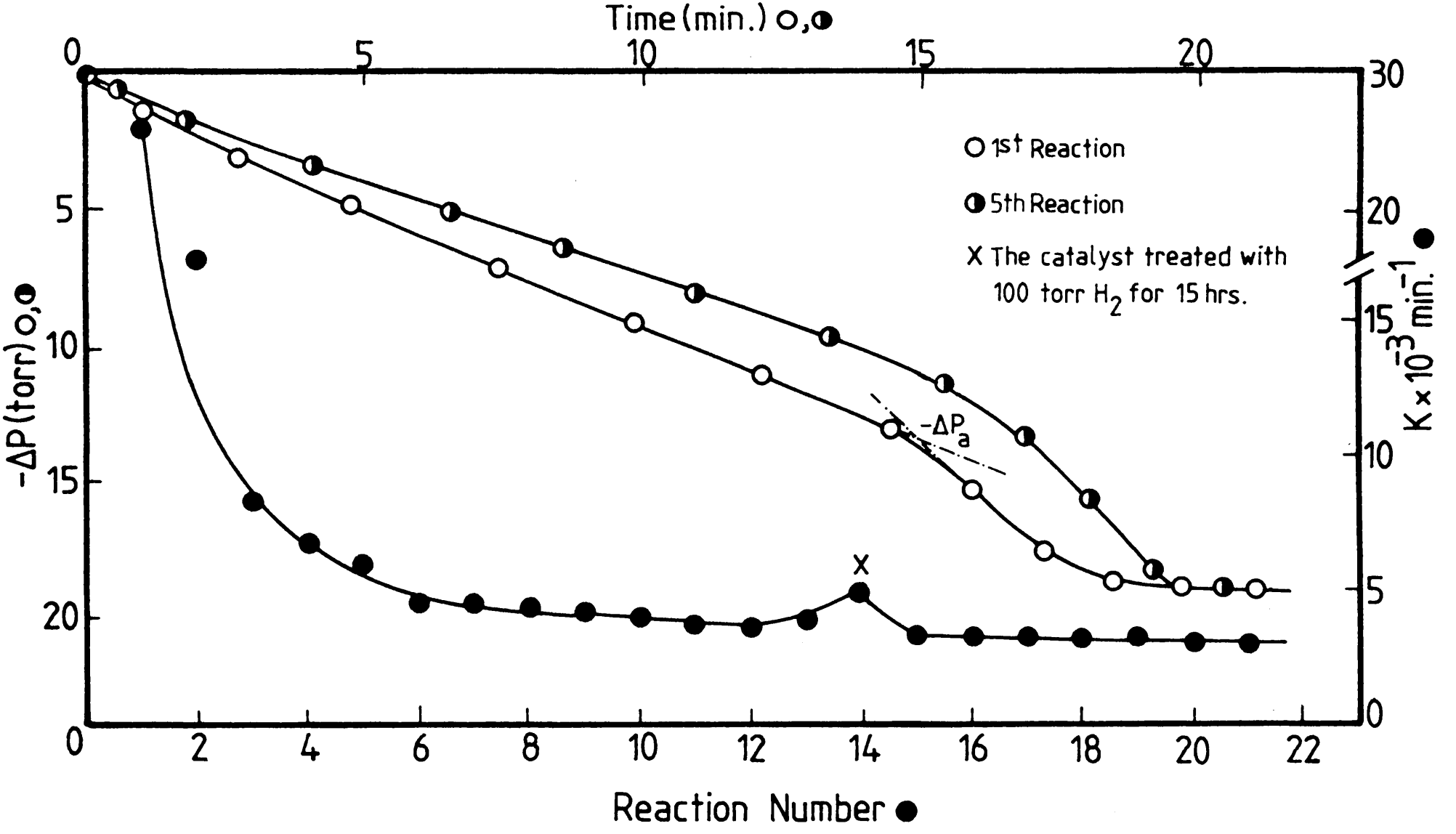

Figure 66. Pressure fall-time curves of 1,3-butadiene hydrogenation on EUROPT-3.

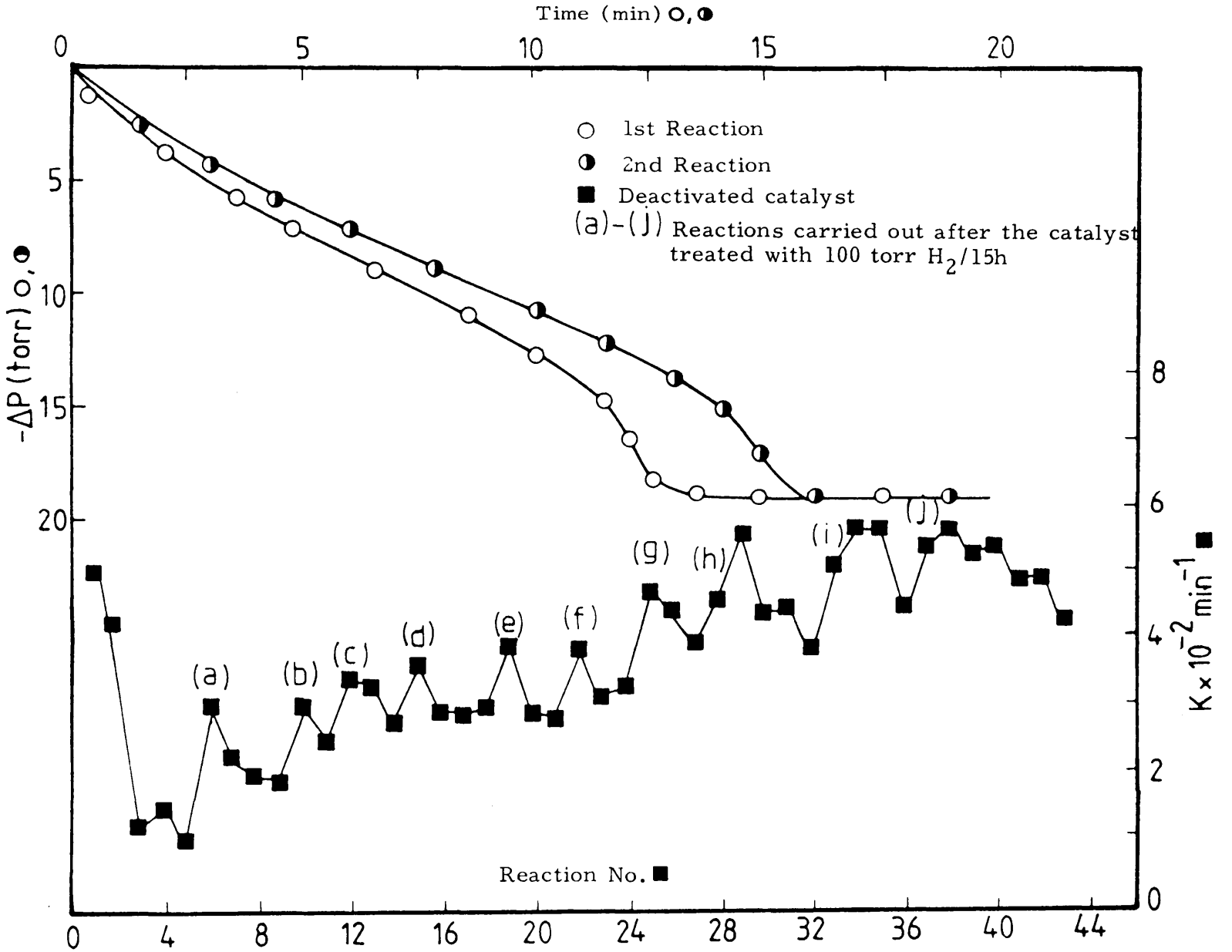

Figure 67. Pressure fall-time curves of buta-1,3-diene hydrogenation on EUROPT-3.

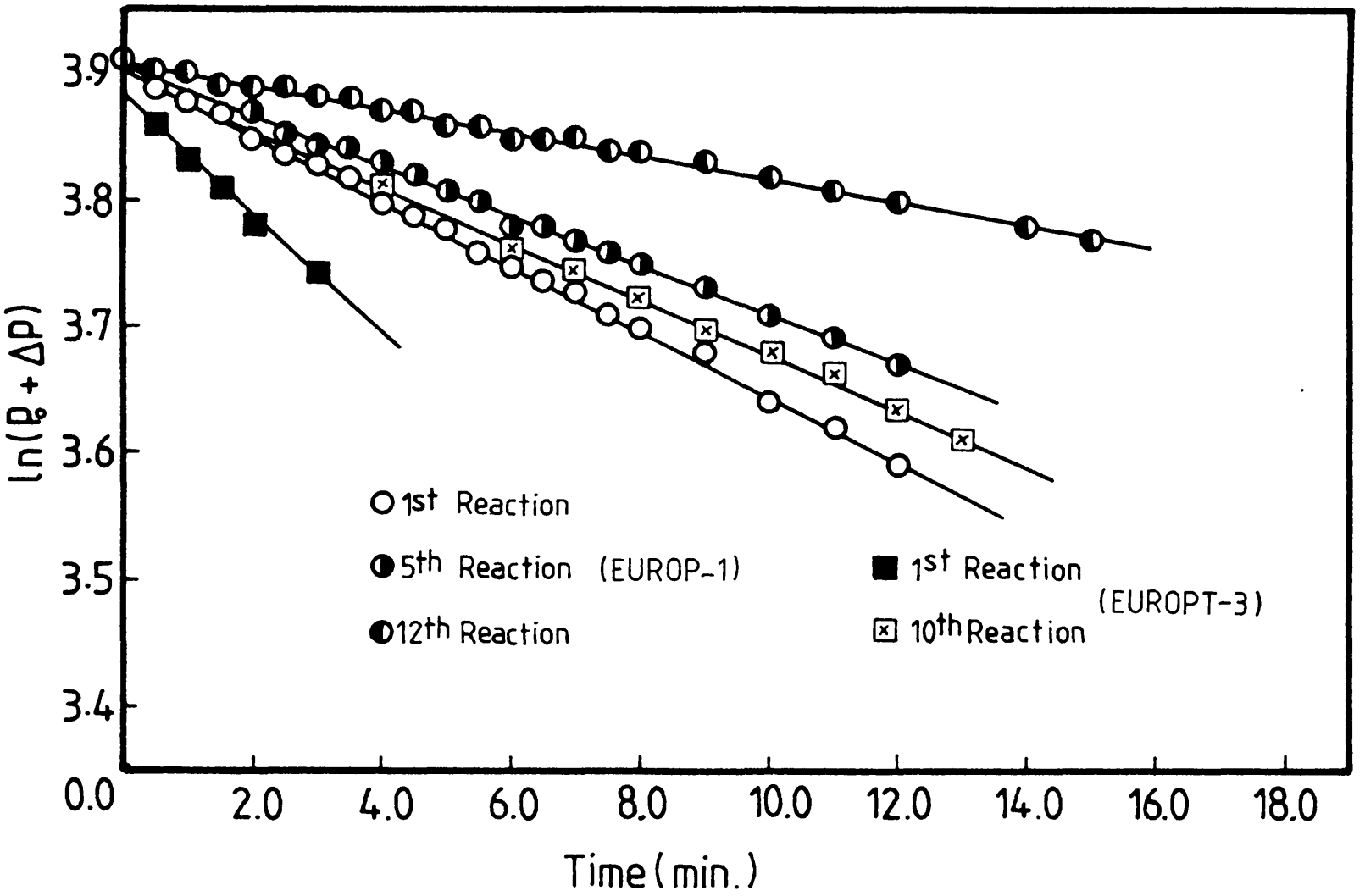

Figure 68. First order plots of buta-1,3-diene hydrogenation on EUROPT-1 and EUROPT-3.

the same catalyst sample. The reaction vessel was evacuated for 30 min after each reaction to remove the gaseous hydrocarbons which had formed. Figures 66 and 67 show the variation of the first order rate constant ($k\ min^{-1}$) with reaction number for both catalysts, from which it can be seen that the rate of the reaction decreased with successive reactions until a constant "steady state" activity was eventually attained. The reaction rate did not tend to zero. However, as it can be noticed (Figure 66) that, during the deactivation process, the activity could be partially restored (points a,b) by leaving the catalyst in contact with H_2 for ~ 15h. The phenomenon of restoring the original activity with H_2 treatment is more pronounced on EUROPT-3 (Figure 67).

8.2 EFFECT OF CATALYST DEACTIVATION ON SELECTIVITY

The change of selectivity ($S = \frac{P_{Butenes}}{P_{Butenes} + P_{n\text{-}B}}$) during the activation process was studied by introducing a mixture of 12.5 Torr 1-3B and 37.5 Torr hydrogen to a freshly reduced catalyst (0.003g EUROPT-1, 0.249g EUROPT-3). Samples were extracted for analysis by gas chromatography at a pressure fall of ~ 10 Torr (~ 65% conversion). This procedure was repeated several times during the process of deactivation. It was found (Table 6) that, within the experimental error, the selectivity on both catalysts showed almost identical values as the reaction number was increased with average values of 0.622 (EUROPT-1) and 0.599 (EUROPT-3). It is important to point out here that, treatment of the catalysts with 100 Torr H_2 for 15h, only increased the selectivity by about 4% for both catalysts for reactions performed immediately after such treatment.

Table 6. Effect of Catalyst Deactivation on Selectivity

(EUROPT-1)		(EUROPT-3)	
Reaction No.	Selectivity	Reaction No.	Selectivity
1	0.609	2	0.530
3	0.632	6	0.590
4	0.603	10*	0.593
5*	0.629	18	0.594
7	0.655	20	0.593
8	0.635	24	0.571
9	0.634	34	0.598
14*	0.620	37*	0.579
16	0.620	39	0.616
18	0.638	42	0.589
20	0.618	43	0.583

* Reactions carried out after the catalyst had been treated in H_2 for 15 h.

8.3 BUTENE DISTRIBUTION ON STEADY STATE CATALYSTS

A series of reactions were carried out to examine the variation of the butene composition and the selectivity with the extent of reaction. 0.007g EUROPT-1 or 0.249g EUROPT-3 was reduced and deactivated by carrying out a series of 1-3B/H_2 reactions, as described in the previous section. Using a hydrogen:1-3B ratio of 3:1, the products were extracted for analysis after a fixed pressure fall of ~ 10 Torr. The

distribution of butenes from these reactions is shown in Figure 69 (EUROPT-1) and Figure 70 (EUROPT-3). On both catalysts, during the first stage of the reaction (up to ~ 100% conversion), the yields of 1-B, t-2-B and c-2-B were almost constant with the compositions 76%, 16% and 6%, respectively. At conversions higher than 100%, the yield of 1-B decreased rapidly with increasing conversion. In the late stages of the reaction (~ completion) the n-B constituted almost ~ 100% of the total product.

The variation of selectivities with respect to conversion are also shown in Figures 69 and 70. The selectivity of EUROPT-3 for butene formation decreased from an initial value of 0.60 to a value of 0.50 at ~ 100% conversion. However, on EUROPT-1, the selectivity showed much slower decrease with % conversion.

8.4 VARIATION ON SELECTIVITY WITH HYDROGEN AND BUTA-1,3-DIENE PRESSURES

In a series of experiments the change in selectivity with the variation in pressures of 1-3B and H_2 was investigated.

Series A

A sample of 0.003g (EUROPT-1) or 0.300g (EUROPT-3) was reduced in H_2 and treated as described in section 3.6. The catalysts were then brought to the steady state as described earlier. Reactions were then carried out with the initial 1-3B pressure being kept constant at 12.5 Torr while the initial H_2 pressure was varied between 10 and 200 Torr. Products were analysed by gas chromatography after a pressure fall of ~ 10 Torr (~ 50% conversion). The results for EUROPT-

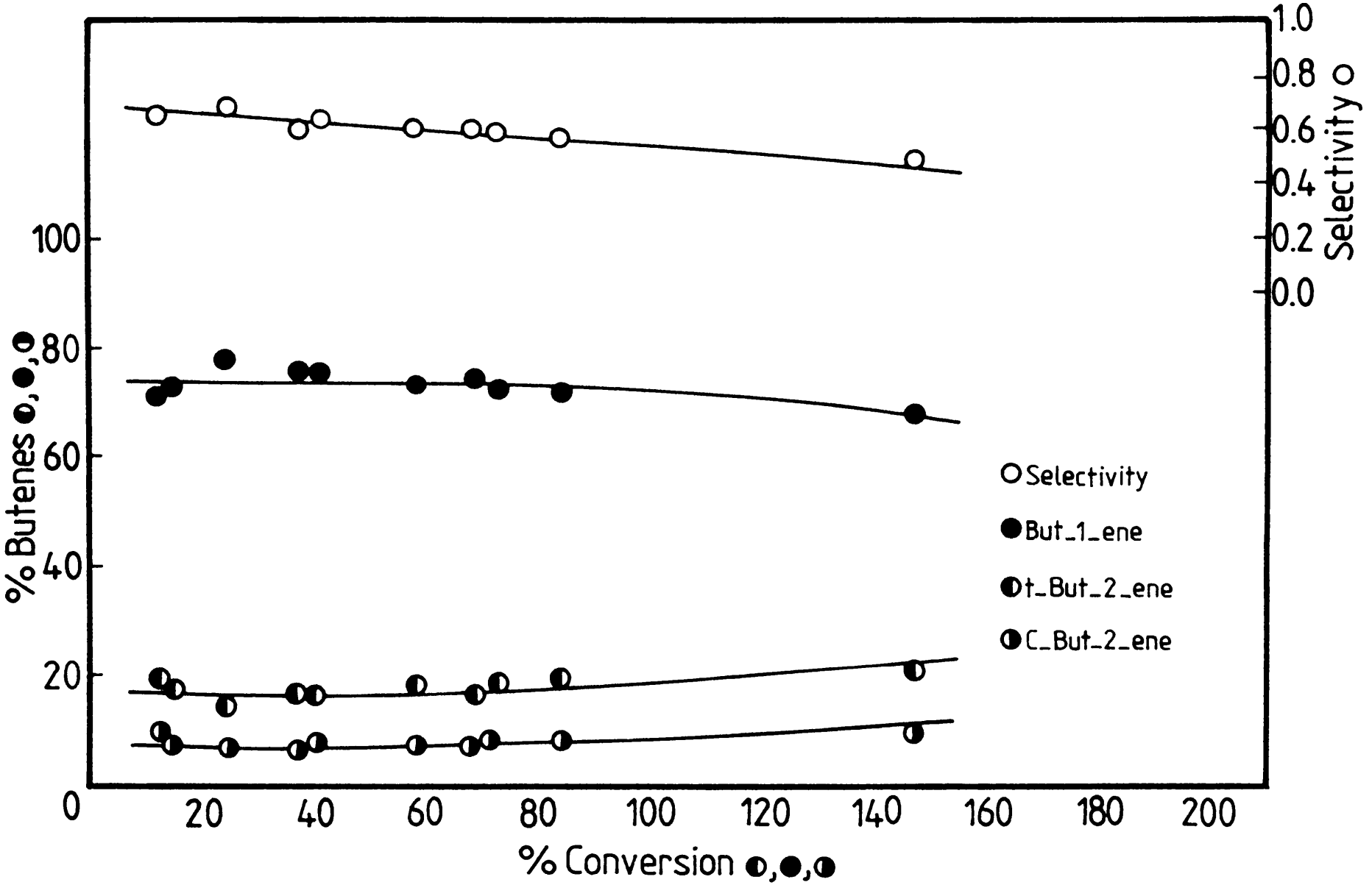

Figure 69. Butene distribution of buta-1,3-diene hydrogenation on EUROPT-1.

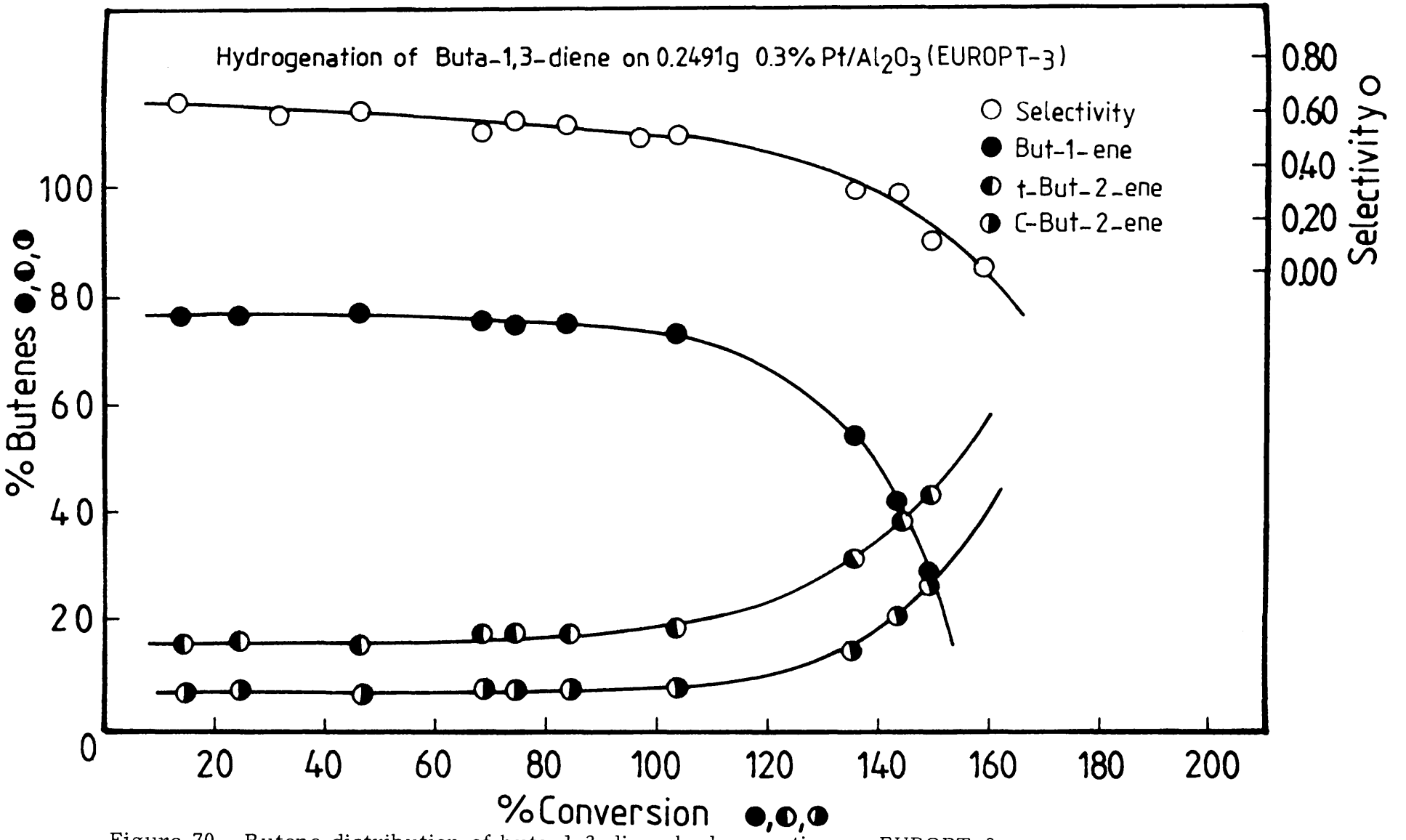

Figure 70. Butene distribution of buta-1,3-diene hydrogenation on EUROPT-3.

1 are shown in Figure 71. From these it can be seen that the butene composition was independent of the initial hydrogen pressure. However, the selectivity showed a slight decrease (~ 7%) as the pressure of H_2 was increased. In contrast with EUROPT-3 (Figure 72), the butene distribution showed some dependence on H_2 pressure. A slight fall in the 1-B yield was observed to occur as the H_2 pressure was extended. This decrease was accompanied by a slight increase in the amounts of isomeric t-2-B and c-2-B produced, although the selectivity showed a steady drop from an initial value of 0.70 to a value of 0.30 as the H_2 pressure increased from 10 Torr to about 110 Torr.

Series B

The catalyst samples which had been used in series A were regenerated statically in 100 Torr H_2, as described in section 3.10, before before being cooled in vacuo to room temperature. These catalysts were then brought to steady state activity using 25 reactions of (3:1), H_2:1-3B, as described in section 8.1. A series of reactions were performed on both catalysts during which the initial 1-3B pressure was varied between 5 and 200 Torr, while that of hydrogen was kept constant at 37.5 Torr. Products were analysed by gas chromatography at a constant pressure fall of ~ 10 Torr (~ 50% conversion). The results presented in Figures 71 (EUROPT-1) and 72 (EUROPT-3) showed that, on both catalysts, the butene distribution and selectivity were independent of initial 1-3B pressure.

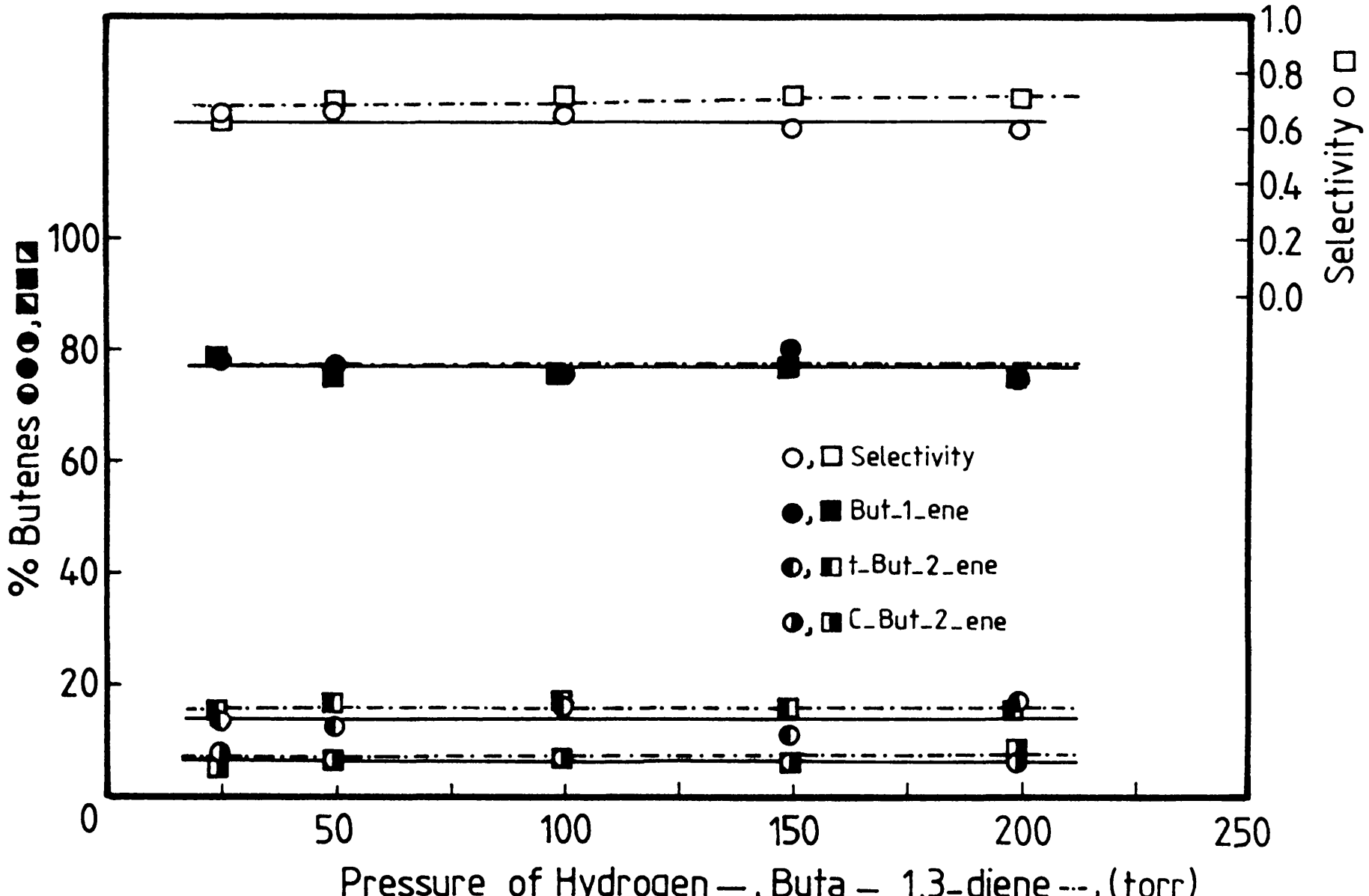

Figure 71. The variation of butenes distribution and selectivity with reactants pressure on EUROPT-1.

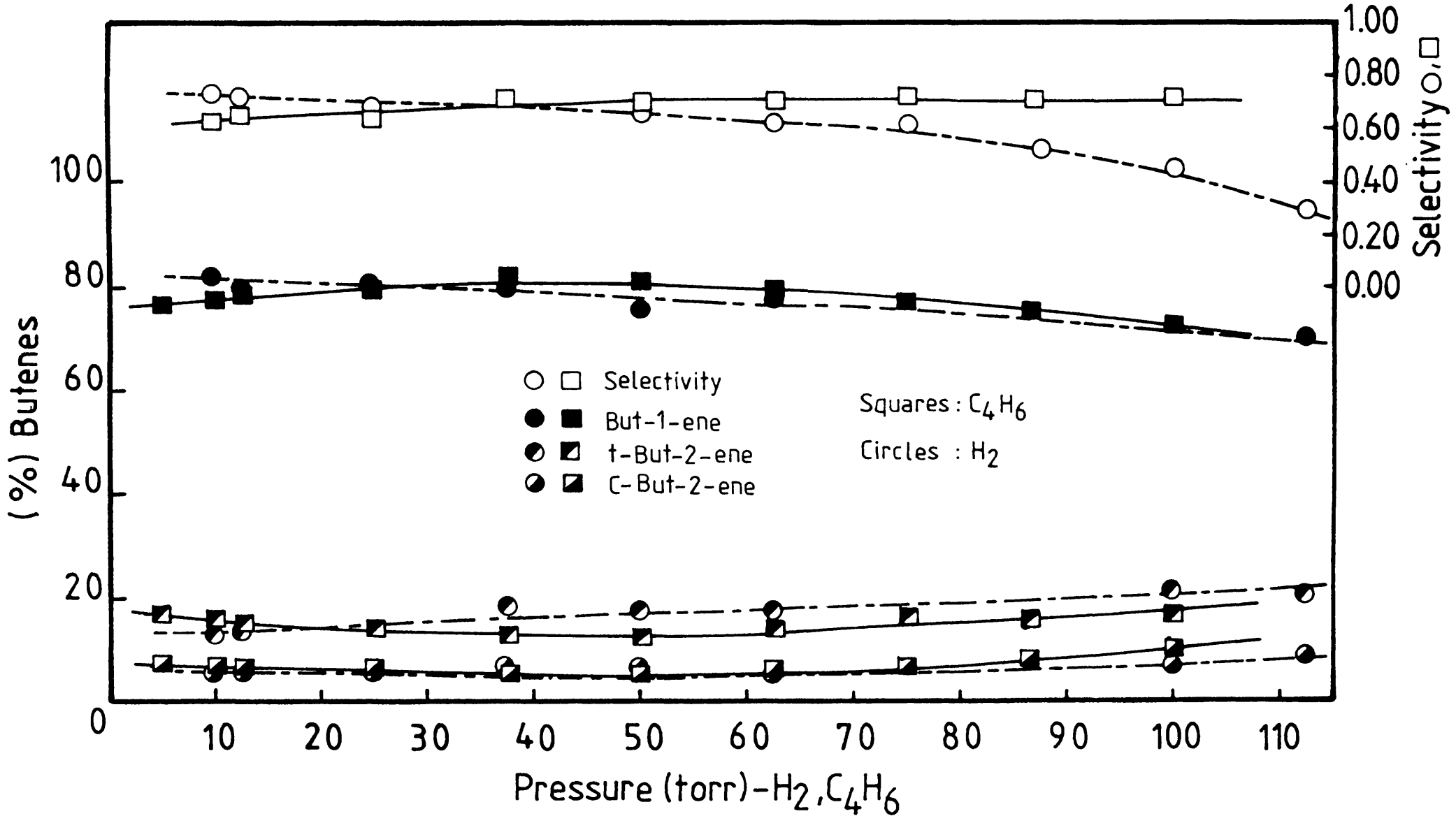

Figure 72. The variation of butenes distribution and selectivity with reactants pressure on EUROPT-3.

8.5 THE REACTION ORDER WITH RESPECT TO HYDROGEN AND BUTA-1,3-DIENE

The catalysts used in section 8.4 were activated according to the standard procedure (section 3.6) and then brought to the steady state activity, as described in section 8.1. These catalysts were used for the determination of reaction orders with respect to hydrogen and 1-3B on EUROPT-1 and EUROPT-3, respectively.

Using EUROPT-1, the order in H_2 was examined by varying its initial pressure between 25 and 150 Torr with a fixed pressure of 1-3B of 12.5 Torr. Figure 73 shows a plot of $\log_{10}$ initial rate against the initial H_2 pressure. From this, the order with respect to hydrogen was found to be first order. The order in 1-3B was determined using initial hydrocarbon pressures between 20 and 150 Torr and a constant hydrogen pressure of 37.5 Torr. From the plot shown in Figure 74, an order of -0.55 ± 0.01 with respect to 1-3B was determined.

With EUROPT-3, the initial hydrogen pressure was varied between 10 and 120 Torr while the pressure of 1-3B was kept constant at 12.5 Torr. The plot of $\log_{10}$ initial rate versus $\log_{10}$ initial hydrogen pressure (Figure 75) yielded a straight line with a slope value of 0.90 ± 0.03. Using pressures of 1-3B of between 10 and 120 Torr and a constant H_2 pressure of 37.5 Torr, the order with respect to 1-3B was found to be -0.60 ± 0.08 (Figure 76).

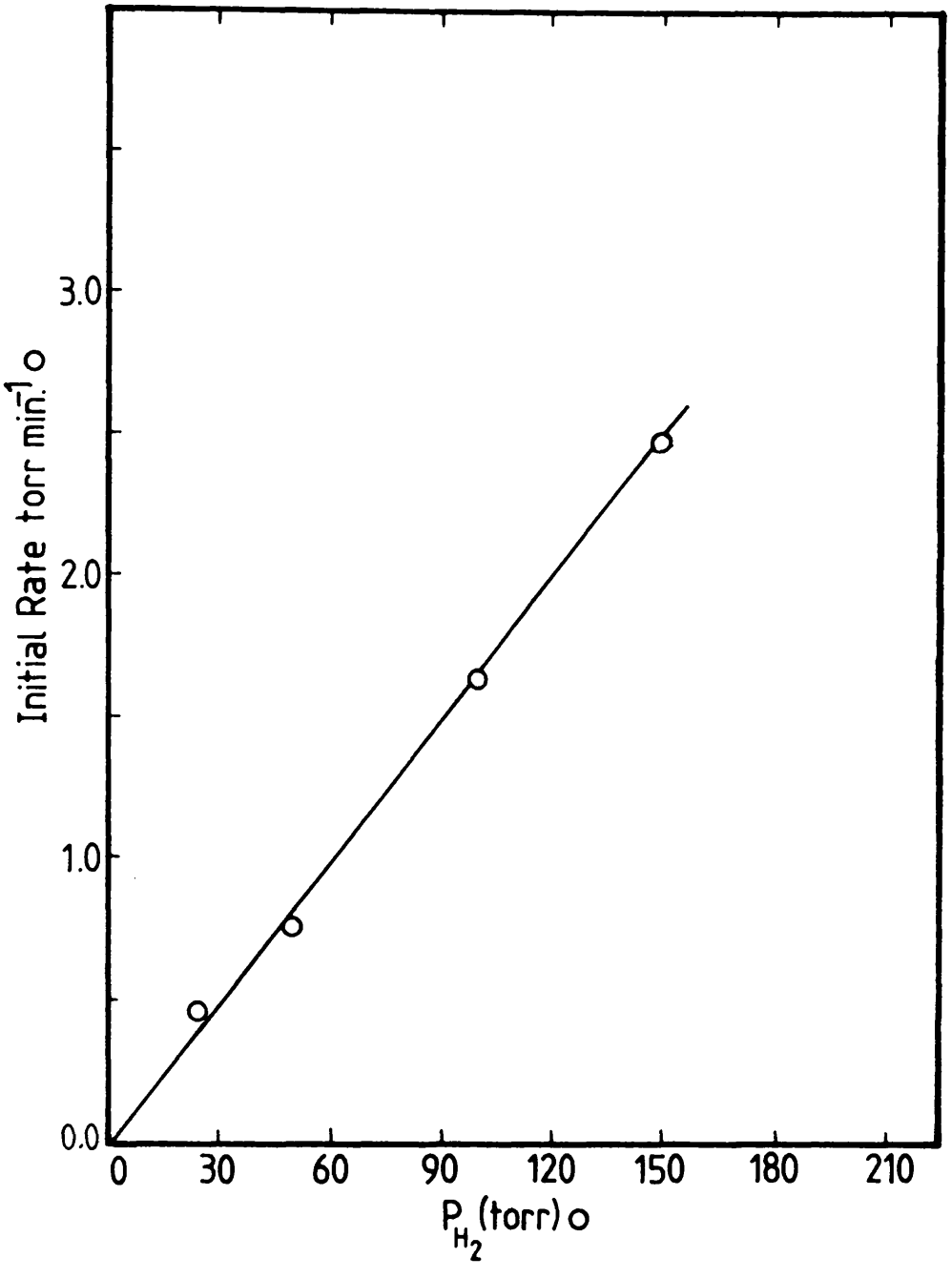

Figure 73. The variation of initial rate with H_2 pressure of buta-1,3-diene hydrogenation on EUROPT-1.

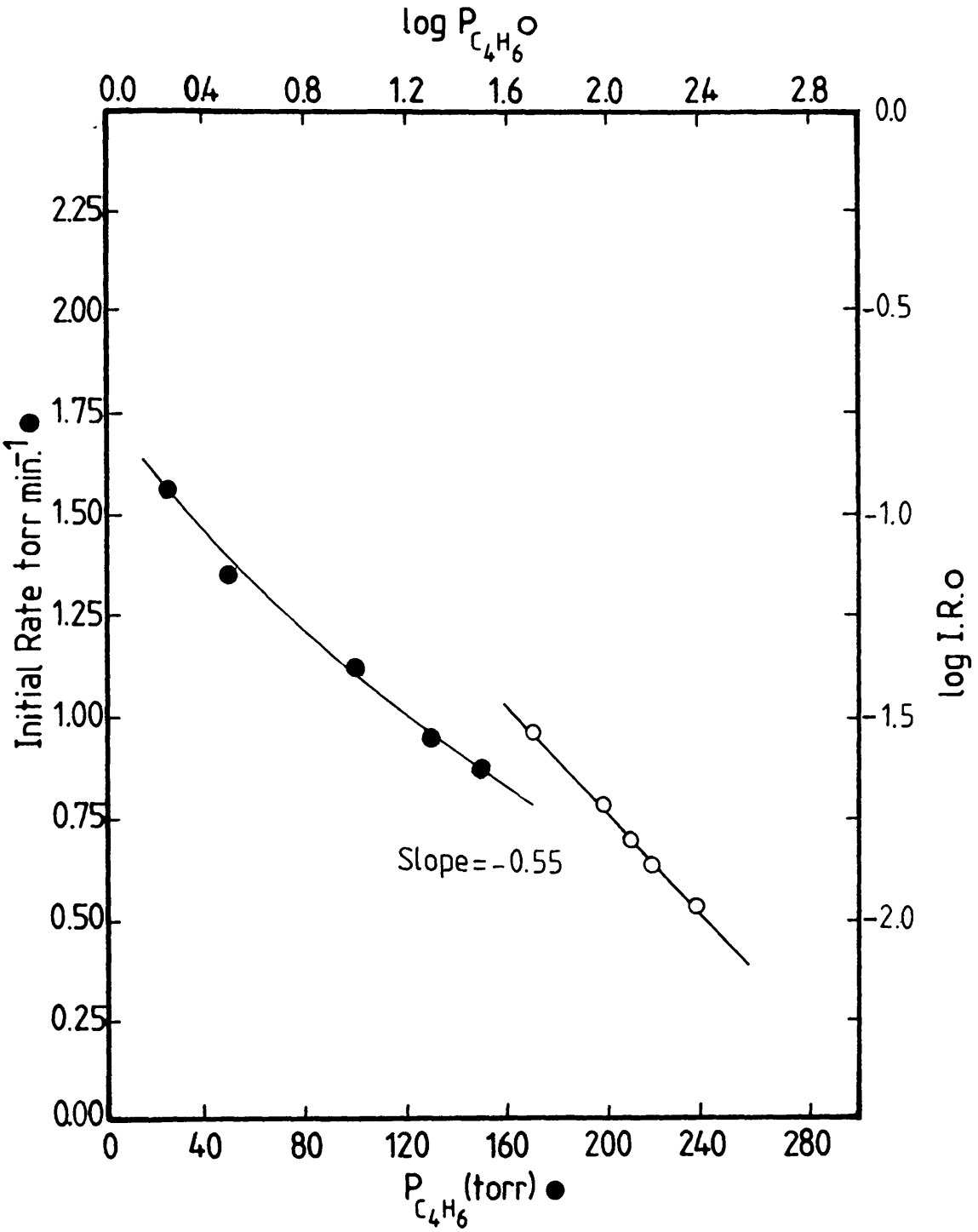

Figure 74. The variation of initial rate with C_4H_6 pressure of buta-1,3-diene hydrogenation on EUROPT-1.

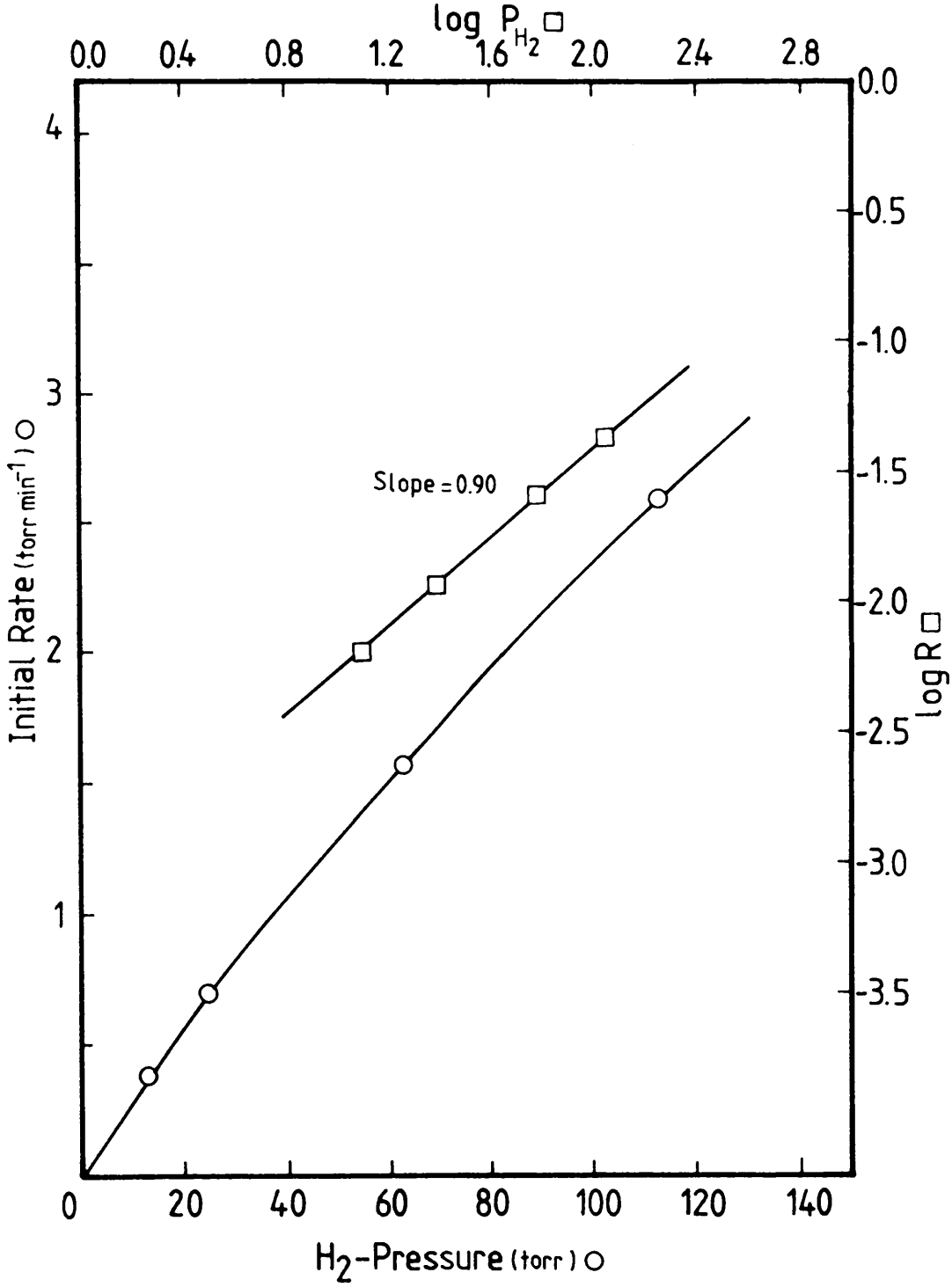

Figure 75. The variation of initial rate with H_2 pressure of buta-1,3-diene hydrogenation on EUROPT-3.

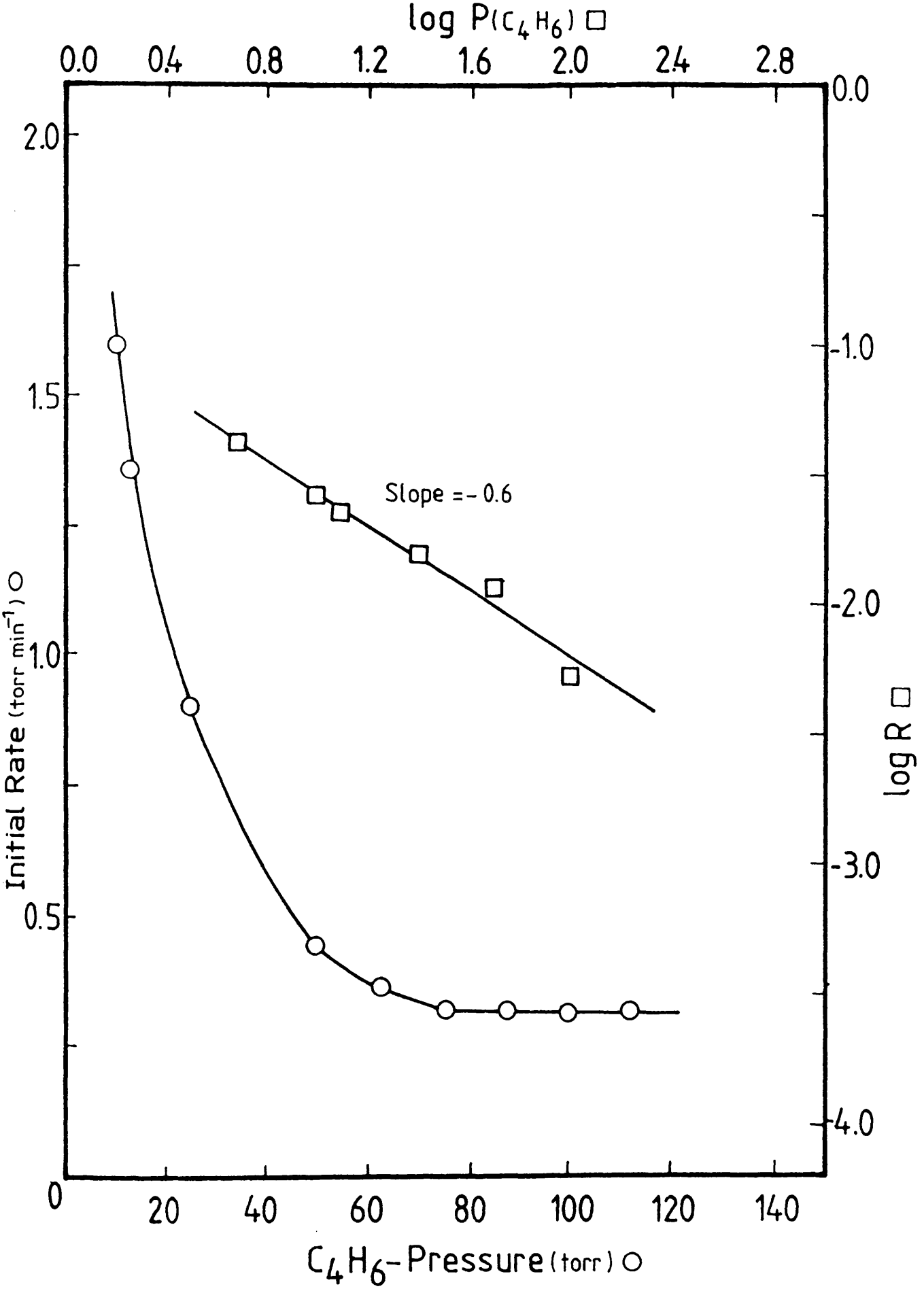

Figure 76. The variation of initial rate with buta-1,3-diene pressure in buta-1,3-diene hydrogenation on EUROPT-3.

8.6 THE TEMPERATURE DEPENDENCE OF THE BUTENE DISTRIBUTION AND THE ACTIVATION ENERGY OF THE REACTION

In a series of reactions over a steady state 0.003g EUROPT-1 catalyst, the variations in butene distribution, selectivity and initial reaction rate were studied as a function of temperature. All the reactions were carried out using a hydrogen:1-3B ration of 3:1 and the products were extracted for analysis by gas chromatography at a pressure fall of ~ 10 Torr (~ 50% conversion). The temperature range studied was between -5 and +180°C. As can be seen from Figure 77, the 1-B yield showed a temperature dependence. It decreased as the temperature was increased, whilst the trans:cis ratio appeared to be almost independent of temperature. The selectivity showed a steady decrease in the temperature range -5° to +100°C, whereas it increased as the temperature was increased from 100° to 180°C.

The plot of $\log_{10}$ initial rate against the reciprocal of absolute temperature (Figure 78) produced a straight line from which an activation energy of 41.05 ± 1 kJ mol^{-1} was obtained.

In a series of reactions, 0.077g steady state EUROPT-3 catalyst was used to investigate the butene distribution and the reaction rate in the temperature range 5-95°C. Samples from the reaction products were again extracted after a pressure fall of ~ 10 Torr (~ 50% conversion) for analysis by gas chromatography. As shown in Figure 79, the selectivity remained constant with increasing the temperature from 5° to 80°C, while it decreased as the temperature was raised > 80°C. The 1-B yield and the trans:cis ratio showed almost no dependence of temperature. An activation energy of 49.64 ± 1 kJ mol^{-1} was obtained from the plot of $\log_{10}$ initial rate versus the reciprocal absolute temperature (Figure 78).

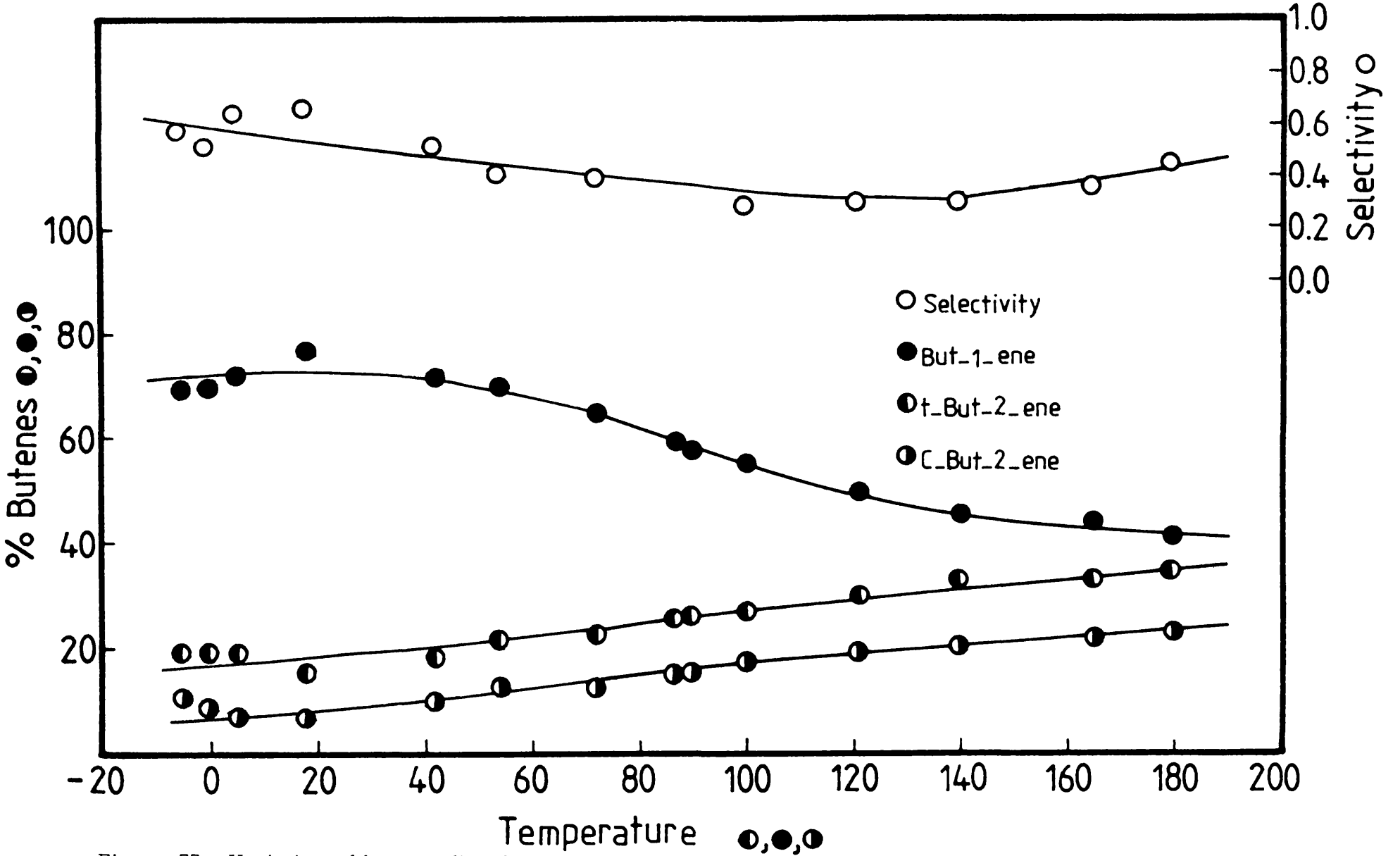

Figure 77. Variation of butene distribution with temperature on EUROPT-1.

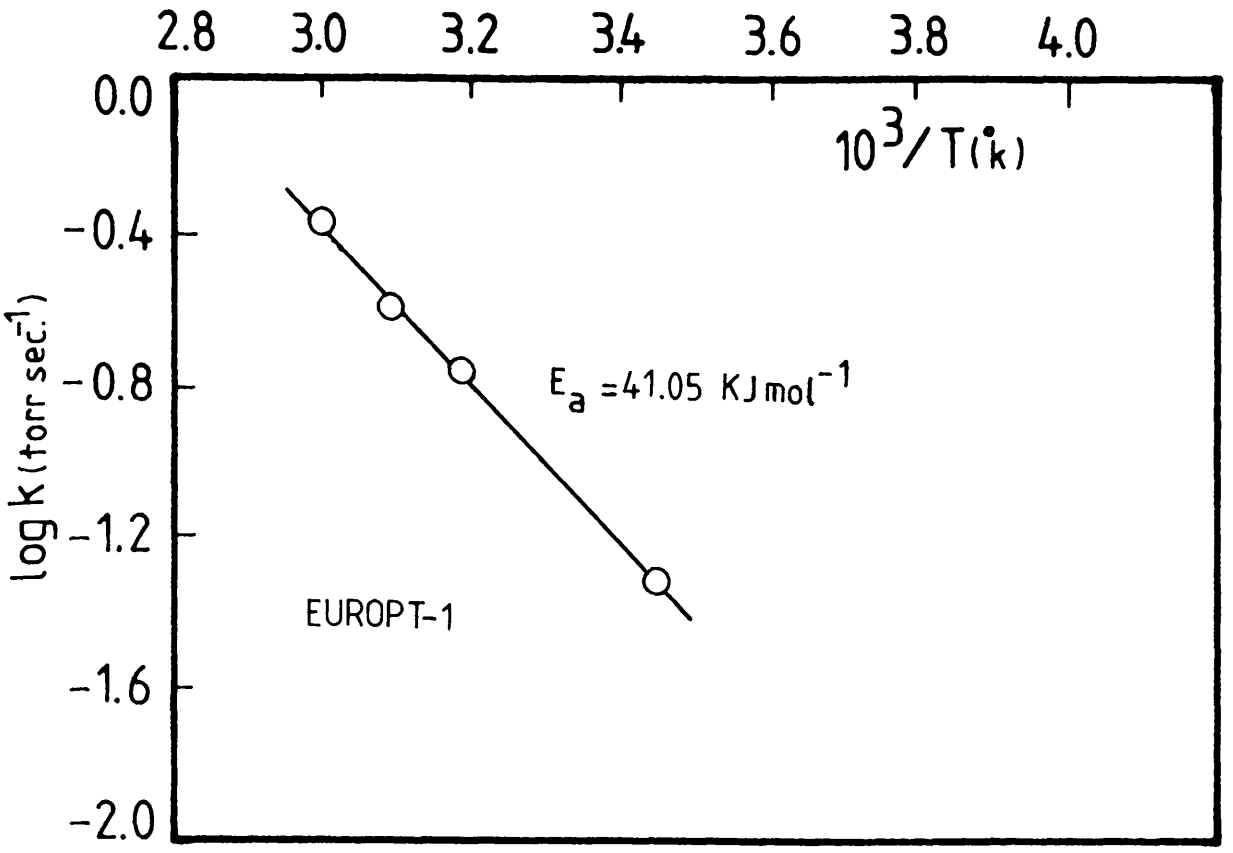

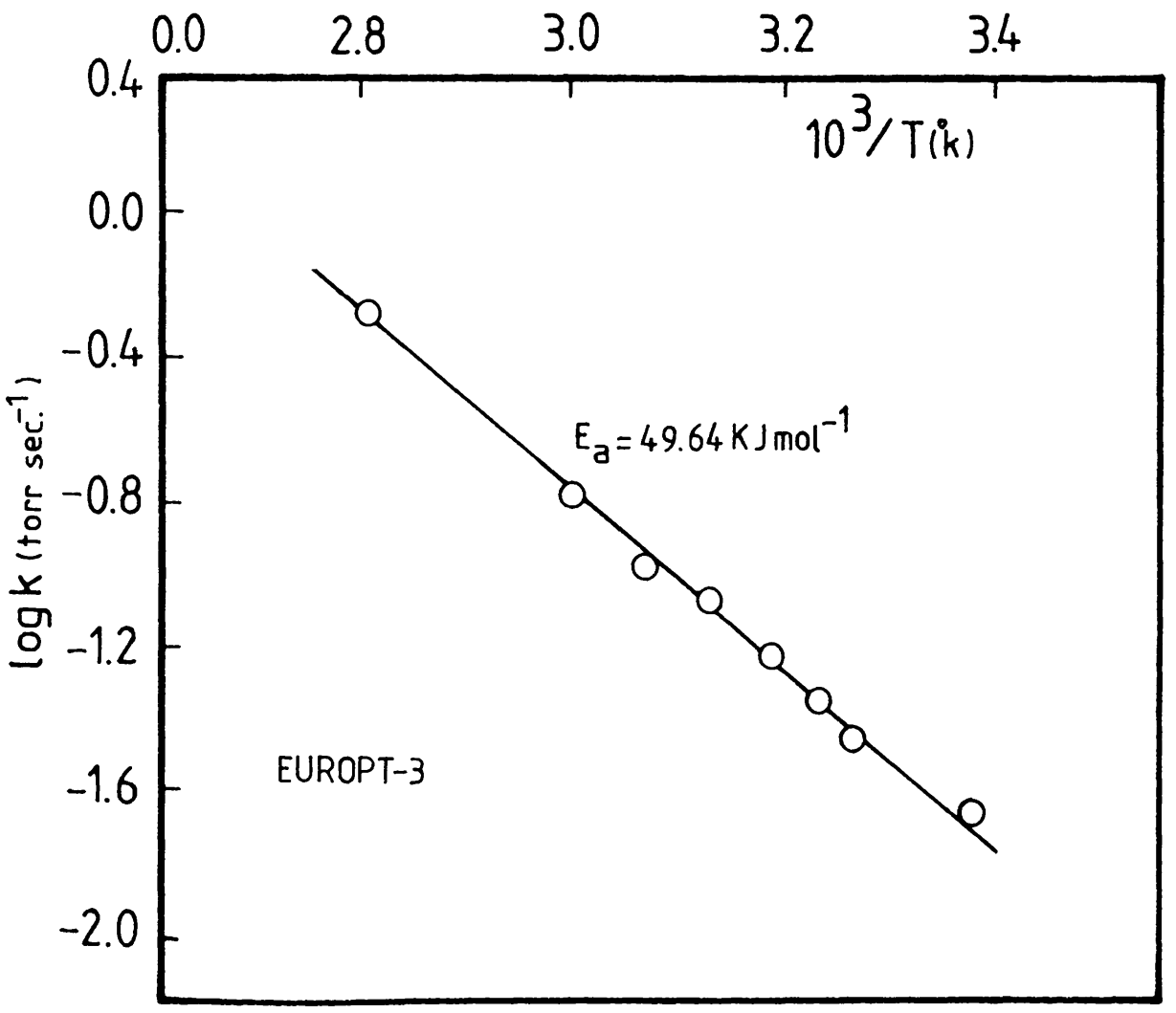

Figure 78. Variation of initial rate with reciprocal of absolute temperature.

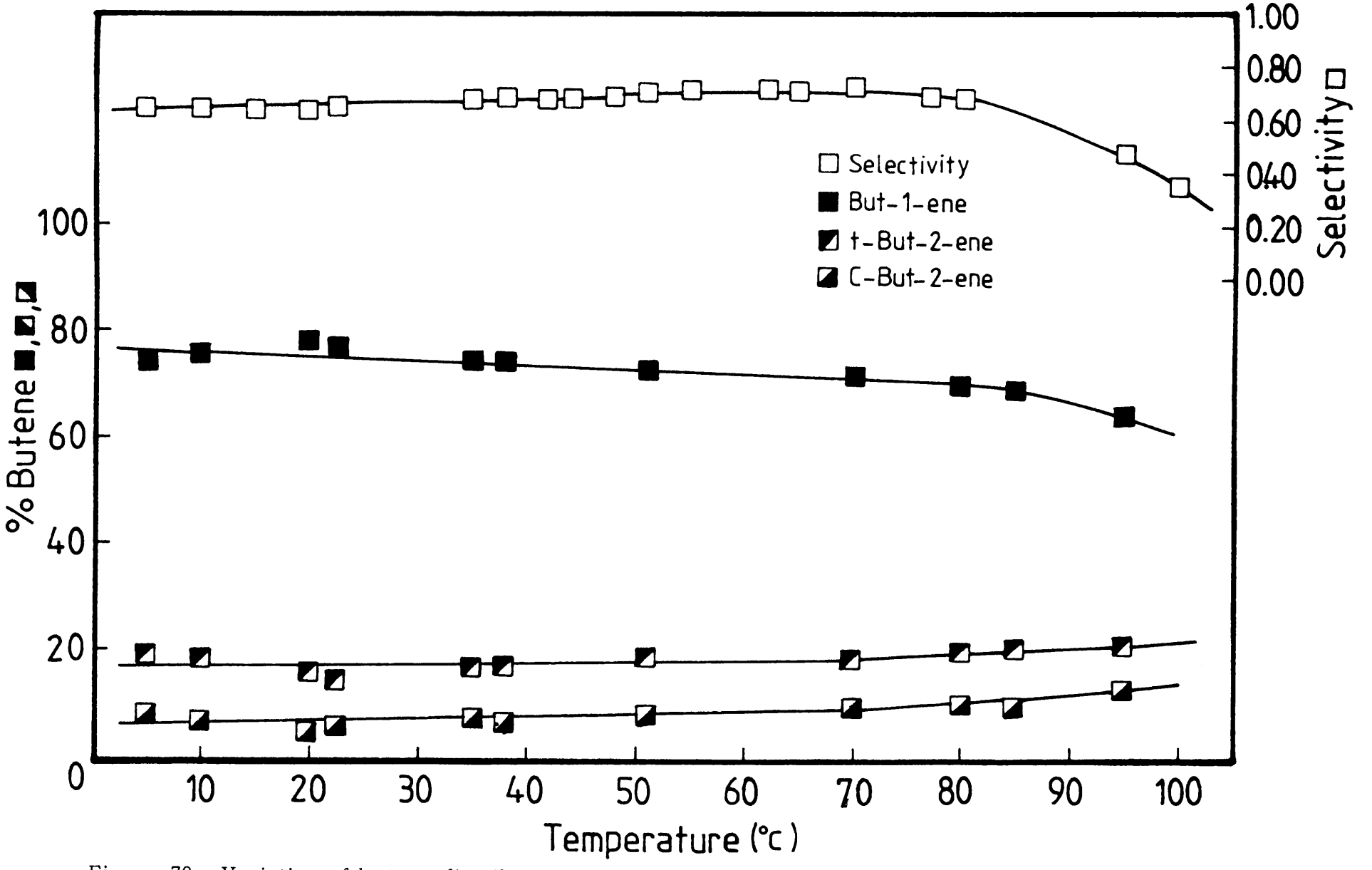

Figure 79. Variation of butene distribution with temperature on EUROPT-3.

CHAPTER NINE

THE SULPHUR POISONING OF PLATINUM CATALYSTS

Sulphur compounds, especially hydrogen sulphide, H_2S, are well known as poisoning agents in heterogeneous catalysis. Their presence can have either beneficial or detrimental effects on catalytic reactions. From the results obtained in this study of acetylene and buta-1,3-diene hydrogenations on EUROPT-1 catalysts, it was apparent that this catalyst possessed a poor selectivity (~ 0.30) for the production of mono-olefins from the corresponding di-unsaturated hydrocarbon. For this reason it was decided to investigate the effects of the adsorption of H_2S on the adsorption characteristics of C_2H_2, C_2H_4 and CO on the selectivity of C_2H_2/H_2 and C_4H_6/H_2 hydrogenation processes on EUROPT-1. Similar H_2S adsorption studies were also conducted on the other catalysts used in this work, namely, EUROPT-3, 0.8% Pt/Al_2O_3 and 0.8% Pt/SiO_2 catalysts for comparative purposes.

9.1 [35-S]-H_2S ADSORPTION ON FRESHLY REDUCED AND STEADY STATE EUROPT-1 CATALYSTS

A 0.1342g EUROPT-1 catalyst was reduced and activated as described in the experimental procedure (section 3.6). Controlled aliquots of [35-S]-H_2S were admitted to the reaction vessel and the surface and gas phase count rates were determined after each addition.

Figure 80 shows an adsorption isotherm for [35-S]-H_2S adsorbed on a freshly reduced catalyst. As in the case of [14-C]-C_2H_2

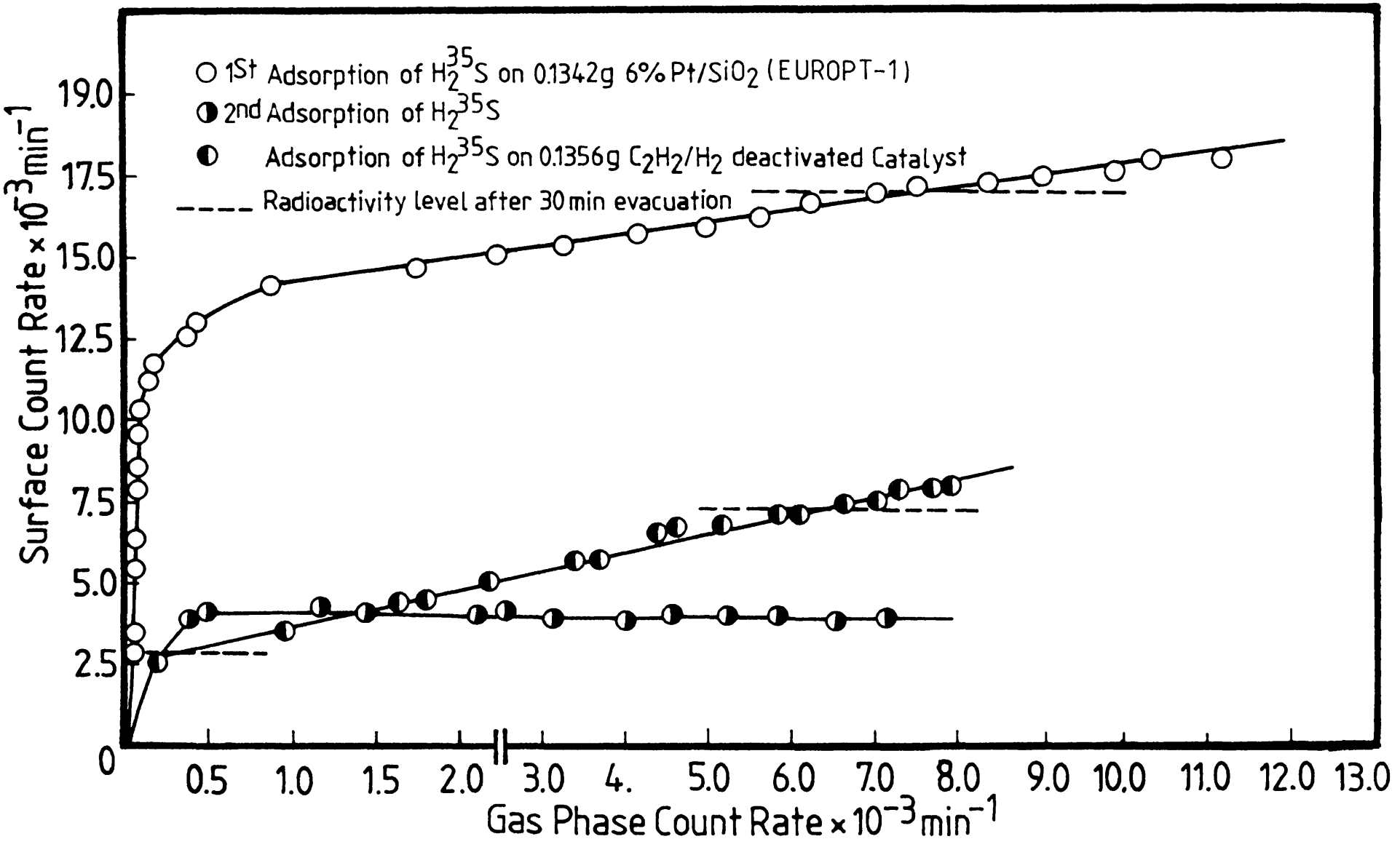

Figure 80. Adsorption isotherms of [35-S]-hydrogen sulphide on EUROPT-1.

and $-C_2H_4$ adsorptions, this showed two distinct regions, a steep primary region followed by a linear secondary region. The secondary region of the adsorption isotherm continued to increase linearly with increasing gas pressure. No plateau region was observed although a gas pressure in excess of ~ 20 Torr was used. However, about 5% of the total amount of the [35-S]-adsorbed species was removed by evacuation for 30 min. Admission of further aliquots of [35-S]-H_2S to the catalyst (2nd adsorption isotherm, Figure 80) showed a continuous build-up of the sulphur species on the catalyst until a plateau region was reached. Subsequent evacuation of the catalyst for 30 min removed ~ 5% of the adsorbed species, that is, the surface count rate dropped from a value of 17967 to 17063 counts min^{-1}. This latter value was taken as to correspond to the completion of monolayer coverage and used to calculate Θ_{H_2S} in the subsequent poisoning experiments.

When [35-S]-H_2S adsorption on a steady state catalyst was investigated, 0.1356g of EUROPT-1 was reduced and treated in the standard manner and was then deactivated to the steady state by 30 reactions using a $1:3::C_2H_2:H_2$ mixture. A [35-S]-H_2S isotherm was built-up on the catalyst by admitting successive aliquots of the radioactive hydrogen sulphide. As can be seen in Figure 80, the extent of sulphur adsorption on the primary region was substantially reduced. Although the amount adsorbed in the secondary region was less than that adsorbed on the freshly reduced catalyst, the isotherm had a similar gradient. Evacuation of the steady state catalyst for 30 min removed ~ 8.8% of the total adsorbed species.

9.2 [14-C]-ACETYLENE ADSORPTION ON [35-S]-H_2S POISONED CATALYSTS

To a 0.1233g sample of EUROPT-1 catalyst, a small pulse of [35-S]-H_2S was admitted and left in contact with the surface for 15 min. The reaction vessel was then evacuated for 15 min to remove any weakly bound species. From the amount of radioactivity recorded after the evacuation process and the sulphur saturation value (see section 9.1), the fractional coverage (Θ_{H_2S}) was determined. A [14-C]-C_2H_2 adsorption isotherm was then determined in the normal manner (section 4.1.1). This process was repeated with another catalyst sample of the same weight using identical counting geometry. Figure 81 shows a series of [14-C]-C_2H_2 adsorption isotherms obtained on [35-S]-H_2S poisoned catalysts. From these it can be seen that, pre-adsorption of sulphur on the catalyst suppressed considerably the amounts of [14-C]-C_2H_2 that could be adsorbed compared with those on a sulphur-free surface. This effect was more pronounced in the secondary adsorption region. Admission of [14-C]-C_2H_2 on to catalysts with high sulphur coverages, $\Theta_{H_2S} > 0.1$, resulted in an interaction between the sulphur and the acetylene molecules leading to a continuous drop in the surface radioactivity. The effect of evacuation on the adsorbed C_2H_2 is also shown in Figure 81.

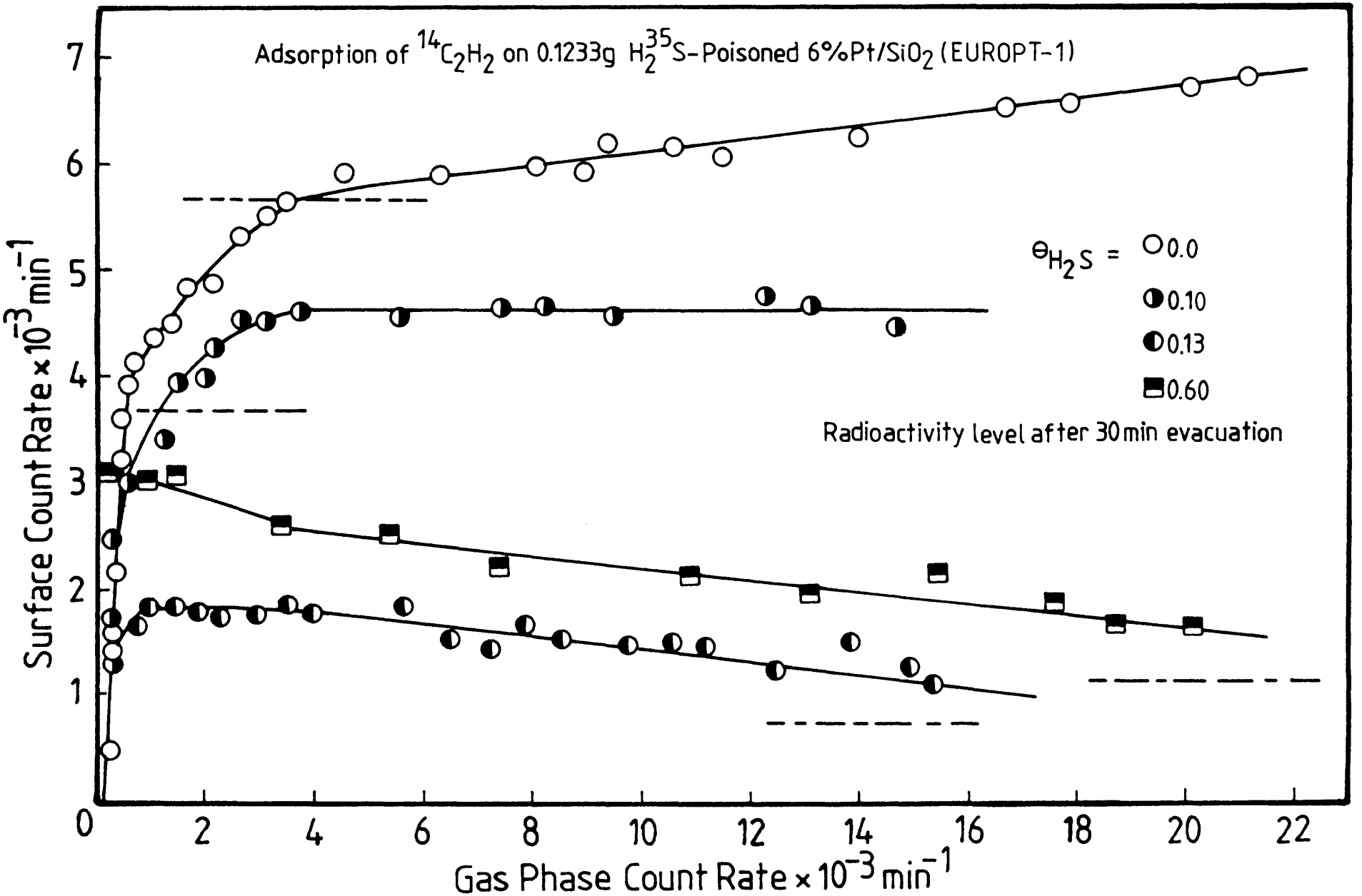

Figure 81. Adsorption isotherms of acetylene on H_2S-poisoned EUROPT-1.

9.3 [14-C]-ETHYLENE ADSORPTION ON [35-S]-H_2S POISONED CATALYSTS

In a series of adsorption experiments on H_2S poisoned catalysts, samples of EUROPT-1 were reduced in flowing H_2 and treated as described in section 3.6. Controlled pressures of [35-S]-H_2S were admitted to these catalysts and left to equilibrate with the surface for 15 min before the system was evacuated for 15 min to remove any weakly adsorbed sulphur species. This was followed by measuring the [14-C]-C_2H_4 adsorption isotherms. Figure 82 shows a series of adsorption isotherms obtained for the adsorption of [14-C]-C_2H_4 on the S-poisoned catalysts. The striking features emerging from these isotherms are that, at Θ_{H_2S} between 0.2 and 0.5, sulphur reduced remarkably the adsorptive capacity of the catalysts for C_2H_4 adsorption in the secondary adsorption region. At $\Theta_{H_2S} > 0.5$, an enhanced uptake of ethylene was observed to occur in particular in the primary adsorption region. However, as the pressures of C_2H_4 were increased, a continuous drop in the surface count rates was observed, suggesting the occurrence of an interaction between the pre-adsorbed sulphur and the C_2H_4 molecules. Evacuation of the reaction vessel for 30 min after each adsorption isotherm resulted in a decrease in the surface count rate to a value corresponding to the turning point of the adsorption isotherms. The extent of sulphur-induced suppression of the adsorption capacity was less with ethylene than with acetylene (Figure 81).

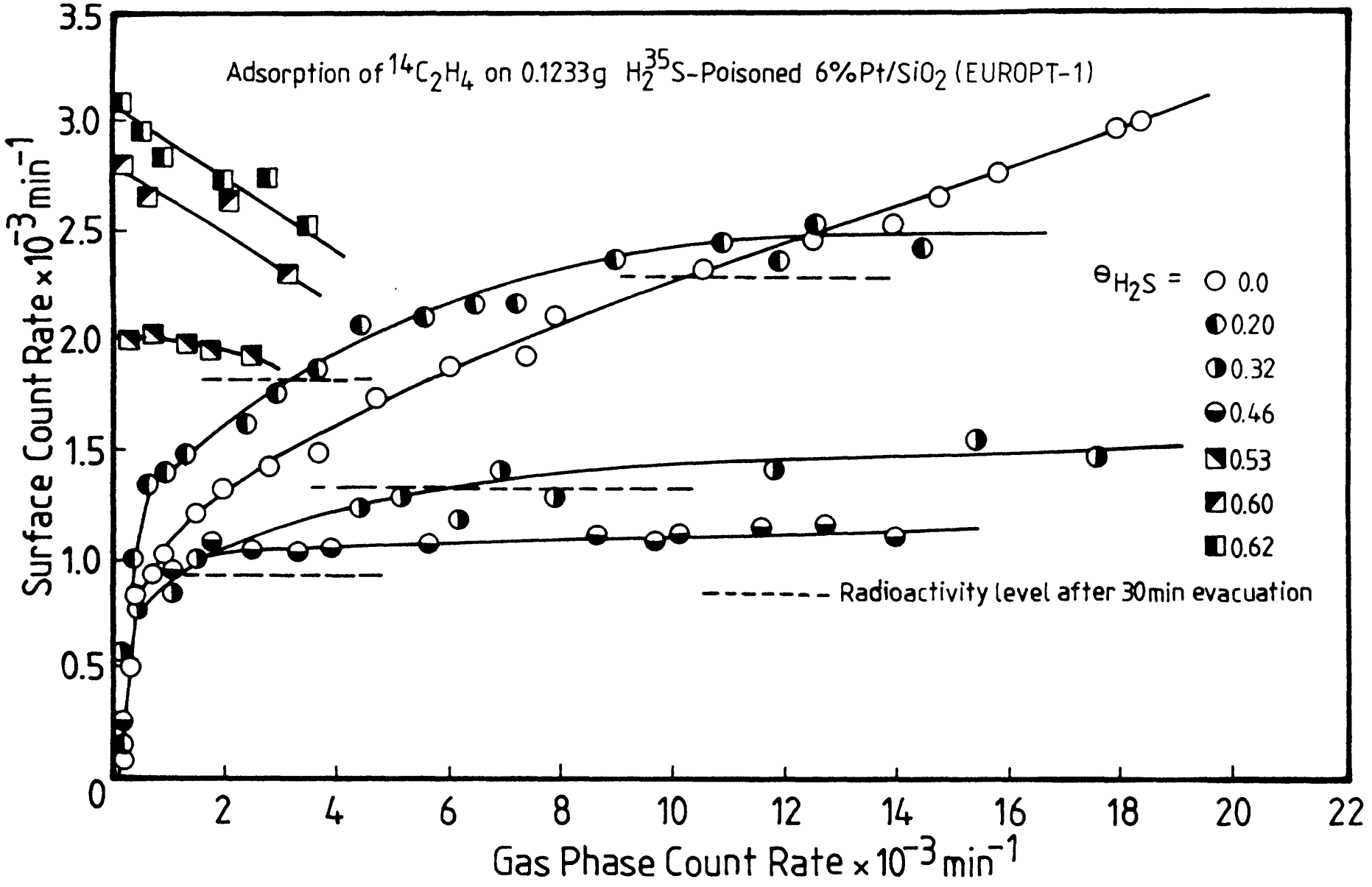

Figure 82. Adsorption isotherms of ethylene on H_2S-poisoned EUROPT-1.

9.4 [14-C]-CARBON MONOXIDE ADSORPTION ON [35-S]H_2S POISONED CATALYSTS

0.0522g samples of reduced EUROPT-1 were used. Controlled quantities of [35-S]-H_2S were admitted to the freshly reduced catalysts and left in contact with the surface for a period of 15 min, after which the reaction vessel was evacuated for 15 min to remove the gas phase and any physically bound H_2S. Carbon monoxide adsorption isotherms were obtained by admitting successive aliquots of [14-C]-CO to the S-poisoned catalysts, as described in section 4.3.1. These shown in Figure 83. Evacuation of the reaction vessel for 30 min resulted in the removal of ca. 10% of the initially adsorbed CO.

9.5 EFFECTS OF [35-S]-H_2S ON THE SELECTIVITY OF ACETYLENE HYDROGENATION

In a series of acetylene hydrogenation reactions using different Pt-catalysts, the selectivities on these catalysts were studied as a function of H_2S-uptake. Controlled pulses of [35-S]-H_2S were admitted to the catalyst surfaces and left to equilibrate for 15 min, followed by 15 min evacuation of the reaction vessel. A $3:1::H_2:C_2H_2$ mixture was then introduced to the reaction vessel and the extent of the reaction was monitored by the pressure transducer. At pressure fall of 10 Torr, the products were analysed by the gas chromatograph. This procedure was repeated with various amounts of pre-adsorbed H_2S.

Figure 84 shows the variation of selectivity with H_2S-coverage (Θ_{H_2S}). From these results it can be seen that, over both EUROPT-1

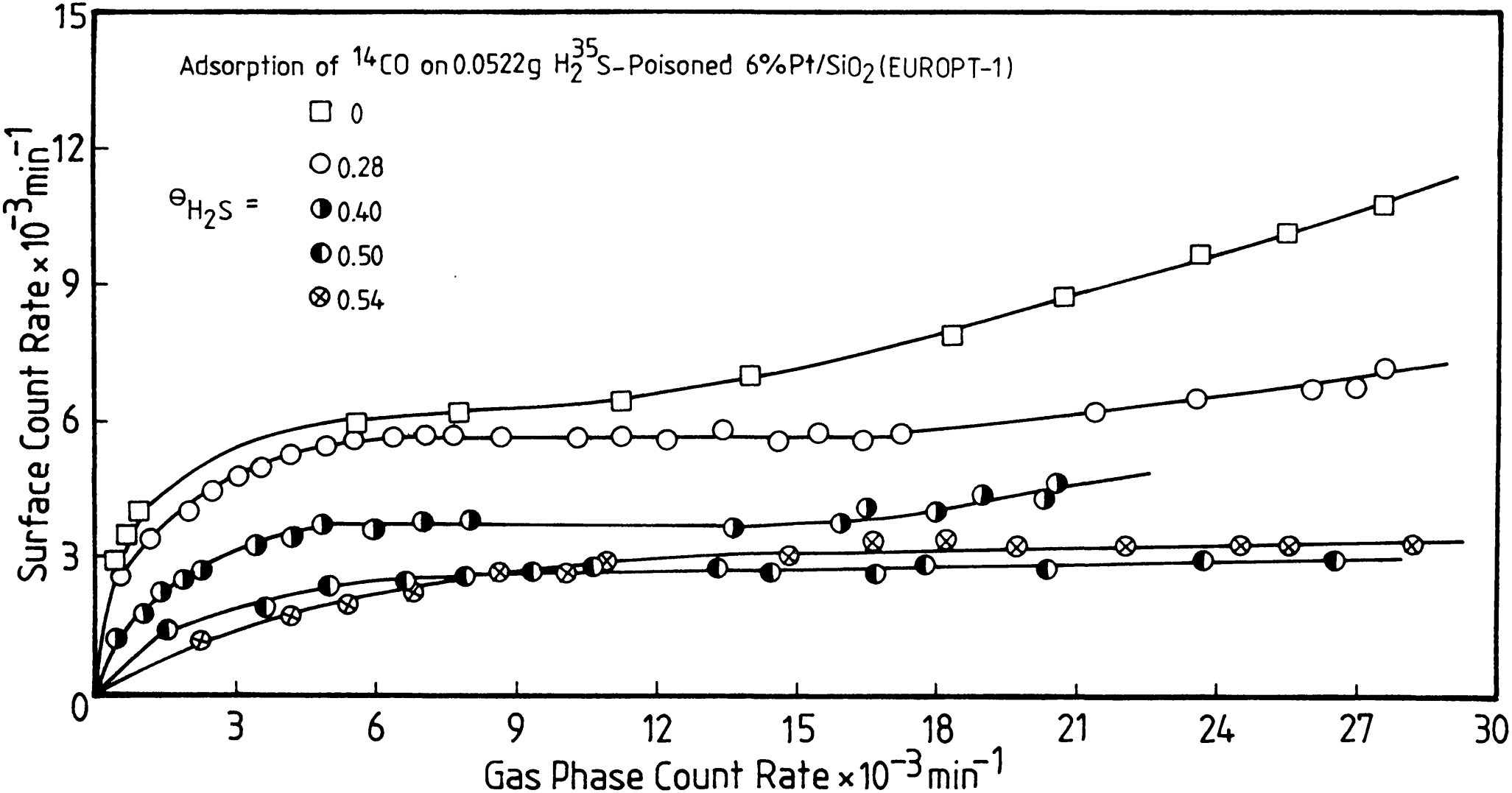

Figure 83. Adsorption isotherms of carbon monoxide on H_2S-poisoned EUROPT-1.

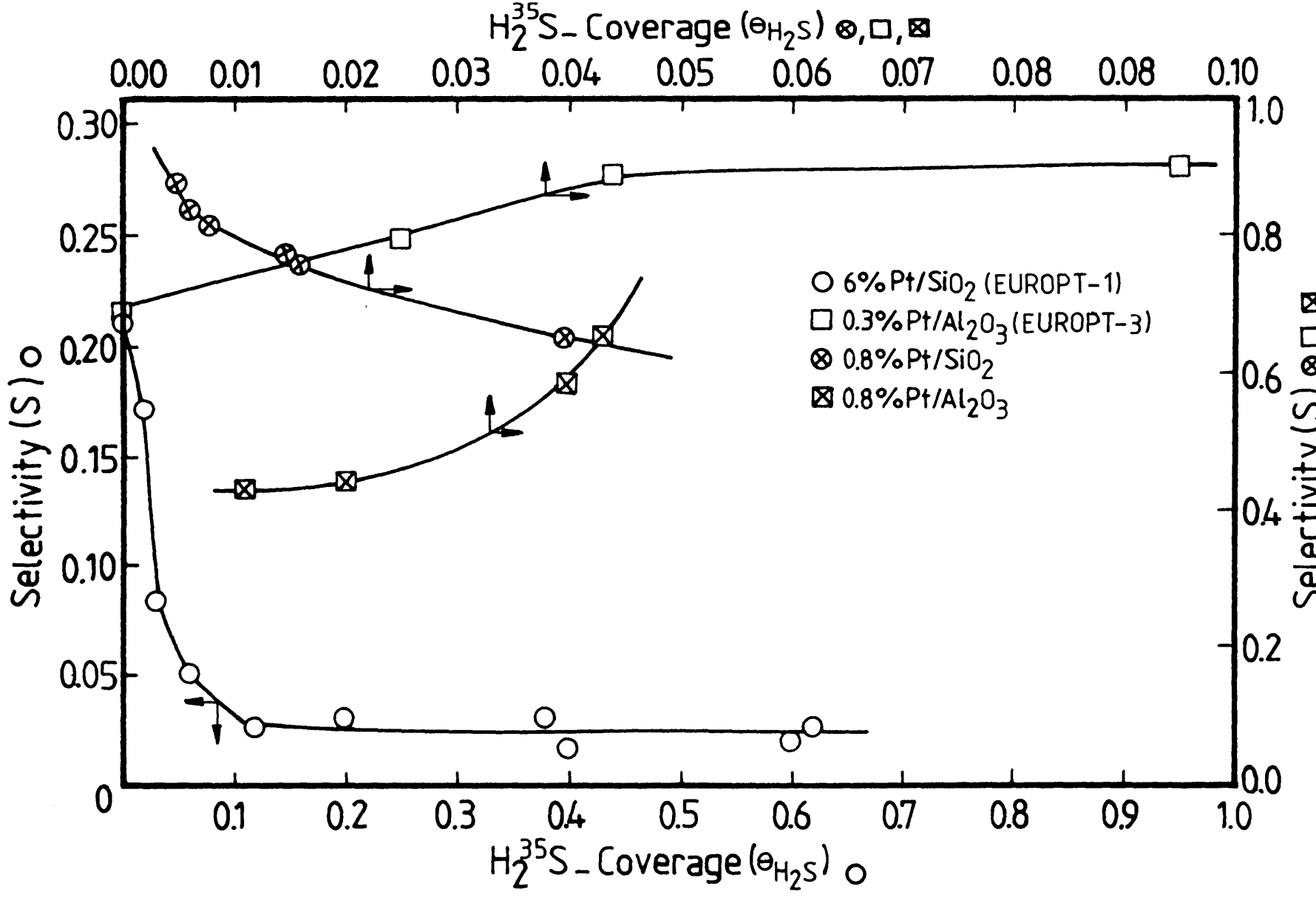

Figure 84. Variation of the selectivity of acetylene hydrogenation on Pt catalysts with sulphur coverage.

(6% Pt/SiO_2) and 0.8% Pt/SiO_2 catalysts, the selectivity decreased considerably as the pressure of H_2S was increased. The effect was greater with the former catalyst as compared with the latter. On EUROPT-3 (0.3% Pt/Al_2O_3) and 0.8% Pt/Al_2O_3 catalysts, the presence of sulphur was beneficial in that a steady increase in the selectivity occurred as the H_2S-coverage was increased. The selectivity did not tend to a zero value as the sulphur coverage was increased.

When [35-S]-H_2S was pre-mixed with the reaction mixtures before the hydrogenation reactions, the effect on the selectivity with each catalyst was identical to that described above.

The hydrogenation of acetylene in the presence of [14-C]-ethylene was also examined on sulphur-poisoned catalysts to gain further knowledge about the effect of sulphur on the different reaction pathways in the acetylene hydrogenation on EUROPT-1 catalysts. 0.233g samples of the reduced catalysts were poisoned with known amounts of sulphur as described in sections 3.6 and 9.1. The amounts of radioactivity in the individual reaction products was determined using radio-gas chromatography. Figure 85 and Table 7 show the results obtained on EUROPT-1 for the hydrogenation of 12.5 Torr C_2H_2 with 37.5 Torr H_2 when 2, 4 and 5 Torr [14-C]-C_2H_4 were added before admission to the reaction vessel containing the poisoned catalysts. As observed on the sulphur-free catalysts (section 5.7), the amount of [14-C]-ethane produced constituted only a small fraction (~ 1%) of the total ethane yield, relative to the amount expected from the amounts of added [14-C]-C_2H_4 present in the reaction vessel.

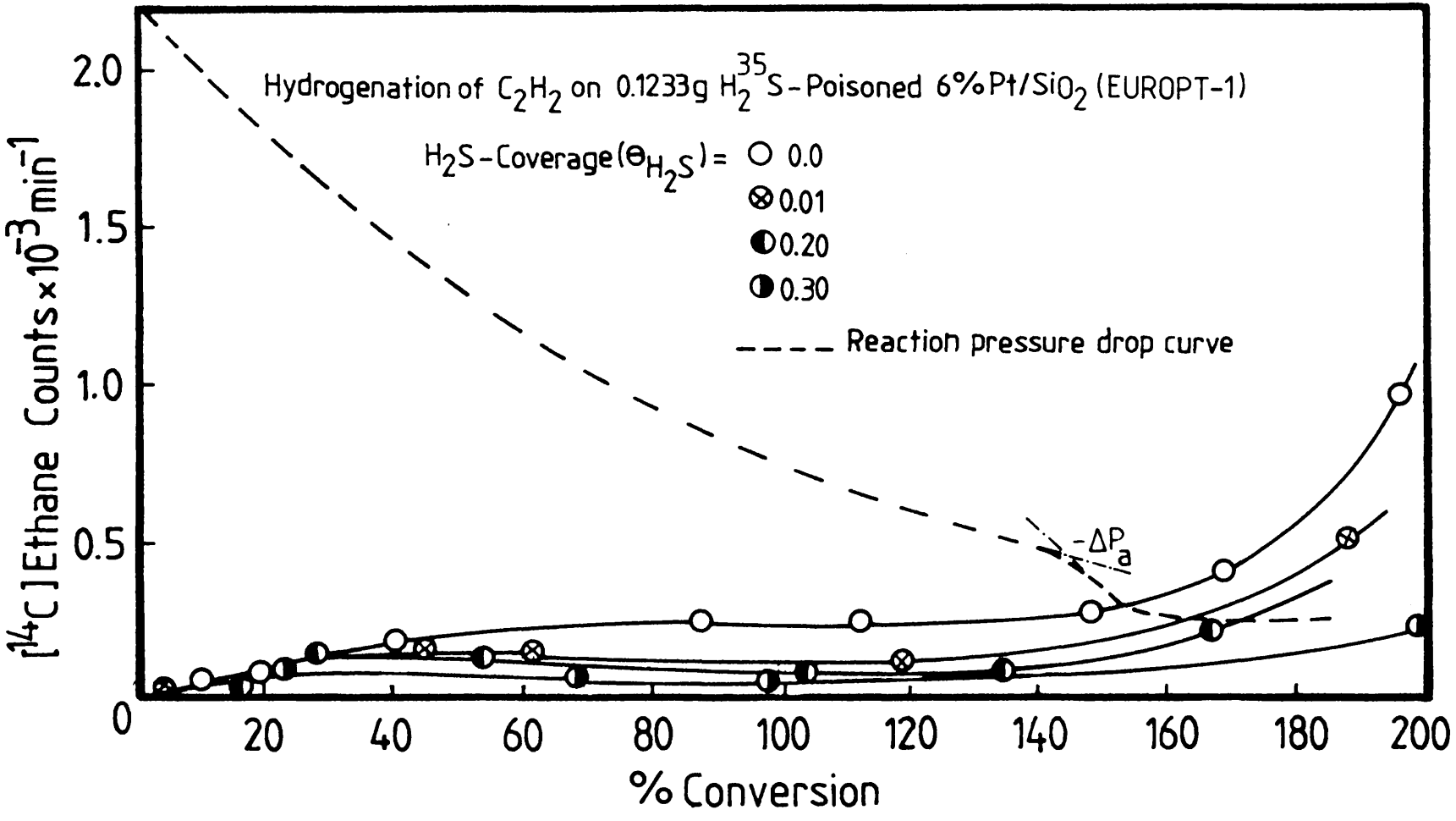

Figure 85. Variation of [14-C] ethane yield during the hydrogenation of acetylene on sulphur-poisoned EUROPT-1 catalyst in presence of added amounts of [14-C]-ethylene.

Table 7. Distribution of C_2-products from the Hydrogenation of 12.5 torr of Acetylene in the presence of 2 torr (Θ_{H_2S} = 0.01), 4 torr (Θ_{H_2S} = 0.20) and 5 torr (Θ_{H_2S} = 0.30) Added [14-C] Ethylene on H_2S-poisoned 0.233g 6% Pt/SiO_2 (Europt-1) catalyst.

P_{H_2} = 37.5 torr temperature = 20 ± 2°C

Θ_{H_2S}	(%) conversion	$P_{^{14}C_2H_6}$ (torr) x 10^{-3}	$P_{^{12}C_2H_4}$ (torr)	Total $P_{^{12}C_2H_6}$ (torr)	Direct $P_{^{12}C_2H_6}$ (torr)	Selectivity (S)	Inherent Selectivity (S')
0.01	10.51	1.25	0.2460	0.4608	0.4606	0.3480	0.3481
-	21.15	7.10	0.3360	0.8929	0.8917	0.2734	0.2740
-	34.61	2.02	0.4104	1.4280	1.4276	0.2232	0.2233
-	45.34	2.43	0.3050	1.7980	1.7976	0.1450	0.1451
-	62.30	1.87	0.3413	2.4380	2.4377	0.1228	0.1228
-	188.00	10.50	0.5110	4.8890	4.8860	0.0946	0.0947
0.20	27.23	10.20	0.5850	1.5030	1.5015	0.28017	0.2804
-	53.84	8.32	0.7550	2.6920	2.6904	0.21903	0.2191
-	77.90	86.00	1.0670	3.3140	3.2906	0.2436	0.2449
-	104.93	4.43	1.1550	4.6960	4.6947	0.1974	0.1974

Table 7 (contd.)

Θ_{H_2S}	(%) conversion	$P_{14_{C_2H_6}}$ (torr) x 10^{-3}	$P_{12_{C_2H_4}}$ (torr)	Total $P_{12_{C_2H_6}}$ (torr)	Direct $P_{12_{C_2H_6}}$ (torr)	Selectivity (S)	Inherent Selectivity (S')
0.20	126.40	77.00	1.0940	4.9230	4.9015	0.1818	0.1825
-	167.00	25.00	0.7680	6.675	6.6702	0.1032	0.1033
0.30	23.10	5.97	0.2580	1.5040	1.5037	0.1464	0.1465
-	40.11	10.80	0.5310	2.2592	2.2581	0.1903	0.1904
-	53.34	22.00	0.6250	2.9178	2.9150	0.1539	0.1766
-	98.00	2.10	0.1640	4.8980	4.8979	0.0324	0.0324

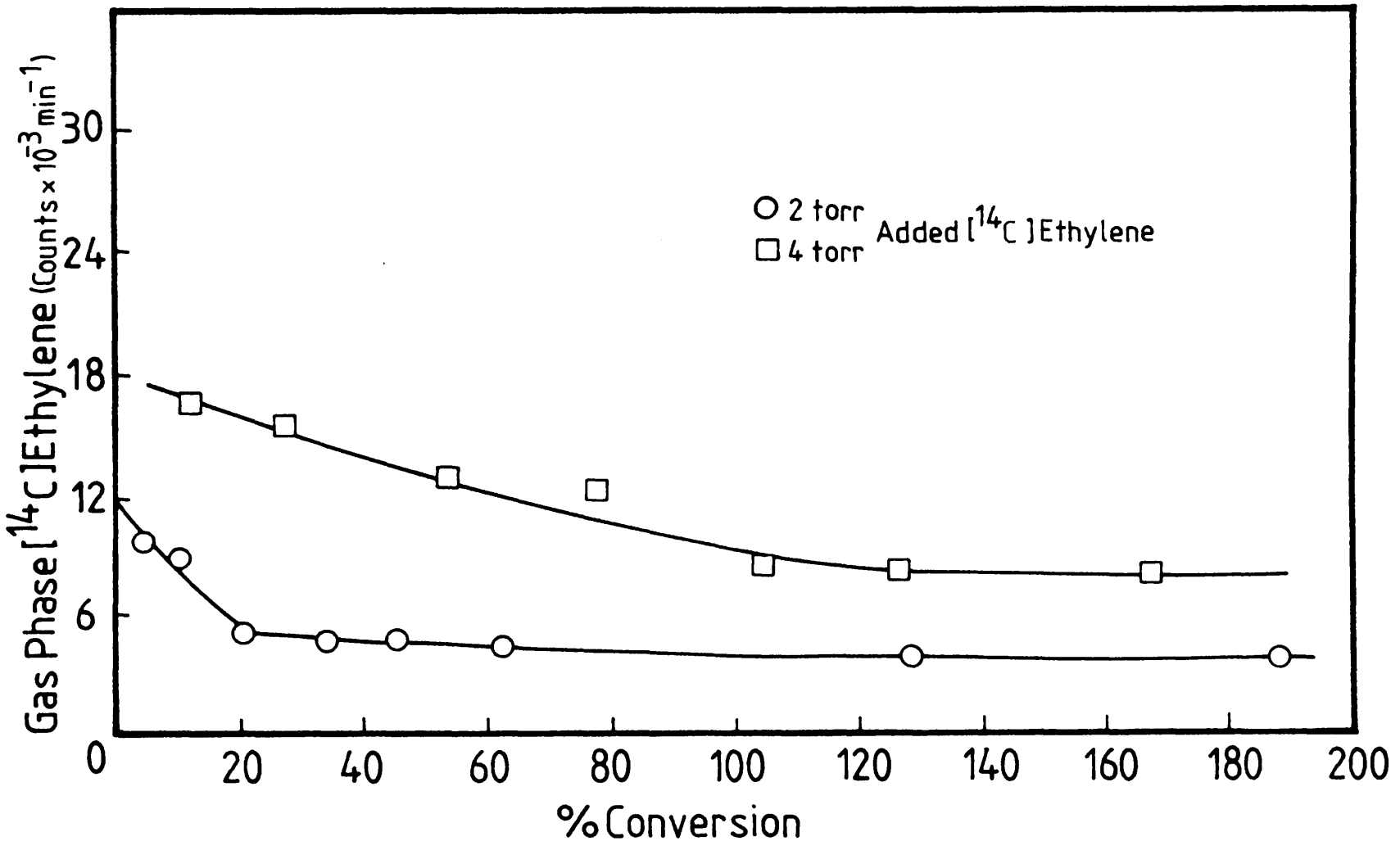

Figure 86. Variation of [14-C] ethylene count rate during the hydrogenation of acetylene on sulphur-poisoned EUROPT-1.

Figure 86 shows the amounts of [14-C]-C_2H_4 present during the hydrogenation reactions as measured by radio-gas chromatography.

The phenomenon of enhanced selectivity on EUROPT-3 with increased H_2S pressure was studied in some detail by examining the adsorptions of acetylene, ethylene and carbon monoxide.

Samples of 0.27g, 0.24g and 0.27g EUROPT-3 were reduced and treated in the standard manner and poisoned with [35-S]-H_2S corresponding to sulphur-coverage of $\Theta_{H_2S} \sim 0.25$ and were used respectively for the determination of [14-C]-C_2H_2, -C_2H_2 and -CO adsorptions. Figure 87 shows the adsorption isotherms of these adsorbates on freshly reduced and H_2S-poisoned catalysts. One of the major differences to be noticed between the poisoned and the clean catalysts was the extent of the severe reduction in the primary adsorption region of all the adsorbates on the poisoned catalysts. In addition, on these catalysts, the shapes of the secondary regions, in particular for C_2H_4 and CO, showed significantly different behaviour from those observed on the freshly reduced catalysts, in the sense that they continued to increase sharply as further gas was admitted to the reaction vessel.

9.6 EFFECTS OF [35-S]-H_2S ON THE SELECTIVITY OF BUTA-1,3-DIENE HYDROGENATION

In order to gain more knowledge concerning the H_2S-poisoning mechanism, the effect of sulphur on selectivity was also examined for buta-1,3-diene hydrogenation on the EUROPT-catalysts.

Samples of 0.051g (EUROPT-1) and 0.427g (EUROPT-3) were used. After reduction pulses of H_2S were introduced to the catalysts

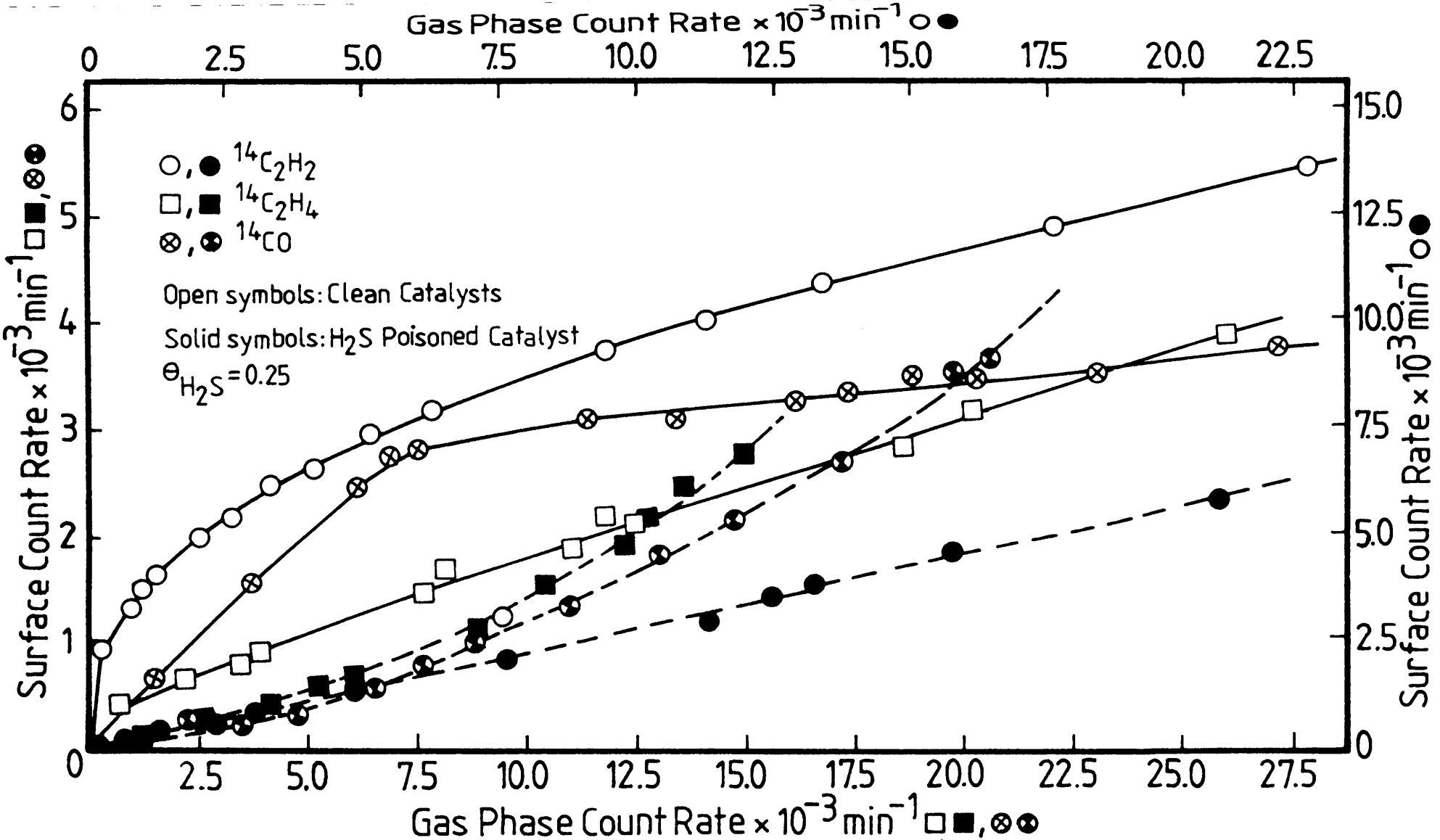

Figure 87. Adsorption isotherms of C_2H_2, C_2H_4 and CO on clean and sulphur-poisoned EUROPT-3.

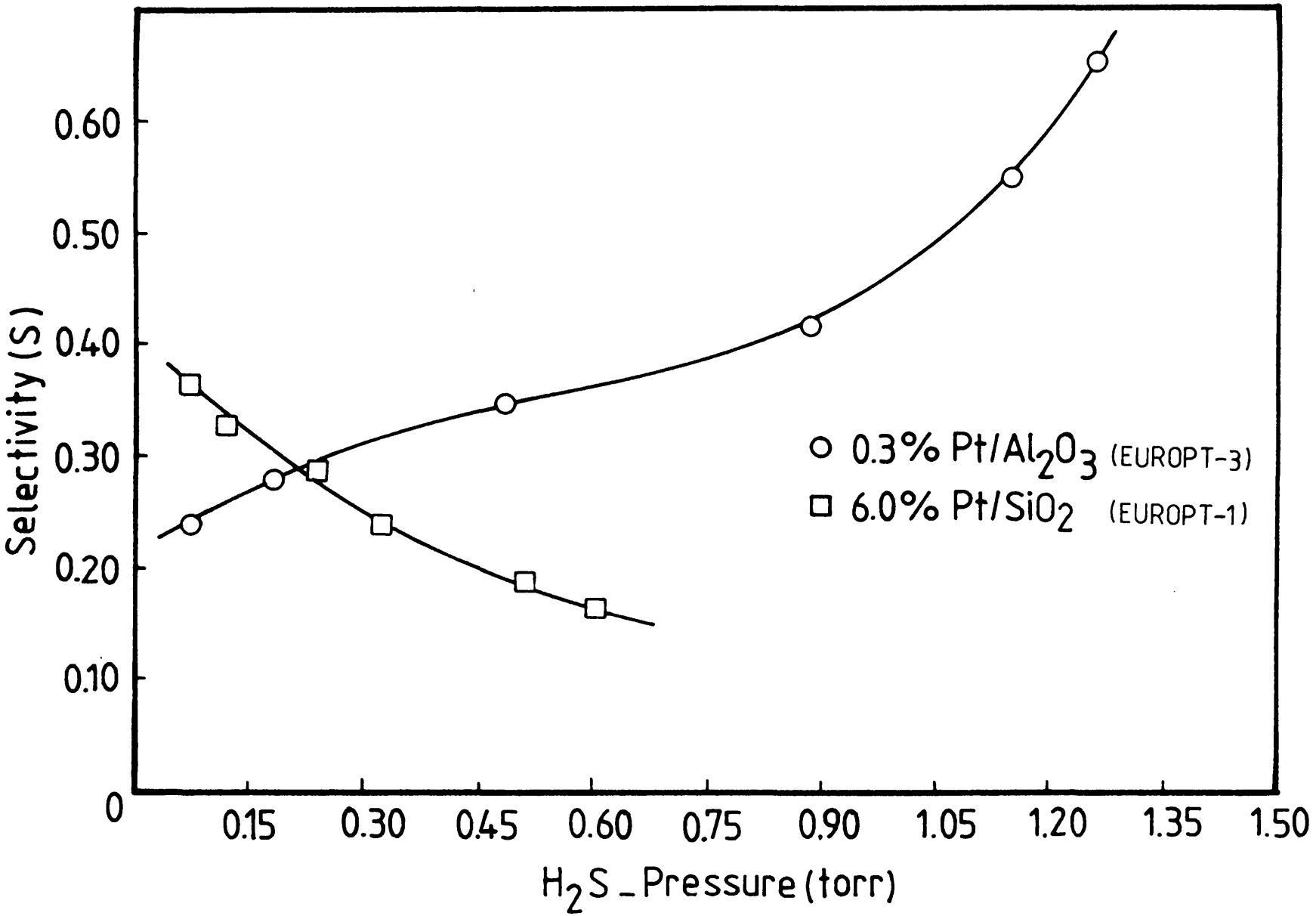

Figure 88. Variation of the selectivity of buta-1,3-diene hydrogenation with sulphur coverage on EUROPT-catalysts.

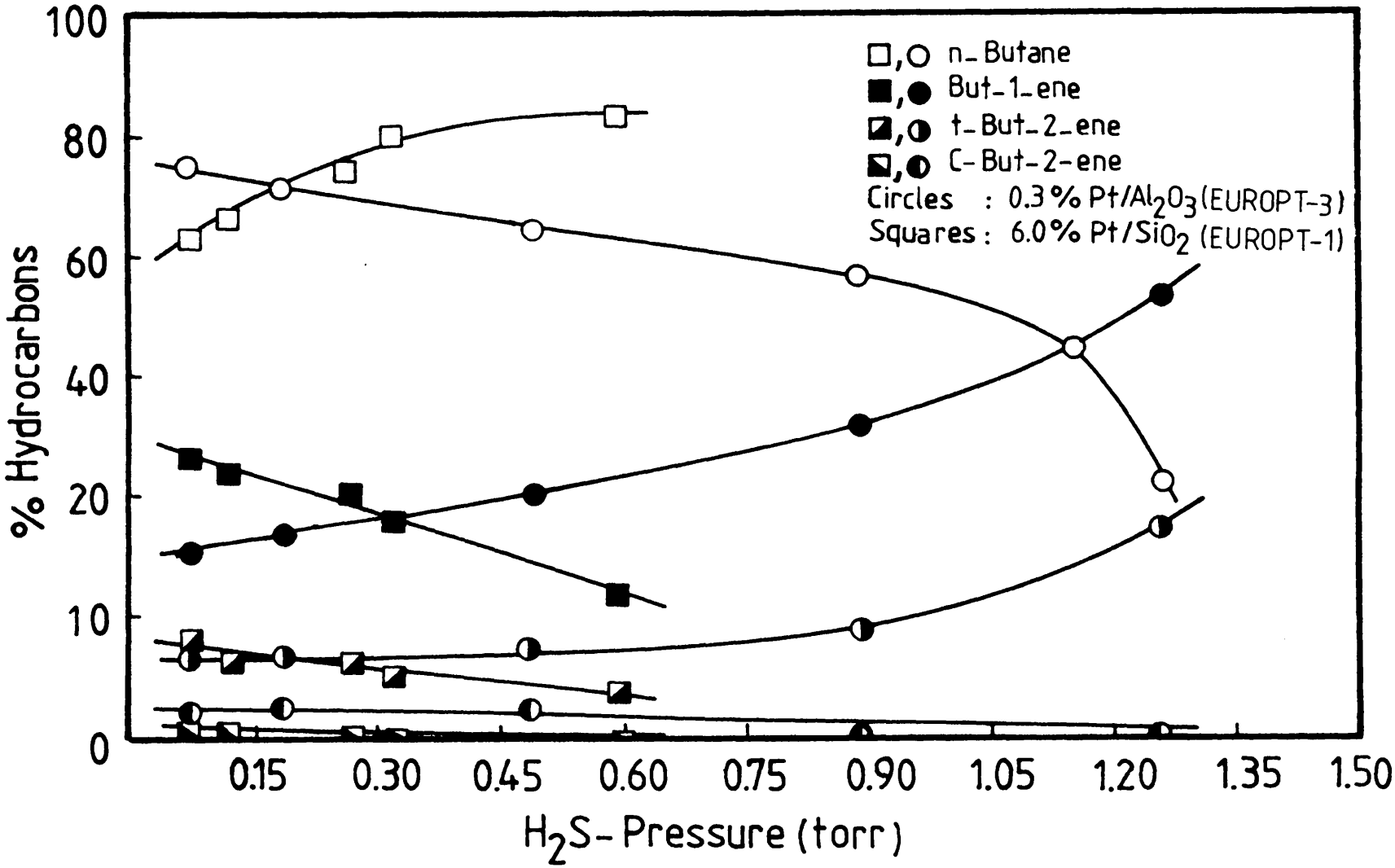

Figure 89. Product distribution curves of buta-1,3-diene on sulphur poisoned EUROPT-catalysts.

before each reaction and the extent of poisoning determined, as described in section 3.6. The products of the hydrogenation reaction were extracted for analysis by gas chromatography at a pressure drop of ~ 10 Torr. The results shown in Figure 88 revealed interesting features, in that, on EUROPT-3, the selectivity for butenes increased noticeably as the pressure of H_2S was increased. However, the reverse was found for EUROPT-1. These effects are clearly shown by the results presented in Figure 89.

CHAPTER TEN

THE FTIR-INFRA RED STUDIES OF THE ADSORBED SPECIES

The nature of the species present on the surface following the adsorption of the various hydrocarbons and carbon monoxide was investigated by Fourier transform infra red spectroscopy. Two methods were used. The catalyst samples which had been subjected to [14-C]-radiotracer adsorption or to C_2H_2/H_2 hydrogenation reactions were examined using the in situ cell (Figure 23). Direct investigation of the adsorption of these molecules by the IR system was performed using the diffuse reflectance cell (DRIFTS) (Figure 24). The details of the experimental procedures employed in these experiments are described in section 3.9. In the DRIFTS experiments, the spectra following the adsorption of C_2H_2 and C_2H_4 on EUROPT-1 at room temperature are shown in Figure 90. The spectrum of the adsorbed species after subtracting the background and gas phase spectra showed a single band at ca. 1293 cm^{-1}. This band, which has also been observed by Beebe et al. (184) for C_2H_2 and C_2H_4 on Pd/Al_2O_3 and can be assigned to the surface ethylidyne species $\equiv C\text{-}CH_3$. In contrast, when the catalyst samples of EUROPT-1 and 0.8% Pt/SiO_2 had been deactivated in a series of acetylene hydrogenation and then examined by FTIR, their in situ IR spectra (Figure 91) displayed small bands in the region 2974-2884 cm^{-1} and intense bands at 2081 cm^{-1}, 1975 cm^{-1}, 1840 cm^{-1}, 1705 cm^{-1}, 1693 cm^{-1} and 1374 cm^{-1}. The bands at 2081 cm^{-1} and 1705 cm^{-1} disappeared as the catalysts were heated to 115°C and flushed with helium for 10 min.

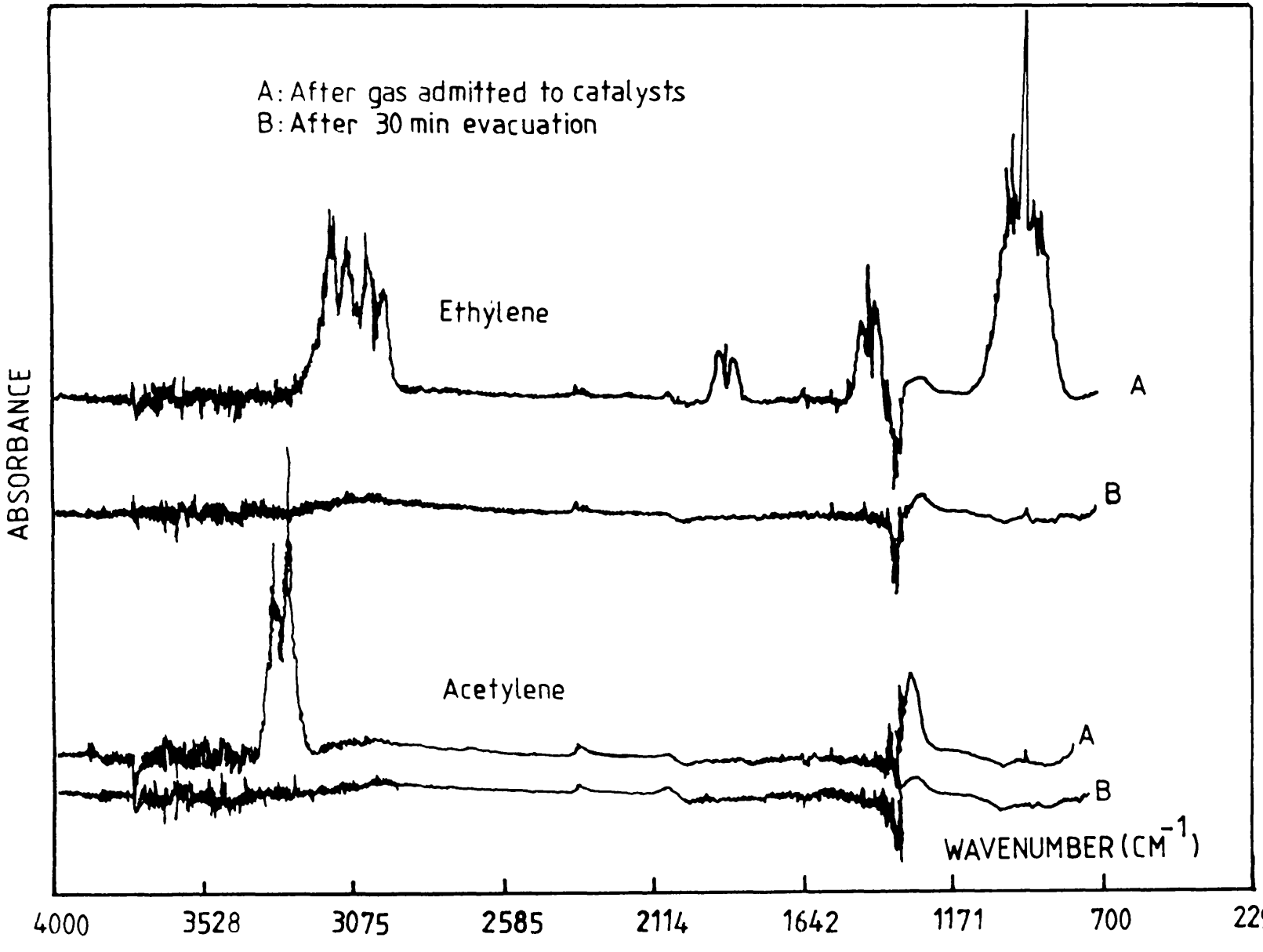

Figure 90. Infra-red spectra of acetylane and ethylene adsorbed on EUROPT-1.

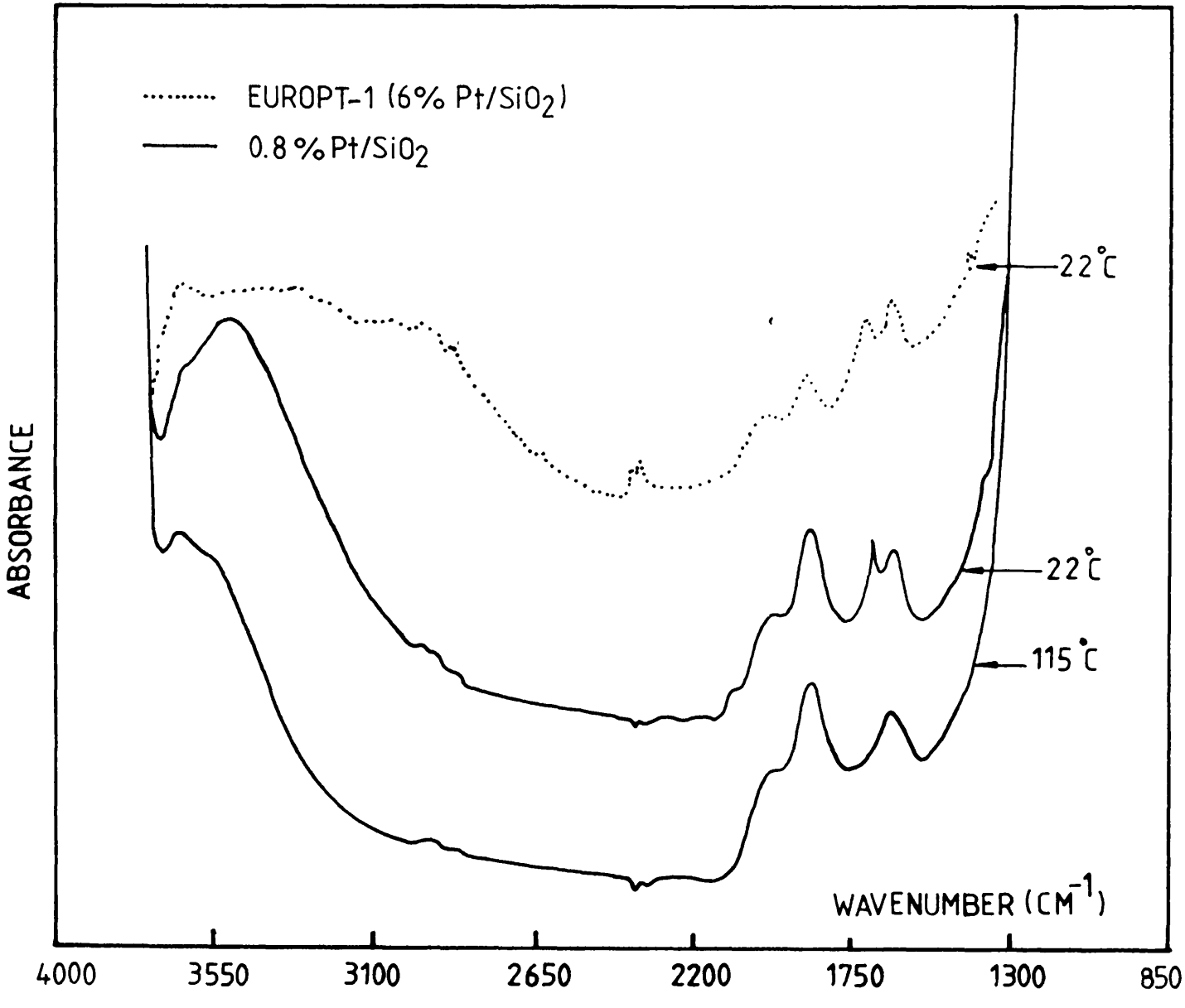

Figure 91. Infra-red spectra of Pt-catalysts deactivated with C_2H_2/H_2 reactions.

Based on the literature data (22,34,35), the bands at 2974-2884 cm^{-1} and 1374 cm^{-1} were assigned to the CH_3 group and are indicative of the presence of surface alkyl species. While the band at 1693 cm^{-1} has been attributed to C=C stretching and is characteristic of a surface species such as PtCH=CHPt. The bands at 2081 cm^{-1}, 1975 cm^{-1} and 1840 cm^{-1} are likely to be due to the adsorption of the hydrocarbon molecules on the support material.

The DRIFTS spectra of the adsorption of CO on the different catalysts are shown in Figure 92 , (EUROTP-1), Figure 93, (0.8% Pt/SiO_2, 0.5% Pt/MoO_3) and Figure 94, (EUROPT-3, 0.8% Pt/Al_2O_3). The spectra of adsorbed CO on EUROPT-1 showed a band at 2086 cm^{-1} and a companion shoulder at 2122 cm^{-1} while, on the 0.8% Pt/SiO_2 and 0.5% Pt/MoO_3 catalysts, CO adsorption, produced a single sharp band at 2086 cm^{-1}. On EUROPT-3 and 0.8% Pt/Al_2O_3 catalysts, CO adsorbed only in the linear form, respectively, giving rise to bands at 2124 cm^{-1}, 2087 cm^{-1} and 2070 cm^{-1}. These bands disappeared completely by the evacuation of the EUROPT-3 catalyst while only thermal treatment (up to 250°C) was required to remove the adsorbed CO from the 0.8% Pt/Al_2O_3 catalyst (except for those species corresponding to the 2124 cm^{-1} band).

The catalyst samples of EUROPT-1, EUROPT-3 and 0.8% Pt/SiO_2 which were first subjected to [14-C]-CO adsorptions in order to look at the shape of their adsorption isotherms were subsequently examined by the IR spectroscopy using the in situ cell. As it can be seen from the spectrum (Figure 95), these catalysts contained moieties which are characteristic of adsorbed hydrocarbon species as indicated by

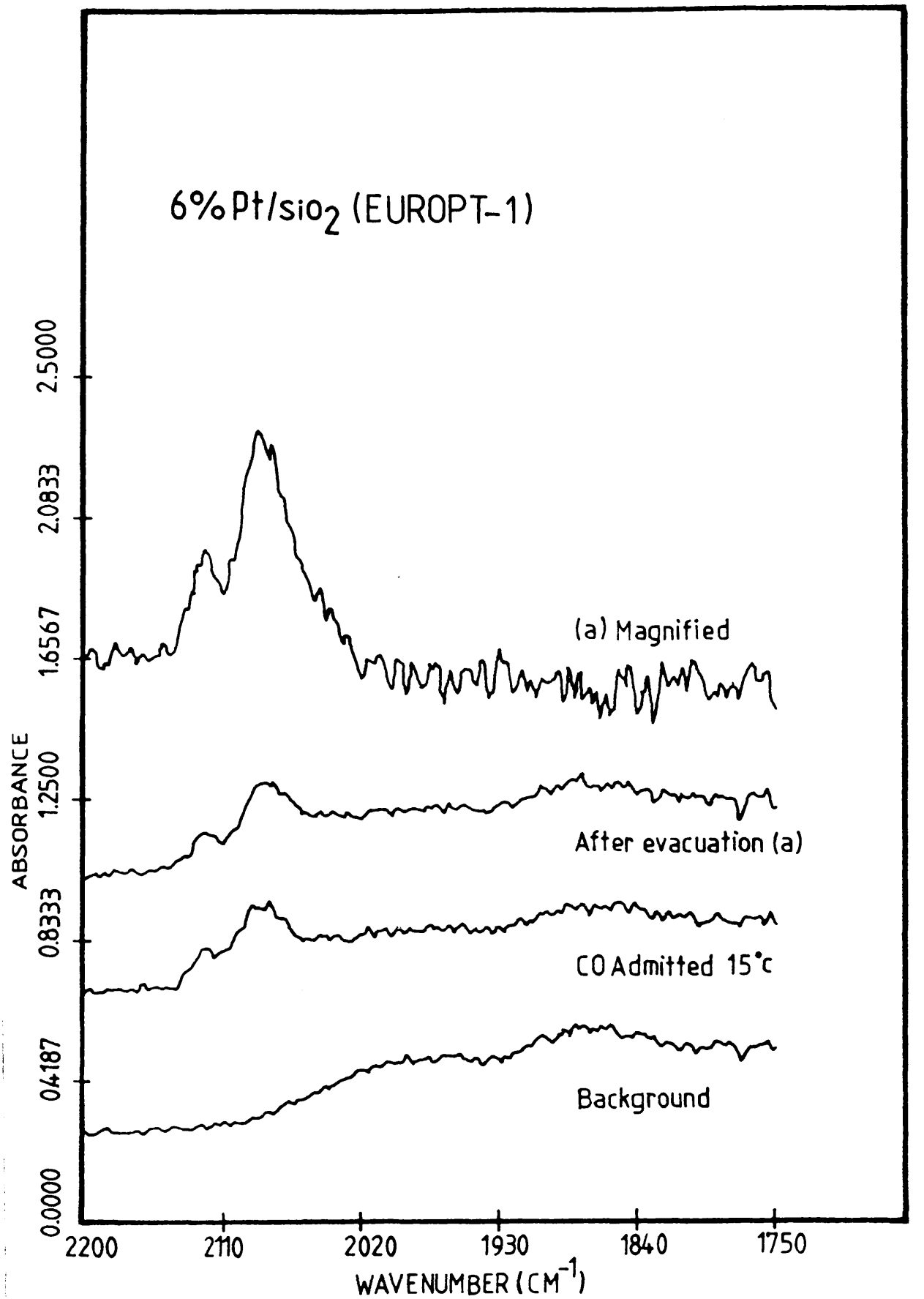

Figure 92. Infra-red spectra of carbon monoxide adsorbed on EUROPT-1.

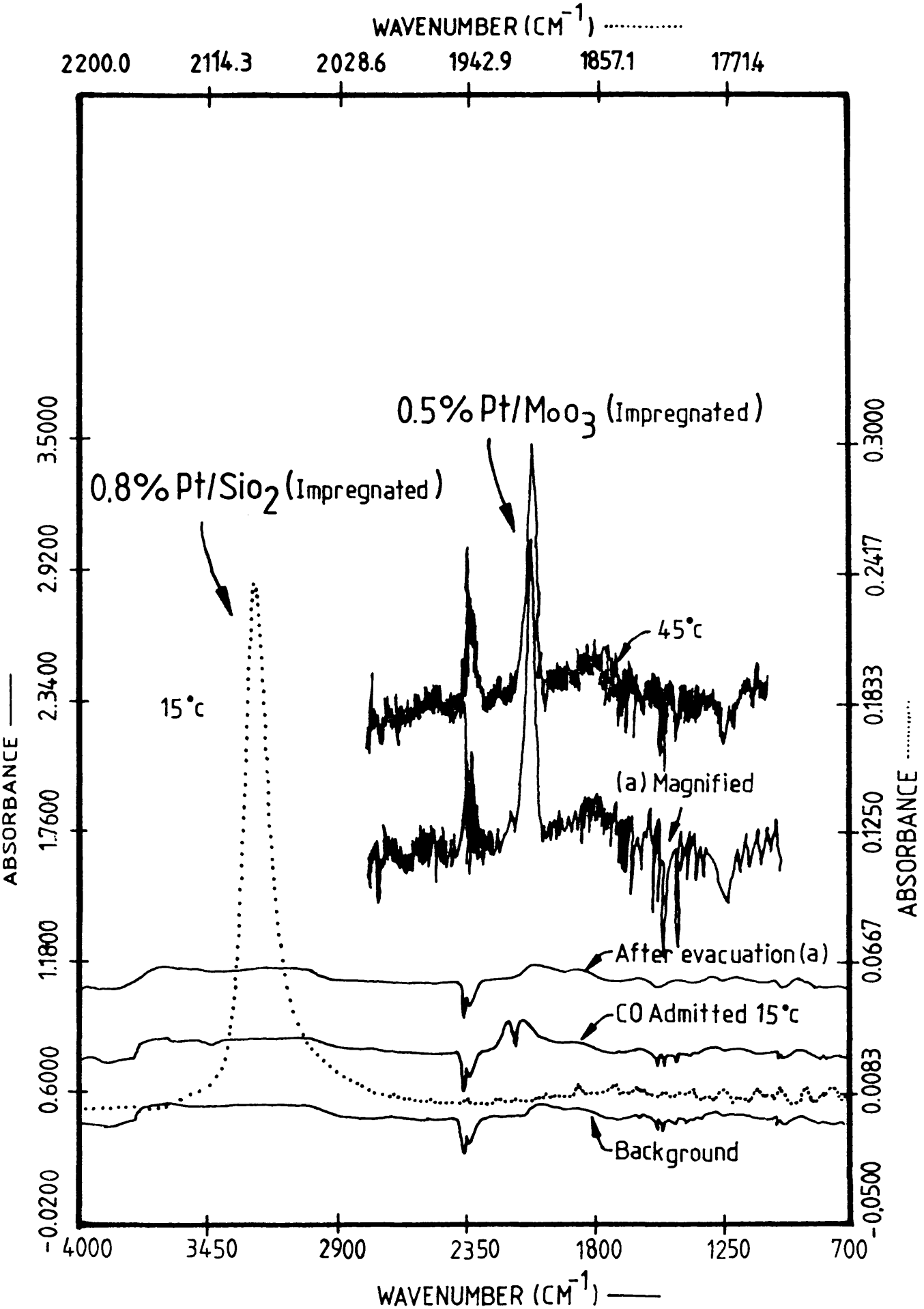

Figure 93. Infra-red spectra of carbon monoxide adsorbed on Pt-catalysts.

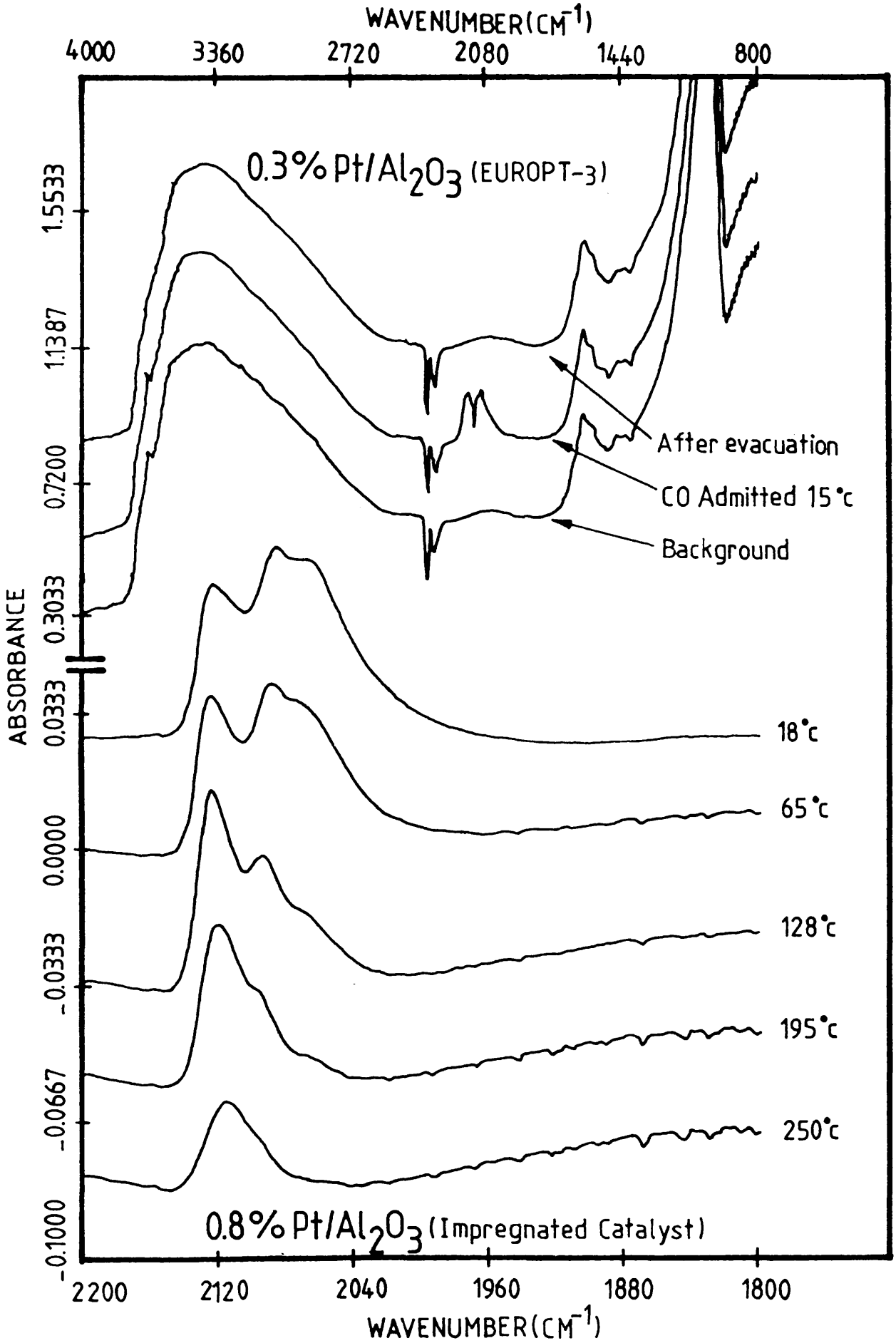

Figure 94. Infra-red spectra of carbon monoxide adsorbed on Pt-catalysts.

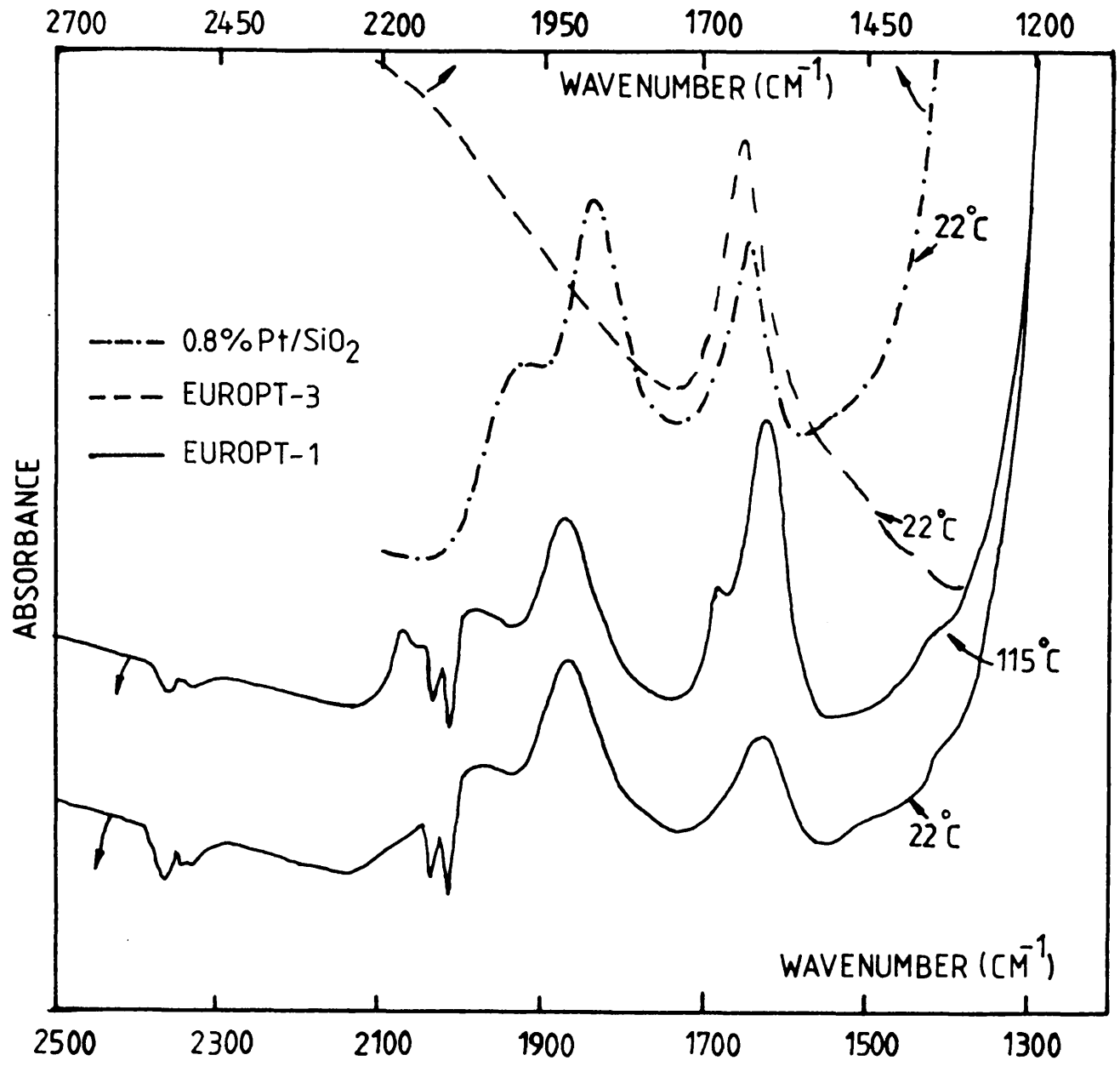

Figure 95. Infra-red spectra of Pt-catalysts deactivated with CO adsorptions.

the bands at 1685 cm^{-1} (C=C), 1632 cm^{-1} (C-C) and 1440 cm^{-1} (CH_3 group). The band at 1685 cm^{-1} appeared as the catalyst (EUROPT-1) was heated at elevated temperatures followed by evacuation. Interestingly, these species were likely to be evolved by the hydrogenation of CO by the H_2 which was retained on the catalyst metal and/or on the support after the reduction process. A band at 1886 cm^{-1} has also appeared in the spectra of the EUROPT-1 and the 0.8% Pt/SiO_2 (Figure 95) which is representative of the adsorbed bridged form of carbon monoxide.

CHAPTER ELEVEN

THE PHYSICAL CHARACTERISATION OF THE Pt-CATALYSTS

11.1 THE TEMPERATURE PROGRAMMED REDUCTION (TPR) OF Pt-CATALYSTS

Samples from the catalysts used in the present studies were subjected to TPR investigation to look at the extent of their reduction. Samples of, 0.158g (EUROPT-1), 0.633g (EUROPT-3), 0.219g (0.8% Pt/SiO_2), 0.530g (0.8% Pt/Al_2O_3) and 0.357g (0.5% Pt/MoO_3) were placed into the TPR cell (Figure 22) and the measurements were conducted as described in section 3.7.

The TPR spectra of these catalysts are shown (Figures 96a-96b). H_2-consumption by EUROPT-1 was observed to start at room temperature ~ 20°C with the TPR spectra showing a broad band with its maxima at 110°C (Figure 96a). This is in accordance with the findings of Bond and Gelsthorpe (183) who reported a reduction temperature between -73°C and 150°C for this catalyst. Similar H_2 uptake behaviour was observed with EUROPT-3 at room temperature. Its TPR spectra displayed two large peaks with maxima at 192°C and 395°C (Figure 96b). The TPR profiles of the impregnated catalysts, 0.5% Pt/MoO_3, 0.8% Pt/SiO_2 and 0.8% Pt/Al_2O_3 showed intense single peaks in the low temperature region, with maxima at 144°, 185° and 214°C, respectively, together with broad bands at the high temperature region 300°-550°C (Figures 96a , 96b , 96c . The 144°C peak of the Pt/MoO_3 catalyst is an indication that this catalyst is likely to exist in the form of the bulk H_2 $[PtCl_6]$ (176,179-182).

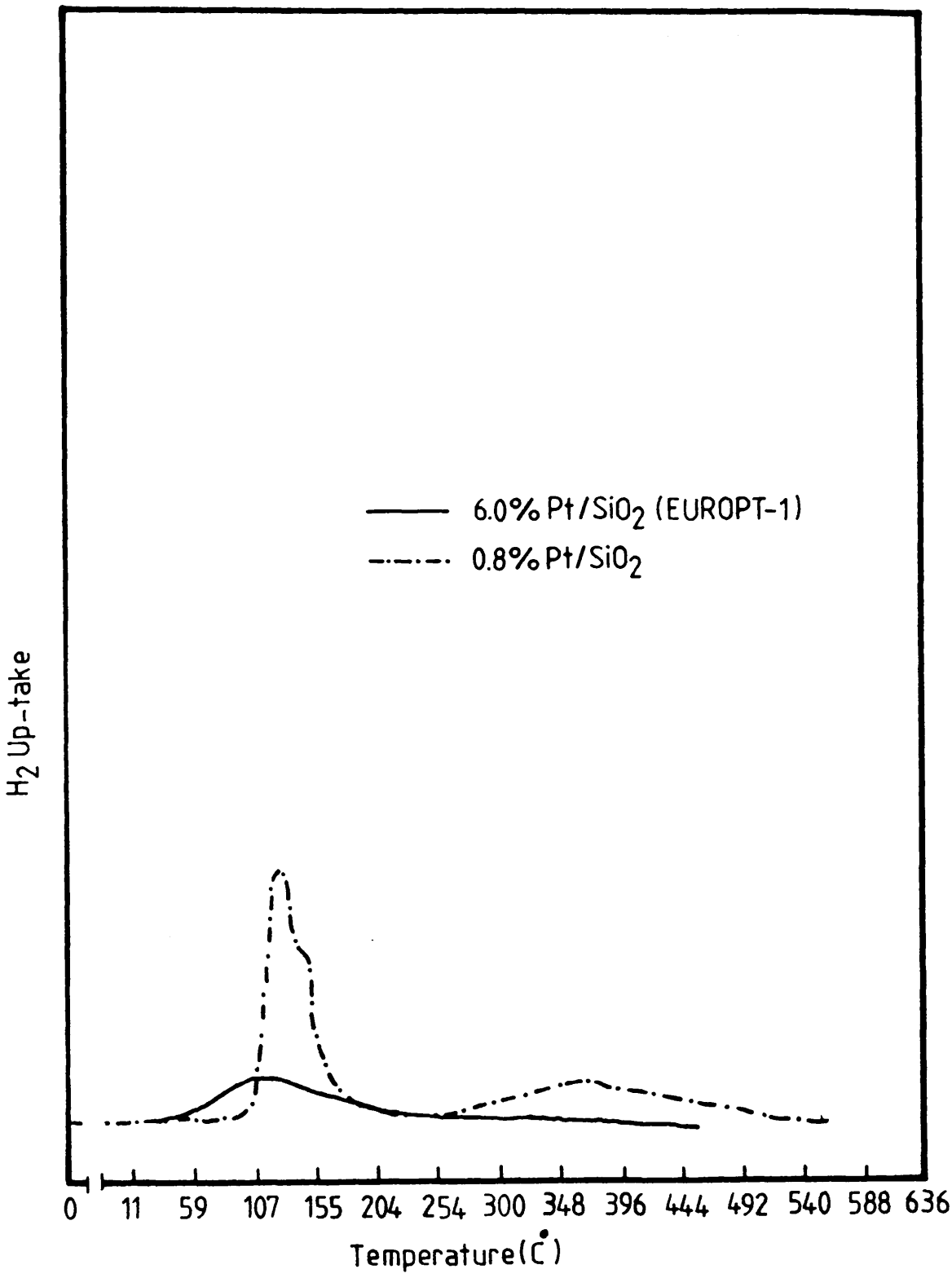

Figure 96a. TPR profiles of Pt-catalysts.

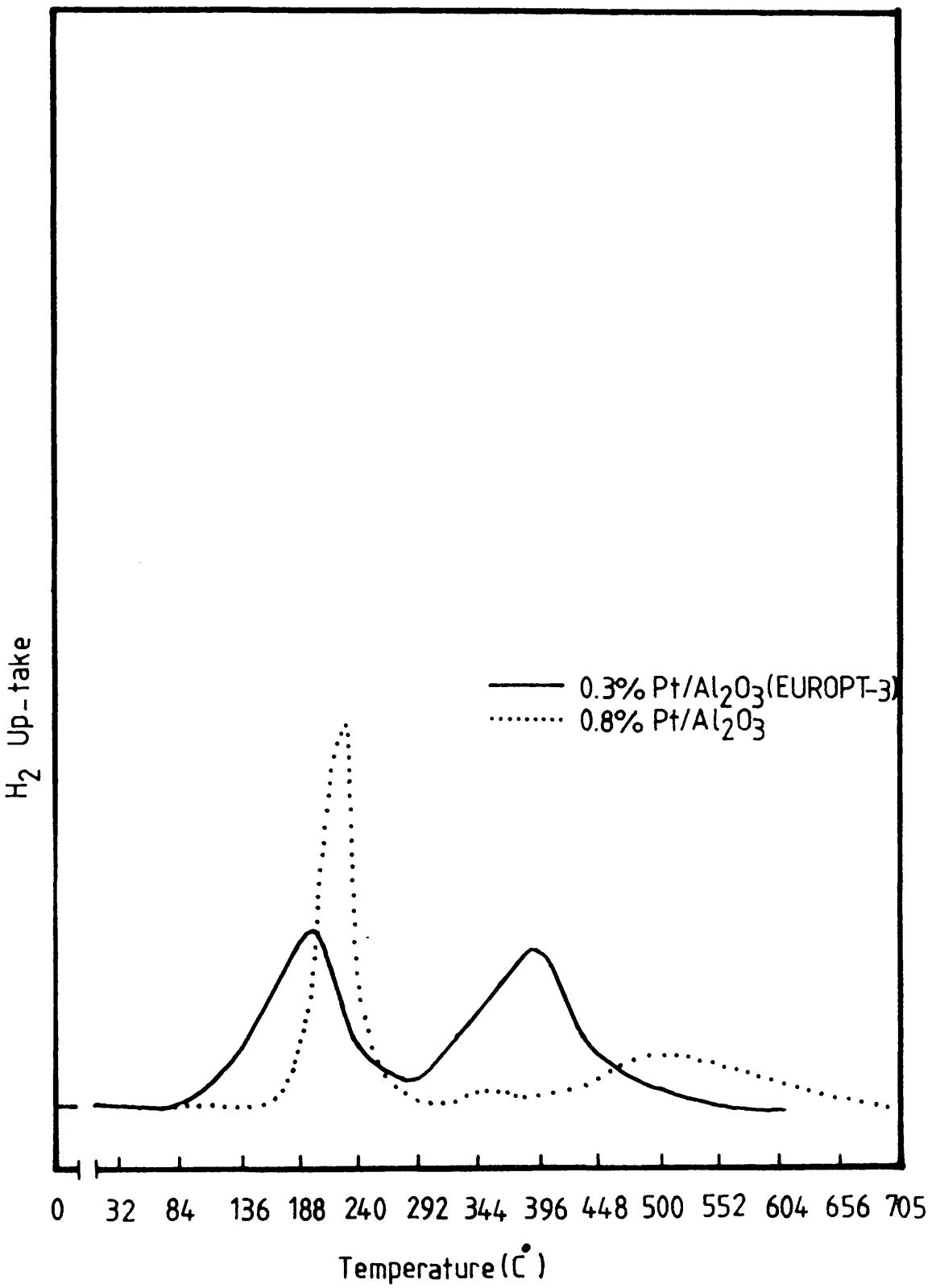

Figure 96b. TPR profiles of Pt-catalysts.

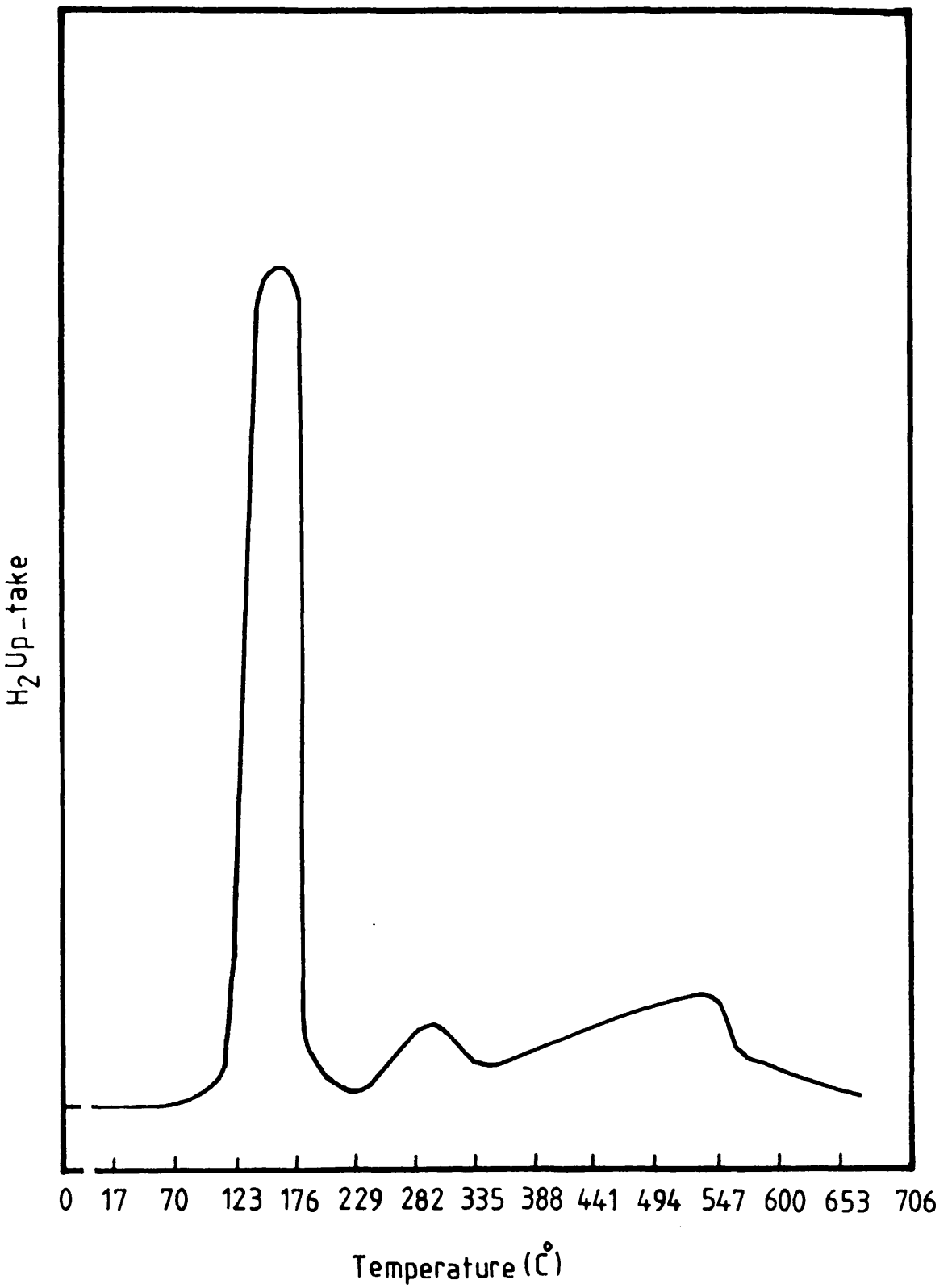

Figure 96c. TPR profiles of Pt/MoO_3 catalyst.

The high temperature bands at > 300°C, are characteristic of the reduction of support materials (189).

11.2 THE ELECTRON MICROSCOPY EXAMINATION OF Pt-CATALYSTS

Samples of EUROPT-1 and EUROPT-3 were examined by transmission and scanning electron microscopy (TEM, SEM) to examine the Pt-particle size and distribution and the effect of hydrocarbon adsorption and hydrogenation on catalyst morphology. The procedures used for the preparation of the catalyst samples for TEM and SEM are described in section 3.8. The Pt-containing particles were imaged on the micrographs as small dark spherical or semi-spherical spots. Ten measurements of ten counts each were used to estimate the average Pt-particle size.

The plates 1-4 show the TEM micrographs of EUROPT-1. Plate 1 is a typical micrograph of the catalyst after it had been reduced in H_2 at 250°C for 2h. From this it can be seen that the Pt-particles are homogeneously dispersed though, in some micrographs, fractions of the Pt-particles are clustered together in the form of aggregates. The particle sizes were calculated as 2.00 ± 0.06 nm, which is consistent with the size range 0.9-3.5 nm, reported by the Council of the Europe Catalysis Group (185). Plate 2 is the TEM of the catalyst after being employed for acetylene hydrogenation. It showed a similar particle size distribution to that of the freshly reduced catalyst (~ 2 nm), indicating that the catalyst is resistant to sintering under the experimental conditions used in this study. However, when EUROPT-1 was used for buta-1,3-diene hydrogenation a growth to the particle size ranging

between 2 and 10 nm was induced. These particles displayed different shapes, vis, spheres, hemi-spheres, squares and hexagonals (Plate 3). The samples of EUROPT-1 which were poisoned with H_2S showed a slight growth in the average particle size from 2.0 to 2.5 nm (Plate 4).

The SEM of the catalyst (Plates 5,6) show the granular morphology of the silica support. No carbon filaments were observed in these or other micrographs of the catalyst in its working condition.

EUROPT-3 also showed an even distribution of Pt-particles after the catalyst had been reduced in H_2 at 250°C for 2h as determined by the TEM. Its particle size was between 3 and 6 nm (Plate 7). The catalyst samples which had been deactivated by a series of acetylene hydrogenation, interestingly displayed carbon filaments in the micrograph (Plate 8).

The SEM micrographs of EUROPT-1 and EUROPT-3 catalysts which had been deactivated to the steady state activity by C_2H_2/H_2 mixtures are shown in Plates 9 and 10.

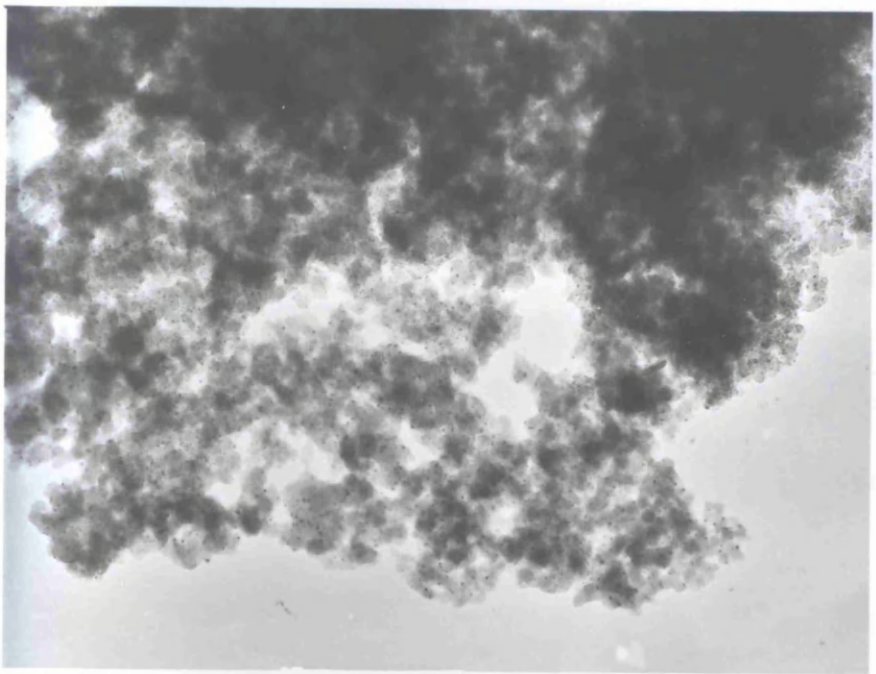

Plate 1. TEM micrograph of EUROPT-1 reduced at 250°C/H_2/2h (x 100 K)

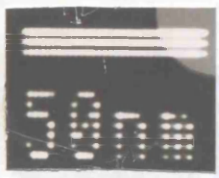

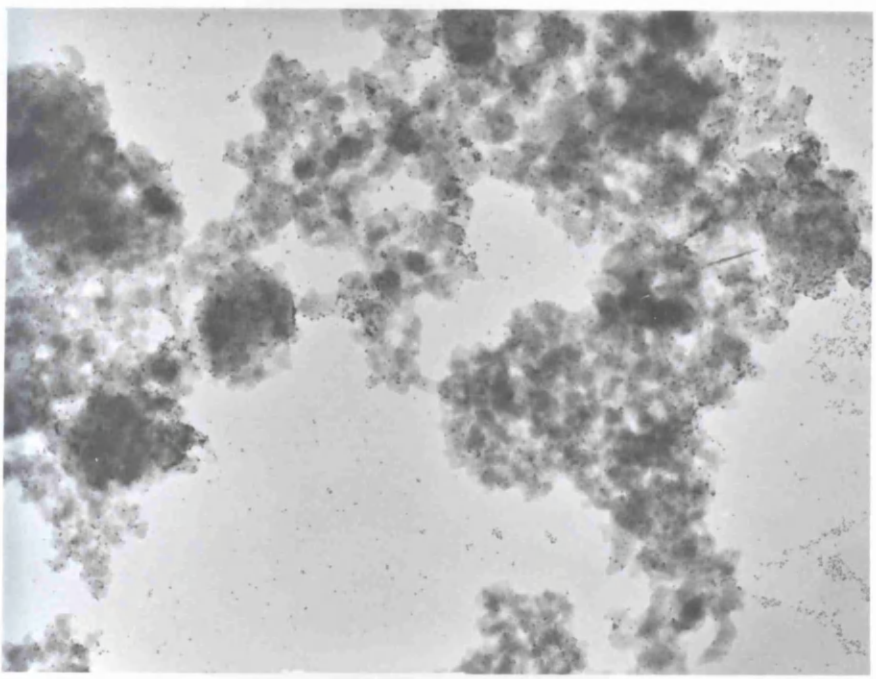

Plate 2. TEM micrograph of EUROPT-1 deactivated with C_2H_2 (x 100 K)

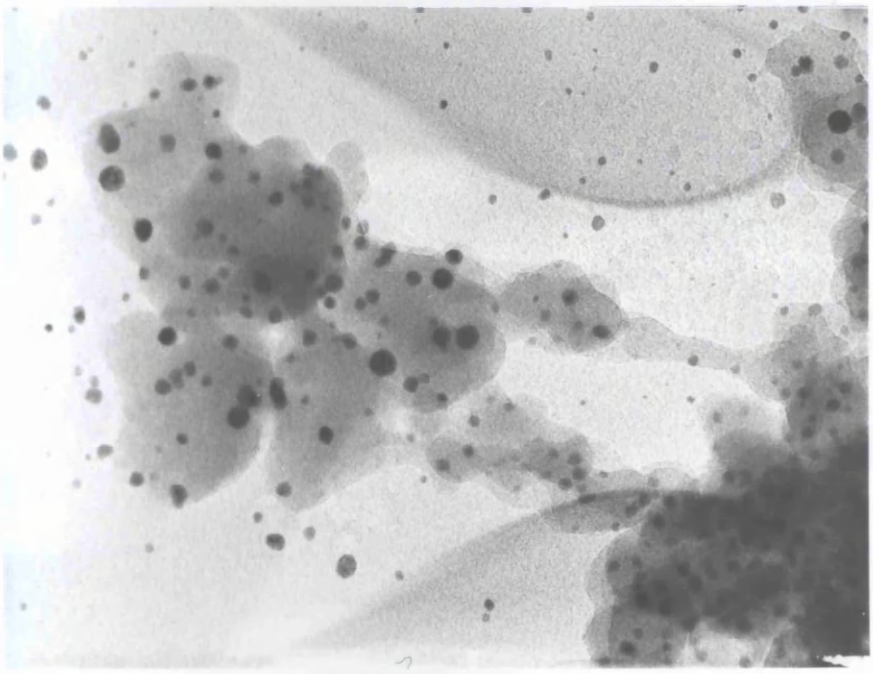

Plate 3. TEM micrograph of EUROPT-1 deactivated with C_4H_6/H_2 (x 200 K)

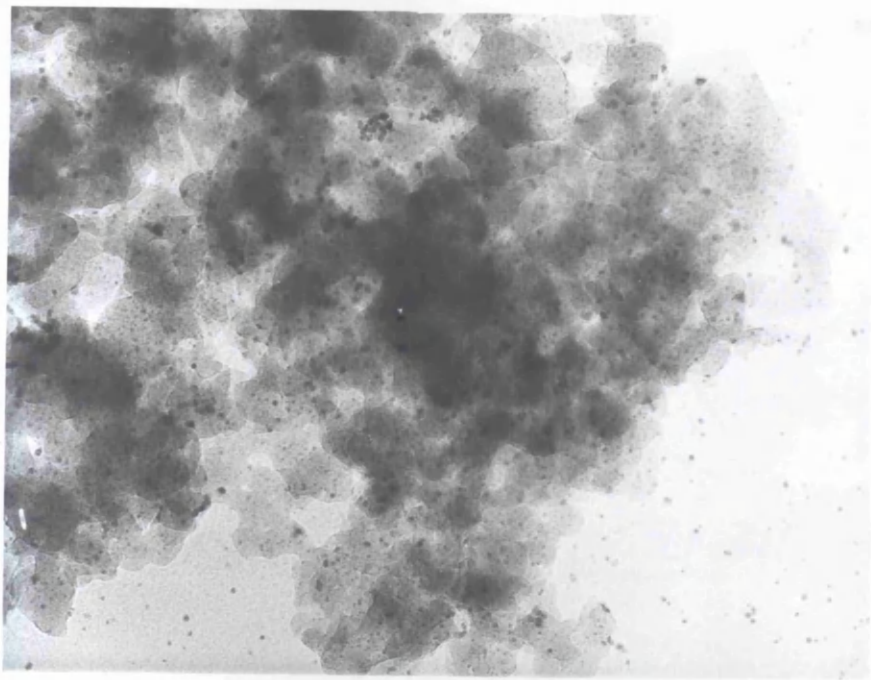

Plate 4. TEM micrograph of EUROPT-1 deactivated with H_2S (x 200 K)

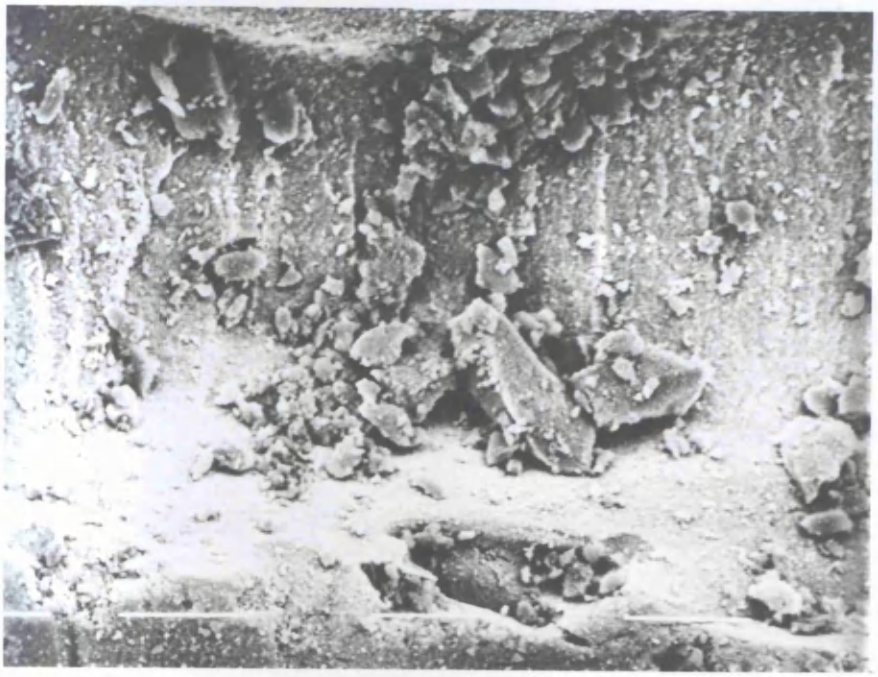

Plate 5. SEM micrograph of EUROPT-1 (x 1.6 K)
(scale = 10 μm)

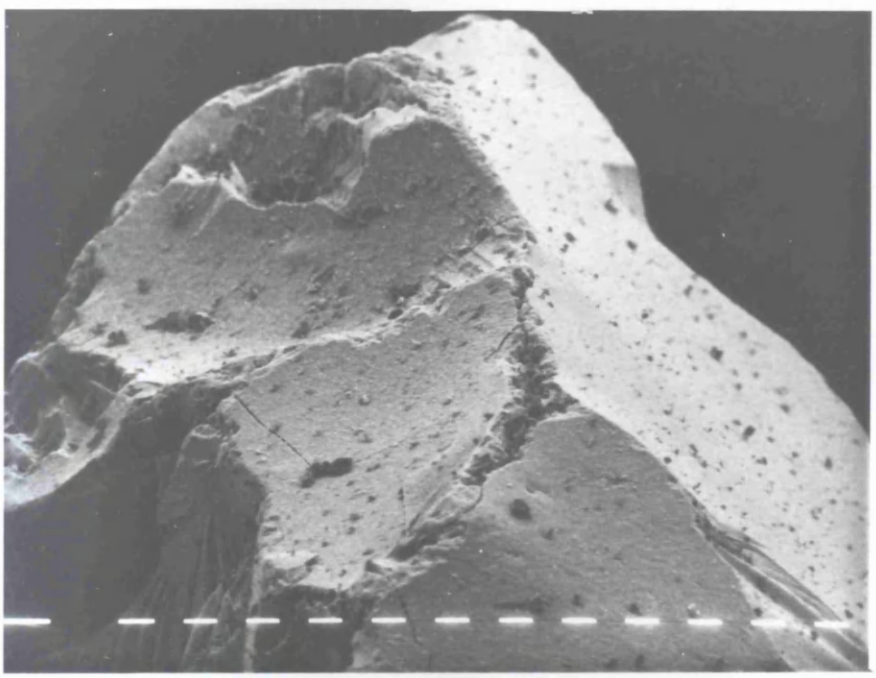

Plate 6. SEM micrograph of EUROPT-1 (x 320 K)
(scale = 10 μm)

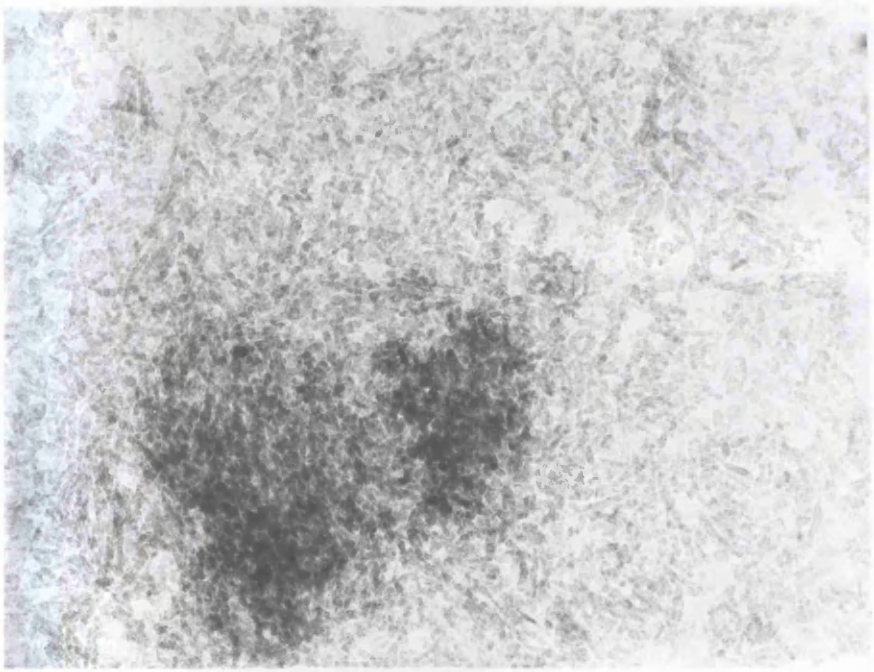

Plate 7. TEM micrograph of EUROPT-3 reduced at 250°C/H_2/2h (x 120 K)

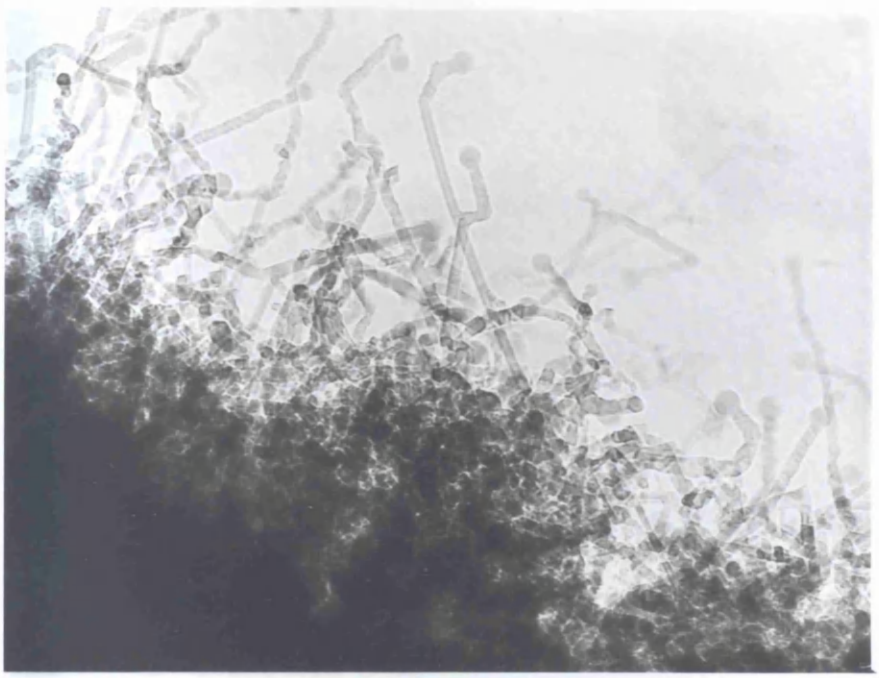

Plate 8. TEM micrograph of EUROPT-3 deactivated with C_2H_2/H_2 (x 120 K)

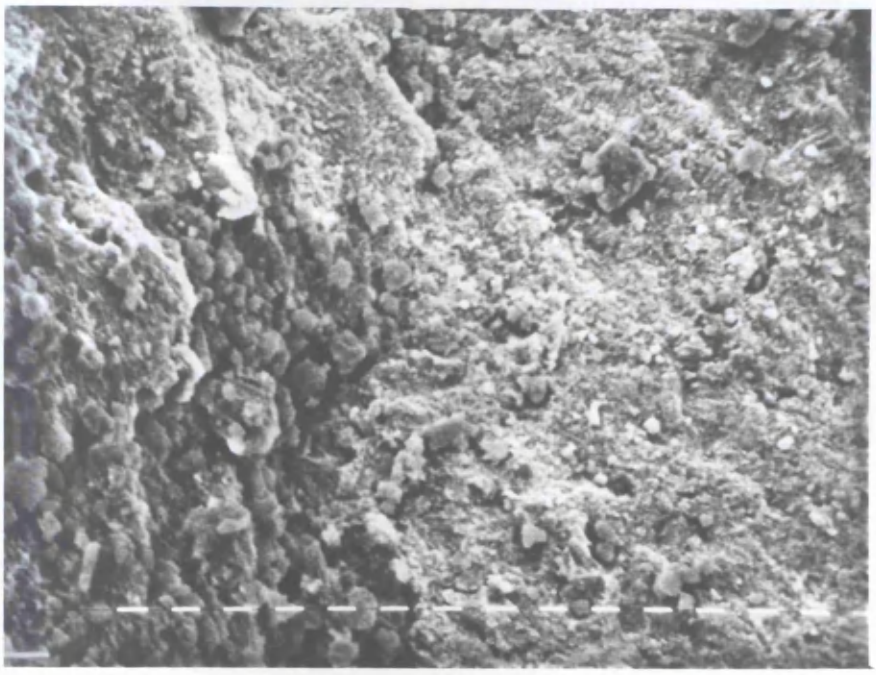

Plate 9. SEM micrograph of EUROPT-3 (x 3.2 K)
(scale = 1 μm)

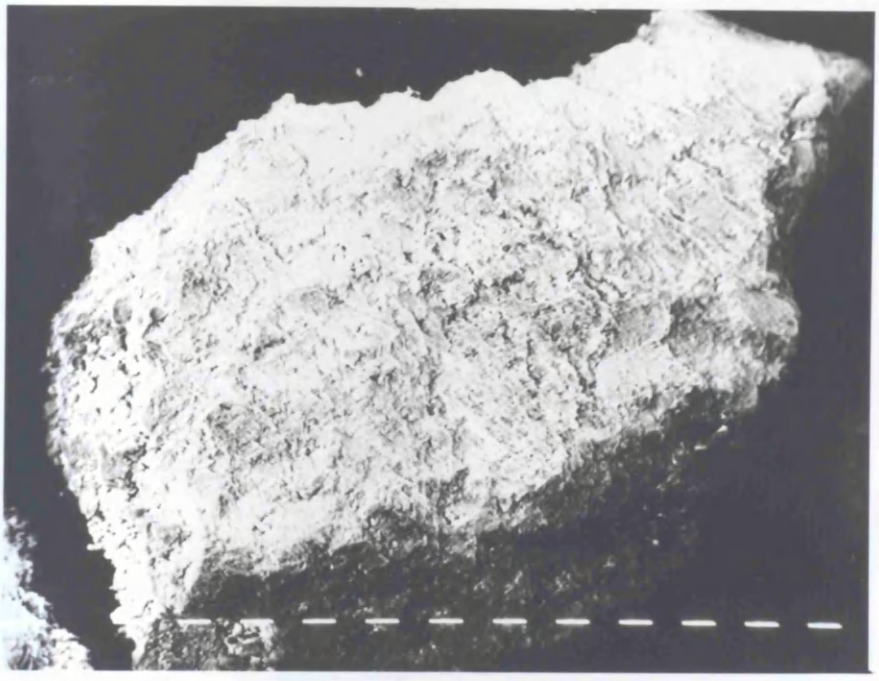

Plate 10. SEM micrograph of EUROPT-3 (x 640 K)
(scale = 10 μm)

SECTION FOUR

DISCUSSION

SECTION FOUR

DISCUSSION

The results presented in Chapters 4-11 show numerous interesting features regarding the adsorption of acetylene, ethylene and carbon monoxide; the hydrogenation of acetylene and buta-1,3-diene; the effects of sulphur poisoning on the adsorption of hydrocarbons and carbon monoxide and on the selectivity of hydrogenation reactions of acetylene and buta-1,3-diene for mono-olefin formation on the Pt-catalysts employed in this work. These, in addition to the results of IR spectroscopy, temperature programmed reduction (TPR) and transmission and scanning electron microscopy (TEM, SEM), will be discussed in detail in the ensuing chapters of the section.

Table 14 shows the relative number of [14-C]-hydrocarbon and carbon monoxide molecules adsorbed in the primary adsorption region on the Pt-catalysts.

CHAPTER TWELVE

THE ADSORPTION OF CARBON MONOXIDE

The adsorption isotherms of carbon monoxide on the catalysts used in this work showed distinct dissimilarities. On EUROPT-1, 0.8% Pt/SiO_2 and 0.8% Pt/Al_2O_3 catalysts, the isotherms (Figures 34, 38) displayed different behaviour from that obtained with the hydrocarbons (acetylene and ethylene) and, interestingly, unlike the expected Langmuir-type CO isotherm for a mono-layer formation, they showed a prolonged secondary region with a positive gradient. The adsorption isotherm of CO on EUROPT-3 (Figure 36) was of a similar shape to the isotherms observed with C_2H_2 and C_2H_4, in which smaller positive gradients for the secondary adsorption regions were observed. However, when EUROPT-3 catalyst was calcined in air at 500°C for 18h, followed by H_2-reduction, the adsorption of CO gave an isotherm of a similar shape to that found with EUROPT-1 (Figure 36). No saturation region was ever observed to occur on these catalysts up to the 5 Torr maximum pressures used in these studies. In contrast, CO adsorption on Pt/MoO_3 exhibited the expected Langmuir-type isotherm in which a saturation plateau was reached, indicative of CO monolayer formation.

Based on the behaviour of CO adsorption on the calcined EUROPT-3 catalyst, the positive gradients of the isotherms observed on the above catalysts suggests that on these catalysts, after reduction and activation, the surface is still partially oxidised, possibly due to interaction of the Pt-particles with water associated with the support material.

This is consistent with the results revealed by the EXAFS spectroscopy conducted by Joyner (121) and the TPR measurements reported (183) by Bond and Gelsthorpe which have indicated that this catalyst is substantially oxidised and contains a disordered Pt-oxide phase. The change in the behaviour of CO adsorption on the calcined EUROPT-3 compared with the uncalcined catalyst can be attributed to the high temperature treatment (500°C, air) which is capable of reducing the high Cl^- content of this catalyst, thus enhancing the possibilities of oxidation of the Pt-particles and increasing the degree of their interaction with the support (Al_2O_3).

From the results in sections 4.3.1.1, 4.3.2.1 and 4.3.3, there is clear evidence that on all the catalysts studied, adsorbed CO exists in two states. One is weakly bound (majority) and can be removed by evacuation or molecular exchange with [12-C]-CO. The other form of CO (~ 15-30%) is more strongly bound to the surface and could not be removed with such treatments from either catalyst.

From the infrared spectroscopic studies (Chapter 10) it is clear that, on each of the catalysts studied, the most abundant CO species at high coverage (~ 4-10 Torr) is adsorbed in the linear form (absorption at 2086 cm^{-1}).

The results of sections 4.3.1.1 and 4.3.2.1 indicate that CO inhibited completely the adsorption of ethylene and to a lesser extent, the adsorption of acetylene, whereas the presence of these hydrocarbons did not prevent completely the CO adsorption. These observations support the postulate that both CO and the hydrocarbons are adsorbed directly on the metal surface and suggesting that, with the hydrocarbon

species are adsorbed on the surface, proportion of the surface sites being left vacant, probably due to geometric restrictions. It is possible, however, that these vacant sites are the active sites for hydrogen adsorption in the hydrogenation reactions.

Although the radiotracer technique does not permit an absolute comparison of the amounts of CO adsorbed on the different catalysts used, nevertheless, it is possible to draw some comparisons regarding the relative number of adsorbed CO molecules and the CO:Pt ratios. From Table 14, the ratio of the number of CO molecules adsorbed on the freshly reduced catalysts to the total number of Pt atoms present, CO:Pt, was found to be, 1.9 (EUROPT-1), 4.0 (EUROPT-3), 0.60 (0.8% Pt/SiO_2), 1.3 (0.8% Pt/Al_2O_3) and 0.3 (0.5% Pt/MoO_3). These values are higher than the reported ratios of 0.60 with EUROPT-1 (98) and of 0.20 (Pt/Al_2O_3) and 0.07 (Pt/SiO_2) reported by Bain et al. (94). From these values, it is clear that there is an overall excess up-take of CO compared with that expected for a (Pt:CO) ratio of unity. Three possible reasons for this can be considered: (i) spillover or adsorption of carbon monoxide on to the support; (ii) an enhanced adsorption of CO in the presence of hydrogen or other species, such as, oxygen, and (iii) a surface reconstruction as the CO adsorption reaches a semi-saturation.

The effect of spillover or adsorption of CO molecules on to the support is unlikely, as has been reported by Kinnaird et al. (96) and as claimed by Levy and Boudart (187), such a phenomenon requires suitable sites on the support.

In studies of co-adsorption of H_2 and CO on Pd and Pt (66, 188) a considerable interaction between the two molecules has been observed to occur, resulting in a shift of the C-O stretching frequencies to higher regions. It has also been reported (43) that Pt-supported catalysts retain considerable quantities of hydrogen which can act as a promotor for carbon monoxide decomposition. However, with regard to EUROPT-1, it has been shown (120) that this catalyst exists in a hydrogen-deficient state under the experimental conditions used (see section 1.7) and hence, such a possibility can be eliminated. Even though EUROPT-1 is of a Pt-O character, rather than as a metallic Pt, the possibility of interaction of CO with oxygen has been investigated (98) and found to have no effect on the IR spectra of adsorbed CO, which is in accordance with the results of the IR studies found in this work (Chapter 10).

The other explanation of the high uptake of CO could be as a result of perturbation of the metal atoms leading to surface reconstruction, probably through migration of the metal atoms in the CO-adlayer. This indeed could be the case since, as observed in this work (Chapter 9) pre-adsorption of sulphur appears to reduce the amount of CO adsorption to give Pt:CO of ~ 1.0. This may be due to the fact that the presence of sulphur stabilises the metal surface to any restructuring similar to that suggested above under the influence of CO alone. The effect of sulphur (H_2S) on the adsorption of CO will be discussed in Chapter 9.

CHAPTER THIRTEEN

THE ADSORPTION OF ACETYLENE AND ETHYLENE

The shape of acetylene adsorption isotherms obtained on the catalysts used in this study (Figures 25, 27, 29) in the pressure range 0-5 Torr, consisted of a steep primary non-linear region, followed (except Pt/MoO_3) by a linear secondary region. No plateau region was observed to occur on these catalysts up to the maximum pressure studied. This is in agreement with the results of Reid et al. (44) and Webb and co-workers (55, 56) on supported Rh, Pd, Ir and Ni catalysts in which primary and secondary adsorption processes were observed to occur with these hydrocarbons. However, the Pt/MoO_3 catalyst showed a non-linear secondary region, which rose sharply as the pressure of C_2H_2 was increased. Even though no specific studies using MoO_3-supported-Pt catalysts have been reported, nevertheless, it is worthwhile considering the possibilities involved in acetylene adsorption on this catalyst. Yashu et al. (186) studied the difference in surface properties between $Pt/MoO_3/SiO_2$ catalysts prepared by different methods. Their results using TPR, ESR and TEM techniques showed that the impregnated catalysts consisted of mixed oxygenated Pt-particles, various molybdenum oxides and a Pt-Mo alloy. The TPR measurements conducted in this work (section 11.1) showed that, on this catalyst a large peak at ~ 144°C accompanied by two broad peaks at 303° and 547°C. It is likely that the low temperature peak corresponds to the reduction of the precursor $H_2[PtCl_6]$ as reported by McNicol et al. (176) and the high temperature peaks may be assigned

to the reduction of the molybdenum oxide species (193). Thus, it is plausible that the primary adsorption region corresponds to the adsorption of C_2H_2 on the Pt-component and that, the secondary region is attributable to adsorption on the molybdenum oxide support.

The adsorption of ethylene on EUROPT-1 and EUROPT-3, also occurred in two stages, but the primary adsorption region showed less adsorption capacity compared with acetylene (ca. 0.25 times that of acetylene) and tended to disappear as the catalysts were brought to their steady-state activity by C_2H_2/H_2 reactions.

When acetylene was adsorbed on the various catalysts, analysis of the gas phase after the build-up of the primary adsorption region showed that with EUROPT-1, ethane and ethylene were present. However, with the other catalysts ethylene was never observed. From the yields of ethane formed, the average composition of the adsorbed hydrocarbon species on the primary region was calculated to be $C_2H_{1.6}$ (EUROPT-1) and $C_2H_{1.8}$ (EUROPT-3). These observations suggest that a range of adsorbed species is present on these catalysts as a result of an extensive dissociation of the C-H bonds. This in turn can lead to two possible processes which may occur independently on the catalyst surface; (i) an extensive dissociation of the adsorbed species to yield multiply bonded species of the form $\underset{**}{C} = CH_2$, $\underset{**}{C} - CH_3$ or $\underset{***}{C} - CH_3$. This latter species has been detected by the IR analysis of adsorbed acetylene and ethylene on EUROPT-1 (Figure 90) in this work and was reported by Ibach et al. (35) and Kesmodel et al. on Pt(111) surface. Consequently, the amount of hydrogen released, together with any hydrogen already present following the reduction process may

react with these species to produce ethane and ethylene; (ii) the dissociated species may react with an adsorbed acetylene or ethylene molecule leading to the deposition of polymeric species on the catalyst surface.

When the primary adsorption region was selectively labelled with [14-C]-acetylene (section 4.1.1.1) or [14-C]-ethylene (section 6.7), followed by a C_2H_2/H_2 hydrogenation reaction, a fraction (ca. 10-20%) of these pre-adsorbed species were permanently retained on the surface, probably as polymeric moieties as suggested above.

With the catalysts at their steady-state activity, the extent of the primary adsorption region was remarkably reduced, 85-90% (acetylene) and 80-85% (ethylene) on both EUROPT-1 and EUROPT-3 catalysts. This clearly is an indication that the steady-state corresponds to the attainment of a steady-state concentration of a strongly retained species with ~ 10-15% of the sites located in the primary region being left vacant, probably due to geometrical restrictions. This is in accordance with the statistical prediction of Campbell and Thomson (171) that, for a random 2-site adsorption, 7% of the metal atoms remain vacant as a single site.

The results of sections 5.1 and 6.1 indicated that the deactivation can only effectively be achieved by treating the catalysts with C_2H_2/H_2 mixtures. When acetylene alone was admitted to the catalysts no deactivation was observed, suggesting that hydrogen is in some way a partner for the deactivation process. Sheppard and Ward (52) from their IR studies of acetylene adsorption in the presence of hydrogen showed that, with various supported metals, surface polymeric species

were formed, although these species were absent when no hydrogen was present on the catalyst surface. This supports the above suggestion that the primary adsorption region consisted of a range of polymeric species of which some may undergo further dissociation, some may be involved in surface polymerisation reactions and others may be active as a hydrogen transfer species. Evidence for such a polymeric species has also been obtained in the IR studies conducted in this work (Chapter 10) when catalyst samples had been deactivated by C_2H_2/H_2 mixtures, bands attributable to CH_3 and CH groups were observed (Figure 92).

Assuming that carbon monoxide adsorption occurs on the exposed metal atoms on the surface, the results of Table 14 show that the relative amounts of adsorbed CO and those of C_2H_2 and C_2H_4 are in the approximate ratios, $CO:C_2H_2$, 1:1 (EUROPT-1), 1.5:1 (EUROPT-3), 15:1 (0.8% Pt/SiO_2), 4.7:1 (0.8% Pt/Al_2O_3) and 0.6:1 (0.5% Pt/MoO_3), with the $CO:C_2H_4$ ratio being 1.8:1 (EUROPT-1) and 7:1 (EUROPT-3). With reference to the adsorption isotherms of CO obtained on these catalysts (Figures 34, 36, 38) and those reported on Rh, Ir, Pd supported catalysts (44, 55, 56), the above CO:hydrocarbon ratios suggest that, the primary adsorption region of these hydrocarbons occur directly on the metal surfaces and the turning point observed in the adsorption isotherms corresponds to monolayer coverage.

From Table 14 and the relevant adsorption isotherm, the adsorptive capacity of EUROPT-1 for acetylene is approximately eight times that for ethylene, compared with a corresponding value of five on EUROPT-3. Furthermore, the extent of retention of the pre-adsorbed species is greater with acetylene than with ethylene. This shows that

there are a large number of sites on these catalysts which are active for acetylene adsorption than for ethylene adsorption, which is consistent with the early observations of Sheridan et al. (122, 123) on Pt-supported catalysts.

With reference to the adsorption isotherms of acetylene and ethylene on freshly reduced catalysts (sections 4.1.1, 4.1.2), it can be seen that at high gas pressures of ~ 5 Torr (~ 1 x 10^4 counts min^{-1}), the amount of adsorbed hydrocarbons is in excess of that adsorbed on the primary adsorption region. Hence, higher ratios of hydrocarbon molecules to the total number of metal atoms are observed. It is also noticeable that in all the subsequent adsorption isotherms (2nd, 3rd,..., adsorptions) determined after the evacuation of the catalysts for 30 min, the extent of the primary adsorption region remained unchanged, bearing in mind that the count rates of these isotherms were corrected for the background activity resulting from the previous adsorption isotherm. The amounts of hydrocarbons removed by either of the treatments, evacuation, H_2, C_2H_2 or C_2H_2/H_2 correspond to an amount of radioactivity equivalent to the secondary region. These observations suggest that the adsorbed species in this region are reactive, which is in agreement with the conclusions of Webb and co-workers (55, 59, 95) that these species are associatively adsorbed on the surface and represent the catalytically active species in the hydrogenation reactions.

In section 4.1.1.4, the co-adsorption of acetylene and ethylene on freshly reduced catalysts was investigated. It was found that acetylene adsorbed in the presence of ethylene, though the adsorption was likely to be weakly in its nature, as ~ 90% of the pre-adsorbed

acetylene was removable by 30 min evacuation. However, ethylene did not adsorb in the presence of acetylene. These findings are an indication that both adsorbates are adsorbing in the same active site of adsorption and that the thermodynamic factor is likely to operate.

The question remains as to the nature of process(es) accompanying the gradient change of the isotherms in the secondary adsorption region. There are three possibilities which have been considered previously (44, 55) and these can be summarised as follows:

a) As the surface reaches a saturation level of adsorption by the hydrocarbon, the adsorption process continues to take place on the support material.

b) The turning point of the adsorption isotherms corresponds to the spillover of the hydrocarbons to the support.

c) The hydrocarbon adsorption process in the secondary region occurs over the dissociatively adsorbed hydrocarbon species of the primary region (overlayer formation).

In their studies Al-Ammar and Webb (55) investigated the phenomenon of hydrocarbon spillover in detail. They treated their catalysts with hexamethyl disilazane to cover the support surface with tri-methylsilyl groups. The extent of the hydrocarbon secondary region was identical to that on the untreated catalysts. Hence, the possibilities of adsorption or spillover of the hydrocarbons to the support were eliminated and a hydrocarbon overlayer formation mechanism was suggested.

However, from the present studies of acetylene and ethylene adsorption on sulphur poisoned catalysts, the results (discussed in Chapter 14) point to a surface reconstruction mechanism as being the likely reason for the turning point in the adsorption isotherms.

CHAPTER FOURTEEN

THE ADSORPTION OF HYDROGEN SULPHIDE (H_2S)

The adsorption of [35-S]-H_2S on EUROPT-1 showed an isotherm (Figure 80), similar in its shape to those obtained with [14-C]-hydrocarbons, in which two adsorption processes were observed. A plateau region was observed to occur at high pressure (ca. 20 Torr). Evacuation of the catalyst for 30 min removed ~ 5% of the pre-adsorbed sulphur species. Pre-deactivation of the catalysts with C_2H_2/H_2 mixtures reduced the extent of H_2S primary adsorption region. These observations suggest that sulphur is adsorbed on the metal surface and are an indication that the adsorption process is partially reversible.

The adsorption of acetylene and ethylene on the sulphur poisoned EUROPT-1 catalysts was found to be considerably suppressed as compared with that on sulphur-free catalysts. The effect was remarkably pronounced in the secondary adsorption region (Figures 81, 82). Evacuation of the catalysts for 30 min, resulted in the removal of the hydrocarbon species adsorbed in this region. At high sulphur coverages, ca. $\Theta_{H_2S} > 0.5$, a continuous drop in the surface count rates was observed to occur, suggesting the occurrence of an interaction between the pre-adsorbed sulphur and the hydrocarbon molecules. These results provide evidence to suggest that a surface reconstruction process takes place as a result of sulphur adsorption, thus limiting the extent of adsorption of C_2H_2 and C_2H_4 to the exposed metal sites left vacant, probably as electron deficient sites. They also provide evidence

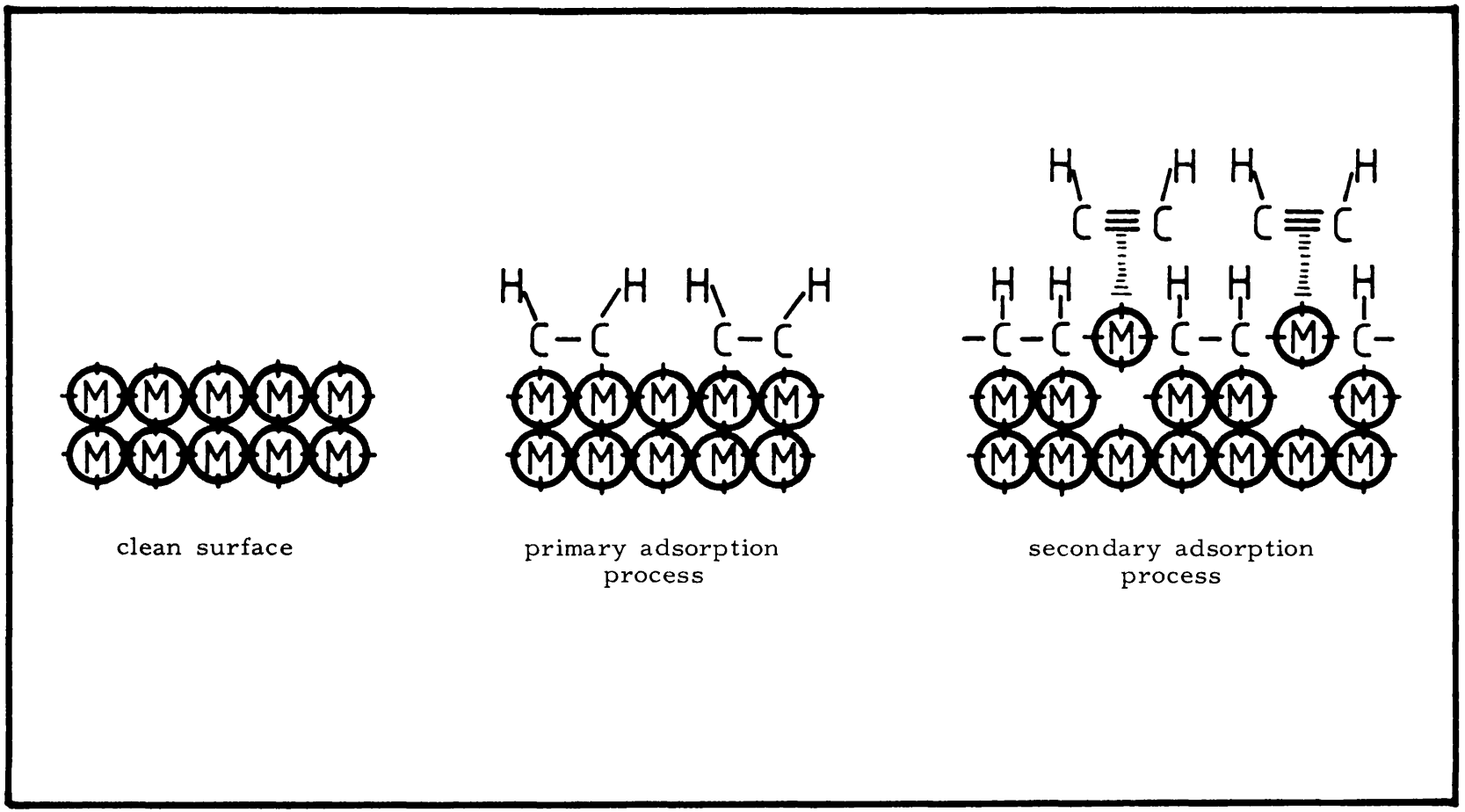

Figure 97. The proposed mechanism of surface reconstruction process.

concerning the secondary adsorption regions observed in the hydrocarbon adsorption isotherms. It is likely that the turning point of these isotherms corresponds to a surface reconstruction process involving the migration of the metal atoms, left vacant at the surface after completion of the primary adsorption process, to form an array with the hydrocarbonaceous residues, as depicted in Figure 97. Hence, the enhancement of C_2H_2 and C_2H_4 adsorption due to the secondary adsorption process which takes place on these modified sites.

The adsorption of C_2H_2 and C_2H_4 on the sulphur-poisoned EUROPT-3 catalysts showed that the extent of the primary adsorption region disappeared completely with a sharp increase in the uptake of these hydrocarbons as their pressures were increased. It is likely that sulphur has completely poisoned the metallic sites of this catalyst whilst, at the same time promoting some adsorption of the hydrocarbons on the support material.

The results presented in Figure 83 show interesting and important differences between the adsorption of CO on freshly reduced and S-poisoned catalysts. At low sulphur coverages, $\Theta_{H_2S} < 0.5$, the adsorption isotherms showed similar shapes to that observed on the clean catalyst, in the sense that the adsorption continued to increase as further CO was admitted to the reaction vessel. At $\Theta_{H_2S} > 0.5$, the CO isotherm showed significantly different behaviour. The surface count rate increased rapidly with increasing the gas pressure until a plateau region was observed (Langmuir type isotherm). These results are also consistent with the suggestion stated above that, in the presence of sulphur, a surface reconstruction process takes place on the catalyst. Such a phenomenon has also been proposed by Somorjai (151).

CHAPTER FIFTEEN

THE REACTION OF ACETYLENE WITH HYDROGEN

The hydrogenation of acetylene over EUROPT-1, EUROPT-3, 0.8% Pt/SiO_2 and 0.8% Pt/Al_2O_3 using a reactant ratio of 3::1 $H_2:C_2H_2$ at room temperature was found to occur in two distinct stages. The onset of the second stage was accompanied by an acceleration in the reaction rate. Plots of $\ell n\ (P_o + \Delta P)$ against time showed that the reaction was first order in total pressure. In the first stage ethylene and ethane were produced, whilst the major process occurring in the second stage was the further hydrogenation of ethylene to ethane. The selectivity was found to remain almost constant as the reaction proceeded. Deactivation of these catalysts with C_2H_2/H_2 mixtures resulted in a progressive decrease in the reaction rate until a steady state activity was achieved. However, treatment of these catalysts with 100 Torr H_2 for 15h resulted in a partial restoration of the original activity. No appreciable reaction between C_2H_2 and H_2 was observed to occur on the 0.5% Pt/MoO_3 catalyst.

The shapes of the pressure-time curves (Figures 39, 54(a), 65), together with the observation that the selectivity remains constant or nearly so until the acceleration point is reached, is an indication that the selectivity for ethylene formation is governed by a thermodynamic factor. Further evidence for the existence of the thermodynamic factor has also been obtained (sections 4.1.1.5, 4.2.2), when no adsorption of ethylene was observed in the presence of acetylene, whilst, acetylene

adsorption took place in the presence of gas ethylene. Such observations make the assumption that the same sites are involved in both acetylene and ethylene adsorption.

The kinetics of acetylene hydrogenation showed a negative order in acetylene and a positive order in hydrogen. This suggests that C_2H_2 was the more strongly adsorbed reactant and that its surface coverage was high, whereas, H_2 was weakly adsorbed and its surface coverage was consequently low. With both EUROPT-1 and EUROPT-3, the decrease in the acceleration point, $-\Delta P_a$, with increasing H_2 pressure is further evidence to suggest that this reactant is weakly adsorbed and unable to compete with acetylene for the adsorption sites, hence, as its initial pressure is increased, an acceleration in the overall reaction rate occurs. The earlier appearance of $-\Delta P_a$ with increasing temperature may have been caused by the decrease in acetylene coverage in the surface and consequently its hydrogenation becomes more pronounced. The increase in the selectivity of ethylene formation with increasing reaction temperature can be related to either (i) a decrease in the surface coverage of hydrogen as the temperature is raised, or (ii) the activation energy of ethylene desorption is higher than its hydrogenation. The activation energy values of 45.15 kJ mol^{-1} (EUROPT-1) and of 40.66 kJ mol^{-1} (EUROPT-3) are in accordance with the value of 38.91 kJ mol^{-1} reported by Bond and Wells (124) on Pt/Al_2O_3 catalyst.

The results presented in sections 5.6 and 6.6 show that, while the hydrogenation of [14-C]-C_2H_2 occurred simultaneously as the reactants were introduced to the freshly reduced catalysts, the reaction on the steady state catalysts showed distinctly different behaviour in

that it led to a continuous build-up of [14-C]-hydrocarbon species, possibly via an exchange mechanism with the [14-C]-hydrocarbon species. present on the catalyst surface.

Figure 50 shows that when a sample of EUROPT-1 was covered with ~ 5 Torr [14-C]-C_2H_2 or -C_2H_4, followed by a 1:3::C_2H_2:H_2 reaction, the pre-adsorbed species underwent hydrogenation. This provides further support to the conclusions presented in Chapter 13, that the catalysis process is associated with the species adsorbed in the secondary adsorption region.

The results presented in Figure 62 show that, during the hydrogenation of acetylene with hydrogen in the presence of added [14-C]-ethylene, C_2H_4 underwent adsorption-desorption cycles. This is confirmation of the phenomena described above and in section 4.1.1.4 and section 4.2.2 in which acetylene and ethylene are competing for the same adsorption sites with the former being more strongly adsorbed.

Assuming that the [12-C]-ethylene formed by the hydrogenation of acetylene behaves in the same manner as the added [14-C]-ethylene, the amount of [14-C]-ethane which was formed via the gas phase intermediate [12-C]-ethylene can be calculated according to the scheme:

$$^{12}C_2H_2 \xrightarrow{+2H} {}^{12}C_2H_4\ (ads.) \begin{cases} \rightarrow C_2H_4\ (g) \\ \xrightarrow{+2H} C_2H_6\ (g) \end{cases}$$

$$^{14}C_2H_4(g) \longrightarrow {}^{14}C_2H_4\ (ads.) \xrightarrow{+2H} {}^{14}C_2H_6\ (g)$$

Hence, by subtracting the amount of [12-C]-ethane formed via the hydrogenation of [12-C]-ethylene from the total yield of [12-C]-ethane, the amount of [12-C]-ethane formed directly can be obtained (Table 3 (EUROPT-1) and Table 5 (EUROPT-3)). From these results, it was possible to calculate the "inherent"selectivity (S'), which is defined as,

$$S' = \frac{P_{C_2H_4}}{P_{C_2H_4} + P^*_{C_2H_6}}$$

where $P^*_{C_2H_6}$ is the amount of ethane produced directly. It is important to note that the inherent selectivity (S') followed a similar pattern of behaviour to the selectivity (S), in that it remained almost constant as the reaction proceeded to about 100% conversion.

It is apparent from Figures 51 and 63 that the hydrogenation of [14-C]-ethylene took place in two distinct stages. In the first stage, up to ~ 100% conversion on EUROPT-3, the yield of [14-C]-ethane was almost constant as the reaction proceeded, indicating that the hydrogenation of [14-C]-ethylene proceeded independently of the amount of acetylene present in the reaction vessel. The second stage (> 100% conversion) which corresponds to the acceleration in the pressure drop curves, showed a rapid increase in the yield of [14-C]-ethane.

From the above results, two interesting features emerge. First, the yield of [14-C]-ethane only constituted a small proportion of the total ethane yield. Secondly, it was possible to hydrogenate [14-C]-ethylene in the presence of acetylene, that is, there are fractions of sites

on the catalyst surfaces active for ethylene hydrogenation, even in the presence of acetylene. This is an indication of the existence of the mechanistic factor to govern the selectivity of ethylene formation. It is important to point out that, whilst it was concluded in Chapter 13 that acetylene and ethylene are competing for the same active site with acetylene preventing ethylene in the adsorption process when both the adsorbates co-exist on the catalyst, the above observation of ethylene undergoing hydrogenation in the presence of acetylene suggests that the third variable in the system, namely, hydrogen, in some way aids the adsorption of ethylene on a fraction of the hydrogenation sites. It is also clear from Tables 3 and 5 that the predominant reaction pathway to ethane is a direct route from acetylene, rather than via ethylene as an intermediate.

The above findings are in general agreement with the model proposed by Al-Ammar and Webb (59) for the selective hydrogenation of acetylene on supported Pd, Rh and Ir catalysts involving separate sites for the conversion of acetylene to ethylene and ethane, and for ethylene to ethane.

The following reaction pathways are possible for acetylene hydrogenation on the supported-Pt catalysts used in this work.

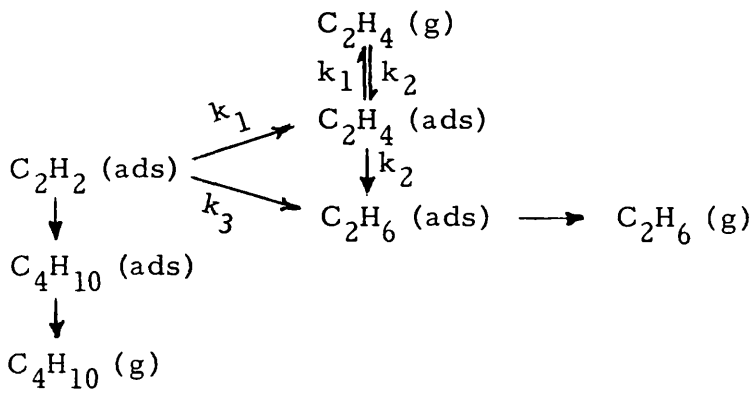

Using the data obtained in Tables 3 and 5, and Figures 53 and 64, the relative values of the reaction rate constants, k_1, k_2 and k_3 in the above reaction scheme could be evaluated quantitively by applying the same method as that used by Berndt et al. (56). Considering that 200% conversion represents complete hydrogenation of acetylene to ethane, the amount of hydrocarbon present at any stage of the reaction can be estimated using equations of the form $\frac{dB}{dH} = k_1 - k_2$, therefore

$$A = A_o - (k_1 + k_3) H \qquad (1)$$

$$B = B_o + (k_1 - k_2) H \qquad (2)$$

$$C = C_o + (k_2 + k_3) H \qquad (3)$$

where A, B and C are the amounts of C_2H_2, C_2H_4 and C_2H_6 respectively. The amount of added [14-C]-ethylene present at any stage of the reaction (B^*) is governed by its dilution with the amount of ethylene formed from the hydrogenation and by conversion to ethane. Thus,

$$B^* = B_o^* - k_2 [B^*/(B^* + B)] H \qquad (4)$$

Substituting equation (2) in equation (4) gives

$$B^* = B_o^*[(B_o + k_1H - k_2H)/(B_o + k_1H)] \qquad (5)$$

Using the results of Figures 53 and 64, where various pressures of [14-C]-ethylene were added at the start of the reaction, the values of $k_1 + k_3$,

Table 8. Distribution of C_2-products from the Hydrogenation of 12.5 torr of Acetylene in the presence of Added* [^{14}C] Ethylene on 0.0947g steady state 6% Pt/SiO_2 (Europt-1) catalyst.

P_{H_2} = 37.5 Torr

Temperature = 20 ± 2°C

Added* $^{14}C_2H_4$ (torr)	(%) conversion	$P_{^{12}C_2H_6}$ (torr)	$P_{^{12}C_2H_4}$ (torr)	$P_{^{12}C_2H_2}$ (torr)	$^{14}C_2H_4$ counts min^{-1}	$k_1 + k_3$	$k_1 - k_2$	$k_2 + k_3$
2*	5.13	0.2452	0.1209	12.09	2384	0.0799	0.0236	0.0478
-	41.34	1.8794	0.5205	8.00	2334	0.1089	0.0126	0.0455
-	83.70	2.5127	1.0154	3.50	2144	0.1075	0.0121	0.0300
-	147.40	5.5864	2.4400	1.09	1813	0.0774	0.0166	0.0379
-	181.90	8.9407	0.4861	0.60	1017	0.0654	0.0027	0.0492
4*	13.00	0.4700	0.1587	10.46	4881	0.1569	0.0122	0.0362
-	45.70	1.7090	0.6401	7.04	4761	0.1195	0.0140	0.0374
-	99.80	4.5678	1.2669	4.60	4420	0.0792	0.0127	0.0458
-	180.00	6.0705	0.7511	0.68	3500	0.0657	0.0042	0.0337
-	184.50	6.8382	0.0655	0.45	2136	0.0653	0.0004	0.0371

Table 9. Distribution of C_2-products from the Hydrogenation of 12.5 torr of Acetylene in the presence of Added* [^{14}C] Ethylene on 2.0345g steady state 0.3% Pt/Al_2O_3 (Europt-3) catalyst.

P_{H_2} = 37.5 Torr Temperature = 20 ± 2°C

Added* $^{14}C_2H_4$ (torr)	(%) conversion	$P_{^{12}C_2H_6}$ (torr)	$P_{^{12}C_2H_4}$ (torr)	$P_{^{12}C_2H_2}$ (torr)	$^{14}C_2H_4$ counts min^{-1}	$k_1 + k_3$	$k_1 - k_2$	$k_2 + k_3$
1*	5.0	0.144	0.326	11.54	5581	0.192	0.065	0.029
-	20.0	0.319	1.382	8.24	5311	0.213	0.069	0.016
-	41.91	0.818	2.506	6.54	5083	0.143	0.060	0.019
-	75.86	1.235	4.019	3.30	4555	0.121	0.053	0.016
-	91.20	1.894	4.956	2.74	3950	0.107	0.054	0.021
-	141.50	3.444	2.601	0.66	2258	0.084	0.018	0.024
-	192.60	8.028	0.602	0.18	463	0.064	0.003	0.042
2*	13.12	0.157	0.958	8.60	10874	0.297	0.073	0.012
-	45.04	0.3577	2.794	4.73	9452	0.173	0.062	0.008
-	93.03	1.5916	3.956	2.31	8411	0.109	0.043	0.017

Table 9.(contd.)

Added* $^{14}C_2H_4$ (torr)	(%) conversion	$P_{12}C_2H_6$ (torr)	$P_{12}C_2H_4$ (torr)	$P_{12}C_2H_2$ (torr)	$^{14}C_2H_4$ counts min^{-1}	$k_1 + k_3$	$k_1 - k_2$	$k_2 + k_3$
2*	113.68	1.8472	4.304	1.070	7823	0.101	0.038	0.016
-	127.11	2.2950	4.491	0.710	6878	0.093	0.035	0.018
-	197.59	7.9903	0.0660	0.082	463	0.063	0.003	0.040
5*	10.85	0.1573	0.725	8.700	21188	0.350	0.067	0.014
-	33.82	0.8030	1.510	6.900	19677	0.166	0.045	0.024
-	65.35	1.3376	3.100	4.400	19838	0.124	0.047	0.020
-	90.81	1.9803	3.640	2.750	18481	0.107	0.040	0.022
-	105.59	2.0870	4.068	1.650	18008	0.103	0.039	0.019
-	168.91	6.0164	1.147	0.640	6902	0.070	0.007	0.036
-	189.67	6.4410	0.3610	0.180	2630	0.065	0.002	0.034

$k_1 - k_2$, $k_2 + k_3$ can be deduced at any stage of the reaction on both catalysts, as shown in Table 8 (EUROPT-1) and Table 9 (EUROPT-3). From these results the relative values of the rate constants k_1, k_2 and k_3 for acetylene hydrogenation on these catalysts at room temperature can be calculated. These values, summarised in Tables 10 and 11, lead to the conclusion that $k_1 < k_3 >> k_2$, that is, the major route in the reaction is via the direct route from C_2H_2 to C_2H_6.

Table 10. Reaction rate constants of C_2H_2/H_2 on EUROPT-1 at 20°C

% Conversion	k_1	k_2	k_3
43.5 ± 2.2	0.014 ± 6.0%	0.001 ± 4.0%	0.101 ± 4.0%
91.6 ± 8.0	0.014 ± 3.0%	0.002 ± 8.0%	0.079 ± 1.5%
183.2 ± 1.3	0.002 ± 4.8%	0.001 ± 3.0%	0.064 ± 1.3%

Table 11. Reaction rate constants of C_2H_2/H_2 on EUROPT-3 at 20°C

% Conversion	k_1	k_2	k_3
12.0 ± 1.5	0.071 ± 4.2%	0.001 ± 0.5%	0.235 ± 4.0%
43.5 ± 1.5	0.070 ± 4.3%	0.008 ± 6.0%	0.090 ± 8.0%
91.9 ± 1.1	0.052 ± 9.0%	0.010 ±10.0%	0.057 ± 7.0%

The results of section 9.5 show that the effect of sulphur poisoning on the selectivity of the catalysts for ethylene formation in the hydrogenation of acetylene was beneficial for the alumina-supported

Table 12. Distribution of C_2-products from the Hydrogenation of 12.5 torr of Acetylene in the presence of 2 torr (Θ_{H_2S} = 0.01), 4 torr (Θ_{H_2S} = 0.20), and 5 torr (Θ_{H_2S} = 0.3) Added [14-C] Ethylene on $H_2{}^{35}S$ poisoned 0.2333g Pt/SiO_2 (Europt-1) catalyst.

P_{H_2} = 37.5 Torr Temperature = 20 ± 2°C

Θ_{H_2S}	(%) conversion	$P_{12}C_2H_6$ (torr)	$P_{12}C_2H_4$ (torr)	$P_{12}C_2H_2$	$^{14}C_2H_4$ counts min^{-1}	$k_1 + k_3$	$k_1 - k_2$	$k_2 + k_3$
0.01	4.25	0.0828	0.3630	12.000	9671	0.118	0.085	0.019
-	10.51	0.4608	0.2460	10.400	8827	0.199	0.023	0.044
-	20.50	0.8385	0.3960	8.900	5017	0.176	0.019	0.041
-	34.61	1.4280	0.4104	7.600	4789	0.142	0.012	0.041
-	45.34	1.7980	0.3050	6.500	4588	0.132	0.007	0.039
-	62.30	2.4380	0.3413	5.600	4266	0.111	0.005	0.039
-	188.44	4.8890	0.5110	0.060	3806	0.066	0.003	0.026
0.20	12.43	0.6720	0.2925	12.200	16650	0.024	0.024	0.054
-	27.23	1.5030	0.5850	11.100	15426	0.051	0.021	0.055
-	53.84	2.6920	0.7550	8.130	12898	0.081	0.014	0.050

Table 12 (contd.)

Θ_{H_2S}	(%) conversion	$P_{^{12}C_2H_6}$ (torr)	$P_{^{12}C_2H_4}$ (torr)	$P_{^{12}C_2H_2}$ (torr)	$^{14}C_2H_4$ counts min^{-1}	$k_1 + k_3$	$k_1 - k_2$	$k_2 + k_3$
0.20	77.90	3.3140	1.0670	5.500	12392	0.089	0.014	0.043
-	104.93	4.6960	1.1550	4.200	8268	0.079	0.011	0.045
-	126.40	4.9230	1.0940	2.640	8100	0.078	0.009	0.039
-	167.42	6.675	0.7680	0.990	7933	0.069	0.005	0.039

catalysts (EUROPT-3, 0.8% Pt/Al_2O_3), but was negative for the silica-supported catalysts (EUROPT-1, 0.8% Pt/SiO_2).

As already discussed in Chapter 14, the effect of sulphur on the adsorption of acetylene and ethylene was to noticeably reduce the extent of the secondary adsorption region. This effect is much more pronounced with C_2H_2 than with C_2H_4 (Figures 81, 82). It is likely that the detrimental effect of sulphur on the silica-supported Pt catalysts is caused by the effective reduction in the number of sites responsible for acetylene hydrogenation, whilst those sites at which ethylene hydrogenation takes place are unaffected. In the presence of excess H_2, the hydrogenation of ethylene becomes more feasible, leading to a decrease in selectivity.

Using the method applied above and the information in Table 12 and Figure 86, it is possible to deduce the relative values of the rate constants of acetylene hydrogenation on the poisoned EUROPT-1 catalyst. These values are presented in Table 13.

Table 13. Reaction rate constants of acetylene hydrogenation on S-poisoned EUROPT-1

% Conversion	k_1	k_2	k_3
10.51*	0.027	0.004	0.172
34.61*	0.026	0.010	0.116
62.30*	0.012	0.007	0.099
-	-	-	-
27.23†	0.025	0.004	0.026
53.84†	0.019	0.005	0.062
79.90†	0.020	0.006	0.069

* $\Theta_{H_2S} = 0.01$, † $\Theta_{H_2S} = 0.002$

An interesting feature emerges when these values are compared with those obtained on the sulphur-free catalyst (Table 10). While the effect of sulphur was negligible on the hydrogenations occurring via the routes k_1 and k_3, it showed a beneficial effect in that a 10-fold increase in the rate of the reaction proceeding via the route k_2 resulted (see reaction scheme above). For this reason EUROPT-1 displayed a substantial decrease in the selectivity as the catalyst was poisoned with sulphur (Figure 84).

The beneficial effect of sulphur on the selectivity of EUROPT-3 and 0.8% Pt/Al_2O_3 for acetylene hydrogenation has been caused by the influence of the acidic sites present on the alumina. This is indeed a possible explanation when the adsorption isotherms of acetylene and ethylene on the sulphur-poisoned catalysts are compared with those obtained on the clean catalysts (Figure 87). The shapes of the secondary adsorption regions of these isotherms continued to increase sharply as further hydrocarbon gas was admitted to the catalyst. This latter behaviour, which has been observed with the adsorption of n-pentane on various supports, such as carbon and $BaSO_4$, is characteristic of a physical adsorption process (190). Thus the possibility exists that, in the presence of sulphur, the gas phase ethylene formed from acetylene hydrogenation is being adsorbed at the chlorinated alumina sites, while their double bond character is retained (195). This, in the presence of hydrogen, would lead to the desorption of ethylene to the gas phase, hence increasing the selectivity.

CHAPTER SIXTEEN

THE REACTION OF BUTA-1,3-DIENE WITH HYDROGEN

Throughout this chapter the terms 1-3B, 1-B, t-2-B, c-2-B and n-B will be used to refer to buta-1,3-diene, but-1-ene, trans-but-2-ene, cis-but-2-ene and n-butane respectively.

The results presented in section 8.1 show that the hydrogenation of 1-3B over EUROPT-1 and EUROPT-3 proceeded in two stages, the onset of the second stage, which occurred very late in the reaction being accompanied by an increase in the reaction rate. The lateness of the acceleration suggests that the hydrogenation of 1-3B and butenes was occurring simultaneously on the catalyst surface.

The negative order in 1-3B and the positive order in H_2 over both catalysts indicates that 1-3B is more strongly adsorbed than H_2 and there is no effective competition for the surface sites between the two reactants.

In section 8.3 it was shown that, over both catalysts, all the three butenes were formed as initial products, in addition to n-B, with the composition 76% (1-B), 16% (t-2-B) and 6% (c-2-B). The distribution of these butenes was found to be independent of the extent of the reaction (up to ~ 100% conversion), even though the selectivity for the formation of these butenes decreased slightly with increasing conversion. These observations suggest that once the butenes are formed, they undergo further reaction at similar rates, rather than desorbing from the surface.

The observations reported in section 8.4 show that, over EUROPT-1, the butene distribution was independent of the initial hydrogen pressure (Figure 71), whereas over EUROPT-3, an increase in the yield of 2-B and a decrease in the yield of 1-B was observed as the initial hydrogen pressure was increased (Figure 72). The independence of the butene distribution on initial hydrogen pressure obtained on EUROPT-1 suggests that the routes to each isomer are equally affected by the change in the availability of adsorbed hydrogen and that the 1-B does not undergo isomerisation to t-2-B and c-2-B. The dependence of the butene composition on the initial hydrogen pressure over EUROPT-3 is an indication that the isomerisation of 1-B is important for the production of the 2-B, as well as the formation of the 2-B directly from 1-3B. However, the magnitude of the effect of hydrogen availability on the butene composition was small, suggesting that the contribution of 1-B isomerisation to the formation of 2-B was also small. The decrease in selectivity observed on this catalyst as the initial hydrogen pressure was increased can be attributed to the increase in the extent of butene hydrogenation relative to desorption, as the availability of adsorbed hydrogen is increased.

It was observed (section 8.6) that over both EUROPT-1 and EUROPT-3, the 1-B:t-2-B ratio decreased with increasing temperature and that of the t-2-B:c-2-B ratio was independent of temperature. The effect is much more pronounced over EUROPT-1 than over EUROPT-3. These observations can be interpreted as showing that the activation energy for 1-B isomerisation is greater than that for its hydrogenation, which is consistent with the observation of Webb (191) using alumina-supported Os and Ru catalysts.

From the above discussion, it appears to be that on both EUROPT-1 and EUROPT-3 catalysts, the 1:2 addition of hydrogen to 1-3B is responsible for 1-B formation and that 1:4 addition is responsible for the t-2-B and c-2-B production. This is consistent with the general mechanism for 1-3B hydrogenation, as proposed previously by Wells et al. (62, 127, 128) (Figure 6) and which can be summarised as follows:

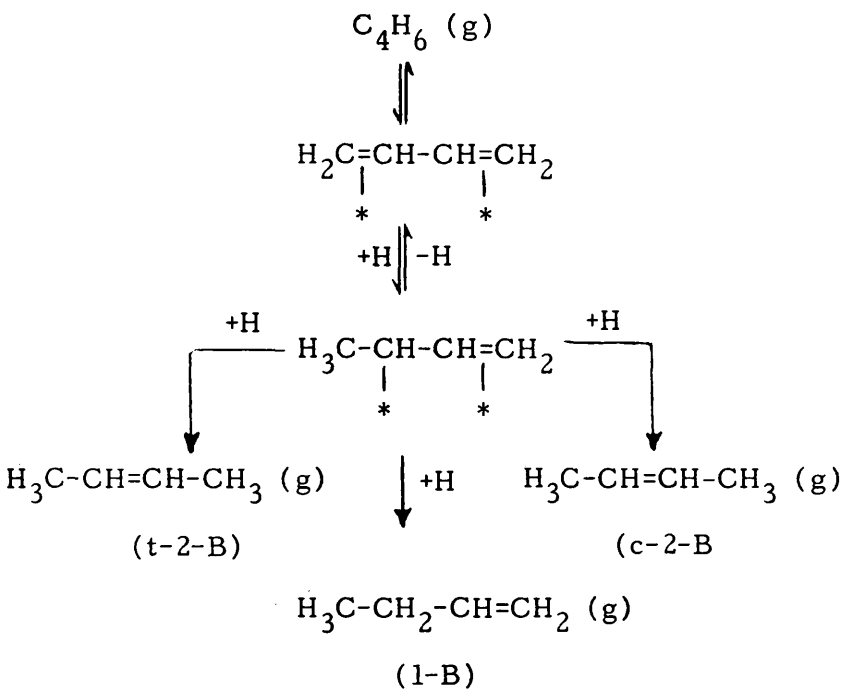

Since the selectivity is less than unity over both catalysts, that is, n-B is produced as an initial product and as it is unlikely that the isomerisation of 1-B to t-2-B and c-2-B takes place over these catalysts, it appears possible that n-B is formed from an adsorbed 1-3B via a route not involving adsorbed 1-B as an intermediate. Such a route may be one involving a 1:4 adsorbed intermediate:

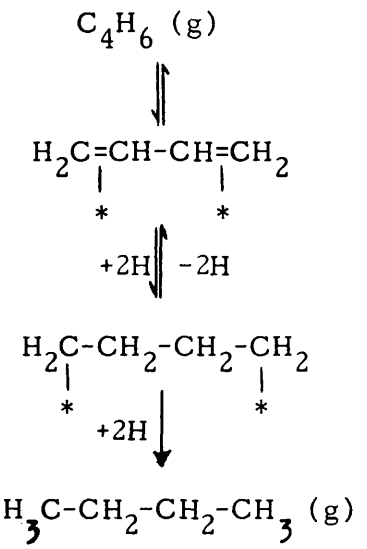

(n-B)

The effects of pre-adsorbed sulphur on the hydrogenation of 1-3B over EUROPT-1 and EUROPT-3 (section 9.6) showed that, while sulphur poisoning was negative for the selectivity over the former catalyst, it was beneficial over the latter catalyst. From the results presented in Figure 89, it can be seen, with EUROPT-1, that sulphur preferentially poisons the sites at which 1-B, t-2-B and c-2-B formation takes place. Similar findings have been reported (73) for the hydrogenation of 1-3B over H_2S-poisoned Pt(100) surface. As a consequence, the availability of adsorbed hydrogen may have increased the extent of 1-3B hydrogenation to n-B. The beneficial effect of pre-adsorbed sulphur over EUROPT-3 was to increase the yields of 1-B and t-2-B while that of n-B decreased as the sulphur coverage was increased (Figure 89). It is tempting to suggest that the increase in the yield of 1-B and probably its isomerisation to t-2-B lies in the possibility

that, sulphur influences the adsorption of 1-3B to the acidic sites present on the alumina support, since it is well established that such sites are good for catalysing the isomerisation of various hydrocarbon adsorbates.

CHAPTER SEVENTEEN

THE EFFECTS OF HYDROGEN AND HYDROGENATION REACTIONS ON THE STRUCTURE OF THE Pt CATALYSTS

The temperature programmed reduction measurements (section 11.1) showed TPR profiles which are indicative of the occurrence of an interaction between the Pt-particles and support surfaces (except Pt/MoO_3). The Pt/MoO_3 catalyst showed a low temperature reduction peak at 144°C which corresponds to that reported (176) for the unsupported $H_2[PtCl_6]$, in addition to two reduction peaks at 303° and 547°C which are characteristic of the reduction of bulk MoO_3 (192). Therefore, sintering of the Pt-particles is likely to be the cause of the inertness of this catalyst for acetylene hydrogenation, reported in Chapter 7. The comsumption of H_2 over EUROPT-1 at ambient temperature and the appearance of a reduction peak at 110°C is characteristic of PtO_2 (193). This is consistent with the results of extended-X-ray absorption fine structure (EXAFS), which indicated that EUROPT-1 contains a disordered Pt oxide phase. The other catalysts used in this work (EUROPT-3, 0.8% Pt/Al_2O_3 and 0.8% Pt/SiO_2) showed main reduction peaks at ~ 200°C, ascribable to the existence of an interaction between the Pt-particles and the supports. Hence, it is assumed that the reduction procedure used in this work (section 3.6) is capable of achieving well-reduced catalysts.

Electron microscopic examinations showed that reducing EUROPT-1 and EUROPT-3 in H_2 at 250°C for 2h produced catalysts containing evenly distributed Pt-particles (Plates 1,7), suggesting that these catalysts are resistant to sintering under the conditions used. However, when EUROPT-3 was subjected to C_2H_2/H_2 reactions, carbonaceous filaments were observed to form on the catalyst surface, with the Pt-particles being located at the heads of these filamentous carbons (Plate 8). Although the mechanism of carbon-filament formation is not well documented in the literature, it is possible that the chlorinated sites located on the alumina of EUROPT-3 acted as a promotor for carbon deposition on the support which in turn diffused progressively to the Pt-particles, forming such carbon tubes. The TEM of EUROPT-1 which had been deactivated with buta-1,3-diene and hydrogen mixtures (Plate 3) showed a growth in the Pt-particles to between 2-10 nm. Moreover, these particles showed interesting variations in shape, such as, spheres, squares and hexagonal , compared with the spherical shapes of the freshly reduced catalyst. Even though such a phenomenon was not observed after the catalysts had been subjected to reaction and deactivated with C_2H_2/H_2 (Plate 2), it is possible that buta-1,3-diene and/or the butenes, in the presence of hydrogen, created a carbon-induced faceting to the Pt-particles similar to that previously reported to occur with Pt/Al_2O_3 catalysts in the presence of various hydrocarbons (152, 194). The effect of sulphur poisoning on EUROPT-1 was to cause only a slight increase in the particle size from ~ 2.0 nm to ~ 2.5 nm (Plate 4) thus demonstrating the remarkable stability of EUROPT-1,

even under treatment with sulphur, which is known to severely disturb the morphology of the metal particles (152, 194). The SEM of EUROPT-1 and EUROPT-3 (Plates 5, 6 and 9, 10, respectively) showed that the morphological texture of the alumina of EUROPT-3 is much softer and more amorphous than the silica of EUROPT-1.

Table 14. Number of adsorbed molecules on Pt-catalysts obtained by the extrapolation of secondary adsorption region to zero pressure.

Catalyst	Θ_{H_2S}	CO molecules $\times 10^{20} g^{-1}$	C_2H_2 molecules $\times 10^{20} g^{-1}$	C_2H_4 molecules $\times 10^{20} g^{-1}$	Condition
EUROPT-1	0.00	3.50	3.98	0.49	F
	0.00	0.70	0.40	0.07	S
	0.10	-	1.64	-	P
	0.13	-	0.66	-	P
	0.20	-	-	0.80	P
	0.28	4.45	-	-	P
	0.32	-	-	0.49	P
	0.40	3.20	-	-	P
	0.46	-	-	0.37	P
	0.54	2.10	-	0.71	P
	0.60	-	1.11	0.98	P
EUROPT-3	0.00	0.36	0.25	0.05	F
	0.00	0.06	0.04	0.01	S
	0.25	0.00	0.00	0.00	P
0.8% Pt/SiO_2	0.00	0.15	0.01	-	F
0.8% Pt/Al_2O_3	0.00	0.33	0.07	-	F
0.5% Pt/MoO_3	0.00	0.05	0.09	-	F

F = freshly reduced , S = steady state (C_2H_2/H_2-deactivated)

P = Sulphur poisoned

- = not determined

REFERENCES

References

1. J.J. Berzelius, Annls. Chim. Phys., 61, 146 (1836).
2. H. Davy, Phil. Trans. Royl. Soc., 107, 77 (1817).
3. I.J. Langmuir, J. Am. Chem. Soc., 38, 2221 (1916).
4. O. Beeck, Disc. Faraday Soc., 8, 118 (1950).
5. J.H. De Boer, in "Chemisorption", ed. W.E. Garner, Butterworths, London (1957) p.27.
6. G.C. Bond, "Catalysis by Metals", Academic Press, New York, (1962).
7. H.M. Freundlich, Kappilar Chemie, Leipzig (1909).
8. M.I. Temkin and V. Pyzhev, Acta Phys. Chem., URSS, 12, 327 (1940).
9. S. Brunauer, P.H. Emmett and E. Teller, J. Am. Chem. Soc., 60, 309 (1938).
10. E.P. Barrett, L.G. Joyner and P.P. Halenda, J. Am. Chem. Soc., 73, 373 (1951).
11. G.C. Bond and R. Burch, in "Catalysis", Specialist Periodical Reports, eds. G.C. Bond and G. Webb, The Chemical Society, Vol. 6 (1983) p.27.
12. "Preparation of Catalysts". Studies in Surface Science and Catalysis, eds., P.A. Jacobs and G. Poncelet, Elsevier, Amsterdam, (1987) Vol. IV.
13. W.F. Taylor, D. Yates and J.H. Sinfelt, J. Phys. Chem., 68, 2962 (1964); J. Catal., 4, 374 (1965).

14. G.M. Schwab, Disc. Faraday Soc., 41, 252 (1966); Adv. Catal., 27, 1 (1978).

15. F. Solymosi, Catal. Rev., 1, 233 (1967).

16. S.J. Tauster, S.C. Fung and R.L. Garten, J. Am. Chem. Soc., 100, 170 (1978).

17. S.J. Tauster, S.C. Fung, R.T. Baker, and J.R. Horsley, Science, 211, 1121 (1981).

18. P.J. Meschter and W.L. Worrel, Mettall. Trans., 7A, 299 (1976).

19. G.J. Denotter and F.M. Dautzenberg, J. Catal., 53, 116 (1978).

20. J.W. Sprys and Z. Mencik, J. Catal., 40, 290 (1975).

21. G.A. Martin, R. Dutartre and J.A. Dalmon, React. Kinet. Lett., 16, 329 (1981); J. Catal., 75, 233 (1982).

22. J.G. Dickinson, L. Katz and R. Ward, J. Am. Chem. Soc., 83, 3026 (1961).

23. F.M. Dautzenberg and H.B.M. Wolters, J. Catal., 51, 26 (1978).

24. T. Huizinga and R. Prins, J. Phys. Chem., 85, 2156 (1981).

25. T.M. Apple, P. Gajardo and C. Dybowski, J. Catal., 68, 103 (1981).

26. J.W.E. Coenen, W.M.T. Schats and R.Z.C. Van Meerten, Bull. Soc. Chim. Belg., 88, 435 (1979).

27. J.A. Szymura and S.E. Wanke, in "Temperature Programmed Reduction for Solid Materials Characterisation", Chemical Industries Vol. 24, eds., A. Jones and B. McNicol, New York, Dekker (1986) p.170.

28. J.R. Katzer, G.C. Schuit and J.H. Van Hooff, J. Catal., 59, 278 (1979).

29. R. Bouwman and P. Biloen, J. Catal., 59, 365 (1979).

30. I. Horiuti and M. Polanyi, Trans. Faraday Soc., 30, 1164 (1934).

31. G.C. Bond and P.B. Wells, Adv. Catal., 15, 91 (1964).

32. G. Webb, in "Surface and Defect Properties of Solids". Specialist Periodical Reports, eds. M.W. Robert and J.M. Thomas, The Chemical Society, Vol. 3 (1974) p.184.

33. S.J. Thomson, in "Catalysis". Specialist Periodical Reports, eds. C. Kemball and D.A. Dowden, The Chemical Society, Vol. 3 (1980) p.1.

34. D.L. Smith and R.P. Merrill, J. Chem. Phys., 52, 5861 (1970); 53, 3588 (1970).

35. H. Ibach, H. Hopster and B. Sexton, Appl. Surf. Sci., 1, 1 (1977).

36. A.M. Baro and H. Ibach, J. Chem. Phys., 74, 4194 (1981).

37. L.L. Kesmodel, L.H. Dubois and G.A. Somorjai, J. Chem. Phys., 70, 2180 (1979).

38. M. Salmeron and G.A. Somorjai, J. Phys. Chem., 86, 341 (1982).

39. S.M. Davis, F. Zaera, B.E. Gordon and G.A. Somorjai, J. Catal., 92, 240 (1985).

40. J.D. Perentice, A. Lesiunas and N. Sheppard, J. Chem. Soc. Chem. Comm., 1976, 76 (1976).

41. D. Cormark, S.J. Thomson and G. Webb, J. Catal., 5, 224 (1966).

42. G.F. Taylor, S.J. Thomson and G. Webb, J. Catal., 12, 191 (1968).

43. J.A. Altham and G. Webb, J. Catal., 18, 133 (1970).

44. J.U. Reid, S.J. Thomson and G. Webb, J. Catal., 29, 433 (1973).

45. G. Webb, in "Catalysis". Specialist Periodical Reports, eds., C. Kemball and D.A. Dowden, The Chemical Society, Vol. 2 (1978) p.145.

46. L.H. Little, N. Sheppard and D.J.C. Yates, Proc. Roy. Soc., A259, 242 (1960).

47. P.J. Page and P.M. Williams, Disc. Faraday Soc., 58, 80 (1974).

48. J.E. Demuth and D.E. Eastman, Phys. Rev. Lett., 32, 1123 (1974).

49. J.E. Demuth, Chem. Phys. Lett., 45, 12 (1977).

50. T.E. Fisher, S.R. Kelemen and H.P. Bonzel, Surf. Sci., 64, 157 (1977).

51. L.L. Kesmodel, P.C. Stairs, R.C. Baetzold and G.A. Somorjai, Phys. Rev. Lett., 36, 1316 (1976).

52. N. Sheppard and J.N. Ward, J. Catal., 15, 50 (1969).

53. S.S. Randhava and A. Rehmat, Trans. Faraday Soc., 66, 235 (1970).

54. P.K. Wang, C.P. Slichter and J.H. Sinfelt, Phys. Rev. Lett., 53, 82 (1984).

55. A.S. Al-Ammar and G. Webb, J. Chem. Soc. Faraday Trans. I, 74, 195 (1978).

56. G.F. Berndt, S.J. Thomson and G. Webb, J. Chem. Soc. Faraday Trans. I, 79, 195 (1983).

57. E.A. Arafa, M.Sc. Thesis, Glasgow University (1985).

58. A.S. Al-Ammar and G. Webb, J. Chem. Soc. Faraday Trans. I, 74, 657 (1978).

59. A.S. Al-Ammar and G. Webb, J. Chem. Soc. Faraday Trans. I, 75, 1900 (1979).

60. G.C. Bond, G. Webb, P.B. Wells and J.M. Winterbottom, J. Catal., 1, 74 (1962).

61. P.B. Wells and A.J. Bates, J. Chem. Soc. A, 3064 (1968).

62. J.J. Phillipson, P.B. Wells and G.R. Wilson, J. Chem. Soc. A, 1352 (1969).

63. A.J. Bates, Z.K. Leszczynski, J.J. Phillipson, P.B. Wells and G.R. Wilson, J. Chem. Soc. A, 2436 (1970).

64. P.B. Wells and G.R. Wilson, J. Chem. Soc. A, 2442 (1970).

65. N.R. Avery, J. Catal., 19, 15 (1970).

66. R.P. Eischens and W.A. Pliskin, Adv. Catal., 10, 2 (1958).

67. A. Ravi and N. Sheppard, J. Phys. Chem., 76, 2699 (1972).

68. C.P. Kulbe and R.S. Mann, Proc. 6th Int. Cong. Catal. Vol. 1, The Chemical Society, London (1977) p.47.

69. Y. Soma, Bull. Chem. Soc. Japan, 50, 2119 (1977).

70. J.L. Gland, K. Baron and G.A. Somorjai, J. Catal., 36, 305 (1975).

71. J. Oudar, S. Pinol and Y. Berthier, J. Catal., 107, 434 (1987).

72. J. Oudar, S. Pinol and C.-M. Pradier and Y. Berthier, J. Catal., 107, 445 (1987).

73. C.-M. Pardier, E. Margot, Y. Berthier and J. Oudar, Appl. Catal., 31, 243 (1987).

74. R. Touroude and F.G. Gault, J. Catal., 32, 288 (1974); 32, 294 (1974); 37, 193 (1975); 60, 15 (1979).

75. M.J. Ledoux, F.G. Gault, A. Bouchy and G. Roussy, J. Chem. Soc. Chem. Faraday I, 76, 1547 (1980).

76. M.J. Ledoux, J. Catal., 70, 375 (1981).

77. R.R. Ford, Adv. Catal., 21, 51 (1970).

78. N. Sheppard and T.T. Nguyen, in "Advances in Infrared and Raman Spectroscopy", eds. R.J. Clarke and R.E. Hester, Wiley, New York (1978), Vol. 4, p.67.

79. R.P. Eischens, S.A. Francis and W.A. Pliskin, J. Phys. Chem., 60, 194 (1956).

80. R.P. Eischens and W.A. Pliskin, Adv. Catal., 10, 1 (1958).

81. G. Blyholder, J. Phys. Chem., 68, 248 (1971).

82. C.W. Garland, R.C. Lord and P.F. Troiano, J. Phys. Chem., 69, 1188 (1965).

83. J.F. Harrod, R.W. Roberts and E.F. Rissman, J. Phys. Chem., 71, 343 (1967).

84. J. Schwank, G. Parravano and H.L. Gruber, J. Catal., 61, 19 (1980).

85. A.C. Yang and C.W. Garland, J. Phys. Chem., 61, 1504 (1957).

86. L. Lynds, Spectrochim. Acta, 20, 1369 (1964).

87. K. Tanaka and J.M. White, J. Catal., 79, 81 (1983).

88. D.M. Haaland, Surf. Sci., 185, 1 (1987).

89. B.E. Hayden and A.M. Bradshaw, 125, 787 (1983).

90. J.E. Crowll, E.L. Garfunkel and G.A. Somorjai, Surf. Sci., 121, 303 (1982).

91. M. Kiskinova, G. Pirug and H.P. Bonzel, Surf. Sci., 133, 321 (1983).

92. P. Paul, Nature, 323, 701 (1986).

93. M.A. Vannice, L.C. Hasselbring and B. Sen, J. Catal., 97, 66 (1986).

94. F.T. Bain, S.D. Jackson, S.J. Thomson, G. Webb and E. Willocks, J. Chem. Soc. Faraday Trans. I, 72, 2516 (1976).

95. N.C. Kuhnen, S.J. Thomson and G. Webb, J. Chem. Soc., Faraday Trans. I, 79, 2195 (1983).

96. S. Kinnaird, G. Webb and G.C. Chinchen, J. Chem. Soc. Faraday Trans. I, 83, 3399 (1987).

97. R.A. Hadden, K.C. Waugh and G. Webb, Catal. Lett., 1, 27 (1988).

98. P.B. Wells, Appl. Catal., 18, 259 (1985).

99. Z. Paal and P.G. Menon, Catal. Rev.-Sci. Eng., 25, 229 (1983).

100. S. Tsuchiya, Y. Amenomiya and R.J. Cvetanovic, J. Catal., 9, 245 (1970).

101. F. Nagy, D. Moger, M. Hegedüs, Gy. Mink and S. Szabó, Acta Chim. Acad. Sci. Hung., 100, 211 (1979).

102. J.J. Stephen, V. Ponec and W.M. Sachtler, J. Catal., 37, 81 (1975).

103. J.P. Candy, P. Fouillox and A.J. Renouprez, J. Chem. Soc. Faraday Trans. I, 76, 616 (1980).

104. P.G. Menon and G.F. Froment, J. Catal., 59, 138 (1978).

105. P.G. Menon and G.F. Froment, Appl. Catal., 1, 31 (1981).

106. J.A. Konvalinka and J.J.F. Scholton, J. Catal., 48, 374 (1977).

107. J.A. Konvalinka, P.H. Van Oeffelt and J.J.F. Scholten, Appl. Catal., 1, 141 (1981).

108. K. Christmann, G. Ertl and T. Pignet, Surf. Sci., 54, 365 (1976).

109. Z. Paàl and S.J. Thomson, Radiochem. Radioanal. Lett., 12, 1 (1972).

110 Z. Paàl and S.J. Thomson, J. Catal., 30, 96 (1973).

111. G.F. Taylor, S.J. Thomson and G. Webb, J. Catal., 8, 388 (1967).

112. B. Lang, R.W. Joyner and G.A. Somorjai, Surf. Sci., 30, 454 (1972).

113. P.B. Wells, J. Catal., 52, 498 (1978).

114. D. Bianchi, M. Lacroix, G. Pajonk and S.J. Teichner, J. Catal., 59, 467 (1979).

115. J.M. Parera, N.S. Figoli, E.L. Jablonski, M.R. Sad and J.N. Beltramini, in "Catalyst Deactivation", eds., B. Delmon and G.F. Froment, Elsevier, Amsterdam (1980 p.571.

116. T. Baird, in "Catalysis". Specialist Periodical Reports, eds., G.C. Bond and G. Webb, The Royal Society of Chemistry, London (1982) Vol. 5, p.172.

117. T. Baird, Z. Paàl and S.J. Thomson, J. Chem. Soc. Faraday Trans. I, 69, 1237 (1973).

118. Y.F. Chu and E. Ruckenstein, Surf. Sci., 67, 517 (1977).

119. R.M.J. Fiederow, B.S. Chahar and S.E. Wanke, J. Catal., 61, 193 (1978).

120. A. Frennet and P.B. Wells, Appl. Catal., 18, 243 (1985).

121. R.W. Joyner, J. Chem. Soc. Faraday I, 76, 357 (1980).

122. J. Sheridan and W.D. Reid, J. Chem. Soc., 2962 (1952).

123. G.C. Bond and J. Sheridan, Trans. Faraday Soc., 48, 651 (1952).

124. G.C. Bond and P.B. Wells, J. Catal., 4, 211 (1965); 65, 419 (1966).

125. G.C. Bond, G. Webb and P.B. Wells, J. Catal., 12, 157 (1968).

126. C. Kemball, W.T. McGown, D.A. Whan and M.S. Scrurell, J. Chem. Soc. Faraday I, 73, 632 (1977).

127. G.C. Bond, G. Webb, P.B. Wells and J.M. Winterbottom, J. Chem. Soc., 3, 3218 (1965).

128. P.B. Wells and A.J. Bates, J. Chem. Soc. A, 3064 (1968).

129. E.B. Maxted, Adv. Catal., 3, 129 (1951).

130. J. Oudar, Catal. Rev.-Sci. Eng., 22, 171 (1980).

131. C.H. Bartholomew, P.K. Agrawal and J.R. Katzer, Adv. Catal., 31 (1982).

132. J. Barbier, in "Deactivation and Poisoning of Catalysts", eds., J. Oudar and H. Wise, Marcel Dekker Inc. (1985) p.109.

133. T.E. Fischer and S.R. Kelemen, J. Catal., 53, 24 (1978).

134. H.P. Bonzel and R. Ku, J. Chem. Phys., 58, 4617 (1973).

135. H.P. Bonzel, Surf. Sci., 27, 387 (1971).

136. J.L. Oliphant, R.W. Fowler, R.B. Pannell and C.H. Bartholomew, J. Catal., 51, 229 (1978).

137. W.D. Fitzharris, J.R. Katzer and W.H. Manogue, J. Catal., 76, 369 (1982).

138. J.M. Saleh, C. Kemball and M.W. Robert, Trans. Faraday Soc., 57, 1771 (1961).

139. J.M. Saleh, Trans. Faraday Soc., 67, 1830 (1971).

140. I.E. Den Besten and P.W. Selwood, J. Catal., 1, 93 (1962).

141. A.Q. Contractor and H. Lal, J. Electroanal. Chem., 96, 175 (1979).

142. H.P. Bonzel and R. Ku, J. Chem. Phys., 59, 1641 (1973).

143. J. Oudar, Proc. Int. Symp. on Fundamental Chemistry of Promotors and Poisons in Heterogeneous Catalysis, American Chemical Society, New York (1986) p.245.

144. E. Protopopoff and P. Marcus, Surf. Sci., 169, L237 (1986).

145. E.S. Argano, S.S. Randhava and A. Rehmat, Trans. Faraday Soc., 65, 552 (1969).

146. C. Besoukhanova, M. Breysse, J. Benard and D. Barthomeuf, in "Catalyst Deactivation", eds., B. Delmon and G.F. Froment, Elsevier, Amsterdam (1980).

147. H.C. Yao, H.K. Stepien and H.S. Gandi, J. Catal., 67, 231 (1981).

148. P. Gallezot, J. Datka, J. Massardier, M. Premet and B. Imelik, Proc. 6th Int. Cong. Catal., London (1976) p.A11.

149. E.J. Erekson, K.S. Chang and C.H. Bartholomew, Appl. Catal., 5, 1323 (1983).

150. R. Maurel, G. Leclercq and J. Barbier, J. Catal., 37, 324 (1975).

151. G.A. Somorjai, J. Catal., 27, 453 (1972).

152. P.J.F. Harris, Nature, 323, 793 (1986).

153. N. Barbouth and M. Salame, J. Catal., 104, 240 (1987).

154. C. Apesteguia and J. Barbier, Bull. Soc. Chim. Fr., 5-6 I, 165 (1982).

155. P.G. Menon and J. Prasad, Proc. 6th Int. Cong. Catal., London (1976) p.1060; (1977) Vol. 2, p.696.

156 M.J. Sterba and V. Haensel, Ind. Eng. Chem. Prod. Res. Dev., 15, 2 (1976).

157. M. Wilde, T. Stolz, R. Feldhaus and K. Anders, Appl. Catal., 31, 99 (1987).

158. H.D. Simpson, Adv. Chem. Ser., 143, 39 (1975).

159. M. Mathieu and M. Primet, Appl. Catal., 9, 361 (1984).

160. F.A. Paneth and W. Vorwerk, Z. Phys. Stoechiom. Verwandschaftt, 101, 445 (1922).

161. S.J. Thomson and G. Webb, in "Heterogeneous Catalysis", eds., T.L. Cottrell, University Chemical Texts, Oliver and Boyd Ltd. (1968).

162. P.H. Emmett, Catal. Rev., 7, 1 (1973).

163. K.C. Campbell and S.J. Thomson, Proc. Surface and Membrane Sci., 9, 163 (1975).

164. G.F. Berndt, in "Catalysis". Special Periodical Reports, The Royal Society of Chemistry, eds., G.C. Bond and G. Webb, London (1983), Vol. 6, p.144.

165. S.J. Thomson and J.L. Wishlade, Trans. Faraday Soc., 58, 1170 (1962).

166. D. Cormack, S.J. Thomson and G. Webb, J. Catal., 5, 224 (1966).

167. D.W. Aylmore and W.B. Jepson, J. Sci. Inst., 38, 156 (1961).

168. T.R. Hughes, R.J. Houston and R. Sieg, Ind. Eng. Chem. Process Design Dev., 1, 69 (1962).

169. S.Z. Roginskii and N.P. Keier, Dokl. Akad. Nauk. SSSR, 57 157 (1947).

170. G.K.L. Granstoun and S.J. Thomson, Trans. Faraday Soc., 59, 2403 (1963).

171. K.C. Campbell and S.J. Thomson, Trans. Faraday Soc., 55, 985 (1959).

172. G. Webb and J.J. MacNab, J. Catal., 26, 226 (1972).

173. J.U. Reid, S.J. Thomson and G. Webb, J. Catal., 5, 244 (1966).

174. F. Schmidt-Bleek and F.S. Rowland, Anal. Chem., 36, 1695 (1964).

175. H.A. Benesi, L.T. Atkins and R.B. Mosely, J. Catal., 23, 221 (1971).

176. B.D. McNicol, N.W. Hurst, S.J. Gentry and A. Jones, Catal. Rev.-Sci. Eng., 24, 233 (1982).

177. G.C. Bond and P.B. Wells, Appl. Catal., 18, 225 (1985).

178. G.M. Bickle, J. Biswas and D.D. Do, Appl. Catal., 36, 259 (1988).

179. B.D. McNicol, J. Catal., 46, 438 (1977).

180. G. Blanchard, H. Charcosset, M.T. Chenebaux and M. Primet, Proc. 2nd Int. Symp. on the Scientific Bases for the Preparation of Heterogeneous Catalysis, Louvain, La-Neuve, Belgium (1978), Paper No. B8.

181. M.F. Johnson and C.D. Keith, J. Phys. Chem., 67, 200 (1963).

182. J.W. Jenkins, B.D. McNicol and S.D. Robertson, Chem. Technol., 7, 316 (1977).

183. G.C. Bond and M.R. Gelsthorpe, Appl. Catal., 35, 169 (1987).

184. T.P. Beebe, Jr., M.R. Albert and J.T. Yates, Jr., J. Catal., 96, 1 (1985).

185. J.W. Geus and P.B. Wells, Appl. Catal., 18, 231 (1985).

186. Y. Yashu, G. Xiexian, L. Huimin, D. Maicun and L. Zhiyin, in ref. 12, p.701.

187. R.B. Levy and M. Boudart, J. Catal., 32, 304 (1974).

188. N.N. Kavtaradze and N.P. Sokolova, Russ. J. Phys. Chem., 44, 93 (1970).

189. G.D. McLellan and G. Webb, unpublished results.

190. C.N. Satterfield, in "Heterogeneous Catalysis in Practice", eds. McGraw-Hill, New York, (1980) p.32.

191. G. Webb, Ph.D. thesis, Hull University (1963).

192. R. Thomas, E.M. Van Oers, V.H.J. de Beer, and J.A. Moulijn, J. Catal., 84, 275 (1983).

193. H.C. Yao, M. Sieg and H.K. Plumer Jr., J. Catal., 59, 365 (1979).

194. P.J.F. Harris, Surf. Sci., 185, L459 (1987).

195. J.B. Peri, Proc. 3rd Int. Cong. Catal., Amsterdam (1964), vol. 2, p.1100.